Autoimmune limbic encephalitis and pathological role of anti-CASPR2 autoantibodies on synaptic function

Alanah Pieters

N°d'ordre NNT : 2019LYS1204

THESE de DOCTORAT DE L'UNIVERSITE DE LYON
opérée au sein de
l'Université Claude Bernard Lyon 1

Ecole Doctorale N° 476
Neurosciences et Cognition

Spécialité de doctorat : Neurosciences
Discipline : Neuroimmunologie

Soutenue publiquement le 17/10/2019, par :
Alanah PIETERS

Autoimmune limbic encephalitis and pathological role of anti-CASPR2 autoantibodies on synaptic function

---

Devant le jury composé de :

Nom,prénom	grade, établissement	Président.e
Devaux, Jérôme	Chargé de recherche CNRS	Rapporteur
Goutebroze, Laurence	Directrice de recherche CNRS	Rapporteure
Baulac, Stéphanie	Directrice de recherche INSERM	Examinatrice
Honnorat, Jérôme	PU-PH Hospices Civils de Lyon	Examinateur
Noraz, Nelly	Chargé de recherche INSERM	Directrice de thèse
Pascual, Olivier	Chargé de recherche INSERM	Co-directeur de thèse

N°d'ordre NNT : 2019LYS1204

THESE de DOCTORAT DE L'UNIVERSITE DE LYON
opérée au sein de
l'Université Claude Bernard Lyon 1

Ecole Doctorale N° 476
Neurosciences et Cognition

Spécialité de doctorat : Neurosciences
Discipline : Neuroimmunologie

Soutenue publiquement le 17/10/2019, par :
Alanah PIETERS

Autoimmune limbic encephalitis and pathological role of anti-CASPR2 autoantibodies on synaptic function

---

Devant le jury composé de :

Nom,prénom	grade, établissement	Président.e
Devaux, Jérôme	Chargé de recherche CNRS	Rapporteur
Goutebroze, Laurence	Directrice de recherche CNRS	Rapporteure
Baulac, Stéphanie	Directrice de recherche INSERM	Examinatrice
Honnorat, Jérôme	PU-PH Hospices Civils de Lyon	Examinateur
Noraz, Nelly	Chargé de recherche INSERM	Directrice de thèse
Pascual, Olivier	Chargé de recherche INSERM	Co-directeur de thèse

RESUME

L'encéphalite limbique à auto-anticorps anti-CASPR2 est une atteinte du système nerveux central, caractérisée par la présence des auto-anticorps (autoAcs) dirigé contre CASPR2 dans le sérum et fluide céphalorachidien. La pathologie affecte majoritairement des hommes âgés présentant l'épilepsie comme symptôme prédominant. CASPR2 est une molécule d'adhésion neuronale, connue pour son rôle d'assemblage des canaux Kv1, régulateurs de l'excitabilité neuronale, à la région juxtaparanodale du nœud de Ranvier, une organisation essentielle pour la conduction saltatoire des flux nerveux.

Un nombre croissant de données dans la littérature suggère un rôle pour CASPR2 dans des fonctions synaptiques et l'activité neuronale. Ceci pourrait expliquer l'épilepsie, un symptôme neurologique qui trouve son origine dans la perturbation de l'activité neuronale, observée chez les patients avec de l'encéphalite limbique anti-CASPR2. Dans ce travail de thèse, j'ai utilisé des autoAcs de patients comme outil pour investiguer le rôle de CASPR2 dans des neurones normalement développés en culture, permettant aussi d'évaluer l'effet des autoAcs des patients sur les fonctions synaptiques et de révéler des mécanismes physiopathologiques possibles sous-jacents à la maladie.

Je me suis d'abord intéressée aux effets des autoAcs des patients sur l'expression et la distribution en surface de CASPR2 et sur l'expression des canaux Kv1.2 dans des neurones hippocampiques matures *in vitro*. J'ai montré que les neurones inhibiteurs sont positifs pour les canaux Kv1.2 et CASPR2 en surface, et que les autoAcs de patients augmentent l'expression de Kv1.2 et n'induisent pas l'internalisation de CASPR2. Dans un second temps, j'ai analysé les effets des autoAcs de patients sur les synapses excitatrices et inhibitrices dans des neurones hippocampiques immatures et matures *in vitro*. Dans les neurones immatures, la densité des épines dendritiques et le contenu des récepteurs AMPA sont augmentés, tandis que dans les neurones matures l'altération de la géphyrin suggère une perturbation de la transmission neuronale après traitement avec des autoAcs de patients. Mes résultats permettent de mieux comprendre les fonctions de CASPR2 dans les processus synaptiques et révèlent des mécanismes pathologiques possibles des autoAcs anti-CASPR2 menant à la présentation clinique des patients atteints d'encéphalite limbique anti-CASPR2.

Mots clés: CASPR2, auto-anticorps, encéphalite limbique auto-immune, synapse, Kv1, épines, AMPA récepteur

ABSTRACT

Anti-CASPR2 autoimmune limbic encephalitis is a central nervous system disorder, characterized by the presence of autoantibodies (autoAbs) directed against CASPR2 in the serum and cerebrospinal fluid. Elderly men are mostly affected, with epilepsy being the predominant symptom. CASPR2 is a neuronal cell adhesion molecule, known for its role in gathering Kv1 channels, regulators of neuronal excitability, at the juxtaparanodal region of the node of Ranvier, an essential organization for saltatory conduction of nervous influxes.

Increasing sets of data in literature point out a role for CASPR2 in synaptic functions and neuronal activity. This could explain the observed epilepsy, a neurological symptom that finds its origin in disturbed neuronal activity, in patients with anti-CASPR2 autoimmune limbic encephalitis. In this work, I used patients' autoAbs as a tool to investigate the role of CASPR2 in normally developed cultured neurons which also allowed me to assess the effects of patients' autoAbs on synaptic functions and reveal possible physiopathological mechanisms underlying the disease.

I first assessed the effects of patients' autoAbs on CASPR2 surface expression and distribution and on Kv1.2 channel expression in mature *in vitro* hippocampal neurons. I provided evidence that inhibitory neurons are positive for both Kv1.2 channels and surface CASPR2, and that patients' autoAbs increase Kv1.2 expression and do not induce CASPR2 internalization. Secondly, I analyzed effects of patients' autoAbs on excitatory and inhibitory synapses *in vitro,* in immature and mature hippocampal neurons. In immature neurons, dendritic spine densities and AMPA receptor content are increased, while in mature neurons alteration of gephyrin suggests disturbed neuronal transmission after treatment with patients' autoAbs. My results allow for a better understanding of CASPR2 functions in synaptic processes and unravel possible pathological mechanisms regarding how anti-CASPR2 autoAbs lead to the clinical presentation of patients with anti-CASPR2 autoimmune limbic encephalitis.

Keywords: CASPR2, autoantibodies, autoimmune limbic encephalitis, synapse, Kv1, spines, AMPA receptor

ACKNOWLEDGEMENTS

I must be honest, when I started my thesis in 2016, I did not really 'believe' in acknowledgements. I estimated words of thanks a form of politeness, or something people do because that is just the way things go. Of course, I read acknowledgements of other peoples' work, but I only saw two-dimensional black words. Not three-dimensional colorful emotions.

During these last three years, my opinion changed, every day a little bit more. Every day that passes by, your thesis takes a bigger part in your life, which can be exciting and bedazzling but also long and frustrating. And thankfully there are people surrounding you and your little thesis cocoon you created, to fix it when it gets broken and you cannot manage on your own, to give you advice when you are looking to closely, to help you out when you get stuck in it, to cheer you up when you are getting lonely inside of it. So, therefore, a genuine thank you to everyone who helped me with and through this thesis.

First of all, I would like to express my sincere gratitude to the members of my jury, professors and doctors Jérôme Devaux, Laurence Goutebroze and Stéphanie Baulac, for accepting to accord their time and investment to the reading and critical evaluation of this work and for their presence and interest at my thesis defense.

I am grateful to Pr. Jérôme Honnorat for accepting me as a PhD student in his laboratory and allowing me to work on this highly interesting subject.

I would also like to thank my supervisor Dr. Nelly Noraz and co-supervisor Dr. Olivier Pascual for accepting to guide me during this thesis project and sharing their knowledge and know-how with me. Thanks to them I learned a lot, in many different domains, that made me grow as a scientist and as a person.

I gratefully acknowledge the help of Denis Resnikoff, for his never-ending patience and guidance during my microscopy and Imaris experiments.

Of course, starting as a pharmacist, unexperienced in neurosciences, I could not have performed this work without my laboratory colleagues. A genuine thank you, Chantal and Naura, for introducing and teaching me, both with your kind and understanding approach, into practical neurosciences. I also wish to thank my (previous) lab colleagues, students, PhD students, postdocs, engineers,… for sharing this adventure with me. A very special thanks goes out to Marie-Eve and Céline, who were always there, in moments of laughter and in moments of tears. Céline, you were like a mentor, professionally and personally. I am grateful for everything you taught me and shared with me, and for all the moments you were there, even when you were not there. Ines and Mélisse, I guess I do not have words for you both. You were always available, from mental status minus ten to plus hundred, inside and outside the lab. Thank you for your presence and help, encouragements and laugthers, insights and reflections,…

The two people I cannot thank enough, Mama, Papa, ‘dank u’ for everything. I do not know where to start, let alone where to end. Thank you for letting me start this adventure, determined as I was to leave Belgium and ‘do a thesis somewhere in Lyon’. Thank you for the hours of listening when I needed to explain every detail, for the encouragements when ‘the dark clouds’ were hanging above my head, for the good advice when I got stuck with the thesis or with myself, for the silly jokes when I needed to put on ‘my pink glasses’,… Thank you for being the best parents I could imagine.

A big thank you as well for my brother and sister, Jade and Morgane. Even though you are not the biggest talkers or huggers in the world, I know I could and still can count on you both. Thank you for trying to listen and understand when I was panicking about everything that was going wrong (or right), and thank you even more for switching those conversations to funnier ones. Thank you for your little gestures, which meant a lot to me during these years.

A very genuine and sincere thank you to you, Vincent. In all simplicity, for simply everything.

Thank you, Julien, for being there and never giving up on me. You believed in me no matter what and have always encouraged me. Thank you for making me believe in myself.

A special thanks to my very good friend, Elodie. We met later during this adventure in Lyon, but time is not an indicator of what you meant to me. We shared joy and sadness, excitation and boredom, serious and silly moments,… Thank you for being part of this (beginning) adventure.

I also wish to thank Tony, for being such a wonderful teacher who profoundly believes in my abilities.

A final word of thank goes out to everyone else I forgot and who in his/her way contributed to this thesis.

“The moment Galileo was set free, he looked up to the sky and down to the ground, and, while stamping his foot, in a contemplative mood, he said, Eppur si muove, that is, and yet it moves, meaning the planet earth.“

- *The Italian Library,* Giuseppe Marco Antonio Baretti, 1757

PREFACE

Limbic encephalitis is a central nervous system disorder, characterized by seizures, short-term memory deficits and psychiatric disorders. In 21% of the cases, limbic encephalitis is autoimmune-mediated, distinguished by the presence of autoantibodies in the serum and/or cerebrospinal fluid of the patient. Patients' autoantibodies can be directed against neuronal intracellular antigens or cell surface antigens. In the case of autoantibodies targeting intracellular antigens, immunomodulatory treatment, aiming at lowering autoantibody concentrations, generally provides unsatisfying results. Hence, these autoantibodies are estimated not to have a direct pathogenic role in the disease. On the other hand, autoantibodies directed against cell surface antigens are supposed to be directly pathogenic, since immunomodulatory treatment drastically improves patients' outcome. Moreover, the clinical presentation of the patient is dependent on the autoantibody present, highlighting the importance of the targeted antigen. Therefore, unraveling the function of the antigen is critical in understanding the pathology and ameliorating patients' outcome.

Initially described as autoantibodies targeting a larger protein complex, autoantibodies directed more specifically against CASPR2 have been recently discovered in patients with autoimmune limbic encephalitis. Given the recent discovery and the rarity of the disease, data in literature on the pathological mechanisms underlying anti-CASPR2 autoimmune limbic encephalitis is scarce. CASPR2 has been identified as a neuronal cell adhesion molecule and the bulk of data on this protein suggests a role for CASPR2 in synaptic processes and neuronal activity. However, the precise function of CASPR2 and the mechanism by which autoantibodies directed against this protein disturb its function has not yet been unraveled.

In my thesis I wished to elucidate the role of CASPR2 in synaptic processes and assess the effects of anti-CASPR2 autoantibodies on their target and on synapses in a normally developed neuronal network. This was anticipated to lead to a better understanding of CASPR2 in neuronal and synaptic functions and a more advanced comprehension of pathological mechanisms in anti-CASPR2 autoimmune limbic encephalitis.

TABLE OF CONTENTS

FIGURES

TABLES

ABBREVIATIONS

4-AP	4-aminopyridine
ADAM22/23	a disintegrin and metalloproteinase domain 22/23
AIE	autoimmune encephalitis
AILE	autoimmune limbic encephalitis
AIS	axon initial segment
AMPA	α-amino-3-hydroxy-5-methyl-4-isoxazolepropionic acid
AMPA-R	α-amino-3-hydroxy-5-methyl-4-isoxazolepropionic acid receptor
AP	action potential
ASD	autism spectrum disorder
AutoAbs	autoantibodies
BBB	blood-brain barrier
CAM	cell-adhesion molecule
CASPR2	contactin-associated protein like 2
CBA	cell-based binding assay
CDFE	cortical dysplasia-focal epilepsy
CNS	central nervous system
CSF	cerebrospinal fluid
DIV	days *in vitro*
DRG	dorsal root ganglion
DTX	dendrotoxin
E	embryonic day
ECM	extracellular matrix
eEPSC	evoked excitatory postsynaptic current
eiPSC	evoked inhibitory postsynaptic current
EPSC	excitatory postsynaptic current
Fab	fragment antigen-binding
FcRn	neonatal Fc receptor
GABA	γ-aminobutyric acid
GABA-R	γ-aminobutyric acid receptor
GlyR	glycine receptor
GPI	glycosylphosphatidylinositol
HEK	human embryonic kidney 293
HLA	human leucocyte antigen
IgG	immunoglobulin G
IPSC	inhibitory postsynaptic current
JXP	juxtaparanode
KA-R	kainate receptor
KD	knockdown
KO	knockout
Kv	voltage gated potassium channel
LE	limbic encephalitis
LGI1/4	leucin-rich glioma inactivated 1/4

mEPSC	miniature excitatory postsynaptic current
mGluR	metabotropic glutamate receptor
mIPSC	miniature inhibitory postsynaptic current
MoS	Morvan syndrome
NF	neurofascin
NMDA	N-methyl-D-aspartate
NMDA-R	N-methyl-D-aspartate receptor
NMT	neuromyotonia
NT	neurotransmitter
P	postnatal day
PN	paranode
PNJ	paranodal junction
PNS	peripheral nervous system
PSD93/95	postsynaptic density 93/95
SIM	structured illumination microscopy
STED	stimulation emission depletion
STORM	stochastical optical reconstruction microscopy
TAG-1	transient axonal glycoprotein-1
VGAT	vesicular GABA transporter
VGKC	voltage gated potassium channel
VGLUT1	vesicular glutamate transporter 1
WT	wild-type

INTRODUCTION

CHAPTER A. AUTOIMMUNE LIMBIC ENCEPHALITIS AND AUTOANTIBODIES

1. HISTORY

Encephalitis is defined by "the presence of an inflammatory process of the brain in association with clinical evidence of neurologic dysfunction" (Tunkel et al., 2008). The syndrome of encephalitis can have an acute or subacute origin and diagnosis is based on epidemiologic, clinical, laboratory and neuro-imaging features (Tunkel et al., 2008; Venkatesan et al., 2013). Although symptoms can vary, they usually comport a combination of fever, headache, altered consciousness, cognitive, neurological and autonomic dysfunction, behavioral changes, and seizures (Tunkel et al., 2008; Venkatesan et al., 2013; Venkatesan & Benavides, 2015).

The term "limbic encephalitis" (LE) was first introduced by Corsellis J. and colleagues in 1968 to define neurological disorders in which "the pathological process has been focused on the limbic gray matter" (Corsellis et al., 1968). They found inflammatory and degenerative changes in the limbic system, which includes the parahippocampal gyrus, cingulate gyrus, hippocampus, amygdala, mammillary bodies, hypothalamus and anterior nuclei of the thalamus (Rajmohan & Mohandas, 2007) **(Figure 1)**.

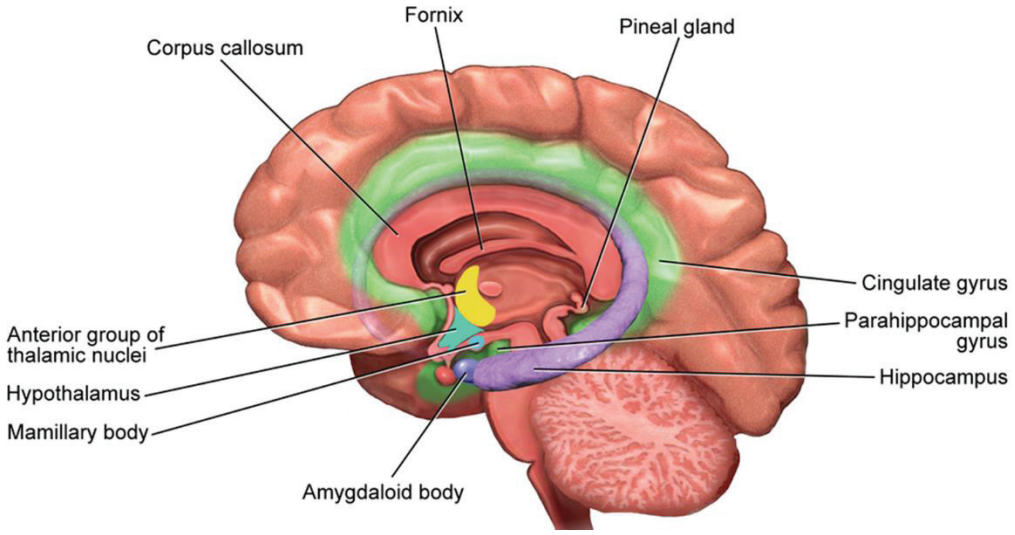

Figure 1. Anatomical components of the limbic system *(adapted from Blausen Medical, n.d., retrieved May 2019 from http://blausen.com).* The different anatomical structures of the limbic system are depicted in different colors. The corpus callosum, fornix and pineal gland are enclosed by the limbic system but do not make part of it.

The limbic system is involved in regulating emotions, memory and autonomic functions, thus explaining the clinical presentation of patients with limbic encephalitis, characterized by short-term memory loss, psychiatric disorders and epileptic seizures (Didelot & Honnorat, 2009).

2. AUTOIMMUNE LIMBIC ENCEPHALITIS

In one of the largest population-based prospective studies on encephalitis, it has been shown that 42% of encephalitides is cause by infection, 37% has an unknown trigger and 21% is autoimmune-mediated (Granerod et al., 2010). In this last case, autoimmune encephalitis (AIE) is characterized by the presence of autoantibodies (autoAbs) in the serum and/or cerebrospinal fluid (CSF). Although the specific target of the autoAb defines the patient's clinical presentation, nearly all forms of encephalitis associated with antibodies directed against neuronal surface antigens share a main syndrome of limbic encephalitis (see chapter A.2.1.2) (Leypoldt et al., 2012). Therefore, these immune-mediated encephalitides are classified as autoimmune limbic encephalitis (AILE).

2.1 TARGETS OF AUTOANTIBODIES

From the discovery of the first type of LE in 1968, which was associated with small-cell lung cancer, until 2001, it was believed that LE always associated with cancer and had generally a poor prognosis. This changed in 2001 with the discovery of serum antibodies against the cell surface voltage gated potassium channel (VGKC) complex in two patients, with and without underlying tumor, who recovered after immunomodulatory therapy or spontaneously respectively (Buckley et al., 2001). Both patients' clinical presentation improved together with the decrease of anti-VGKC antibodies (Buckley et al., 2001). In 2005, Ances et al. discovered an intense surface staining of the hippocampal and cerebellar neuropil with several other patients' antibodies presenting with LE. Importantly all patients had a drastic clinical and neuroimaging improvement after immunomodulatory treatment (Ances et al., 2005). This discovery led to the first classification of antibody-associated encephalitis, with the clinical presentation, treatment and outcome depending on the target of the antibody present. The individual characterization of other antibodies in autoimmune encephalitis and autoimmune limbic encephalitis followed rapidly.

2.1.1 ANTIBODIES DIRECTED AGAINST INTRACELLULAR ANTIGENS

Several autoAbs directed against intracellular antigens are known, which include nuclear antigens Hu (ANNA-1) (Graus et al., 1987), Ri (ANNA-2) (Luque et al., 1991), Ma1 (Dalmau et al., 1999), ANNA-3 (Chan et al., 2001), Ma2 (Ta) (Voltz et al., 2002) and SOX1 (AGNA) (Sabater et al., 2008), and cytoplasmic antigens Yo (PCA-1) (Furneaux et al., 1990), CV2 (CRMP5) (Honnorat et al., 1996), PCA-2 (Vernino & Lennon, 2000), Zic4 (Bataller et al., 2004) and GFAP (Fang et al., 2016) **(Table 1)**.

AutoAbs targeting more specifically synaptic intracellular proteins are also categorized in this group and include anti-AK5 (Tüzün et al., 2007), anti-amphiphysin (De Camilli et al., 1993) and anti-GAD65 (Solimena et al., 1988) **(Table 1)**.

Antigen	Clinical features	Associated tumors
AGNA[93] (SOX1)	LEMS, limbic encephalitis, neuropathy	Highly associated with small cell lung cancer, especially with LEMS
Amphiphysin[94]	Wide clinical spectrum: stiff person syndrome, cerebellar degeneration, limbic encephalitis, encephalomyelitis, myelopathy, peripheral neuropathy, opsoclonus myoclonus	~85% (breast, small cell lung cancer)
ANNA-1[45] (anti-Hu)	Wide clinical spectrum: sensory neuronopathy, limbic encephalitis, cranial neuropathies, cerebellar degeneration, encephalomyelitis, partial epilepsy, status epilepticus, autonomic dysfunction including intestinal pseudoobstruction, opsoclonus myoclonus	~80% (small cell lung cancer, neuroblastoma, prostate cancer)
ANNA-2[47] (anti-Ri)	Opsoclonus myoclonus, brainstem encephalitis, cerebellar degeneration	~60% (breast, gynecologic, lung, bladder cancer)
ANNA-3[95]	Cerebellar degeneration, encephalomyelitis, sensory neuronopathy	~60% (lung cancer)
CRMP-5[96] (anti-CV2)	Wide clinical spectrum: cerebellar degeneration, limbic encephalitis, optic neuritis, retinopathy, uveitis, chorea, encephalomyelitis, sensorimotor neuropathy	~75% (small cell lung cancer, thymoma)
GAD-65[97,98]	Wide clinical spectrum: encephalitis, stiff person syndrome, cerebellar ataxia, seizure disorder. With cancer more likely to see opsoclonus myoclonus syndrome and encephalomyelitis	~10% (lung cancer, neuroendocrine tumor, thymoma, breast cancer)
GFAP[5,6]	Encephalitis, meningoencephalitis, myelitis, encephalomyelitis, neuropathy, meningitis, ataxia	34% with malignancy, most often ovarian teratoma
Anti-Ma1,[99] Ma2[48](Ta)	Ma1 and Ma2: cerebellar and brainstem dysfunction. Ma2 (only): limbic encephalitis, hypothalamic dysfunction, brainstem encephalitis	> ~90% (Ma1 and Ma2—breast, colon, parotid, non-small cell lung cancer; Ma2 (only)—germ cell testicular)
PCA-1[100] (anti-Yo)	Paraneoplastic cerebellar syndrome: ataxia, dysarthria, nystagmus, peripheral neuropathy	~90% (breast, gynecologic, lung cancer)
PCA-2 (MAP1B)[101]	Encephalomyelitis, cerebellar degeneration, LEMS	~90% (lung cancer)
ZIC[103]	Encephalomyelitis, cerebellar degeneration, opsoclonus	Highly associated with small cell lung cancer

Table 1. Intracellular antigens *(adapted from Bradshaw et al., 2018)*. List of known intracellular antigens targeted by autoantibodies, clinical features of the autoimmune disease and possibility of tumor association.

Intracellular autoAbs occur more frequently in presence of a tumor. Importantly, the autoAb present can serve as a biomarker, since each autoAb is mainly associated with a specific tumor

type **(Table 1)**. Autoimmune disorders associated with intracellular autoAbs are presumed to be mediated by cytotoxic T-cells, causing the observed neuronal damage. Therefore, the autoAbs present are considered to rather be an immunological epiphenomenon than having a direct pathogenic role (Bien et al., 2012; Dalmau & Rosenfeld, 2008). This also explains why immunotherapy, aiming at lowering autoAbs titers, shows unsatisfying results in most cases (Shin et al., 2018).

2.1.2 ANTIBODIES DIRECTED AGAINST CELL SURFACE ANTIGENS

Cell surface antigens (or membrane antigens) targeted by autoAbs are mainly synaptic proteins. They were discovered more recently than intracellular antigens but have known substantial growth over the last decade. They include synaptic receptors such as mGluR1 (Smitt et al., 2002), NMDA-R (Dalmau et al., 2007), GlyR (Hutchinson et al., 2008), AMPA-R (Lai et al., 2009), $GABA_B$-R (Lancaster et al., 2010), mGluR5 (Lancaster et al., 2011) and $GABA_A$-R (Petit-Pedrol et al., 2014), more general receptors including DR2 (Dale et al., 2012) and DNER (de Graaff et al., 2012), ion channel (subunits) such as P/Q type VGCC (Mason, 1997) and DPPX (Piepgras et al., 2015), cell-adhesion proteins like IgLON5 (Sabater et al., 2014) and neurexin-3α (Gresa-Arribas et al., 2016), and the initially collectively grouped proteins, targeted by so-called anti-VGKC autoAbs (see chapter A.3.1), LGI1 (Sarosh R Irani et al., 2010; M. Lai et al., 2010), CASPR2 (Irani et al., 2010; Lancaster et al., 2011), contactin-2 (Sarosh R Irani et al., 2010) and Kv1 (Irani et al., 2010; Kleopa et al., 2006) **(Table 2)**.

In contrast with autoAbs directed against intracellular antigens, the association with a tumor is much less frequent but also depends on the specific antigen **(Table 2)**. The autoAbs of this category seem to play a direct pathogenic role in the disease, which is supported by the clinical improvement of patients after immunomodulatory treatment. Moreover, patients presenting with autoAbs against cell surface antigens share a core symptomatology, but certain symptoms are more frequently associated with a specific autoAb **(Table 2)**. This points out that the function of the targeted antigen is important in generating the clinical presentation (Dalmau et al., 2017).

Antigen	Clinical features	Associated tumors
AMPAR[106]	Limbic encephalitis; may occur with pure psychiatric manifestations	~70% (lung, breast, thymoma)
CASPR2[91]	Encephalitis, Morvan's syndrome, neuromyotonia	~0–40% (thymoma)
DPPX[108]	Encephalitis with CNS hyperexcitability: confusion, psychiatric manifestations, tremor, myoclonus, nystagmus, hyperekplexia, PERM-like symptoms, ataxia	Rare B cell neoplasms reported
$GABA_AR$[109]	Refractory seizures, status epilepticus, or epilepsia partialis continua. Low-titer antibody: stiff person syndrome, opsoclonus	Infrequent
$GABA_BR$[110]	Limbic encephalitis, prominent seizures, status epilepticus	~50% (lung, neuroendocrine)
GlyαR[111]	Wide clinical spectrum: stiff person syndrome, PERM, limbic encephalitis, cerebellar degeneration, or optic neuritis	Infrequent
IgLON5[112,113]	Abnormal sleep movements and behaviors, obstructive sleep apnea, stridor, dysarthria, dysphagia, ataxia, chorea	None reported
LGI-1[91]	Limbic encephalitis, faciobrachial dystonic seizures, REM sleep behavior disorder, myoclonus ~60% with hyponatremia	<~10% (small cell lung cancer, thymoma)
mGluR1[114,115]	Cerebellar degeneration, very few cases	Hodgkin's lymphoma; may occur without tumor
mGluR5[116]	Ophelia syndrome: limbic encephalitis, myoclonus; very few cases	Hodgkin's lymphoma; may occur without tumor
Neurexin-3α[118]	Encephalopathy/encephalitis, seizures	None
NMDAR[33] (GluN1)	NMDAR encephalitis: progression through psychiatric manifestations, insomnia, reduced verbal output, seizures, amnesia, movement disorders, catatonia, hypoventilation, autonomic instability, coma	Age-dependent: ~10–45%, most often ovarian teratomas, rarely carcinomas, rare in children
PCA-Tr[119] (anti-DNER)	Cerebellar degeneration, 1/28 patients with possible limbic encephalitis	~90% (Hodgkin's lymphoma)
VGCC[120] (P/Q, N-type)	P/Q and N: LEMS P/Q: cerebellar degeneration, seizures N: variable; includes encephalopathy, seizures	LEMS: ~50% (small-cell lung cancer)

Table 2. Cell surface antigens *(adapted from Bradshaw et al., 2018)*. List of known cell surface antigens targeted by autoantibodies, clinical features of the autoimmune disease and possibility of tumor association.

2.2 ORIGIN OF AUTOANTIBODIES IN AUTOIMMUNE LIMBIC ENCEPHALITIS

Although characterization of specific autoAbs' targets in AILE has known substantial improvement the last decade, the origin and thus the cause of a sudden presence of autoAbs in patients with AILE remains a matter of debate. The most studied hypotheses will here be discussed.

2.2.1 INFECTION BY MICROORGANISMS

Two main hypotheses that could explain the presence of autoAbs in AILE rely on the assumption of previous exposure to infectious triggers. The infectious agents could be fungi, bacteria, viruses or other parasites, but most data currently come from bacteria and viruses. The first hypothesis is the "autoimmune molecular mimicry hypothesis" where viral or bacterial surface proteins molecularly resemble self-proteins, causing development of autoAbs after infection with the bacterium or virus (Platt et al., 2017). This is the case for *Campilobacter jejuni* infections, where infection with a specific bacterial strain is suspected to cause Guillain-Barré syndrome (GBS), an autoimmune-mediated neuromuscular disorder, and atypical GBS-related diseases such as Miller Fisher syndrome and Bickerstaff brainstem encephalitis (Al-din et al., 1982; Hadden et al., 2001; Sauteur et al., 2015). These diseases implicate autoAbs raised against peripheral and central neuronal gangliosides, which share epitopes with the lipo-oligosaccharides on the bacterial surface (Ang et al., 2002; Koga et al., 2005; Platt et al., 2017). In the same way, infections with Group A *Streptococcus* can cause Sydenham's chorea, an autoimmune neurological disease, due to molecular mimicry between the bacterial surface and brain neuronal gangliosides (Kirvan et al., 2003; Krisher & Cunningham, 1985). In systemic lupus erythematosus, autoAbs that cross-react with the viral Epstein-Barr nuclear antigen-1 and human Ro-protein target the central nervous system (CNS) and are found frequently early in the disease (Diamond et al., 2013; Platt et al., 2017).

Intriguingly, in a retrospective study, Prüss et al. (2012) showed presence of anti-N-methyl-D-aspartate receptor (NMDA-R) autoAbs in 30% of patients admitted with herpes simplex encephalitis, which is caused by infection with herpes simplex virus-1 (HSV-1). The autoAbs were present at hospital admission or developed shortly after (Prüss et al., 2012). The link between HSV-1 and anti-NMDA-R autoAbs has been extensively studied, but up to date no similar epitope between the virus and the NMDA-R has been found, ruling out the molecular mimicry hypothesis in this case. Moreover, anti-NMDA-R autoAbs have been detected after infection with other herpesviruses than HSV-1, such as Epstein-Barr virus, varicella zoster virus and human herpesvirus 6 (Hou et al., 2019; Linnoila et al., 2016; Solís et al., 2016). In addition, in patients infected with these viruses, autoAbs other than anti-NMDA-R autoAbs, have been found (Armangue et al., 2014; Linnoila et al., 2016). This suggests a post-infectious immunological mechanism which is not specific for a precise viral antigen. These observations

lead to a second hypothesis, which supposes that a viral trigger could create a pro-inflammatory environment, causing neuronal damage and subsequent self-antigen exposure. In addition to this, a recent study showed that exposure to different flaviviruses causes an upregulation in expression of immune-related genes (Clarke et al., 2014). Altogether, these changes may lie at the basis of CNS immune dysregulation, rendering self-antigens harmful (Clarke et al., 2014; Venkatesan & Benavides, 2015).

2.2.2 TUMORS

The association of autoAbs with the presence of a tumor is more frequent in cases of AILE with autoAbs directed against intracellular antigens, although tumors can also occur in cases of autoAbs directed against neuronal surface proteins. These pathologies are classified as paraneoplastic syndromes of the CNS. The frequency and the type of the tumor are dependent on the syndrome and the autoAb present. For example, in NMDA-R AIE 40% of patients has an underlying neoplasm, with 93% of this group being female with almost exclusively ovarian teratoma (94%) (Titulaer et al., 2013), while in leucine-rich glioma-activated (LGI1) AILE only 11% of the cases presents with an underlying tumor (Lai et al., 2010). Two possible mechanisms for the development of autoAbs in presence of a tumor have been proposed. First, tumor cells can ectopically express neuronal antigens on the surface which are normally present in brain nervous tissue. This causes the immune system to misdirect an immunological response against neuronal self-antigens (Dalmau et al., 2017). Secondly, autoAbs can be raised against tumoral intracellular proteins, which have been released by apoptotic tumor cells. In both cases however, the precise mechanism behind the breaking of self-tolerance remains unknown (Dalmau et al., 2017; Diamond et al., 2013). Interestingly, ovarian teratomas for example always contain neuronal tissue, expressing the NMDA-R, but presence of this type of teratomas does not always induce anti-NMDA-R autoAb production (Mangler et al., 2013; Tabata et al., 2014). This suggests tumor specific characteristics in NMDA-R AIE.

2.2.3 GENETIC PREDISPOSITION

Another less explored explanation for presence of autoAbs in AILE is a genetic predisposition. Currently, only a few studies have been reported, the majority of them having very small

samples sizes. All studies have focused on the human leucocyte antigen (HLA) gene complex, which encodes proteins responsible for regulating the human immune system.

A possible genetic susceptibility has been proposed for anti-IgLON5 autoAbs, where six patients all had a very unusual HLA haplotype in common (Gelpi et al., 2016) and for anti-LGI1 autoAbs, where a strong association was evidenced between two HLA alleles and non-tumorous anti-LGI1 AILE (van Sonderen et al., 2017). In a recent study with 61 Chinese patients presenting with anti-NMDA-R AIE, a significant association was found with the HLA DRB1*16:02 allele (Shu et al., 2019). A larger genome-wide association study on the German population demonstrated a significant association of anti-LGI1 AILE and several single-nucleotide polymorphisms (SNPs) in the HLA region, but no association with anti-NMDA-R encephalitis was detected (Mueller et al., 2018).

It may be clear that studies investigating a possible genetic predisposition remain sparse, given the rarity of the disease, the need for a large cohort both for patient and control groups, and the time-consuming process of genetical analysis. Moreover, HLA alleles are highly polymorphic and show heterogenicity between different ethnic groups, making generalized conclusions regarding the disease difficult (Dean & Dresbach, 2006; Parham, 1988).

2.3 PRODUCTION SITE OF AUTOANTIBODIES: CROSSING THE BLOOD BRAIN BARRIER

Even though presence of autoAbs in the CSF in AILE is well documented, their production site, central or peripheral, is still a matter of debate. A first hypothesis states that autoAbs are produced intrathecally by activated plasmocytes, thus circumventing the need of passing through the BBB. Although extensively studied, no clear evidence for this possibility has been found yet. One study though showed a clear increase of plasmocytes in meninges and brain parenchyma in patients with anti-NMDA-R AIE (Martinez-Hernandez et al., 2011).

The second hypothesis presumes the production of autoAbs to take place outside the brain. This hypothesis is strongly favored in cases of peripheral tumor presence, but even in absence of a tumor peripheral autoAb production is estimated the most plausible. However, in order to reach the CNS, the peripheral produced autoAbs have to cross the blood-brain barrier (BBB). This is a highly specialized structure of endothelial cells, pericytes and astrocytes, organized in a tight manner to hinder passage of cells, pathogens and blood proteins into the

brain parenchyma. Therefore, breaching of the BBB is necessary for autoAbs to enter the CNS (Diamond et al., 2009).

A first hypothesis for breaching the BBB is endothelial activation **(Figure 2A)**. Endothelial cells ensure anchoring between neighboring cells by tight junctions. Rupture of these tight junctions allows for paracellular transport of autoAbs in the brain. On the other hand, modulating the permeability of endothelial cells can alter endocytosis capacity and thus promote transcellular transport. Different possibilities of endothelial activation have been proposed. Bacterial derived substances, present under pathological conditions, such as lipopolysaccharides (LPS) bind to endothelial Toll-like receptor 4 expressed on the BBB and alter its permeability (Diamond et al., 2009). In the same way, circulating cytokines can bind to endothelial cytokine receptors, modulating the BBB permeability (Banks, 2005). This is also possible for local cytokines, inducing a local immune response via microglial activation. Moreover, expression of the autoAb specific antigen on the endothelium causes autoAb binding, altering barrier integrity (Diamond et al., 2009). Finally, physical conditions, such as stress and trauma, and molecules from foreign sources, such as nicotine and cocaine, enhance adrenaline secretion, allowing its binding with the endothelial adrenergic receptor, changing barrier properties (Kuang et al., 2004).

The BBB can also be breached without endothelial activation **(Figure 2B)**. Kuhlmann et al. (2009) suggested endothelial expression of the NMDA-R, implying a self-enhancing mechanism for anti-NMDA-R autoAbs, facilitating their own CNS uptake upon binding with their antigenic target. Neuronal axons that protrude towards the lumen of BBB capillaries can transport autoAbs retrogradely into the brain parenchyma (Diamond et al., 2009). Furthermore, autoAbs can be carried by leukocytes during their transendothelial migration and released once they entered the brain (Diamond et al., 2009; Engelhardt & Wolburg, 2004).

A last possible way of autoAb entry into the brain is by the neonatal Fc receptor (FcRn) and possibly by other FcRs **(Figure 2C)**. Their function is to expulse Abs that have reached the brain (Siegelman et al., 1987; Zhang & Pardridge, 2001). Alterations of these receptors may cause autoAb entry into the brain (Diamond et al., 2009).

Importantly, molecules synthesized in the brain or cytokines that have crossed the BBB can cause the so-called 'inside out mechanism', in which these internal brain molecules activate cells secreting barrier modulating substances that result in increased BBB permeability (Diamond et al., 2009). Since the sensory circumventricular organs lack tight barrier

properties, they allow for a more easily initial passage of molecules through the BBB at this site, and may thereby facilitate the cascade of the 'inside out mechanism' (Roth et al., 2004).

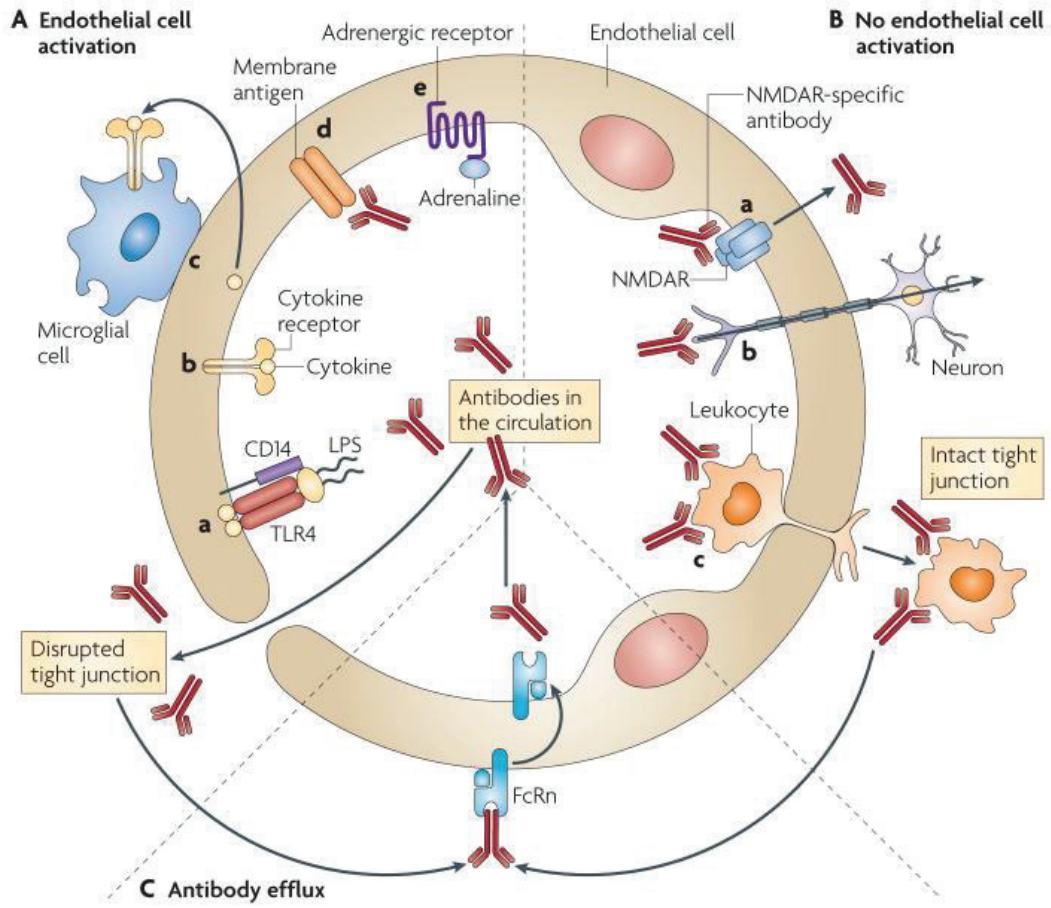

Figure 2. Possible mechanisms for autoAbs in the circulation to cross the BBB *(Diamond et al., 2009).* **A)** Mechanisms causing endothelial cell activation. a) Bacterial substances such as LPS bind to Toll-like receptor 4 (TLR4), b) circulating cytokines bind to endothelial cytokine receptors, c) local cytokines activate microglia, d) binding of the autoAb to its endothelial receptor, e) binding of adrenaline with the endothelial adrenergic receptor. **B)** Passage mechanisms without endothelial cell activation. a) Endothelial expression of the NMDA-R facilitates passage of anti-NMDA-R autoAbs, b) retrograde axonal transport via neurites protruding into the capillary lumen, c) uptake by transendothelial migrating leucocytes. **C)** Efflux of autoAbs into the circulation via the neonatal Fc receptor (FcRn).

3. ANTI-CASPR2 AUTOIMMUNE LIMBIC ENCEPHALITIS

3.1 DISCOVERY OF ANTI-CASPR2 AUTOANTIBODIES

For long time autoAbs against contactin-associated protein-like 2 (CASPR2), leucine-rich glioma inactivated 1 (LGI1) and transient axonal glycoprotein 1 (TAG-1) were not distinguished

from autoAbs against VGKCs due to, at that timepoint unnoticed, methodological shortcomings. All aforementioned autoAbs were thus wrongly collectively classified as anti-VGKC autoAbs. The origin for this wrong classification sprouts in the early '90s.

In 1994, Browne et al. provided strong evidence for the association between point mutations in the *KCNA1* gen, coding for Shaker-related Kv channels, and episodic ataxia and myokymia. At the same time, increasing data pointed towards a possible autoimmune-mediated mechanism in the etiology of neuromyotonia (NMT), where myokymia is a clinical feature (Halbach et al., 1987; Newsom-Davis & Mills, 1993; Sinha et al., 1991). This prompted Shillito et al. (1995) to screen serum from patients with NMT for anti-VGKC autoAbs. Detection of these autoAbs initially took place by radioimmunoprecipitation, an approach in which VGKCs from human cortical lysates were radiolabeled with ^{125}I-α-dendrotoxin (Hart et al., 1997; Shillito et al., 1995). Patient serum was then added to the labeled extract and immunoprecipitated using anti-human antibodies. The possibly co-immunoprecipitated VGKCs were detected by analyzing radiation with a gamma counter. Using this approach, Shillito et al. (1995) showed the presence of anti-VGKC autoAbs in patients with NMT and provided evidence for a possible causal link between these autoAbs and peripheral nerve conduction alterations. Causality was later confirmed by Hart et al. (1997), who showed target specificity of anti-VGKC autoAbs in NMT. Using the same radioimmunoprecipitation method, anti-VGKC autoAbs were also found in patients with LE (Buckley et al., 2001), Morvan syndrome (MoS) (Liguori et al., 2001) and faciobrachial dystonic seizures (Irani et al., 2008). In a study with 17 patients presenting with NMT, MoS or LE 11 sera labeled the juxtaparanodal region of the node of Ranvier (see chapter B.2.2.1) colocalizing with Kv1.1 and Kv1.2 channels (Kleopa et al., 2006). All patients' sera were capable of recognizing different Kv1 subunits. However, except for the association between LE and a preferential binding of autoAbs with Kv1.1 subunits, no straightforward link between the targeted Kv subunit and the different clinical presentations obviously stood out (Kleopa et al., 2006). Other studies aiming to investigate the specificity for Kv1 channels of patients with anti-VGKC autoAbs were in the majority of cases not able to demonstrate Kv1 staining by patients' sera (Irani et al., 2010; Lai et al., 2010). This led to the discovery of proteins other than Kv channels targeted by anti-VGKC autoAbs, namely TAG-1, LGI1 and CASPR2 (Irani et al., 2010; Lai et al., 2010). As previously mentioned, the initial inability to distinguish these proteins from VGKCs lays in the detection method. When preparing cortical lysates for radioimmunoprecipitation, digitonin

was used as detergent to solubilize proteins. However, this is a mild detergent, allowing proteins strongly bound to Kv channels to remain attached and consequently to be recognized by autoAbs different from anti-VGKC autoAbs. Indeed, it was later evidenced that the juxtaparanodal staining observed with serum from LE patients did not correspond to Kv1 channels, but to CASPR2, presenting the same distribution pattern as Kv1 channels in this area (Lancaster et al., 2011; Poliak et al., 1999).

The discovery of VGKC associated proteins and autoAbs also led to a better understanding of the clinical presentation of patients with anti-VGKC autoAbs, which initially consisted of a large variety of closely linked symptoms. Specific symptoms could now be more clearly restricted to the precise autoAb present. Furthermore, the direct pathogenic effect of anti-LGI1 and anti-CASPR2 autoAbs in AILE was strongly suggested in a study assessing the effects of immunoadsorption therapy, a selective apheresis method in which antibodies are removed from plasma without the necessity for plasma exchange (Onugoren et al., 2016; Paroder-Belenitsky & Pham, 2019). The authors hypothesized that removal of serum autoAbs would consequently cause a decrease in CSF autoAbs, and thus ameliorate CNS symptoms (Onugoren et al., 2016). Indeed, autoAbs in both serum and CSF of patients with anti-LGI1 or anti-CASPR2 AILE were decreased by immunoadsorption, which was accompanied with a rapid clinical improvement, supporting a direct role of these autoAbs in the disease (Onugoren et al., 2016). Nevertheless, the relative recent discovery of anti-CASPR2 AILE together with its low prevalence, makes large cohort studies difficult. They are necessary though for better understanding and thus treatment of the disease. A rapid and clear symptom recognition is essential, since this improves clinical treatment and patients' outcome.

3.2 CLINICAL PRESENTATION

Anti-CASPR2 autoAbs have been found in serum and/or CSF of patients with neuronal peripheral and/or central symptoms (Irani et al., 2010; Lancaster et al., 2011) **(Figure 3)**. A first possible clinical presentation is NMT also known as Isaacs' syndrome. Only peripheral nervous system (PNS) symptoms are present in form of a syndrome of peripheral nerve hyperexcitability, characterized by spontaneous muscular activity, muscle rigidity, muscle cramps, pain, stiffness and myokymia (Isaacs, 1961; Newsom-Davis & Mills, 1993). The second possible presentation is pure AILE with only CNS symptoms. The third possibility is MoS, in

which patients present with a combination of NMT and CNS symptoms, such as insomnia, confusion, hallucinations, agitation and anxiety (Morvan, 1890; Lee et al., 1998). This manuscript will be focused on anti-CASPR2 autoAbs found in pure AILE.

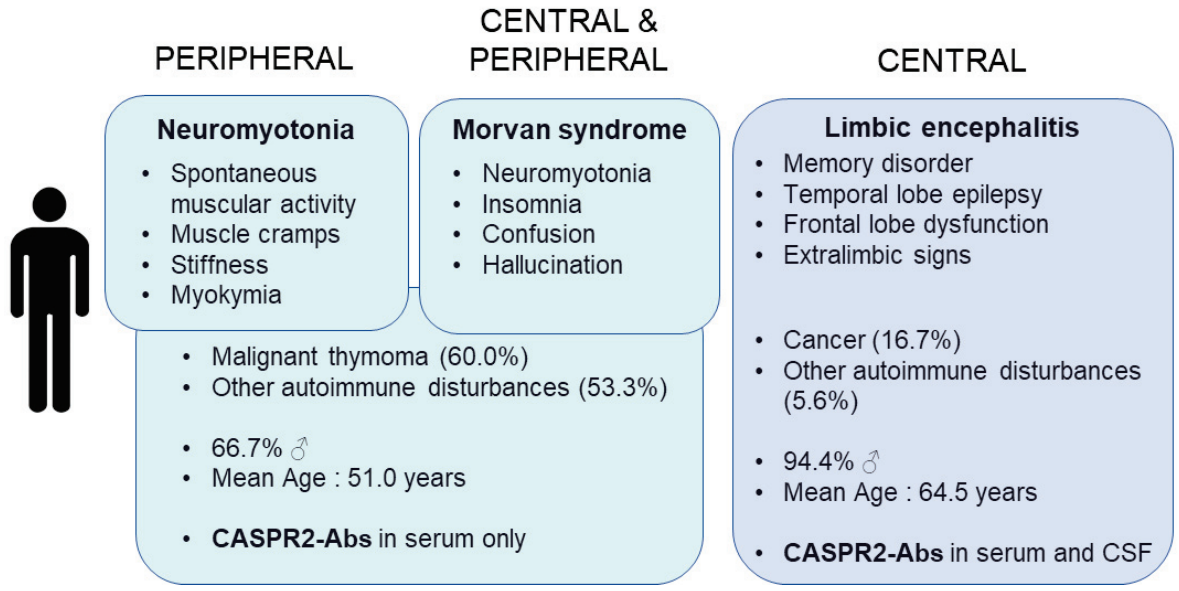

Figure 3. Comparison of anti-CASPR2 autoAb-mediated autoimmune disorders *(adapted from Saint-Martin et al., 2018).* Anti-CASPR2 autoAbs can be found in neuromyotonia, characterized by exclusively peripheral symptoms, Morvan syndrome, characterized by a combination of central and peripheral symptoms, and limbic encephalitis, characterized by exclusively central symptoms. Malignant thymoma and other autoimmune disturbances are less frequently associated with limbic encephalitis. The percentage of males and mean age is higher for limbic encephalitis. Anti-CASPR2 autoAbs are not found in the cerebrospinal fluid (CSF) of patients with neuromyotonia or Morvan syndrome.

In a study of Joubert et al. (2016) the authors retrospectively included patients with anti-CASPR2 autoAbs in the CSF and compared them with patients diagnosed with NMT or MoS and positive for anti-CASPR2 autoAbs in the serum. The group with autoAbs in the CSF were also tested for anti-CASPR2 autoAbs in the serum and all were found positive. All patients of this group presented with AILE. Interestingly, in the NMT/MoS group no CSF autoAbs were detected. This was the first study to provide strong evidence that anti-CASPR2 autoAbs in the CSF give rise to the clinical entity of non-paraneoplastic pure AILE, while when present exclusively in the periphery are associated with NMT or MoS (Joubert et al., 2016) **(Figure 3)**. Patients with AILE positive for anti-CASPR2 autoAbs are predominantly men (94,4%) with an age ranging from 53 to 75 (median age 64.5) (Joubert et al., 2016) **(Figure 3)**. The main symptoms leading to hospital admission are partial temporal seizures (72.2%) and progressively evolved memory disorders (27.8%) (Joubert et al., 2016). Other symptoms

develop over a time course ranging from 1 day until 18 months and include seizures, temporal lobe epilepsy, anterograde and episodic memory disorders, frontal lobe dysfunction and psychiatric disorders such as depression and persecutory thoughts, which are a reflection of limbic and hippocampal involvement (Joubert et al., 2016). The cohort of 18 patients examined by Joubert et al. (2016) did not show signs of confusion or behavioral disorders, typical symptoms in other types of AILE. Other, more seldom extra-limbic symptoms found in anti-CASPR2 AILE are (paroxysmal) cerebellar ataxia, sleep disorders, NMT, neuropathic pain, movement disorders and weight loss (Bien et al., 2017; Joubert et al., 2017, 2016; van Sonderen et al., 2016).

In patients with anti-CASPR2 NMT or MoS cancer association is frequent whereas this is rare in anti-CASPR2 AILE (Joubert et al., 2016; van Sonderen et al., 2016). In the study of Joubert et al. (2016) 60.0% of patients with NMT or MoS presented with malignant thymoma, whereas only 16.7% of patient with AILE had a previous or concomitant history of cancer, importantly thymoma was absent **(Figure 3)**. In the same way, other auto-immune comorbidities were more frequently reported in NMT or MoS (53.3%) than in AILE (5.6%) (Joubert et al., 2016) **(Figure 3)**.

3.3 DIAGNOSIS AND DETECTION OF ANTI-CASPR2 AUTOANTIBODIES

For each type of AI(L)E a rapid and clear diagnosis is necessary, since this allows for adjusted treatment and consequently improves patient's outcome. Diagnosis is based on the clinical presentation of the patient, together with paraclinical examinations such as MRI, PET and EEG. Prompt tumor screening is important since tumor presence influences the chosen treatment and outcome. The differential diagnosis between other pathologies sharing similarities with AI(L)E is crucial, since treatment differs and is directly linked with a favorable outcome for the patient. On the other hand, the chosen treatment also depends on the specific autoAb present. So specific antibody detection is extremely important in confirming diagnosis but also decides the required medication. Considering that autoAbs are not necessarily simultaneously present in serum and CSF, it is strongly recommended to screen for presence of autoAbs in both liquids. It must be kept in mind that the detected autoAb titers have limited clinical importance for several reasons. Detected titers are variable between methods, laboratories and disease progress, making them not very conclusive regarding the patient's disease status,

especially when comparing between different hospitals (Lancaster, 2016). They are also not very informative with respect to disease severity and phase, i.e. high titers do not necessarily mean a severe clinical presentation or advanced disease status and vice versa (Gresa-Arribas et al., 2014; Lancaster, 2016).

Multiple autoAb screening methods exist and the choice is mainly laboratory dependent. It must be mentioned that these tests are not unambiguous and diagnosis must not only depend on positive autoAb testing but also on clinical presentation. For example, it has been shown that non-neuronal antibodies against thyroperoxidase are present in 10 to 12% of the normal population (Feldt-Rasmussen, 1996). Low serum titers for anti-VGKC autoAbs, in absence of anti-LGI1 or anti-CASPR2 autoAbs, without clinical manifestations have also been reported (Paterson et al., 2014).

Treatment can alter autoAb titers, so it is preferable to perform sampling before treatment installation. In our *Centre de référence des syndromes neurologiques paranéoplasiques et encéphalites auto-immunes*, samples from patients with suspicion of AILE are first screened by immunohistochemistry on sagittal rat brain slices. Since each autoAb is directed against a specific antigen, which shows a precise localization in the brain, this technique allows for a first global impression of the characteristic autoAb staining pattern. The downside is that the recognized epitope must share sufficient homology between rat and human. For CASPR2 this homology amounts to 94%.

A positive first screening gives an idea of the possible autoAb present, based on the staining pattern. This allows for further identification of the specific autoAb by cell-based binding assay (CBA), a technique in which a panel of cell lines expressing different possible antigens are incubated with the patient's serum or CSF. The targeted antigen shows a positive immunofluorescent reaction after incubation with fluorescent anti-human secondary antibodies. Our Center uses HEK cells transfected with CASPR2 allowing surface CASPR2 expression, although other cell lines can be used as well. Other possible antigen detection methods are ELISA techniques or western blotting. The latter is less used since conformational epitopes of the antigen are lost due to the required denaturation step in western blotting protocols.

3.4 TREATMENT AND OUTCOME

Proper treatment of patients with AI(L)E is challenging, given the rarity of the disease and consequently limited clinical and evidence-based treatment. Therefore, chosen treatment is mainly depending on the patient's status and clinical judgement (Shin et al., 2018). Used medication ranges from broad immunosuppressors to molecules targeting specific steps in the disease.

In the rare cases of anti-CASPR2 AILE in association with a tumor, tumor resection is required and chemo or immunotherapy applied if necessary (van Sonderen et al., 2016). First line treatment consists in intravenous immunoglobulins (IgGs), plasmapheresis and/or corticosteroids (Lancaster, 2016). Corticosteroids inhibit the inflammatory process by binding to the intracellular glucocorticoid receptor and inhibiting transcription of proinflammatory genes. They are not very specific and show many systemic side-effects. Intravenous IgGs is a pooled IgG extract obtained from plasma of over a thousand donors (Shin et al., 2018). In high doses intravenous IgG therapy has anti-inflammatory and immunomodulatory effects. Removal of autoAbs and other possible pathogens from the patient's plasma by plasmapheresis is another option and is generally used when foregoing treatments are less tolerated (Shin et al., 2018). Plasmapheresis has the capacity of altering the immune system by changing B and T cell numbers and activation, and lymphocyte proliferation and function (Reeves & Winters, 2014).

If first line therapy does not provide the desired effect, second line therapy can be installed to improve the patient's outcome and decrease relapses (Shin et al., 2018). Furthermore, in some patients two or three concomitant treatments can be required (Joubert et al., 2016; van Sonderen et al., 2016). In anti-CASPR2 AILE rituximab and cyclophosphamide are mostly used as a second line treatment. Rituximab is a monoclonal antibody that targets CD20 on the surface of B cells and subsequently causes B cell and short-lived plasma cell depletion. Cyclophosphamide is an alkylating immunosuppressant which inhibits B and T cell proliferation. Another less administered medication in anti-CASPR2 AILE is mycophenolate mofetil. It is considered useful when second-line therapy does not ameliorate the patient and has a selective antiproliferative effect on lymphocytes (Shin et al., 2018).

Even though adequate therapy in most cases assures a positive recovery of the patient, relapses are possible. They mainly occur between the first seven months and two years after

initial admission and predominantly include increase in seizure activity and occur more often in untreated patients (Joubert et al., 2016; van Sonderen et al., 2016). Full recovery is often observed after immunomodulatory treatment, whereas some of the patients recover spontaneously (Joubert et al., 2016). Other patients recover partially, but rarely display severely life altering symptoms. Death is very seldom and is most likely not immediately linked to the foregoing anti-CASPR2 AILE.

3.5 PROPERTIES OF ANTI-CASPR2 AUTOANTIBODIES

3.5.1 SERUM VERSUS CSF, IGG1 VERSUS IGG4

Antibodies or IgGs can be divided into different subclasses ranging from IgG1 to IgG4, based on their molecular composition, dictating their effector functions (Vidarsson et al., 2014). The relative serum abundance is as follows in the normal population IgG1 > IgG2 > IgG3 = IgG4, with IgG1 representing 60% and IgG4 around 4% of total serum IgGs (Aalberse et al., 2009; Vidarsson et al., 2014).

In the previously mentioned study of Joubert et al. (2016) (see chapter A.3.2), where patients with NMT/MoS only displayed anti-CASPR2 autoAbs in the serum and patients with AILE presented with autoAbs in both serum and CSF, the authors further analyzed the characteristics of the present anti-CASPR2 autoAbs in both groups **(Table 3)**. IgG1 was the predominant IgG subclass in the serum of the NMT/MoS group and was present in all sera and 59% of CSF from patients with AILE (Joubert et al., 2016). IgG1 Abs are capable of aggregating the targeted antigen, causing its internalization (Vidarsson et al., 2014). They also have strong affinity for the Fcγ receptor and can efficiently activate complement, inducing complement-mediated cell-toxicity (Vidarsson et al., 2014). Interestingly, all patients with anti-CASPR2 AILE who showed signs of hippocampal atrophy presented with IgG1 autoAbs in the CSF, supporting the involvement of complement-mediated neuronal cell death (Joubert et al., 2016). This idea is supported by another study, where complement deposits and neuronal degeneration were found in a hippocampal surgical resection of a patient with anti-CASPR2 AILE (Körtvelyessy et al., 2015). Moreover, these observations suggest a direct pathogenic role of the autoAb in the pathology (Bien et al., 2017; Joubert et al., 2016).

On the other hand, IgG4 Abs were present in the serum and CSF of all patients with AILE, compared with only 41% in the NMT/MoS group (Joubert et al., 2016) **(Table 3)**. The high abundance of this IgG subclass in patients with AILE, compared with very low titers in the healthy population, is indicative for a pathological mechanism. Importantly, the IgG4 subclass can exchange fragment antigen-binding (Fab) regions, rendering them epitope bispecific (Aalberse et al., 2009; van der Neut Kolfschoten et al., 2007). This makes them functionally monovalent, not being able to cross-link antigens and cause their internalization (Aalberse & Schuurman, 2002). Moreover, IgG4 has low affinity for the Fcγ receptor and does not cause complement activation and cytotoxicity (Vidarsson et al., 2014). Thus the pathological effect of IgG4 autoAbs must take place via other mechanisms such as blocking interactions of the targeted antigen with other molecules (Davies & Sutton, 2015).

	No./Total No. (%)		
Characteristic	Patients With Anti-CASPR2 Antibodies in the CSF	Patients With NMT or MoS	*P* Value
No. of patients	18	15	
Male	17/18 (94.4)	9/15 (60.0)	.03
Age, y, median (range)	64.5 (53-75)	51 (1 mo-75 y)	.002
Serum titers, median (range)	1/15 360 (1/10 240-1/81 920)	1/800 (1/20-1/5120)	<.001
CSF titers, median (range)	1/1280 (1/80-1/10 240)	0	<.001
Detected IgG4 anti-CASPR2 antibodies			
Serum	11/12 (91.7)	5/12 (41.7)	.03
CSF	17/17 (100)	0	<.001
Detected IgG1 anti-CASPR2 antibodies			
Serum	12/12 (100)	10/12 (83.3)	.48
CSF	10/17 (58.8)	0	<.005
Recognition of discoidin and laminin G1	18/18 (100)	11/11 (100)	>.99
Additional epitopes	10/18 (55.6)	8/11 (72.7)	.45
Malignant thymoma	0	9/15 (60.0)	.001
Other cancers	3/18 (16.7)	0	.23
Other autoimmune disturbances	1/18 (5.6)	8/15 (53.3)	.004

Table 3. Baseline characteristics and immunological findings of patients with anti-CASPR2 autoAbs in the CSF compared with patients with anti-CASPR2 autoAbs in the serum *(Joubert et al., 2016)*. Patients diagnosed with anti-CASRP2 AILE are compared with patients diagnosed with NMT or MoS positive for anti-CASPR2 autoAbs. Patients with anti-CASPR2 AILE present with anti-CASPR2 autoAbs in the CSF and serum whereas patients with NMT or MoS present with anti-CASPR2 autoAbs only in the serum. Basic characteristics and immunological findings are represented for both groups. Age differences were compared by Mann-Whitney U test. All other represented results were compared by Fisher exact test. Statistical significance was set at $p<0.05$ and obtained p-values are represented.

Another important observation in the study of Joubert et al. (2016) is the difference in anti-CASPR2 IgG serum titers: AILE patients had a significantly higher serum IgG endpoint dilution compared with the NMT/MoS group (median 1:15360 and 1:800 respectively) **(Table 3)**. This can be related to the presence of IgG4 in AILE patients. The IgG4 subclass has strong binding capacities compared with other IgG subclasses (Aalberse & Schuurman, 2002). Low IgG4 concentrations are sufficient to bind the antigen, explaining the high endpoint dilutions in the group of patients with AILE.

Interestingly, in a retrospective study Bien et al. (2017) initially found by multivariate logistic regression that anti-CASPR2 autoAbs serum titers and presence of a so-called 'encephalitic MRI' were good predictors for the diagnosis of anti-CASPR2 AILE. Bien and colleagues then divided patients with anti-CASPR2 autoAbs in the serum, for which they already knew the diagnosis, into three groups: group one with a serum endpoint dilution <1:64, group 2 with a serum endpoint dilution ranging from 1:64 to 1:512 and group 3 with a serum endpoint dilution >1:512. Using the established predictive model, the authors found that group 1 had low probability of anti-CASPR2 AILE (indeed, none of the patients in this group presented with AILE), group 2 had intermediate chance of anti-CASPR2 AILE and group 3 had the highest chance of AILE (Bien et al., 2017). Importantly, in group 3 the presence of encephalitic MRI was not of value for the diagnosis of AILE (i.e. serum autoAbs titers sufficed for diagnosis with the model), and indeed all patients categorized in this group presented with AILE (Bien et al., 2017). Although using a predictive model, these results are in line with the results of Joubert et al. (2016) and reinforce the observation that higher serum endpoint dilutions are found in patients with anti-CASPR2 AILE than in patients with anti-CASPR2 NMT/MoS.

3.5.2 TARGETED EPITOPES

Anti-CASPR2 serum and CSF autoAbs all recognize the N-terminal discoidin-like and laminin G-like domain (see chapter B.1.1) (Joubert et al., 2016; Olsen et al., 2015; Pinatel et al., 2015) **(Figure 4)**. The 30 amino acids linker between both domains is not recognized (Olsen et al., 2015) and up until now the function of these domains is not known. Importantly, patients' autoAbs target multiple epitopes. Most of them are located in the first N-terminal half of the protein and recognition of at least some of these epitopes does not appear to be dependent

of tertiary structure or glycosylation (Olsen et al., 2015). However, more experiments are necessary to confirm this supposition.

As mentioned, all patients with anti-CASPR2 AILE present with autoAbs from the IgG4 subclass, which have the particularity of being capable of bispecific epitope recognition. Thus, binding to two different neighboring domains, discoidin-like and laminin G-like, by anti-CASPR2 autoAbs can occur either due to polyclonality, with one antibody binding to one domain, or due to IgG4 bispecificity, with each Fab fragment of one autoAb binding a different domain **(Figure 4)**.

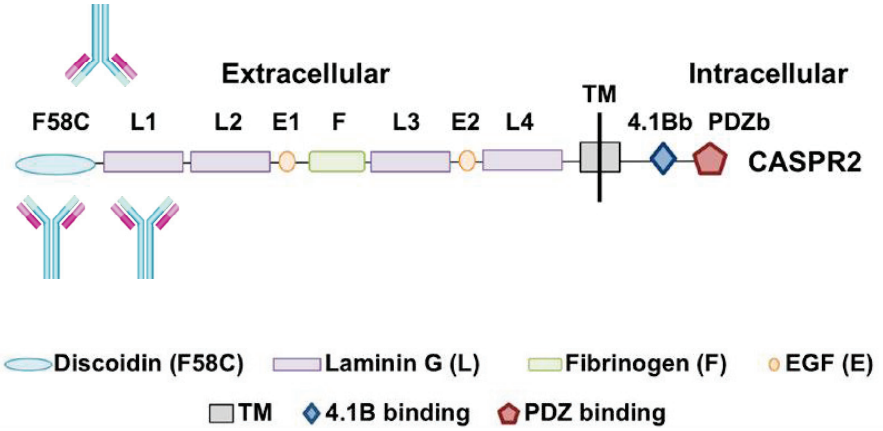

Figure 4. Secondary structure of CASPR2 and epitopes targeted by autoAbs *(adapted from Saint-Martin et al., 2018)*. CASPR2 consists in a long extracellular and short intracellular domain. Anti-CASPR2 autoAbs all recognize the N-terminal discoidin-like and laminin G-like domains. Binding of the two neighboring domains can occur due to autoAbs IgG4 bispecificity (upper presentation) or due to polyclonality (lower presentation).

CHAPTER B. CONTACTINE-ASSOCIATED PROTEIN LIKE 2 (CASPR2)

1. STRUCTURE OF CASPR2

CASPR2 was first discovered by Poliak et al. (1999) as a member of the neurexin superfamily. Proteins belonging to this superfamily are transmembrane proteins, mediating neuronal anchoring. They are mainly located at the synapse and ensure interactions between the pre- and postsynaptic neuron (Ushkaryov et al., 1992). The neurexin superfamily can be divided into the neurexin family (Ushkaryov et al., 1992), the NCP (Neurexin IV, CASPR/Paranodin) family (Bellen et al., 1998) and axotactin (Yuan & Ganetzky, 1999). CASPR2 belongs to the NCP family, which is implicated in neuron-glia interactions (Baumgartner et al., 1996). CASPR2 is the mammalian ortholog of the *Drosophila* Neurexin IV (Poliak et al., 1999).

1.1 SECONDARY STRUCTURE

CASPR2 is encoded by the *CNTNAP2* gene, which is located at the human chromosomal region 7q35-q36.1 and with its 24 exons spanning 2.3 Mbp is one of the largest genes in the human genome (Nakabayashi & Scherer, 2001). The CASPR2 protein contains a sequence of 1331 amino acids, coding for a large transmembrane protein (Poliak et al., 1999). Starting from the N-terminus its secondary structure consists in eight extracellular domains, one transmembrane domain and two intracellular C-terminal motifs **(Figure 5)**. Moving from the N-terminus towards the transmembrane domain (TM), its extracellular part consists of following domains: a discoidin-like or coagulation factor 5/8 type C-like domain (F58C), a first laminin G-like domain (L1), a second laminin G-like domain (L2), a first epidermal growth factor (EGF)-like domain (E1), a fibrinogen-like domain (F), a third laminin G-like domain (L3), a second EGF-like domain (E2) and a last laminin G-like domain (L4) (Poliak et al., 1999) **(Figure 5)**. The transmembrane domain follows and hereafter the short intracellular part is found. It contains a protein-4.1B binding motif (4.1Bb), which binds to the FERM domain of protein 4.1B, connecting CASPR2 to the cytoskeleton (Denisenko-Nehrbass et al., 2003; Poliak et al., 1999) and a C-terminal PSD95/Disc large/Zona occludens-1 (PDZ) binding motif (PDZb), allowing interactions with scaffolding proteins (Horresh et al., 2008; Poliak et al., 1999) **(Figure 5)**.

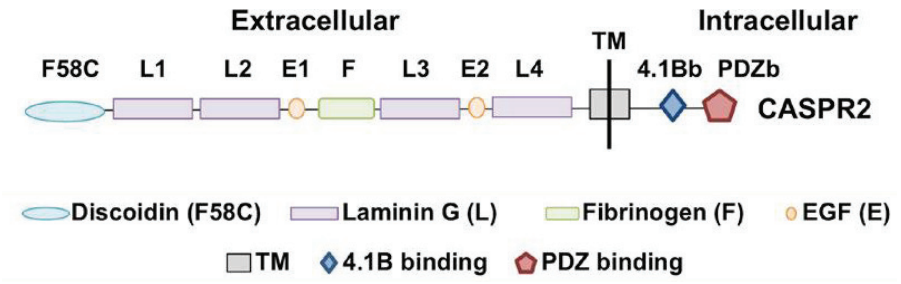

Figure 5. Secondary structure of CASPR2 *(adapted from Saint-Martin et al, 2018)*. CASPR2 shows a linear secondary structure, composed of a long extracellular domain containing the N-terminus, a transmembrane domain (TM) and a short intracellular domain containing the C-terminus.

Interestingly, an isoform of CASPR2, consisting in only its intracellular C-terminal domain, has been discovered in mouse cortical and hippocampal lysates (Chen et al., 2015). This isoform (called isoform 2) is present in similar amounts in WT and KO mice, but at a more than ten-fold lower amount compared with the full length CASPR2 in WT (Chen et al., 2015).

1.2 TERTIARY STRUCTURE

CASPR2 has a complex, F-shaped 3D structure (Rubio-Marrero et al., 2016). Electron microscopy studies pointed out that CASPR2's extracellular tertiary structure consists of three lobes: a major lobe, containing the F58C, L1 and L2 domain, a middle lobe, containing the F and L3 domain, and a small lobe, containing the L4 domain (Lu et al., 2016) **(Figure 6)**. These lobes are highly flexible with respect to each other, thanks to the EGF domains between the lobes (Lu et al., 2016). The high freedom in flexibility allows multiple possible conformations of CASPR2 (Lu et al., 2016; Rubio-Marrero et al., 2016). CASPR2's ectodomain, with dimensions of ~ 145 Å long X ~ 90 Å wide X ~ 50 Å thick, has been proposed to be capable of adapting two main orientations: a vertical and a horizontal position (Lu et al., 2016) **(Figure 6)**. The orientation of CASPR2 could be of importance regarding possible interactions with other proteins and subcellular localization.

With 12 putative N-linked glycosylation sites (Poliak et al., 1999), CASPR2 has also been found to be highly glycosylated (Canali et al., 2018; Falivelli et al., 2012; Lu et al., 2016; Rubio-Marrero et al., 2016). This can largely affect many important factors such as binding properties, tertiary structure and flexibility (Rubio-Marrero et al., 2016).

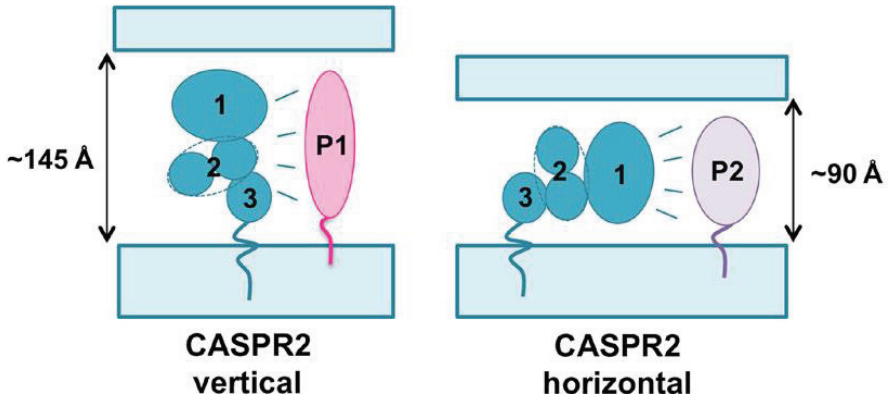

Figure 6. Tertiary structure of CASPR2 *(adapted from Saint-Martin et al., 2018)*. The tertiary structure of CASPR2 consists of three major lobes (1, 2, 3), with the second lobe containing two smaller lobes, which are highly flexible respective to each other. Depending on the orientation of the lobes CASPR2 could adopt a vertical position measuring ~ 145 Å or a horizontal position measuring ~ 90 Å. The proposed orientations of CASPR2 could also influence its interaction with possible partners, represented as P1 for a vertical orientation and P2 for a horizontal orientation.

2. TISSULAR AND CELLULAR EXPRESSION

2.1 TISSUE LEVEL

2.1.1 IN THE BRAIN

In human, CASPR2 mRNA has been found primarily in nervous tissue (spinal cord and brain) and in low quantities in prostate and ovaries (Poliak et al., 1999). In mouse whole brain lysates the CASPR2 protein has been first detected at embryonic day 14 (E14) by western blot (Peñagarikano et al., 2011). Gordon et al. (2016) generated a reporter mouse line in which the first exon of CASPR2 was replaced by tau-LacZ allowing to visualize brain areas expressing CASPR2. Although this study provides valuable information regarding to the expression of CASPR2 in the brain, it must be kept in mind that with this approach the activity of the *Cntnap2* promotor is observed and not the actual CASPR2 mRNA or protein. Staining of mouse brain slices started at E18 and pointed out that CASPR2 displays a gradually increasing expression, moving from posterior to anterior, which is completed at adult age (Gordon et al., 2016; Poliak et al., 1999) **(Figure 7)**.

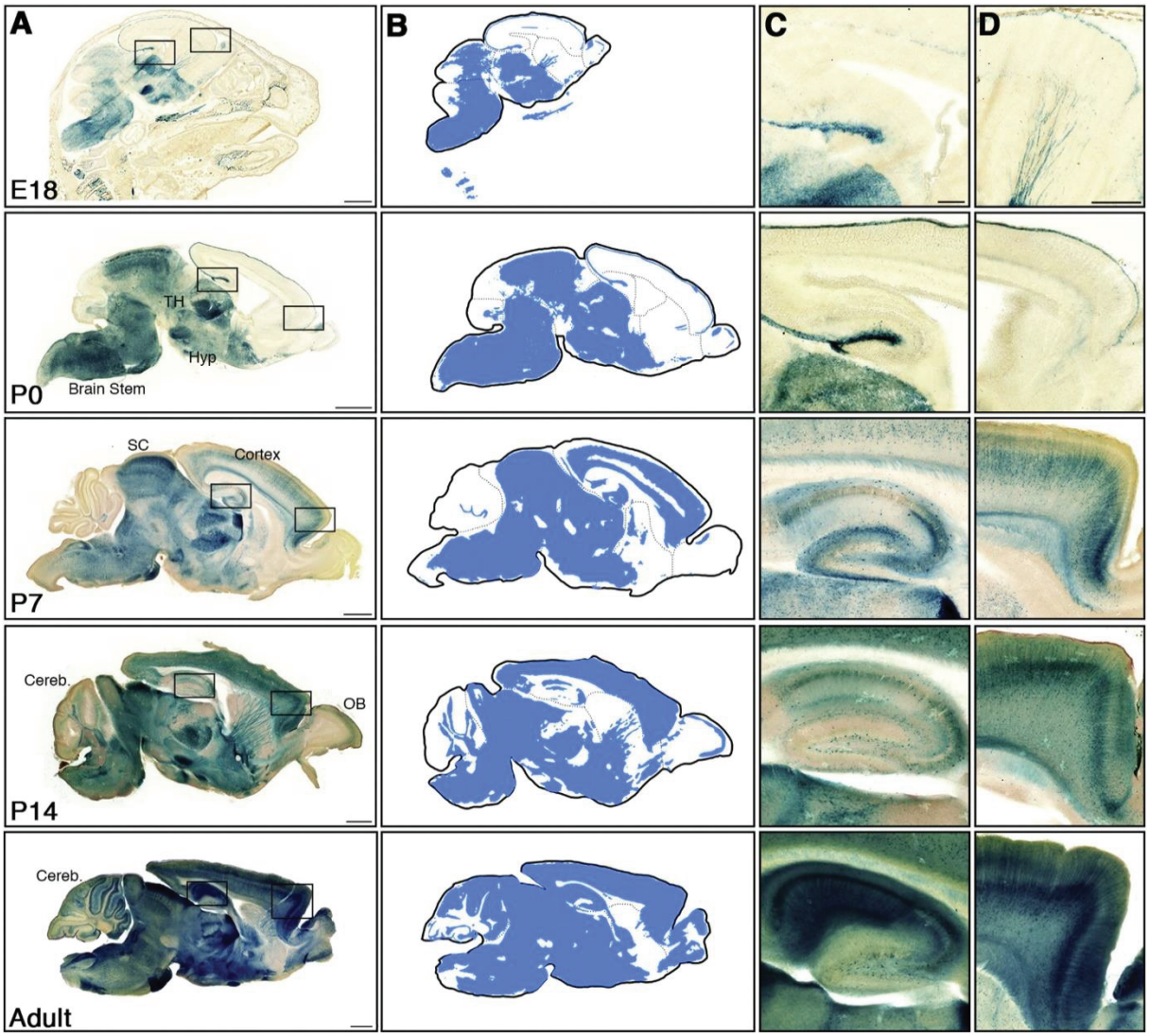

Figure 7. CASPR2 temporal and spatial distribution in the mouse brain *(Gordon et al., 2016)*. A reporter mouse line was created by replacing the first exon of CASPR2 by tau-lacZ, allowing for visualization of CASPR2. **A)** Sagittal brain slices show a gradual posterior to anterior increase in CASPR2 expression starting from embryonic day 18 (E18) into adulthood. **B)** Schematic representation of the results shown in A). **C)** High magnification of the hippocampus corresponding with the black quadrant in A). CASPR2 expression starts in the dentate gyrus and shifts towards higher expression in the CA1-CA3. **D)** High magnification of the cortex corresponding with the black quadrant in A). CASPR2 expression progresses into deeper cortical layers during development.
TH: thalamus, Hyp: hypothalamus, SC: superior colliculus, Cereb: cerebellum, OB: olfactory bulb. Scale bars represent 1 mm (A), 200 µm (C) and 500 µm (D).

At E18, CASPR2 is detected in the hypothalamus, thalamus, brain stem, dentate gyrus and the marginal zone of the cortex. During development, its expression in the dentate gyrus diminishes and shifts towards a higher expression in the CA1, CA2 and CA3 region of the cornu ammonis (CA). In the cortex CASPR2 expression gradually increases, migrating into deeper cortical layers. At postnatal day 0 (P0) its expression is still limited to the marginal zone of the

cortex, while at P7 CASPR2 is detected in many cortical layers, to be fully expressed in all layers at P14. At this stage CASPR2 is also found in the olfactory bulb and in white matter tracts of the cerebellum. In the adult mouse brain, CASPR2 is strongly expressed in the cortex, hippocampus, substantia nigra, interpeduncle nucleus, pontine nucleus, amygdala and mammillary bodies.

In the adult mouse and rat hippocampus CASPR2 staining is restricted to the CA1-CA3 stratum radiatum and stratum oriens (Lancaster et al., 2011) **(Figure 8A)**. The stratum oriens contains cell bodies of inhibitory neurons and basal dendrites of pyramidal excitatory neurons of the CA **(Figure 8B)**. These dendrites receive axonal afferents from other pyramidal cells, septal fibers and commissural fibers from the collateral hippocampus. In the stratum radiatum the apical dendrites of pyramidal neurons receive innervation mainly from axons of the CA3 pyramidal neurons, called Schaffer collateral fibers, interneurons and afferences from the entorhinal cortex. The stratum pyramidale contains the cell bodies of pyramidal neurons and CASPR2 expression is not observed in this hippocampal layer (Lancaster et al., 2011) **(Figure 8)**.

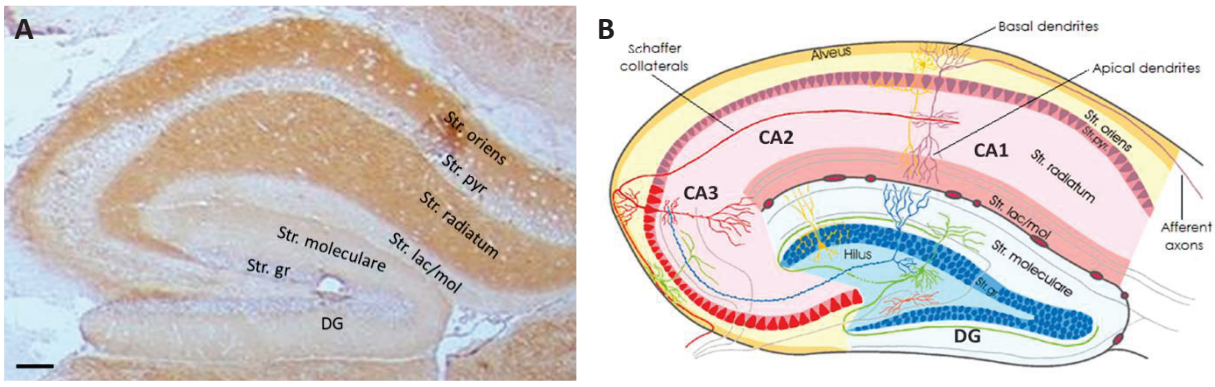

Figure 8. Hippocampal staining pattern of CASPR2 in the adult rat brain and schematic representation of the hippocampus *(A) adapted from Lancaster et al., 2011, B) adapted from Veterinär-Anatomisches Insitut Leipzig, n.d., retrieved April 2016 from http://anatomie.vetmed.uni-leipzig.de).* **A)** CASPR2 staining is observed in the CA1-CA3 stratum oriens (Str. oriens) and stratum radiatum (Str. radiatum) of the adult rat hippocampus. Staining is absent in other hippocampal layers and the dentate gyrus (DG). **B)** The stratum pyramidale (Str. pyr) contains cell bodies of hippocampal pyramidal cells. Their basal dendrites extend into the str. oriens and receive inputs from afferent axons. Pyramidal cell apical dendrites reach into the str. radiatum and are contacted by CA3 Schaffer collateral fibers, interneurons and afferences from the entorhinal cortex. Apical dendrites extend further into the stratum lacunosum moleculare (Str. lac/mol).
CA: cornu ammonis, Str. gr: stratum granulosum, Str. moleculare: stratum moleculare. Scale bar represents 100 µm.

When performing immunohistochemistry on rat and human brain, a more precise cortical staining of CASPR2 has been reported. In adult rat brain, CASPR2 staining is visible in cell bodies and dendrites of neurons of the fifth pyramidal layer of the cerebral cortex (Poliak et al., 1999). These long dendrites extend towards the second layer. In human, CASPR2 expression is observed in layers II-V of the temporal lobe cortex in child (aged 6) and adult (aged 58) brain (Bakkaloglu et al., 2008). Intriguingly, *in situ* hybridization experiments demonstrated an enrichment of *CNTNAP2* in the anterior temporal and prefrontal cortex of human fetal brain tissue, which is not observed in E17 mouse or E21 rat brain tissue (Abrahams et al., 2007) **(Figure 9)**. These brain areas are specific for human cognitive specializations, such as language, which suggests a role for CASPR2 in higher evolved cognitive functions (Abrahams et al., 2007).

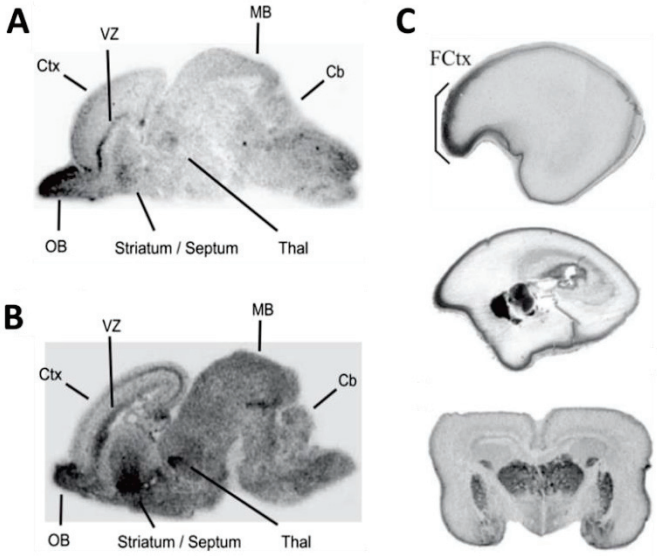

Figure 9. *CNTNAP2* expression in rodent and human developing brain *(adapted from Abrahams et al., 2007)*. In situ hybridization experiments were performed on sagittal (A, B, C) or coronal (C, lowest) brain slices to identify *CNTNAP2* expression. **A)** E17 mouse brain shows broad expression of *Cntnap2* with highest expression levels in the olfactory bulb (OB), ventricular zones (VZ), striatum and thalamus (Thal). **B)** E21 rat brain displays a *Cntnap2* expression similar with E17 mouse brain. **C)** 19 to 20-week-old human fetal brain shows enrichment of *CNTNAP2* in the anterior temporal and prefrontal cortex. A restricted expression is observed in the putamen, amygdala, dorsal thalamus and caudate.
Cb: cerebellum, Ctx: cortex, FCtx: frontal cortex, MB: midbrain.

2.1.2 IN SENSORY MODALITIES

The mouse brain areas that express CASPR2 are mainly involved in sensory pathways (Gordon et al., 2016). For example, at adult age CASPR2 is expressed in the solitary tract nucleus and

dorsal cochlear nucleus of the brain stem, which are connected with gustatory and auditory organs respectively. The piriform cortex, important for olfactory processes, also shows high expression of CASPR2. In the thalamus CASPR2 is found in the ventral posteromedial and posterolateral thalamic nuclei and in the ventral and dorsal medial geniculate nuclei, areas involved in sensory processing. Moreover, this relation with sensory pathways is affirmed when analyzing tissues other than the brain, where CASPR2 at adult age is found in areas related to all the five different senses (Gordon et al., 2016). In the visual system CASPR2 is expressed, among others, in the retina and the optic nerve. In the auditory system CASPR2 is present in the cochlea and spiral ganglion cells, as for the gustatory system its expression is observed all along the gustatory information pathway, starting at tongue nerve endings. Regarding the somatosensory system, the dorsal horn, dorsal root ganglions, footpad and whisker innervations show CASPR2 staining. The most extensive staining of CASPR2 is found in the olfactory system, including sensory olfactory neurons, the vomeronasal organ and the olfactory bulb. In conclusion, CASPR2 is expressed in all sensory modalities, starting from the primary sensory organ to the related cortical information processing zones (Gordon et al., 2016).

This particular expression is interesting regarding to the commonly proposed link between CASPR2 disruption and autism spectrum diseases (ASD) (see chapter B.4.2), since abnormalities in behavioral responses and sensory processing for all sensory modalities are an ubiquitous feature in ASD patients (Marco et al., 2011).

2.2 CELLULAR LEVEL

2.2.1 IN MYELINATED NEURONS

CASPR2 was first discovered as a protein present at the juxtaparanodal region of the node of Ranvier (NOR) in myelinated neurons (Poliak et al., 1999). The NOR is an essential organization for the saltatory conduction of nervous influxes.

As the name indicates, myelinated neurons are neurons whose axons are wrapped with layers of myelin, a substance highly enriched in lipids. Myelin is provided by Schwann cells in the PNS and by oligodendrocytes in the CNS. These myelinating glia enwrap axons in intervals which are separated by NORs **(Figure 10)**. The space between two NORs is called the internode

(Figure 10). In the PNS the entire myelin unit is surrounded by a basal lamina and the outermost side of Schwann cells, at the node, shows small protrusions called microvilli (Ichimura & Ellisman, 1991) **(Figure 10)**. In the CNS the basal lamina is absent and instead some of the nodes are contacted by processes from perinodal astrocytes (Black & Waxman, 1988) **(Figure 10)**.

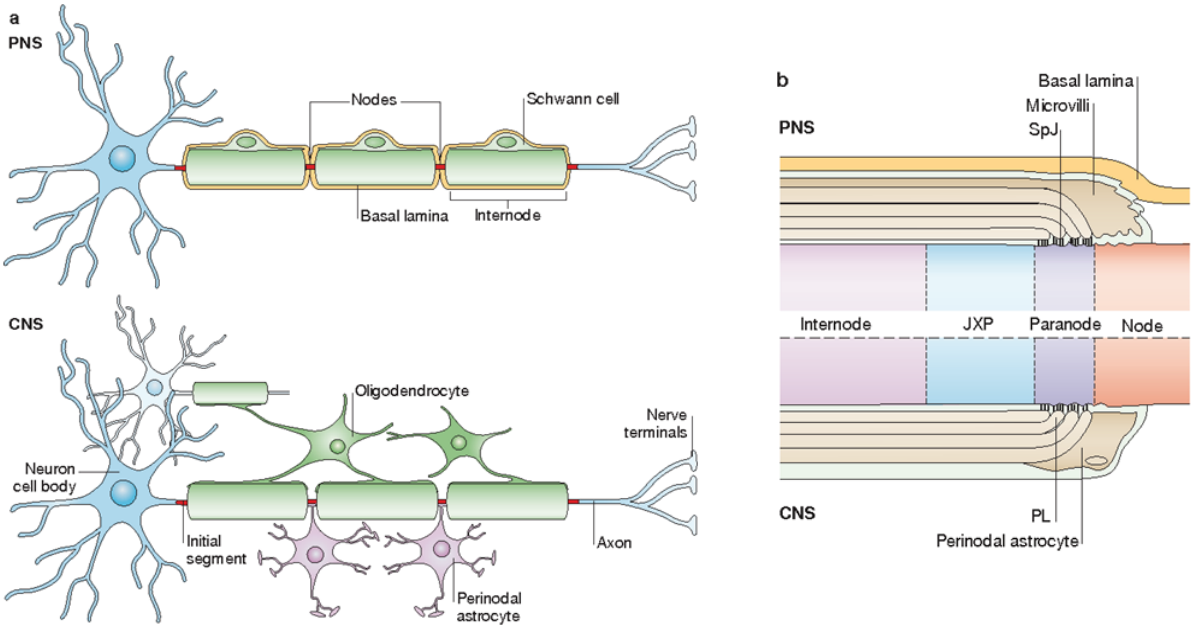

Figure 10. Structure of myelinated neurons *(adapted from Poliak & Peles, 2003).* **A)** Myelinating cells cover neuronal axons in myelin sheets. They cover the axons in intervals, forming nodes of Ranvier (NORs) where they leave a gap. The space between two NORs is the internode. In the PNS one Schwann cell myelinates one internode and the entire myelin unit is surrounded by a basal lamina. In the CNS oligodendrocytes myelinate different axons and multiple internodes per axon. Perinodal astrocytes contact the nodes in the CNS. **B)** Longitudinal section of a myelinated neuron in the CNS and PNS, representing a heminode. The node, paranode, juxtaparanode (JXP) and internode are represented in different colors. Paranodal loops (PL) of myelin form a septate-like junction (SpJ) with the axon. In the PNS the outermost aspect of Schwann cells present microvilli at the node, whereas in the CNS the node is contacted by perinodal astrocytes.

For long time it was believed that myelin only plays a passive role in action potential (AP) propagation, namely ensuring higher AP conduction velocities by reducing the capacitance and increasing the resistance of the axolemma. However, active roles, such as regulation of axonal diameters and axonal survival, have also been assigned to myelinating glia (de Waegh et al., 1992; Griffiths et al., 1998). Importantly, the present glia are not only necessary for myelin provision. A reciprocal glia-axon communication ensures the creation of the NOR, highly adapted for the rapid saltatory conduction of nervous influxes (Poliak & Peles, 2003;

Rasband & Peles, 2016). The NOR can be divided into distinct molecular, structural and functional zones: the node itself, the paranode (PN) and the juxtaparanode (JXP) **(Figure 10B)**. At the level of the PN the spiraling of multiple myelin sheets around the axon creates so-called paranodal loops, who form a septate-like junction (SpJ) with the axon **(Figure 10B)**.

2.2.1.1 FUNCTION AND ORGANIZATION OF THE NODE

The nodal area of the NOR is essential for AP propagation. To ensure correct conduction of nervous influxes, rapid de- and repolarization are required, explaining the high abundance of sodium (Na^+) and potassium (K^+) channels at the node (Waxman & Ritchie, 1993).

Na^+ channels are pore-forming ion channels, ensuring ion flux through the axolemma. Their β1-subunit binds with contactin in the CNS node, and this interaction might be important for regulating Na^+ channel surface expression (Kazarinova-Noyes et al., 2001) **(Figure 11B)**. The node is also enriched in K^+ channels, which regulate excitability (Battefeld et al., 2014; King et al., 2014). Kv3.1b is mostly found in the CNS (Devaux et al., 2003), whereas Kv7.2 and Kv7.3 are expressed in PNS and CNS nodes (Devaux et al., 2004) **(Figure 11)**.

Na^+ and K^+ channels are anchored to the βIV spectrin cytoskeleton by the scaffolding protein ankyrin G (Berghs et al., 2000; Kordeli et al., 1995) **(Figure 11B)**. Ankyrin G also binds transmembrane cell-adhesion molecules (CAMs) of the immunoglobin (Ig) superfamily, neurofascin 186 (NF186) and neuron-glia-related CAM (NrCAM), which in their turn interact with the extracellular matrix (ECM) (Davis, Lambert, & Bennett, 1996). The composition of the ECM differs between the CNS and PNS **(Figure 11)**.

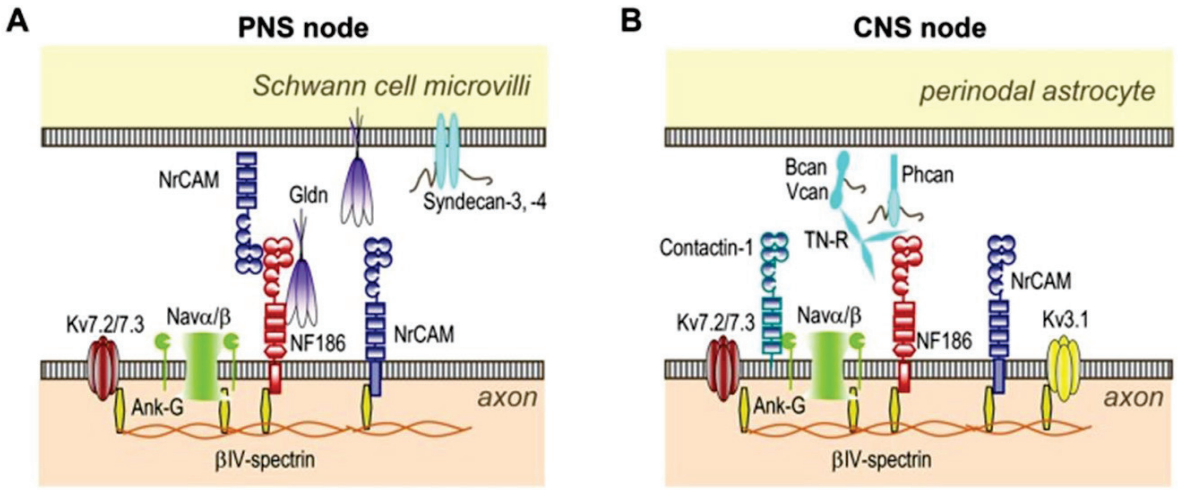

Figure 11. Molecular organization of the node *(adapted from Faivre-Sarrailh & Devaux, 2013).* **A)** Molecular organization of the PNS node. Ankyrin G (Ank-G) connects the βIV spectrin cytoskeleton with the cytoplasmic part of Na^+ channels consisting in α and β-subunits (Navα/β), Kv7.2/7.3 channels and transmembrane cell-adhesion molecules (CAMs) neurofascin 186 (NF186) and neuron-glia-related CAM (NrCAM). Both CAMS interact with the extracellular matrix (ECM), containing several proteins secreted by Schwann cell microvilli. NF186 interacts directly with secreted NrCAM and gliomedin (Gldn). Gldn can also occur anchored to the Schwann cell membrane, together with proteoglycans such as syndecan-3 and 4. **B)** Molecular organization of the CNS node. The molecular organization of the CNS node is very similar with the PNS node. Additionally, Ank-G binds the cytoplasmic part of Kv3.1 channels. The CAM contactin-1 is anchored in the axonal membrane and interacts with the Nav β-subunit. The ECM is enriched in proteoglycans such as tenascin-R (TN-R), brevican (Bcan), versican (Vcan) and phosphacan (Phcan), secreted by perinodal astrocytes.

2.2.1.2 FUNCTION AND ORGANIZATION OF THE PARANODE

At both sides of the node lie the paranodes. The paranodal region has several important functions: attachment of the myelin to the axolemma, separation of nodal from internodal electrical activity and preventing the lateral diffusion of axonal proteins (Poliak & Peles, 2003; Rasband & Peles, 2016). It also plays a role in the formation and maintenance of nodal and juxtaparanodal domains.

A key player in these functions is the complex between glial NF155 and the axonal glycosylphosphatidylinositol (GPI) anchored contactin or contactin-1 and CASPR1 or paranodin (Charles et al., 2002; Rios et al., 2000) **(Figure 12)**. The contactin-1/CASPR1 interaction can be considered the molecular homolog of the juxtaparanodal TAG-1/CASPR2 interaction (see chapter B.2.2.1.3 and B.3.3.1). Interaction of contactin-1 with CASPR1 is necessary for transport of CASPR1 to the axolemma, where it stabilizes the formed complex (Faivre-Sarrailh et al., 2000). CASPR1 binds with its cytoplasmic tail to protein 4.1B (Denisenko-

Nehrbass et al., 2003; Gollan et al., 2002), which connects the protein to the cytoskeleton, consisting of αII and βII spectrin (Chang et al., 2014; Ogawa et al., 2006) **(Figure 12)**. The intracellular interaction between CASPR1 and protein 4.1B is necessary for the paranodal localization of βII spectrin (Brivio et al., 2017).

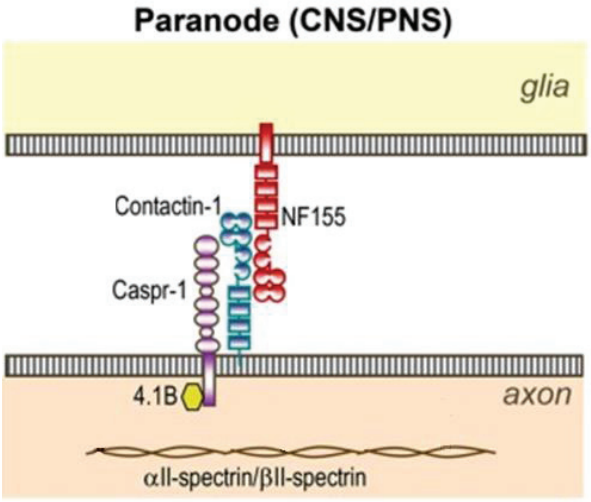

Figure 12. Molecular organization of the CNS and PNS paranode *(adapted from Faivre-Sarrailh & Devaux, 2013)*. Axonal CASPR1 binds with axonal anchored contactin-1, which in its turn interacts with glial neurofascin 155 (NF155). Protein 4.1B (4.1B) binds the cytoplasmic tail of CASPR1, anchoring the formed CAM complex to the αII and βII spectrin cytoskeleton.

Mice knocked out for CASPR1 or contactin-1 lack the septate-like junctions and show a widening of the space between the axolemma and the myelin loops (Bhat et al., 2001; Boyle et al., 2001). Moreover, in these mice, K^+ channels, normally localized at the JXP, disperse into the PN and reduced nerve conduction is observed (Bhat et al., 2001; Boyle et al., 2001). This highlights the role of the septate-like junctions but more importantly of the CAM-complex holding them into place.

2.2.1.3 FUNCTION AND ORGANIZATION OF THE JUXTAPARANODE

Moving further away from the node, the JXP can be found next to the PN. It is at the JXP that CASPR2 is located, together with its main partners Kv1 channels and transient axonal glycoprotein-1 (TAG-1) (Poliak et al., 1999; Traka et al., 2002) **(Figure 13)**. These three proteins form the core of the so-called VGKC-complex and their assembly will be described in chapter B.3.3.

The JXP complexes assure two functions: establishing axoglial contacts and concentrating Kv1 channels. These are delayed rectifier K^+ channels from the Shaker family, which form

heterotetramers consisting in subunits Kv1.1 and Kv1.2 and the auxiliary subunit Kvβ2 (Rasband & Trimmer, 2001; Rasband et al., 1998; Rhodes et al., 1997). At the JXP they stabilize AP conduction by blocking repetitive firing and maintaining the internodal membrane resting potential, and this especially during moments of (re)myelination (Devaux et al., 2017; Rasband et al., 1998; Vabnick et al., 1999).

Figure 13 gives an overview of the proteins present at the JXP. These proteins and their interactions will be discussed in chapter B.3.

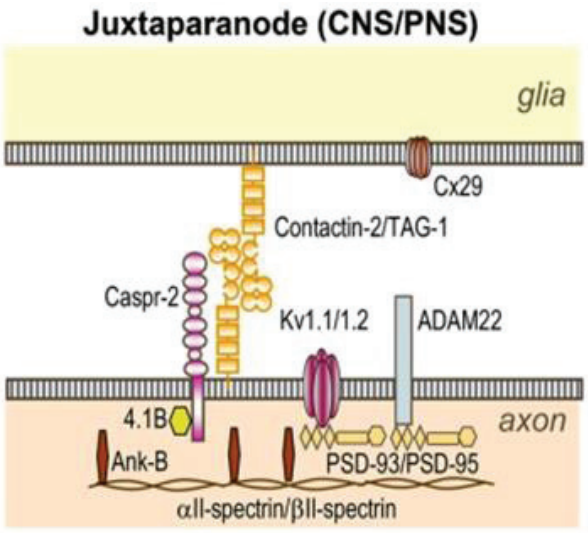

Figure 13. Molecular organization of the CNS and PNS juxtaparanode *(adapted from Faivre-Sarrailh & Devaux, 2013)*. Transmembrane axonal CASPR2 binds with axonal anchored contactin-2 or TAG-1, which presumably interacts with a glial form of TAG-1. Protein 4.1B (4.1B) binds the cytoplasmic tail of CASPR2, anchoring the formed CAM complex to the ankyrin B (Ank-B), αII spectrin and βII spectrin cytoskeleton. PSD93 and PSD95 interact intracellularly with Kv1.1/1.2 channels and ADAM22. The hemichannel connexin 29 (Cx29), probably involved in axo-glial communication via electrical synapses, is present at the glial membrane.

2.2.2 IN UNMYELINATED CULTURED NEURONS

In myelinated neurons the reciprocal interaction between glial and axonal proteins together with the presence of myelin, gives rise to the distinct domains of the NOR. In *in vitro* cultured neurons, myelinating oligodendrocytes and Schwann cells are lacking, causing axons to be mainly unmyelinated. Therefore, in these cultured neurons NORs are absent and proteins normally restrained at a specific region of the NOR are still present but show a different distribution.

In *in vitro* unmyelinated rat hippocampal neurons transfected and endogenous CASPR2 knows a polarized expression that arises gradually over time (Bel et al., 2009; Pinatel et al., 2015). From 2 days *in vitro* (DIV) until DIV 6 CASPR2's intracellular and extracellular expression is observed at the neuronal somatodendritic compartment and along axons, including the axon initial segment (AIS) (Bel et al., 2009; Pinatel et al., 2015). At DIV 7 polarization starts, and at DIV 8 surface CASPR2 puncta remain only faintly at the somatodendritic compartment and are clearly localized on the axonal surface (Bel et al., 2009; Pinatel et al., 2015). The polarized expression is maintained over time and is achieved because of an endocytosis signal in the cytoplasmic tail of CASPR2 (Bel et al., 2009). This signal causes selective elimination of surface CASPR2 from the somatodendritic compartment, without altering axonal surface CASPR2. The axonal surface expression is observed in inhibitory axons, and is evenly distributed along the axon, no AIS enrichment is observed (Bonetto et al., 2019; Pinatel et al., 2015).

The precise subcellular localization, and especially a possible synaptic localization, of CASPR2 in *in vitro* cultured neurons is still a matter of debate. This will be discussed in chapter C.2.1.

3. PRINCIPAL PARTNERS OF CASPR2

3.1 TRANSIENT AXONAL GLYCOPROTEIN-1 (TAG-1)

The main partner of CASPR2 is TAG-1 or contactin-2 or axonin-1, a CAM belonging to the Ig superfamily (Furley et al., 1990).

3.1.1 STRUCTURE OF TAG-1

TAG-1 is a protein which is exclusively extracellular (Furley et al., 1990). It does not contain a transmembrane or intracellular domain and is anchored to the membrane via a GPI linkage (Karagogeos et al., 1991). TAG-1 can also occur in a soluble form (Karagogeos et al., 1991). The structure of TAG-1 consists of six N-terminal Ig domains and four C-terminal fibronectin (Fn) III domains **(Figure 14A)**.

Starting with the obtention of the crystal structure of certain regions of TAG-1, the 3D-structure of the protein could be identified (Freigang et al., 2000; Kunz et al., 2002; Mörtl et al., 2007). A *cis* homophilic interaction is possible via the C-terminal Fn3 and Fn4 domains

(Kunz et al., 2002) **(Figure 14B)**. On the other hand, the N-terminal Ig domains form a compact U-shape, by interactions between Ig1 and 4 and between Ig3 and 2 of the same protein (Freigang et al., 2000). Two U-shapes from opposing TAG-1 molecules interact in *trans*, anchoring the two facing membranes (Freigang et al., 2000; Rader et al., 1993) **(Figure 14B)**. Both interactions are necessary for maintaining the cell-cell binding, thus creating a cooperative so-called *cis*-assisted *trans*-binding (Kunz et al., 2002). On the other hand, deglycosylated TAG-1 can also occur folded on itself, in a horseshoe form, not allowing homophilic *cis*- nor *trans*-interactions (Kunz et al., 2002; Rader et al., 1996) **(Figure 14B)**.

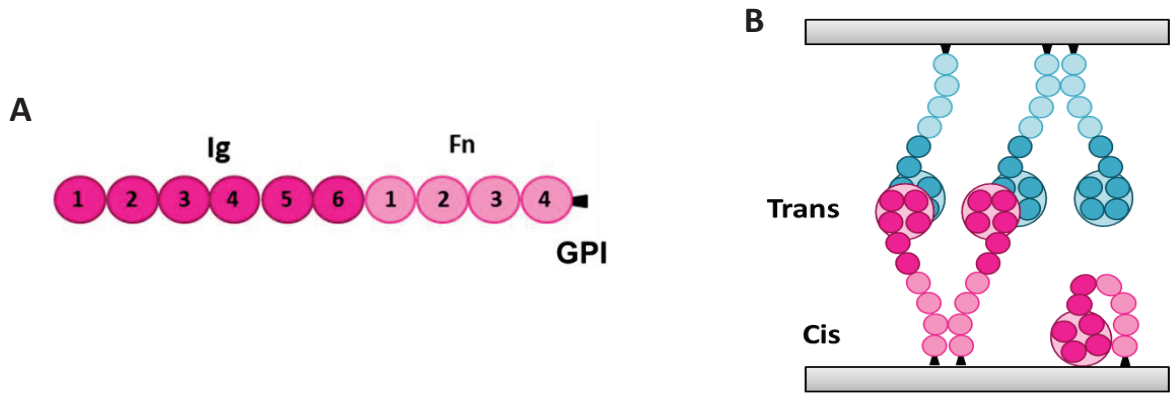

Figure 14. Secondary structure and possible configurations of TAG-1 *(adapted from Caractérisation des anticorps anti-CASPR2 de patients atteints d'encéphalite limbique auto-immune et impact sur le complexe CASPR2/TAG-1/KV1.2 by Saint-Martin M., 2018)*. **A)** TAG-1 is composed of six N-terminal immunoglobulin (Ig) domains, four C-terminal fibronectin (Fn) III domains and a glycosylphosphatidylinositol (GPI) linkage. **B)** TAG-1 can present a *cis* homophilic interaction between the Fn3 and Fn4 domains of two TAG-1 molecules (left). The N-terminal Ig1-4 domains form a compact U-shape and can assist in a *trans* interaction between the same domains of an opposing TAG-1 molecule. TAG-1 can occur folded on itself not participating in homophilic interactions (right).

3.1.2 FUNCTION OF TAG-1

TAG-1 is present at the neuronal membrane and at the surface of myelinating glia in the CNS and PNS. It is transiently expressed during development and knows a predominant expression in the developing brain, which is related to its implication in neuronal migration, neurite outgrowth, axonal guidance and neuronal fasciculation (Denaxa et al., 2001; Furley et al., 1990; Karagogeos et al., 1991; Stoeckli et al., 1991). During these processes, TAG-1 assures cell-cell and cell-matrix interactions. It binds with several neuronal CAMs, such as NrCam and NgCam, and with extracellular matrix proteins (Buttiglione et al., 1998; Kuhn et al., 1991; Milev

et al., 1996). Some of these heterophilic TAG-1 bindings can induce or impact intracellular signaling processes. Moreover TAG-1 can bind with itself, assuring homophilic interactions (Rader et al., 1993). Interestingly, its ligand-binding capacities are maintained across species, making comparison between species possible.

Surprisingly, immunohistochemistry of mice TAG-$1^{-/-}$ brain slices does not reveal morphological alterations (Fukamauchi et al., 2001). Compensatory mechanisms upon TAG-1 deletion are a possible explanation. However, it was later evidenced that TAG-$1^{-/-}$ mice present altered NORs in the CNS, with an absence of clustering of Kv channels and CASPR2 at the JXP and their dispersion into the internode (Savvaki et al., 2008). These internodes show a shortened length in the cerebral and cerebellar white matter (Savvaki et al., 2008). Interestingly co-expression of TAG-1 with Kv1.2 channels in HEK cells renders these channels less voltage dependent and reduces their activation threshold (Gu & Gu, 2011). This suggests a role for TAG-1 in regulating Kv1 channel activity. In addition to this, re-excitation is more prone to occur in shortened internodes in PNS myelinated neurons (Zhou et al., 1999).

The observed morphological alterations in TAG-$1^{-/-}$ mice most probably lie at the basis of the hyperexcitable phenotype of these mice. Indeed, TAG-$1^{-/-}$ mice show increased seizure susceptibility, characterized by increased severity of induced seizures and increased mortality, visible around P34 (Fukamauchi et al., 2001). In addition to this, learning and memory capacities are disturbed in adult TAG-$1^{-/-}$ mice, as well as sensory and motor function (Savvaki et al., 2008). A decreased spontaneous activity, abnormal gait coordination and increased response latency to thermal noxious stimuli are observed (Savvaki et al., 2008).

3.2 VOLTAGE GATED POTASSIUM CHANNELS (KV CHANNELS)

The second main partner of CASPR2 are Kv1 channels formed by the Kv1.1 and Kv1.2 subunits from the Shaker delayed-rectifier type.

3.2.1 STRUCTURE OF KV CHANNELS

Kv1 channels are heterotetramers consisting in four α-subunits, together creating a transmembrane pore allowing K^+ passage (Lai et al., 2006; Wang et al., 1993) **(Figure 15)**. Each α-domain is built of six α-helical transmembrane segments (S1-S6) **(Figure 15)**. The fourth

segment contains multiple arginine residues, giving it a positive charge, and functions as the main responsible voltage sensor. The S5 and S6 segments are the pore formers of the channel. The different helices are linked with alternate intracellular and extracellular loops, the first linking S1 and S2 being extracellular. The loop linking S5 and S6 has a re-entrant pore, forming the narrowest part of the pore. Each α-subunit is linked via its N-terminal T1 domain with an auxiliary cytoplasmic β2-subunit (Gulbis et al., 2000; Rhodes et al., 1997) **(Figure 15)**. The T1 domain is necessary for channel subunit tetramerization whereas the auxiliary β2-subunit modifies channel expression, functional properties and subcellular localization. A direct example of this is the capacity of the β2-subunit to enter the pore and thus by a ball-and-chain mechanism block K^+ efflux (Campomanes et al., 2002; Gulbis et al., 2000; Shi et al., 1996). The C-terminal cytoplasmic tail of the α-subunit contains a PDZI and PDZII binding motif which can bind PDZ proteins (Kim et al., 1995).

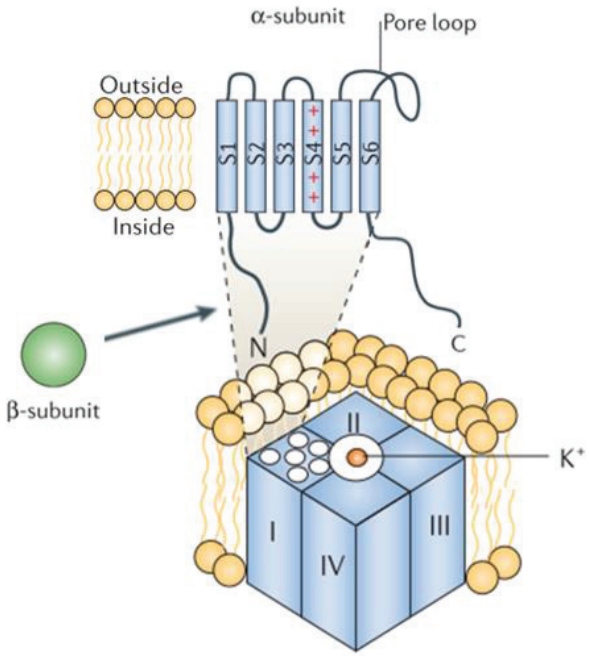

Figure 15. Structure of Kv channels *(adapted from Lai et al., 2006).* Kv channels are heterotetramers, consisting in four α-subunits. Each α-subunit contains six α-helical transmembrane segments (S1-S6). S4 is enriched in arginine, giving it a positive charge. S5 and S6 form the pore of the channel which is permeable for potassium (K^+) ions. The transmembrane segments are connected via alternating extracellular and intracellular loops. The loop between S5 and S6, the pore loop, has a re-entrant pore. Each α-subunit is linked with an auxiliary cytoplasmic β2-subunit via its N-terminal domain.

3.2.2 FUNCTION OF KV CHANNELS

The Kv1 subfamily has an important role in shaping the AP, regulating firing patterns and controlling neuronal excitability (Robbins & Tempel, 2012). These channels are activated at low electric potentials and show a sustained K^+ efflux with a delay after membrane depolarization. The K^+ efflux allows for a rapid repolarization of the axon membrane.

At the NOR, the function of Kv1.1 and Kv1.2 channels evolves gradually during development, in parallel with their progressing localization and the development of the myelinated nerve (Devaux et al., 2002; Vabnick et al., 1999). In the first rat postnatal week Kv channels are not detected in PNS sciatic nerves by immunostaining, but are most probably present, since application of 4-aminopyridine (4-AP), a K^+ channel blocker, slows down the falling phase of APs (Vabnick et al., 1999). Kv channels become detectable at approximately 1 week of age at the PNS node but mainly at the PN (Vabnick et al., 1999). Their expression shifts towards the JXP in the developmental period of ~ 2-4 weeks of age. From approximately P0 to P10 Kv channels are involved in AP generation, speeding membrane repolarization and declining the refractory period (Vabnick et al., 1999). After this period, neurons become highly sensitive to repetitive firing. At this time point, present Kv channels function to prevent this bursting behavior by decreasing the refractory period (Vabnick et al., 1999). However, these observations, evidenced by application of 4-AP, diminish over time during development of the NOR. At 6 weeks of age the effect of 4-AP is almost completely abolished (Vabnick et al., 1999). CNS and PNS mature myelinated neurons show attenuated responses to pharmacological actors such as 4-AP and dendrotoxin (DTX) (Devaux et al., 2002; Devaux & Gow, 2008; Vabnick et al., 1999). Indeed, at this time point Kv channels are electrically isolated, since myelin sheets are properly formed and the NOR has been correctly assembled, explaining absence of effects upon application of Kv channel blockers. However, increasing evidence has shown that Kv channels underneath the myelin sheets can be activated by nodal action currents passing via short pathways through or beneath paranodal myelin (Chiu et al., 1999; Devaux & Gow, 2008; Rosenbluth et al., 2013). Furthermore, currents can flow not only anterogradely but also retrogradely. Retrograde currents could reactivate Na^+ channels at remote nodes, which would cause repetitive firing (Rosenbluth et al., 2013). It is thus supposed that the function of Kv channels in mature myelinated neurons is to prevent retrograde channel activation and consequently repetitive firing and maintain the internodal resting membrane potential

(Rosenbluth et al., 2013). Nevertheless, the unaltered nerve conduction of mature myelinated neurons in presence of K^+ channels blockers implies that Kv channels exert little effect in normal situations of electrical activity (Rosenbluth et al., 2013). Their possible more widespread role in nerve conduction or in altered electrical activity remains to be elucidated. Mice lacking the Kv1.1 subunit display a limbic seizure phenotype, reminding of temporal lobe epilepsy (Robbins & Tempel, 2012; Smart et al., 1998). Spontaneous seizures begin at early developmental ages and become recurrent during adolescence (Smart et al., 1998). Only half of the Kv1.1 KO mice survive into adulthood (Smart et al., 1998). Electrophysiological measurements in the sciatic nerve evidenced that in these mice AP conduction is altered with a prolonged depolarization and an increase in refractory period (Smart et al., 1998). Mice knocked out for the Kv1.2 subunit on the other hand display brainstem seizure phenotype, with a sudden onset followed by tonic-clonic activity (Brew et al., 2007). They only survive into P19 (Brew et al., 2007).

3.3 ASSEMBLY OF THE VGKC COMPLEX

3.3.1 THE VGKC COMPLEX AT THE JUXTAPARANODE OF MYELINATED NEURONS

CASPR2 has a major anchoring and organizing role at the JXP. In teased sciatic and optic nerves from CASPR2 KO mice, TAG-1 is almost completely absent from the JXP (Poliak et al., 2003) **(Figure 16)**. Moreover, Kv1 channels are redistributed along the internode in CNS optic nerves and long-range cortical axons and in PNS sciatic nerves (Poliak et al., 2003; Scott et al., 2017) **(Figure 16)**. In the latter the Kv1 channels are additionally packed closely to the PN (Poliak et al., 2003) **(Figure 16)**. Despite the clear alteration of Kv1 distribution in CASPR2 KO mice, nerve conduction is not altered (Poliak et al., 2003). On the other hand, knock out of TAG-1 causes a similar phenotype, namely a redistribution of CASPR2 and Kv1.2 along the internode (Poliak et al., 2003; Traka et al., 2003). This demonstrates an interdependence between these three proteins, and importantly a role for CASPR2 and TAG-1 in gathering and maintaining Kv1 channels at the JXP (Poliak et al., 2003; Traka et al., 2003).

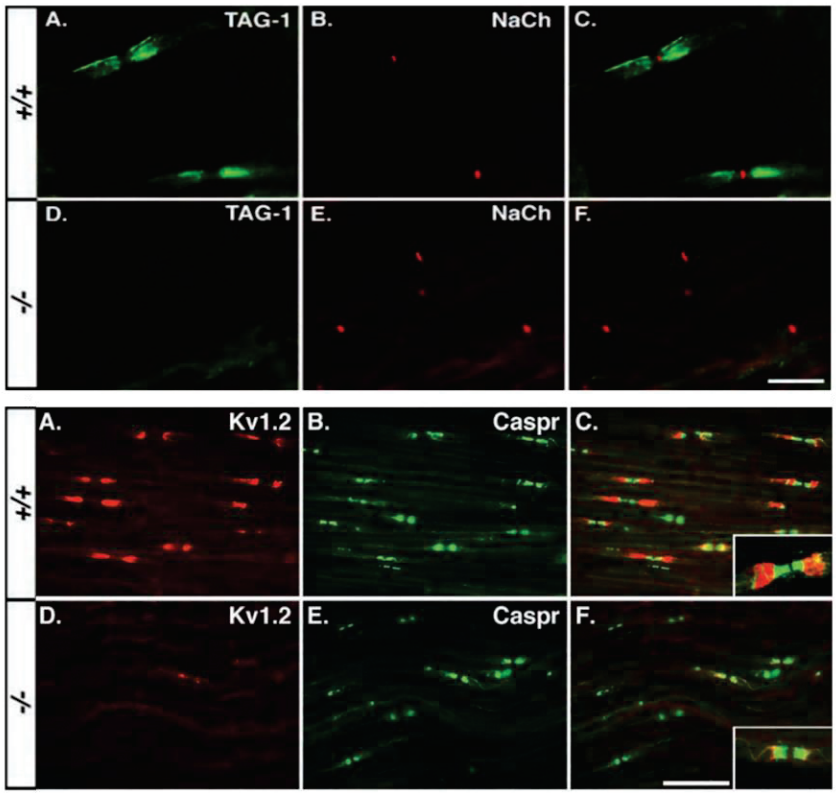

Figure 16. Absence of TAG-1 and reduced clustering of Kv1.2 channels at the JXP in CASPR2 KO teased sciatic nerves *(Poliak et al., 2003)*. Upper panel: CASPR2 KO sciatic nerves are absent from TAG-1 at the JXP. The node is visualized by staining against Na^+ channels (NaCh). Lower panel: Kv1.2 channels are redistributed along the internode and in some cases packed against the PN in CASPR2 KO sciatic nerves. The PN is visualized by staining against CASPR. Scale bars represent 20 µm.

An important CAM-interaction complex is formed between CASPR2 and TAG-1, in which CASPR2 recruits axonal TAG-1 in *cis* and clusters Kv1 channels at the JXP (Poliak et al., 2003; Traka et al., 2003). It has been proposed that glial TAG-1 participates in a homophilic *trans* interaction with the formed CASPR2/TAG-1 complex, promoting Kv1 channel clustering (Poliak et al., 2003; Traka et al., 2002, 2003). This hypothesis has been questioned by results obtained in transgenic mice expressing TAG-1 exclusively in oligodendrocytes. Savvaki et al. (2010) demonstrated that expression of only glial TAG-1 was sufficient for restoring correct JXP assemblance. They postulated that an interaction between glial TAG-1 and CASPR2 could gather Kv1 channels, without the necessity of axonal TAG-1. Moreover, by expressing only glial TAG-1, the behavioral deficits in sensorimotor gating and motor coordination witnessed in TAG-$1^{-/-}$ mice were restored (Savvaki et al., 2010). The *trans* interaction between glial TAG-1 and CASPR2 has been confirmed by co-immunoprecipitation assays and experiments using HEK cells (Savvaki et al., 2010). However, these results were contradicted in a study using

cocultures of hippocampal neurons and HEK cells. Neuronal CASPR2 was unable to cluster Kv1.2 channels in presence of *trans* TAG-1 expressed by HEK cells (Gu & Gu, 2011). In addition, the *trans*-homophilic TAG-1 interaction was sufficient to position Kv1.2 channels on neuronal membranes (Gu & Gu, 2011). Thus, the interactions of the CASPR2/TAG-1/Kv complex have not been completely resolved yet. An important factor in the aforementioned studies is the possible presence of soluble TAG-1, released by both neurons and glia (Karagogeos et al., 1991; Traka et al., 2002). In case of the study by Savvaki et al. (2010), soluble TAG-1 could bind in *cis* with CASPR2, permitting the interaction with glial TAG-1 to consequently gather Kv channels, thus leading to false conclusions. Regarding the study by Gu & Gu (2011), the released form of TAG-1 could bind with TAG-1 expressed by the cells, thus impeding interaction with CASPR2 in *cis* or in *trans*.

In the same manner, many results point out an interaction, albeit indirect, between CASPR2 and Kv1 channels, but the exact mechanism has not been established yet. The cytoplasmic tail of CASPR2 is necessary for its association with Kv1 channels and the assembly of the complex at the JXP (Horresh et al., 2008; Poliak et al., 1999, 2003) **(Figure 17)**. Since the cytoplasmic part of CASPR2 contains a type II PDZ binding domain (Poliak et al., 1999) and it was already established that Kv1.1/1.2 channels bind the PDZ1 and PDZ2 domain of PSD95 via their α-subunit C-terminal cytoplasmic tail (Kim et al., 1995), it was supposed that the interaction between both proteins takes place via a common PDZ containing protein. PDZ-containing proteins that are present at the central and peripheral JXP include the membrane-associated guanylate kinases (MAGUKs) PSD93 and PSD95 (Horresh et al., 2010). However, it has been shown that CASPR2 does not bind PSD95 (Tanabe et al., 2015). In addition, mice knocked out for PSD93, PSD95 or PSD93 and PSD95 mice show normally assembled nodes, PNs and JXPs in the CNS and PNS (Horresh et al., 2008; Rasband et al., 2002). Moreover, CASPR2 deleted for its PDZ binding domain is still capable of co-immunoprecipitating Kv1.2 and forms correctly assembled JXPs in teased sciatic nerves (Horresh et al., 2008) **(Figure 17)**. Thus, the association between CASPR2 and Kv1.2 does not depend on CASPR2's PDZ binding domain. On the other hand, localization of PSD93/95 at the JXP depends on CASPR2, since they fail to accumulate at the JXP in CASPR2 KO mice (Horresh et al., 2008) **(Figure 17)**.

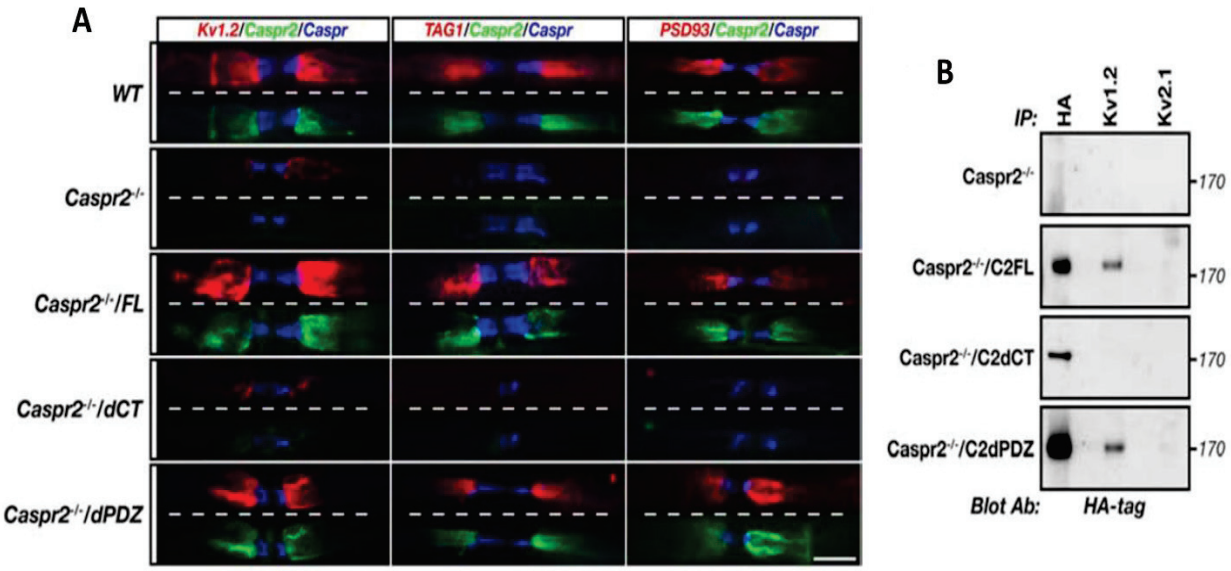

Figure 17. Juxtaparanodal assembly of Kv1.2 channels, TAG-1 and PSD93 is dependent from CASPR2's cytoplasmic domain but not from its PDZ binding domain in teased sciatic nerves *(Horresh et al., 2008)*. Transgenic mice expressing HA-tagged CASPR2 constructs (CASPR2 full length (C2FL), CASPR2 lacking its cytoplasmic C-terminal domain (C2dCT) and CASPR2 lacking its PDZ binding domain (C2dPDZ)) were crossed with CASPR2$^{-/-}$ mice. **A)** In teased sciatic nerves Kv1.2, TAG-1 and PSD93 are absent at the JXP in CASPR2$^{-/-}$ mice and in CASPR2$^{-/-}$/dCT mice but are present at the JXP in CASPR2$^{-/-}$/dPDZ mice. **B)** Brain membrane lysates from the crossed transgenic mice were prepared, immunoprecipitated by antibodies against HA, Kv1.2 or Kv2.1 and western blotted against the HA-tag. C2FL and C2dPDZ co-immunoprecipitate with Kv1.2 whereas C2dCT does not.
Scale bar represents 10 µm.

An important interaction takes places between the four point one, ezrin, radixin, moesin (FERM) domain of protein 4.1B, a cytoskeletal adaptor protein, and the intracellular tail of CASPR2 (Denisenko-Nehrbass et al., 2003). This interaction allows the attachment of the VGKC complex to the cytoskeleton, consisting of ankyrin B, αII and βII spectrin (Denisenko-Nehrbass et al., 2003; Horresh et al., 2010). Indeed, at the JXP of PNS and CNS nerves, protein 4.1B KO mice show a redistribution of CASPR2, TAG-1, PSD93 and Kv1 channels (Cifuentes-Diaz et al., 2011; Einheber et al., 2013; Horresh et al., 2010).

Even though CASPR2, TAG-1 and Kv1 channels are the main components of the initially described VGKC complex, over the years other proteins, including a disintegrin and metalloproteinase (ADAM) 22, ADAM23, leucin-rich glioma inactivated (LGI) 1 and LGI4, have been identified. However, their functional role in maintaining the correct assembly of the VGKC complex is seemingly less important with respect to the core proteins CASPR2, TAG-1 and Kv1 channels.

LGI4 is expressed in and secreted by glial cells and plays a role in myelination (Ozkaynak et al., 2010). It has been shown that LGI4 released by Schwann cells binds with the extracellular part of ADAM22/23, which are membrane-anchored proteins. It has thus been proposed that LGI4 creates an interface between molecules at the JXP (Kegel et al., 2014; Sagane et al., 2008). LGI1 is also important for myelination, but only weak staining at the JXP has been observed (Ogawa et al., 2010; Schulte et al., 2006). Using immunoprecipitation experiments it has been shown that LGI1 can bind ADAM22/23 (Sagane et al., 2008). Effects of deletions of LGI1/4 on CASPR2 or its partners have not been assessed yet. Regarding ADAM22 it has been demonstrated that its deletion impedes PSD93/95 clustering at the JXP, but has no effect on Kv1 channels or CASPR2 in the CNS (Ogawa et al., 2010).

Figure 18 gives an overview of the established and presumed interactions of the VGKC complex proteins at the JXP.

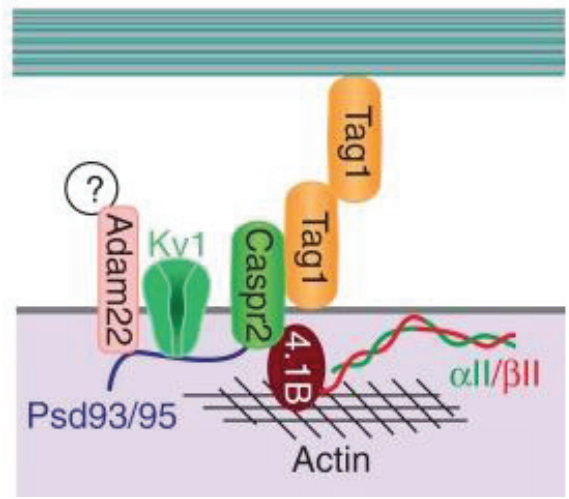

Figure 18. Interactions of the VGKC complex at the juxtaparanode *(Rasband and Peles, 2016)*. Axonal CASPR2 binds in *cis* with axonal anchored TAG-1, which presumably interacts with a glial form of TAG-1 in *trans*. Protein 4.1B (4.1B) binds the cytoplasmic tail of CASPR2, anchoring the formed CAM complex to the αII and βII spectrin and actin cytoskeleton. PSD93 and PSD95 interact intracellularly with ADAM22 and Kv1 channels. CASPR2 interacts indirectly with Kv1 channels and is necessary for PSD93/95 localization at the JXP, but the precise mechanisms behind these interactions have not yet been unraveled. The function of ADAM22 at the JXP remains unknown.

3.3.2 THE VGKC COMPLEX AT THE AXON INITIAL SEGMENT OF MYELINATED NEURONS

Proteins of the VGKC complex are also present at the AIS of myelinated neurons. The AIS follows immediately after the axon hillock, which emerges from the neuronal soma, and

generates and shapes the AP before its propagation along the axon **(Figure 19)**. In order to execute its function in neuronal excitability, the AIS is highly concentrated in voltage gated Na^+ and K^+ channels (Leterrier, 2018) **(Figure 19)**. These channels and other proteins such as CAMs, are attached to ankyrin G, which is essential for the structural organization of the AIS (Nelson & Jenkins, 2017). Indeed, ankyrin G serves as a scaffold between these proteins and the actin/spectrin cytoskeleton. This anchoring restricts surface diffusion of proteins and allows the AIS to execute a second function, namely to serve as a boundary between the somatodendritic and axonal compartment (Rasband, 2010).

In myelinated neurons, the axonal region following the AIS is present as a heminode (Duflocq et al., 2011) **(Figure 19)**. The beginning of myelin sheets starts here and a paranodal-like and juxtaparanodal-like compartment are found, referred to as para-AIS and JXP-AIS respectively (Duflocq et al., 2011) **(Figure 19)**.

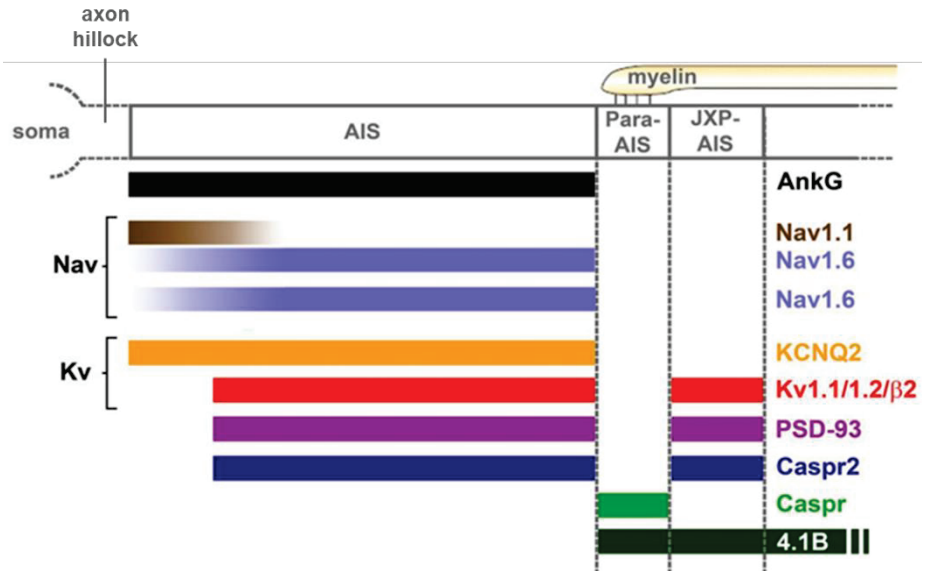

Figure 19. Schematic representation of protein distribution at the AIS in myelinated neurons *(adapted from Duflocq et al., 2011).* The neuronal soma is followed by the axon hillock which is adjacent to the AIS. The first myelin sheets start at the heminode next to the AIS. The heminode contains a para-AIS followed by a JXP-AIS. The different ion channels and proteins from the VGKC complex present at the AIS regions are shown in different colors.
AIS: axon initial segment.

In myelinated neurons CASPR2, Kv1 channels and PSD93 are present at the distal part of the AIS and at the JXP-AIS (Duflocq et al., 2011; Inda et al., 2006; Ogawa et al., 2008) **(Figure 19)**. Assembling mechanisms of the VGKC complex are the same in both aforementioned AIS regions, but differ from those described previously at the JXP. In contrast with the situation at the JXP, clustering of Kv1 channels at the AIS and JXP-AIS is independent from CASPR2, TAG-1

or PSD93 (Duflocq et al., 2011; Ogawa et al., 2010; Ogawa et al., 2008). At the AIS normal positioning of Kv1 channels has also been demonstrated in absence of PSD95 or ADAM22 (Ogawa et al., 2010). Protein 4.1B is absent from the AIS but present at the para-AIS and JXP-AIS (Duflocq et al., 2011) **(Figure 19)**. As for the JXP, protein 4.1B plays a major role in assembling the VGKC complex at the JXP-AIS (Duflocq et al., 2011). Its absence causes a redistribution of PSD93, CASPR2 and Kv1 channels into the para-AIS (Duflocq et al., 2011).

3.3.3 THE VGKC COMPLEX IN CULTURED UNMYELINATED NEURONS

The proteins of the VGKC complex have also been assessed in *in vitro* cultured unmyelinated neurons. As mentioned, these neurons lack NORs and JXPs. This implies not only a different distribution of VGKC proteins in cultured unmyelinated neurons, but also discrepancies in their interactions compared with the situation at the JXP and AIS of myelinated neurons.

In vitro, surface CASPR2 is distributed all along the axon of hippocampal inhibitory neurons together with surface TAG-1 (Bonetto et al., 2019; Pinatel et al., 2017) **(Figure 20)**. However, TAG-1 is enriched at the AIS, which is not the case for CASPR2 (Bonetto et al., 2019; Pinatel et al., 2017) **(Figure 20)**. Deletion of L2 and EGF1 in CASPR2 (CASPR2Δ2) causes an enrichment of CASPR2 at the AIS and moreover increases its co-immunoprecipitation with TAG-1 (Pinatel et al., 2017). Thus, the absence of these domains may cause a tighter binding between TAG-1 and CASPR2 possibly by conformational changes. Moreover, in cultured hippocampal neurons established from TAG-1 KO mice, only half of the original inhibitory neuronal population expressing CASPR2 still expresses CASPR2 along the axon (Pinatel et al., 2017). Since not all CASPR2 expressing neurons are affected, this indicates that TAG-1 is necessary for CASPR2 proper expression but other mechanisms may be involved as well. These results also confirm the *cis*-interaction between TAG-1 and CASPR2 as observed at the JXP. A possible *trans*-interaction is still a matter of debate. Neurons transfected with TAG-1 show increased binding of CASPR2-Fc, a CASPR2 chimera allowing to detect CASPR2 binding sites, compared with untransfected neurons at DIV 8 (Pinatel et al., 2015). This suggests that TAG-1 and CASPR2 may interact in *trans* as well. However, CASPR2-Fc chimeras may adopt different conformations. Consequently, the observed interaction between TAG-1 and CASPR2-Fc can also represent a *cis* interaction.

In parallel with CASPR2 and TAG-1, Kv1.1 and Kv1.2 channels are expressed *in vitro* in hippocampal inhibitory neurons (Bonetto et al., 2019) **(Figure 20)**. Intracellular staining experiments demonstrated that they are present along the axon and at the soma of parvalbumin (PV) positive and somatostatin (SST) positive neurons (Bonetto et al., 2019). Kv1.1 channels are more faintly expressed compared with Kv1.2 channels **(Figure 20)**, rendering Kv1.2 channels the most abundantly expressed subunit of Kv1 channels in inhibitory hippocampal neurons (Bonetto et al., 2019). Staining for total Kv1.1 and Kv1.2 channels showed that in inhibitory neurons these channels are also enriched at the AIS, whereas in excitatory neurons they are exclusively expressed at the AIS (Bonetto et al., 2019). The positioning of Kv1 channels at the AIS does not depend on PSD93 or PSD95 or ADAM22 (Ogawa et al., 2008). Moreover, in contrast with the situation at the JXP, knock out for CASPR2, TAG-1 or protein 4.1B does not alter Kv1.2 expression *in vitro* (Bonetto et al., 2019), pointing out different Kv1 clustering mechanisms in cultured hippocampal inhibitory neurons.

Although the intracellular molecule protein 4.1B is dispensable for proper Kv1.2 channel expression *in vitro*, it is necessary for correct CASPR2 and TAG-1 distribution (Bonetto et al., 2019). Protein 4.1B is expressed along inhibitory axons but only faintly at their AIS, which differs from the surface distribution of CASPR2 and TAG-1 (Bonetto et al., 2019; Ogawa et al., 2008) **(Figure 20)**. Nevertheless, knockout of protein 4.1B causes a decrease of surface CASPR2 axonal expression of 50% compared with WT (Bonetto et al., 2019). In addition, surface TAG-1 expression is completely abolished from some inhibitory neurons in absence of protein 4.1B, whereas an increased number of neurons present with an AIS-restricted expression (Bonetto et al., 2019). The different impacts on CASPR2 and TAG-1 upon protein 4.1B knockout suggest that protein 4.1B may associate in a complex with both CAMs and influence their axonal distribution, but that other mechanisms are most likely involved as well.

The interactions of the more recently evidenced VGKC complex proteins have been more extensively studied in *in vitro* cultured hippocampal neurons than at the JXP. ADAM22 is colocalized with TAG-1 in inhibitory hippocampal neurons, intracellularly it appears along the axons of inhibitory neurons, with an enrichment at the AIS (Bonetto et al., 2019) **(Figure 20)**. Interestingly ADAM22 co-immunoprecipitates with TAG-1 in HEK cells, whereas ADAM23 does not (Hivert et al., 2019). Both proteins are capable though of co-immunoprecipitating CASPR2, an interaction that most likely takes place via CASPR2's ectodomain (Hivert et al., 2019). Furthermore, TAG-1 and CASPR2 seem to have different effects on ADAM23 when they are

transported together in intracellular vesicles. When co-transfected with TAG-1, ADAM23 shows AIS enrichment, whereas co-expression with CASPR2 causes a faint distribution of ADAM23 along the axon (Hivert et al., 2019). Thus, these CAMs interact together, influencing one another's axonal distribution.

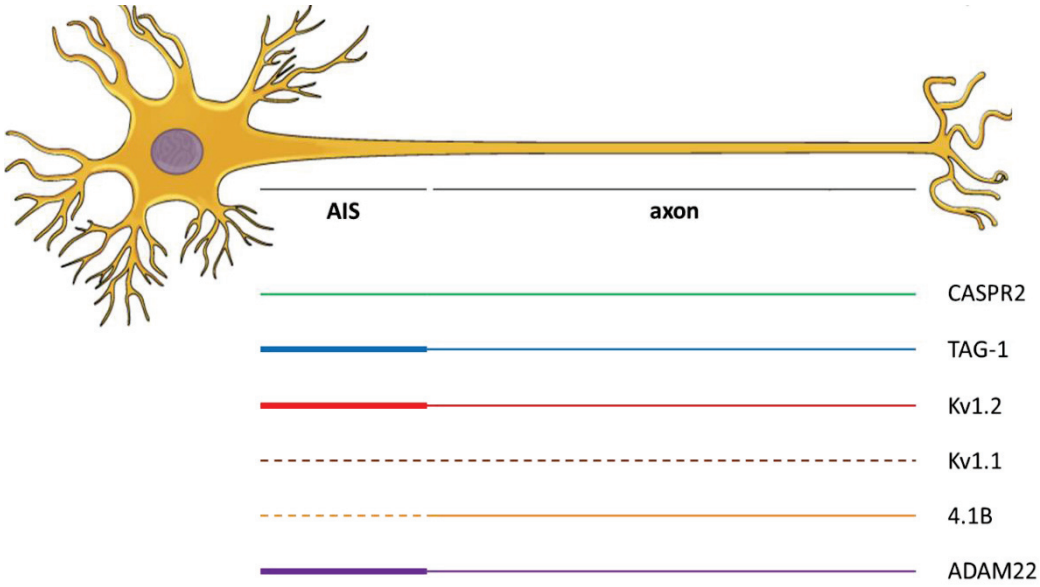

Figure 20. Schematic representation of the distribution of VGKC complex proteins in *in vitro* inhibitory hippocampal unmyelinated neurons. An *in vitro* inhibitory hippocampal unmyelinated neuron is represented and the axonal initial segment (AIS) and axon are indicated. Presence of the individual VGKC complex proteins at these regions is represented by a line, with each color representing a different protein. For CASPR2 and TAG-1 the line represents surface expression, whereas for other proteins total expression is represented. An enriched presence is indicated by a thick line. A faint presence is indicated by a dashed line.

LGI1 is the main partner of ADAM22/23. Their interaction has been extensively studied at the synapse, where two soluble LGI1 proteins form a bridge between presynaptic ADAM23 and postsynaptic ADAM22 (Fukata et al., 2010; Fukata et al., 2006; Sagane et al., 2008). Interestingly co-transfection of LGI1 with ADAM23 in *in vitro* hippocampal neurons causes less enrichment of Kv1.2 at the AIS (Hivert et al., 2019).

4. DISEASES ASSOCIATED WITH CASPR2

4.1 GENETIC ALTERATIONS OF *CNTNAP2* LINKED WITH DISEASE

The first description of a disorder linked with perturbation of the *CNTNAP2* gene was by Verkerk et al. (2003). It involved a complex translocation/inversion/deletion affecting

chromosomes 2 and 7 in a father and his two children. The common denominator in all three patients was the heterozygous insertion of chromosome 2p21-p23 into chromosome 7q35-q36, the *CNTNAP2* chromosomal region (Verkerk et al., 2003). However, the father only presented with obsessive-compulsive disorder whereas the children additionally displayed Gilles de la Tourette syndrome and mental and growth retardation. After this discovery, many other cases with chromosomal rearrangements involving the *CNTNAP2* gene were reported. Since in many cases multiple genes were affected, straightforward conclusions regarding *CNTNAP2* gene alterations are not possible. However, the increasing bulk of case reports made it possible to determine that patients with mutations only for the *CNTNAP2* gene always present with a combination of following phenotypes: seizures, autistic traits, intellectual disability and language impairments (Rodenas-Cuadrado et al., 2014). *CNTNAP2* disruptions have also been more seldomly found in patients with schizophrenia, attention deficit hyperactivity disorder (ADHD) and developmental delay. All these data strongly suggest that *CNTNAP2* is involved in CNS neurodevelopmental diseases. Only one case of peripheral neuropathy, Charcot-Marie-Tooth disease, has been reported in two sisters with a duplication of exon 4 of *CNTNAP2* (Høyer et al., 2015).

Neurodevelopmental diseases linked with *CNTNAP2* mutations mainly know an early childhood onset and affect males in 61% of the cases (Saint-Martin et al., 2018). Most mutations are heterozygous, suggesting that disturbance of only one allele is sufficient to perturb CASPR2 function (Rodenas-Cuadrado et al., 2014). Important results came from an Old Order Amish family, in which 13 children presented with a homozygous mutation (3709delG) in exon 22, causing a frameshift which led to a premature stop codon (Strauss et al., 2006). The predicted protein is non-functional due to a lack of its intracellular and transmembrane domain (Strauss et al., 2006). All children presented with cortical dysplasia-focal epilepsy (CDFE) as primary symptom (Strauss et al., 2006), a neuronal migration disorder resulting in a complex syndrome of childhood onset epileptic seizures, mental retardation, language regression, hyperactivity and in two third of the patients ASD. The same mutation was found in a heterozygous manner in their parents and four other non-affected individuals, suggesting that homozygous mutations lead to a more severe clinical phenotype (Rodenas-Cuadrado et al., 2014; Strauss et al., 2006). Three more cases with homozygous deletions for *CNTNAP2* have been reported so far, all presenting with severe neurological disorders. In two cases the deletion caused a premature stop codon and patients presented with severe

intellectual deficiency and epilepsy as primary symptom (Rodenas-Cuadrado et al., 2016; Watson et al., 2014). In the third case the deletion caused loss of the N-terminal discoidin-like and laminiG-like domains and patients presented with Pitt-Hopkins-like mental retardation as primary symptom (Zweier et al., 2009). Interestingly, a higher rate of *CNTNAP2* deletions or duplications impacts the discoidin-like domain coding exons in patients presenting with neurological disorders and *CNTNAP2* mutations compared with the healthy population (Saint-Martin et al., 2018). This may be interesting regarding the fact that patients' autoAbs in anti-CASPR2 AILE are mainly directed against this domain.

Even though in literature the amount of cases presenting with *CNTNAP2* mutations and neurological disorders is increasing, there is reasonable doubt for a causal link between *CNTNAP2* gene disturbances and neurodevelopmental disorders (Poot, 2015, 2017; Rodenas-Cuadrado et al., 2014). First of all, its large gene size increases the probability of genetic alterations to occur. Secondly, heterozygous mutations have also been found in the healthy population, questioning the value of *CNTNAP2* mutations. Furthermore, the large spectrum of clinical phenotypes associated with *CNTNAP2* alterations make it difficult to assign a specific role for CASPR2 in these disorders. Therefore it has been proposed that *CNTNAP2* mutations may rather be a clinical risk factor in generating neurological disorders than a primary cause (Rodenas-Cuadrado et al., 2014). Given the highly evolutionary conservation of *CNTNAP2*, other authors suggested that the gene can be considered as a node in a combinatorial genetic network that regulates brain development, serving as a bridge to connect different cellular functions (Poot, 2015, 2017). Disrupting such important 'genetic bridges' that link several functions and interactions consequently gives rise to a variety of clinical phenotypes.

4.2 CASPR2 AND AUTISM SPECTRUM DISORDER (ASD)

Even though a direct causal link between *CNTNAP2* gene alterations and neurodevelopmental disorders remains doubtable and the clinical spectrum observed in patients with *CNTNAP2* mutations is large, particular attention has been invested in the association of CASPR2 and ASD. Initially described as a pure behavioral syndrome, it is now generally accepted that ASD is a phenotypically and genetically highly heterogenous neurodevelopmental disorder (Takumi et al., 2019). Interestingly the core characteristics found in ASD patients are the same as the main clinical phenotypes found for *CNTNAP2* mutations.

Patients suffering from ASD present with three core behavioral abnormalities visible at early age: social interaction impairments, language and communication deficits and repetitive, restricted sensory-motor behavior (APA, 2013). In mice knocked out for *Cntnap2* the same behavioral deficits are present starting at P3 (Peñagarikano et al., 2011). *Cntnap2*$^{-/-}$ mice emit less ultrasonic calls with their mother at birth and interact less with novel mice at P21. In the three-chamber social interaction test *Cntnap2*$^{-/-}$ mice do not show a preference of a novel mice over an object. The restricted and repetitive behavior is observed in the T maze test, where these mice show less alterations between the different arms. Moreover, grooming time is increased compared to wild-type (WT) littermates. Interestingly, epileptic seizures, hyperactivity and hypersensitivity to sensory stimuli, neurological features that are frequently associated with ASD, are also observed in *Cntnap2*$^{-/-}$ mice (Peñagarikano et al., 2011; Peñagarikano & Geschwind, 2012).

In addition to the behavioral similarities between the *Cntnap2*$^{-/-}$ model and ASD, the altered neurophysiological features observed in *Cntnap2*$^{-/-}$ mice further support the idea that CASPR2 disturbance could contribute to the pathology. Mice lacking CASPR2 show cortical neuronal migration abnormalities (Peñagarikano et al., 2011). First of all this strongly supports the hypothesis that *CNTNAP2* mutations and CDFE are linked (see chapter B.4.1) (Peñagarikano et al., 2011; Strauss et al., 2006). Secondly, neuronal migration is crucial for correct neuronal network formation, putting forward a role for CASPR2 in developing neurons (Peñagarikano et al., 2011; Peñagarikano & Geschwind, 2012). This proposed role is further supported by the observation that *Cntnap2*$^{-/-}$ mice display an asynchronous neuronal firing pattern, most likely due to network dysfunction (Peñagarikano et al., 2011). Electrophysiological studies also point out a role for CASPR2 in developing neuronal networks and will be discussed in chapter C.2.2.2. ASD is considered to be a cerebral dysconnectivity disorder, characterized by altered brain circuit connections as a result from anomalies that can occur at different brain developmental stages (Mohammad-Rezazadeh et al., 2016; Peñagarikano & Geschwind, 2012). Hence, given the function of CASPR2 in developing neuronal networks, its disturbance might contribute to the development of ASD. In addition, *Cntnap2*$^{-/-}$ mice display a decreased number of parvalbumin positive interneurons, most probably due to defects in their differentiation and/or activity (Peñagarikano et al., 2011; Vogt et al., 2018). This could lead to altered neuronal excitation/inhibition balance, another mechanism proposed to underly ASD physiopathology (Rubenstein & Merzenich, 2003). Furthermore, human CASPR2 is strongly

expressed in cortical areas implicated in higher evolved cognitive processes such as language, whose normal development is disturbed in ASD (Abrahams et al., 2007; Gordon et al., 2016). Interestingly, it has been shown that brain-reactive autoAbs can be more frequently found in mothers of children with ASD than in mothers of childbearing age or mothers of children without developmental disorders (Brimberg et al., 2013; Singer et al., 2007). For this reason, some recent studies have assessed the possibility of anti-CASPR2 autoAbs to cross the fetal BBB and cause ASD-like behavior and morphological features in the progeny. In a first study monoclonal anti-CASPR2 autoAbs cloned from a mother with an ASD child were injected *in utero* in pregnant mice (Brimberg et al., 2016). The progeny showed ASD-like behavior starting at 10-14 weeks of age. Interestingly, these mice presented with a decreased dendritic arborization and spines and decreased inhibitory interneurons, morphological features which are also present in CASPR2 KO mice (Anderson et al., 2012; Brimberg et al., 2016; Peñagarikano et al., 2011). Another study used a more biologically relevant maternal-to-fetal transfer mouse model, in which anti-CASPR2 autoAbs from two different patients with AILE were injected intraperitoneally in the pregnant mice (Coutinho et al., 2017). This study assessed the long-term effects of autoAbs on the progeny and consequently examined only adult mice. Similar results were found, with ASD-like behavior witnessed around 6-8 months old and morphological changes resembling the CASPR2 KO model, such as decreased cortical GluA1 density (Coutinho et al., 2017; Varea et al., 2015).

Intriguingly, in these studies, ASD-like behavioral and morphological features occurred more frequently in the male progeny than in the female progeny (Brimberg et al., 2016; Coutinho et al., 2017). This is in line with the fact that ASD mainly affects the male sex (Christensen et al., 2018). Interestingly, administration of estrogen agonists in zebrafish *cntnap2*$^{-/-}$ larvae suppresses the *cntnap2*$^{-/-}$ behavioral phenotype (Hoffman et al., 2016). In addition, we have shown in a recent paper that anti-CASPR2 AILE almost exclusively occurs in male patients (Joubert et al., 2016).

Altogether, foregoing data strongly suggest an implication of CASRP2 disturbance in ASD. They also point out a capacity of anti-CASPR2 autoAbs in generating ASD-like behavior. Interestingly, albeit by autoAbs or genetic alterations, perturbation of CASPR2 is more frequently observed in the male sex, which is in line with the higher prevalence of ASD in males.

CHAPTER C. CASPR2 AND THE SYNAPSE

1. THE SYNAPSE

1.1 SYNAPTIC TRANSMISSION

The human brain counts around 10^{11} neurons, each one of them participating in ~ 10 000 synaptic contacts (Garner et al., 2002). These synaptic contacts are functional contacts between neurons, rendering communication between both neurons possible. Depending on how the communication is performed, synaptic contacts can be categorized into electrical and chemical synapses (Purves et al., 2013). Electrical synapses pass the current between two cells directly via communicating channels. Chemical synapses transmit the presynaptic AP to the postsynaptic neuron in form of neurotransmitters (NTs). The neuronal AP causes depolarization of the presynaptic terminal, followed by opening of voltage gated calcium (Ca^{2+}) channels and entering of Ca^{2+} into the presynaptic bouton. The entered Ca^{2+} causes fusion of vesicles, containing NTs, with the presynaptic membrane, releasing more than a hundred NT molecules into the synaptic cleft, a small space between the pre- and postsynaptic membrane. In the synaptic cleft, NTs bind with postsynaptic membrane receptors, located at the postsynaptic density (PSD), a highly specialized structure for neuronal transmission. Subsequently, postsynaptic electrical responses are generated and transmitted through the neuron.

Depending on the NT released, synapses can be excitatory, inhibitory or modulatory in nature. Excitatory synapses use glutamate as NT and are formed on dendritic spines, whereas inhibitory synapses use γ-aminobutyric acid (GABA) or glycine as NT and occur on dendritic shafts and cell bodies **(Figure 21)**. Modulatory NTs are not restricted to the synaptic cleft and involve for example dopamine, acetylcholine, neuropeptides and many others. They are beyond the scope of this manuscript and will not be discussed.

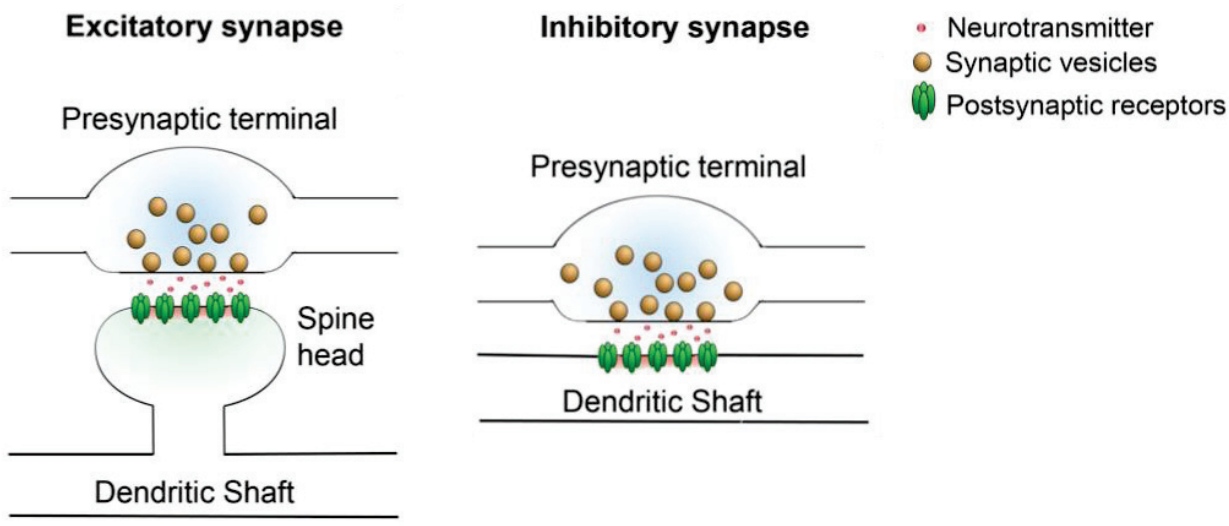

Figure 21. Schematic global representation of excitatory and inhibitory synapses *(adapted from Arikkath, 2012)*. Excitatory synapses are formed by a presynaptic terminal contacting a dendritic spine, a protrusion of the dendritic shaft (left). Inhibitory synapses are formed by a presynaptic terminal contacting the dendritic shaft directly (right). Presynaptic terminals contain synaptic vesicles, which release their contained neurotransmitters in the synaptic cleft. The released neurotransmitters bind to postsynaptic receptors.

1.2 EXCITATORY SYNAPSES

The majority of existing synapses are excitatory, and use glutamate as NT. The glutamate released in the synaptic cleft can bind with different kinds of receptors: ionotropic or metabotropic receptors (Dingledine, 1991; Traynelis et al., 2010). Ionotropic receptors are ligand-gated ion channels, where binding of the ligand induces a conformational change of the ion channel, causing the transmembrane pore to open or close. They are divided into three classes, depending on their pharmacology and structural homology: α-amino-3-hydroxy-5-methyl-4-isoxazolepropionic acid receptors (AMPA-Rs), NMDA-Rs and kainate receptors (KA-Rs). Metabotropic receptors on the other hand are G-protein coupled receptors. Only the metabotropic glutamate receptor (mGluR) belongs to this group.

Glutamate receptors are mainly located at the PSD of postsynaptic dendritic spines (see chapter C.1.2.3 and C.1.2.4). However, they can also be found in presynaptic nerve terminals to regulate vesicular glutamate release (Meir et al., 1999), perisynaptically (i.e. the direct synaptic environment) (Zhang & Diamond, 2006) and extrasynaptically (Traynelis et al., 2010). Even though in this work not all types of excitatory receptors have been the subject in our studies, I estimate it important to have a basic description of the current understanding of the

existing different receptors to be capable of placing my obtained results in a global context. Therefore, I will describe briefly all excitatory receptors, with a main focus on the AMPA-R and the NMDA-R.

1.2.1 IONOTROPIC GLUTAMATE RECEPTORS

Ionotropic glutamate receptors are large integral membrane proteins, forming tetramers, with each subunit counting over 900 amino acids (Traynelis et al., 2010). The four subunits form a central pore for ion passage upon ligand binding. Each subunit functions in a semiautonomous way with respect to the other subunits and consists of following domains: the extracellular amino-terminal domain, the extracellular ligand-binding domain, the transmembrane domain, which consists in three membrane spanning domains and one re-entrant domain, and an intracellular carboxyl-terminal domain (Traynelis et al., 2010) **(Figure 22)**.

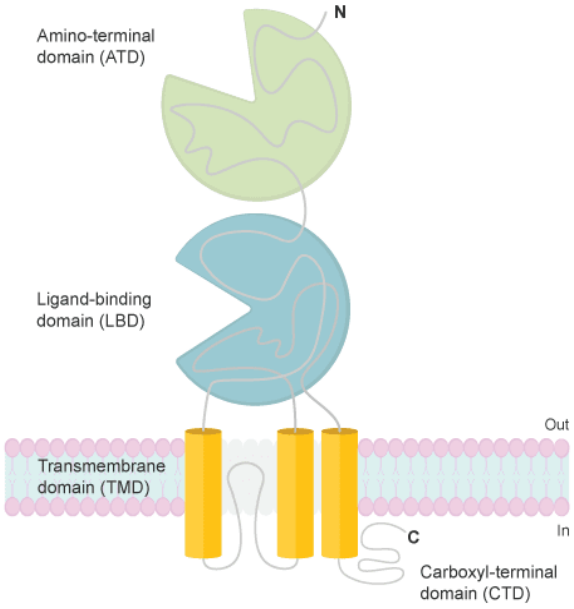

Figure 22. Schematic representation of the ionotropic glutamate receptor subunit *(adapted from Traynelis et al., 2010)*. Each subunit from ionotropic glutamate receptors contains an extracellular amino-terminal domain (ATD), followed by a ligand-binding domain (LBD). The transmembrane domain (TMD) is built of three membrane spanning domains and one reentrant loop. The intracellular carboxy-terminal domain (CTD) is attached to the last membrane spanning domain.

1.2.1.1 THE α-AMINO-3-HYDROXY-5-METHYL-4-ISOXAZOLEPROPIONIC ACID RECEPTOR (AMPA-R)

AMPA-Rs, in contrast with NMDA-Rs, mediate fast excitatory transmission in the CNS (Jacobi & von Engelhardt, 2018). They exhibit low affinity for glutamate and the channel pore is permeable for Na^+ and K^+ ions.

The subunits forming the AMPA-R include GluA1, GluA2, GluA3 and GluA4 (also known as GluR1-GluR4). They can assemble into homo or heterotetramers, but mostly occur as tetramers of two dimers from the same subunit (dimers of dimers) (Mansour et al., 2001). The different subunit composition is a major player in functional channel properties and depends on multiple factors such as brain region, cell type and developmental stage (Schwenk et al., 2012). Immunoprecipitation experiments demonstrated that hippocampal pyramidal neurons consist in two major populations of AMPA-Rs: mainly tetramers of GluA1/2 followed by tetramers of GluA2/3 (Wenthold et al., 1996). The GluA4 subunit is only expressed during the first 10 postnatal days in the hippocampus, and is replaced by the GluA2 subunit in an activity dependent manner (Zhu et al., 2000).

AMPA-Rs play an important role in synaptic transmission, strength and stabilization. Their number at the synapse is positively correlated with synaptic strength (Jacobi & von Engelhardt, 2018). AMPA-R surface expression at the synapse is regulated by exo- and endocytosis. Inhibition of AMPA-R exocytosis at the synapse or disrupting the GluA2 subunit causes a decrease in the amplitude of AMPA-R excitatory postsynaptic currents (EPSCs), whereas inhibition of endocytosis provokes the inverse effect (Lüscher et al., 1999). Importantly, given the low affinity of AMPA-Rs for glutamate, a precise localization at the postsynaptic membrane, with respect to the presynaptic terminal and glutamate release sites, is necessary (Nair et al., 2013).

Superresolution imaging has pointed out nanodomains in which AMPA-Rs are concentrated instead of being diffused at the PSD (see chapter C.1.2.3) (Nair et al., 2013). These concentrations of AMPA-Rs are stabilized at the synapse by interaction with MAGUKs, the most important being PSD95, via the AMPA-R auxiliary subunit stargazin (Bats et al., 2007; Santos et al., 2009). Stabilization takes place during development, together with synapse formation and maturation. More importantly, these receptors show increased lateral diffusion of the extrasynaptic receptor pool with increased synaptic activity, indicating that AMPA-R mobilization at the synapse is regulated by neuronal activity (Groc et al., 2004). NMDA-R

mobility was not affected in this study, which fits with the hypothesis that during synaptic maturation activation of the NMDA-R stabilizes previously 'silent' or labile AMPA-Rs at the synapse, favoring neuronal transmission (Groc et al., 2006).

1.2.1.2 THE N-METHYL-D-ASPARTATE RECEPTOR (NMDA-R)

NMDA-Rs exhibit some unique properties, which will be described hereafter, that distinguish them from other glutamate receptors. As for AMPA-Rs, subunit composition is critical for biophysical and pharmacological channel properties. Seven different subunits exist, categorized into three subfamilies depending on their sequence homology: GluN1, GluN2 (containing GluN2A, GluN2B, GluN2C and GluN2D) and GluN3 (containing GluN3A and GluN3B). Together they form heterotetramers, consisting in two obligatory GluN1 subunits and two GluN2 subunits or a combination of GluN2 and GluN3 subunits (Paoletti et al., 2013). Importantly, the NMDA-R subunit composition changes during development throughout the brain (Paoletti et al., 2013). The most important subunit switch is the one from GluN2B to GluN2A. This spatiotemporal plasticity depends on neuronal activity and sensorial experience and is crucial in remodeling the neuronal network and adaptation to precedent events (Dumas, 2005). Growing evidence shows that this subunit plasticity also takes place at mature synapses, where it is the neuronal correlate of efficient information encoding and storage (Hunt & Castillo, 2012).

NMDA-Rs show high affinity for glutamate, but channel activation requires binding of glutamate together with a co-agonist, glycine or D-serine (Johnson & Ascher, 1987; Kleckner & Dingledine, 1988). The requirement of a co-agonist adds a regulatory level to NMDA-R mediated synaptic activity (Hansen et al., 2018). Moreover, the subunits of NMDA-Rs contain binding sites for positive or negative allosteric modulators, such as protons, zinc ions and polyamines, adding another regulatory level to these receptors (Paoletti et al., 2013). The channel pore itself is permeable for Na^+ and K^+ but mostly for Ca^{2+} ions. However, in its resting state the pore is subjected to a voltage dependent block by Mg^{2+}, which is released by membrane depolarization (Mayer & Westbrook, 1987; Nowak et al., 1984). Furthermore, NMDA-R activation requires this membrane depolarization to be simultaneous with glutamate release. Altogether, the specific requirements for NMDA channel activation allow NMDA-Rs to function as 'co-incidence' detectors of presynaptic NT release and postsynaptic depolarization (Tabone & Ramaswami, 2012).

NMDA-Rs mediate EPSCs with a slow activation and longer duration compared with AMPA-Rs (Gibb & Colquhoun, 1992). This contributes to their important role in long-term potentiation (LTP) and long-term depression (LTD), an activity-dependent increase or reduction respectively in synaptic strength over time (Hansen et al., 2018; Traynelis et al., 2010).

All these specific properties of NMDA-Rs make them capable of transforming neuronal activity patterns into long-term synaptic morphological and structural changes, most possibly underlying higher cognitive functions (Paoletti et al., 2013). The description of these processes is outside the scope of this work.

1.2.1.3 THE KAINATE RECEPTOR (KA-R)

The KA-R has been less studied than AMPA-Rs and NMDA-Rs because of the lack of adequate pharmacological tools. After obtaining the required pharmacological agents, it has become clear that the KA-R is a unique receptor, with a very complex signaling. The channel pore is permeable for Na^+ and K^+, and ranges from Ca^{2+} permeable to non-permeable, depending on small differences in subunits (Evans et al., 2019; Traynelis et al., 2010). Five subunits exist, from GluK1 to GluK5. GluK1-3 show low affinity for kainate and form homotetramers or heterotetramers. GluK4-5 on the other hand show high affinity for kainate but can only form functional heterotetramers with low-affinity subunits.

KA-Rs are considered “modulatory” receptors. In contrast with AMPA-Rs and NMDA-Rs, their main role does not lie in excitatory transmission (Contractor et al., 2011). This is reflected in the distribution of KA-Rs, which is ubiquitous in the CNS (Bahn et al., 1994). KA-Rs can be found presynaptically, where they modulate inhibitory and excitatory NT release (Huettner, 2003). Postsynaptically they only appear in a subset of excitatory neurons, to mediate excitatory neurotransmission (Huettner, 2003; Sihra et al., 2014). Finally, they are also located extrasynaptically, where they finetune and enhance neuronal excitability (Contractor et al., 2011). Interestingly, a small fraction of KA-Rs can be found coupled to G-protein mediated signaling pathways, thus acting as metabotropic receptors (Rodríguez-Moreno & Lerma, 1998). Given their role as modulating receptors of neurotransmission, it is not surprising that they are implicated in short and long-term plasticity (Jane et al., 2009; Sihra et al., 2014).

1.2.2 METABOTROPIC GLUTAMATE RECEPTORS

Metabotropic glutamate receptors (mGluRs) are G-protein coupled receptors. Binding of glutamate activates a signaling cascade, which depends on the type of receptor. Eight different mGluR subtypes exist, all exhibiting the same general structure: an N-terminal extracellular glutamate binding Venus fly-trap domain, a cysteine-rich domain, seven transmembrane domains and an intracellular carboxy terminal domain (Conn, 1997) **(Figure 23)**. This last domain modulates G- protein coupling, receptor signaling and trafficking (Suh et al., 2018).

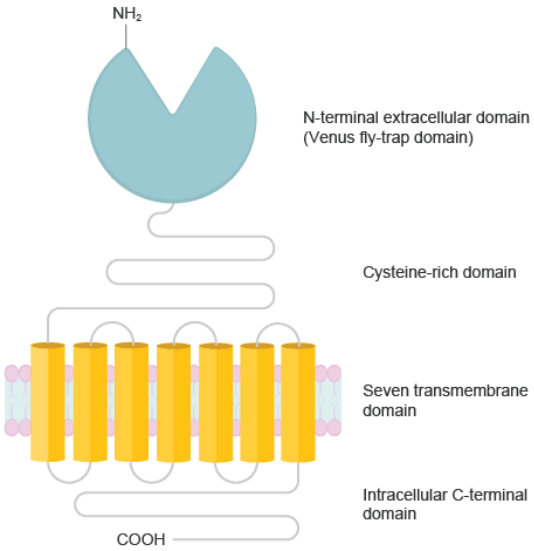

Figure 23. Schematic representation of the metabotropic glutamate receptor *(adapted from Kenny & Markou, 2004)*. Metabotropic glutamate receptors all contain an extracellular N-terminal Venus fly-trap domain followed by a cysteine-rich domain. The transmembrane domain consists of seven transmembrane helices which is followed by an intracellular C-terminal domain.

MGluRs can be divided into three different groups, depending on their pharmacological properties, sequence homology and second messengers (Suh et al., 2018; Willard & Koochekpour, 2013). Group I contains mGluR1 and mGluR5, their activation causes stimulation of phospholipase C and subsequent increase in intracellular Ca^{2+} concentration and activation of protein kinase C. MGluR2 and mGluR3 belong to group II whereas mGluR4, mGluR6, mGluR7 and mGluR8 belong to group III. They share the same signaling pathway but are different in their agonist preferences. Activation of these two groups causes an inhibition of adenylate kinase C, causing a decrease in cAMP which in its turn causes activation of protein kinase A. The signaling cascades following the mentioned initial canonical pathways are far more complex (Willard & Koochekpour, 2013).

MGluRs form functional homo or heterodimers which are present in all CNS areas, except for mGluR6, which is found exclusively in the retina (Doumazane et al., 2011; Suh et al., 2018). Additionally, mGluR3 and mGluR5 can also be found on the glial surface (Aronica et al., 2003; Schools & Kimelberg, 1999). As for the other glutamatergic receptors, all mGluRs are involved in neuronal excitability, synaptic transmission and plasticity throughout the CNS. Group I is situated postsynaptically, whereas group II and III are located presynaptically (Suh et al., 2018). Group II is found further away from glutamate release sites, whereas group III is present at the presynaptic active zone. These presynaptic mGluRs have a rather modulatory and fine tuning role in neuronal transmission and generally depress NT release (Pinheiro et al., 2008).

1.2.3 THE POSTSYNAPTIC DENSITY (PSD)

NTs released from the presynaptic neuron enter the synaptic cleft to bind with postsynaptic receptors. These receptors are attached to the PSD, a highly specialized structure located beneath the postsynaptic membrane, crucial for synaptic transmission and efficacy (Boeckers, 2006). The PSD was first discovered by electron microscopy as a fuzzy, electron-dense postsynaptic zone (Gray, 1959). It appears as a thick, disc-shaped structure, present immediately underneath the postsynaptic membrane of both inhibitory and excitatory synapses **(Figure 24)**. However, PSD dimensions are more important in excitatory synapses, where they show a range in thickness from ~ 30 to 50 nm compared with ~ 12 nm for inhibitory synapses (Tao et al., 2018) **(Figure 24)**.

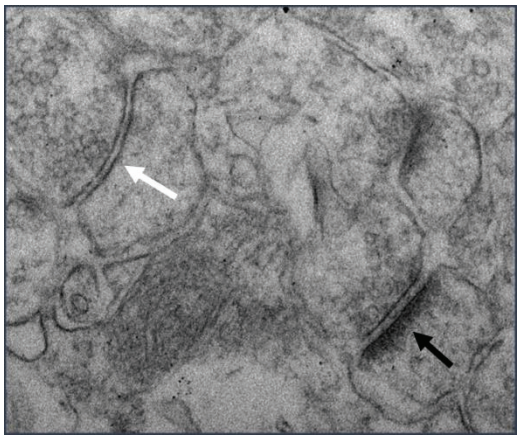

Figure 24. Electron microscopy image of the inhibitory and excitatory PSD. The postsynaptic density (PSD) occurs as a fuzzy, electron-dense zone immediately beneath the postsynaptic membrane. The PSD is less thick and nearly indistinguishable from the postsynaptic plasmamembrane for inhibitory synapses (white arrow) whereas it can clearly be seen as a dense, dark zone in excitatory synapses (black arrow).

In order to execute its important role in neuronal signaling, the PSD shows a mesh-like structure highly enriched in a variety of proteins which can be categorized in membrane receptors and ion channels, cell-adhesion proteins, scaffolding and adaptor proteins, signaling molecules such as kinases and phosphatases and cytoskeletal proteins (Boeckers, 2006) **(Figure 25)**. The prototype and one of the most characterized proteins of the PSD is the MAGUK PSD95. Via its PDZ domain it binds to AMPA-Rs and NMDA-Rs, anchoring and stabilizing them at the postsynaptic membrane (Petralia et al., 2005) **(Figure 25)**. As for other MAGUKs present, the interaction of PSD95 with membrane receptors also regulates their surface expression.

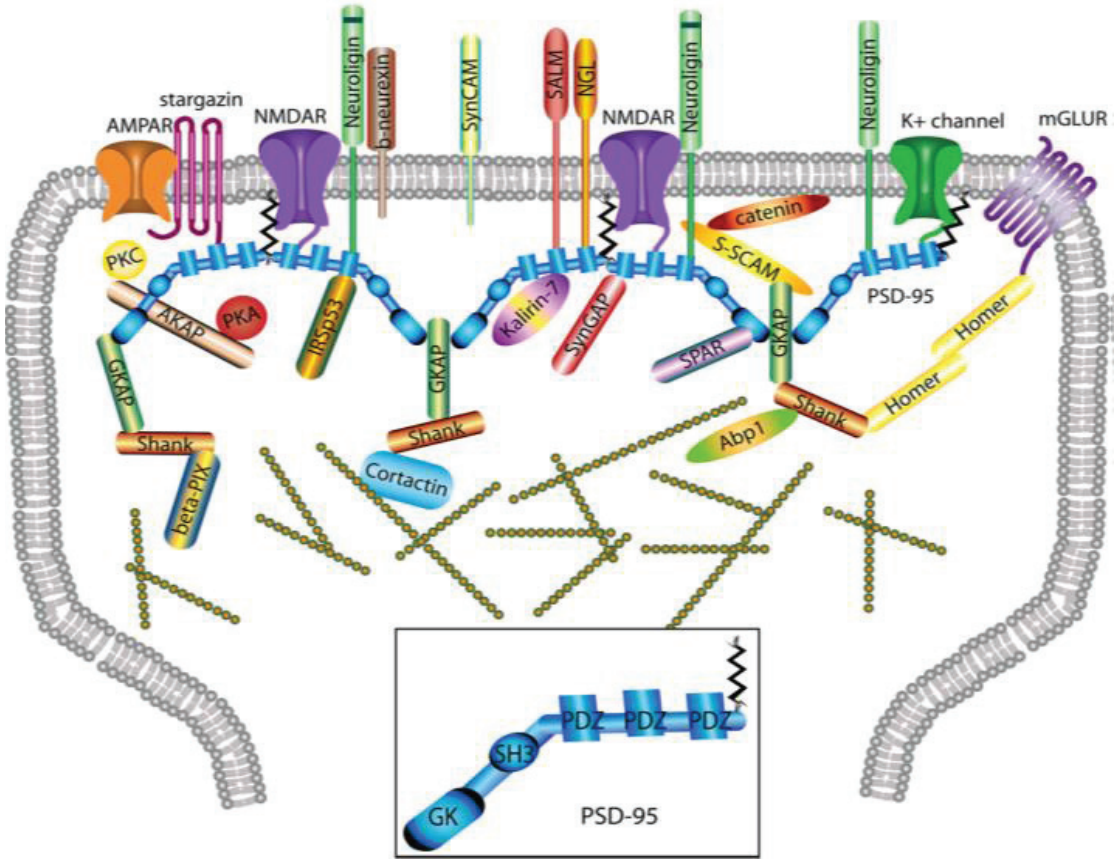

Figure 25. Molecular composition of the PSD *(adapted from Keith & El-Husseini, 2008).* The PSD contains a variety of proteins, involved in synaptic functioning, morphology, trafficking, signaling and anchoring of molecules and receptors. The main receptors, ion channels, cell-adhesion proteins, signaling molecules and scaffolding and anchoring proteins are represented. PSD95 is the main scaffolding protein of the PSD and binds many different proteins. An important domain is the PDZ domain, allowing anchoring and stabilization of the NMDA-R and the AMPA-R, via stargazin, at the postsynaptic membrane. Other proteins can bind the PDZ domain as well.

1.2.4 DENDRITIC SPINES

At the level of excitatory synapses, the postsynaptic compartment forms small protrusions of the dendritic membrane. These protrusions were discovered by Ramón y Cajal in 1888 and referred to as dendritic spines. Dendritic spines can be found in a certain type of neurons, such as pyramidal neurons in the cortex, Purkinje cells in the cerebellum, medium spiny neurons in the basal ganglia and pyramidal and granule cells in the hippocampus (Harris & Weinberg, 2012; Kasai et al., 2010). They consist of a spine neck and a spine head. The PSD is present at the top of the spine head and occupies ~ 10% of the total spine head volume (Harris & Stevens, 1989). The cytoskeleton lies underneath the PSD and is mainly built of F-actin, on which proteins attach to ensure the structure of the spine (Okabe, 2007).

Depending on their morphology dendritic spines can be artificially categorized into different spine classes **(Figure 26)**: filopodia, long fine spines without a spine head; stubby spines, small protrusions where distinction between spine head and neck is not possible; thin spines, which have a long and narrow neck followed by a small head, and mushroom spines, which have a short neck and a large head (Jones & Powell, 1969; Peters & Kaiserman-Abramof, 1970). This categorization is artificial, in this meaning that spine morphology is not static but shows a dynamic rearrangement over time, occurring in a timespan from seconds to minutes (Parnass et al., 2000). Spines are considered the molecular correlate of learning and memory, and undergo morphological changes depending on neuronal transmission (Harris & Stevens, 1989; Harris, 1999; Harris et al., 1992). Indeed, with increased synaptic transmission, spines evolve from a stubby to a thin spine into a mushroom spine. An important linear structure-function relationship between the PSD and spine morphology exists (Harris & Jensen, 1992). During the development into a stabile mushroom spine, the spine head expands. Consequently, the PSD and its content increase **(Figure 26)**. During this process the surface expression of the AMPA-R increases and is dependent from the NMDA-R (Nusser et al., 1998; Takumi et al., 1999). These synaptic rearrangements, referred to as “synaptic plasticity”, occur with increased synaptic strength and are the molecular correlates of learning and memory.

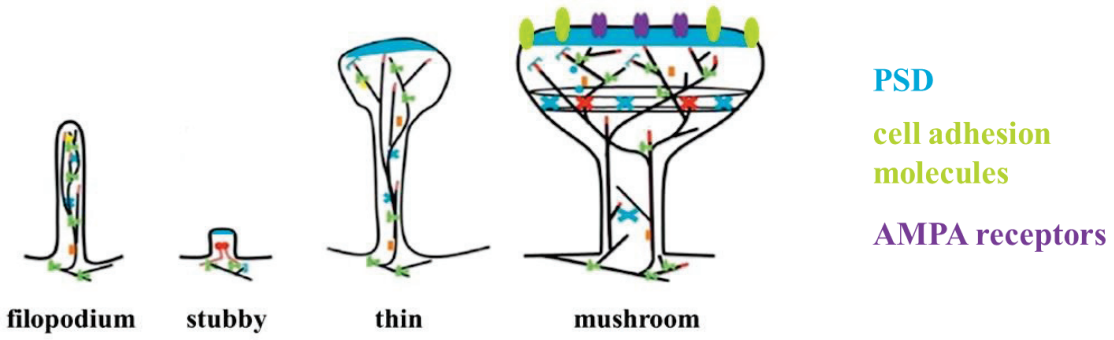

Figure 26. Spine class morphologies *(adapted from Hotulainen & Hoogenraad, 2010).* During their development, spines undergo morphological changes, allowing artificial division into different spine classes. Filopodia are long spines without a spine head, stubby spines are short spines with an equal neck length and head width, thin spines are long, narrow spines with a small spine head and mushroom spines are large spines with a short neck and a big spine head. With increased neuronal transmission, the spine head increases, together with the PSD, its content and surface AMPA receptors. Cell adhesion molecules attach postsynaptic dendritic spines to the presynaptic compartment.

The role of filopodia is not entirely clear yet. Most studies consider these spines to be short-living spines, initiating synaptogenesis by contacting facing axons (Fiala et al., 1998; Holtmaat et al., 2005; Saito et al., 1992). However, different models of synaptogenesis involving spines, called spinogenesis, are proposed which are not necessarily mutually exclusive (Yuste & Bonhoeffer, 2004) **(Figure 27).** The Sotelo model proposes that spine development is independent from the facing axon and thus intrinsically regulated. According to the Miller/Peters model the presynaptic axon terminal contacts the dendritic shaft and triggers spinogenesis. The filopodial model is derived from Vaughn's synaptotropic hypothesis, which postulates that filopodia 'search' a facing axon to attract it towards the dendrite. Upon this attraction the axon develops a presynaptic terminal and the filopodium develops into a stabile spine.

On the other hand, while some spines get stabilized into a highly active mushroom spine, others get removed, which is called synaptic pruning (Colman et al., 1997; Holtmaat et al., 2005; Rakic et al., 1986). The removal of unnecessary synapses is accompanied by a morphological shrinking of the spine and reduced synaptic strength. This process is necessary to refine connections and is presumed to be necessary for optimizing learning and memory processes.

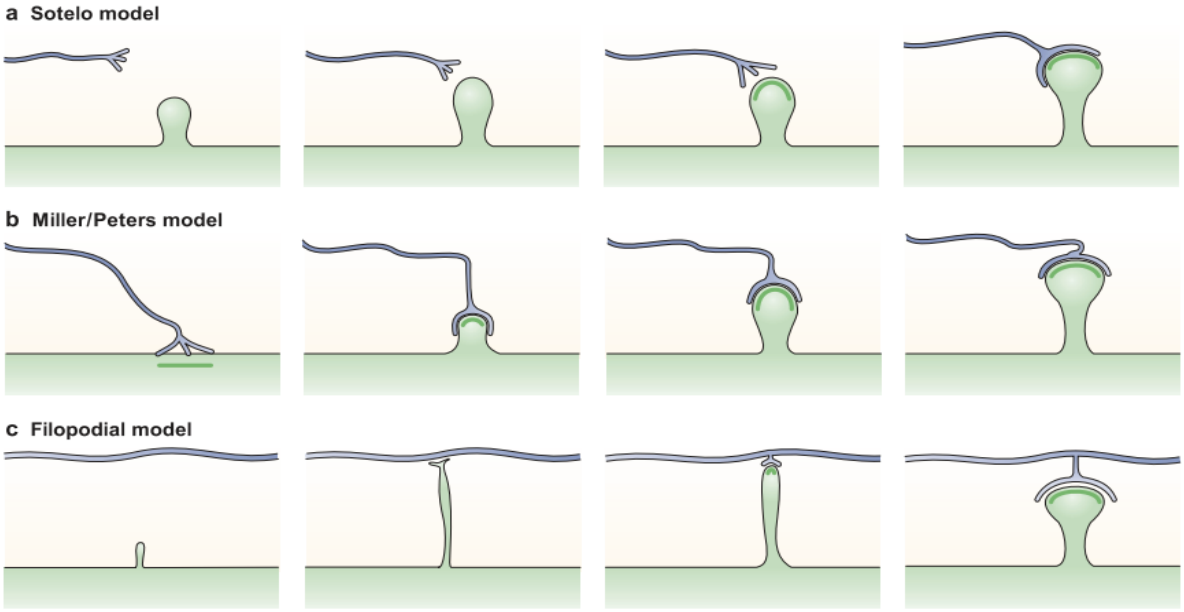

Figure 27. Different models of spinogenesis *(Yuste & Bonhoeffer, 2004).* **A)** In the Sotelo model the spine directly emerges from the dendritic shaft, independently from the facing axon. The spine further develops and gets contacted after initial development by a presynaptic axon terminus. **B)** The Miller/Peters model suggests an initial contact of the dendritic shaft by the presynaptic axon terminal, allowing the outgrowth of a dendritic spine which then further develops into a mature spine. **C)** In the filopodial model a small dendritic protrusion develops into a filopodium that 'searches' for a presynaptic axon. Upon contact, the axon develops a presynaptic terminal and the filopodium matures into a stable spine.

Spine size, shape and number vary highly depending on many factors such as species studied, age, time, brain area and neuron type. Comparison between different studies is extremely tricky since several parameters influence the results, ranging from basic setups (e.g. *in vitro* versus *in vivo*) to detailed experimental processes (e.g. seeding density in *in vitro* studies). Since categorization is mainly based on subjective visual detection, high variability between different observers, and even for one same observer, occurs. One *in vitro* study even showed highly variable results amongst three repeated experiments with the exact same experimental setup (Jammalamadaka et al., 2013). The majority of studies however do not categorize spines based on visual detection, but use (semi)automatic detections, with spine classifications based on measured parameters such as spine head width and neck length. However, up to date no consensus has been proposed for mathematical calculations in order to categorize spines into different spine classes. This adds another degree of complexity to the direct comparison of results obtained in for example different laboratories. Moreover, since spine shapes are a continuum, not all detected shapes can be categorized. This non-classifiable spine fraction can account for up to 30% of total spines (Harris et al., 1992). Here as well, no consensus has been

established about whether to consider this fraction for calculations of the total and subclass spine density or not.

It may thus be clear that absolute numbers related to spine dimensions and classes should be interpreted with caution and are not very useful for comparison between studies. However, some generalities can be deduced out of the many studies performed. Spine dimensions generally range from ~ 0.04 to 0.5 µm for spine neck diameter and ~ 0.2 to 2.0 µm for spine neck length, although neck diameters and lengths up to 1.0 µm and 6.50 µm respectively can be found in the CA3 hippocampal area (Chicurel & Harris, 1992; Sorra & Harris, 1999). The spine head width measures approximately 0.1 to 1.6 µm (Bourne & Harris, 2011). Mature dendrites show spine densities ranging from 1 to 10 spines/µm (Sorra & Harris, 1999). Early spines mainly consist in filopodia, whose density decreases during spine maturation. This is accompanied with an overall increase in spine density, increase in spine head width and decrease in spine neck length (Harris et al., 1992; Sorra & Harris, 1999).

1.3 INHIBITORY SYNAPSES

Inhibitory transmission is required to dampen excitatory activity, control neuronal transmission and synchronize neuronal networks. The NTs of the inhibitory synapse are GABA and glycine, which bind the GABA receptor (GABA-R) and glycine receptor (GlyR) respectively. As for glutamatergic receptors, these receptors occur mainly postsynaptically, but can also be localized presynaptically. In contrast with the excitatory synapse, inhibitory synapses occur on dendritic shafts and cell bodies. They do not exhibit postsynaptic dendritic spines to rely on for structural organization and stability. Therefore, the cytoskeleton and scaffolding proteins play an important role in maintaining structural and functional integrity of the inhibitory synapse (Groeneweg et al., 2018). The major scaffolding protein of the inhibitory postsynaptic element is gephyrin.

For the same reason mentioned for the excitatory receptors, I will briefly describe all inhibitory receptors, with a focus on the $GABA_A$-R.

1.3.1 THE γ-AMINOBUTYRIC ACID RECEPTOR (GABA-R)

Two types of GABA-Rs exist: the ionotropic $GABA_A$-R and the metabotropic $GABA_B$-R.

1.3.1.1 THE IONOTROPIC $GABA_A$-R

The $GABA_A$-R belongs to the Cys-loop receptor family, for which members all share the same pentameric structure of five subunits forming a central pore. Each $GABA_A$-R subunit contains approximately 450 amino acids and roughly half of the subunit is located extracellularly at the N-terminus (Sigel & Steinmann, 2012). The N-terminus is followed by four transmembrane helices, containing a short intracellular loop between helix 1 and 2, and a large intracellular loop between helix 3 and 4 (Tretter et al., 2012) **(Figure 28)**. These loops are the only possible intracellular interaction points. It is the transmembrane helix 2 of each subunit that forms the ion pore. The short C-terminus is located extracellularly **(Figure 28)**.

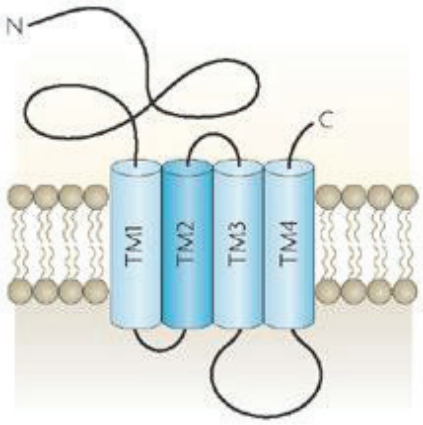

Figure 28. Schematic representation of the $GABA_A$ receptor subunit *(Jacob, Moss, & Jurd, 2008)*. Each subunit of the $GABA_A$-R has a long extracellular N-terminus followed by four transmembrane (TM) helices. TM1 and TM2 are connected by a short intracellular loop, TM2 and TM3 by a short extracellular loop and TM3 and TM4 by a long intracellular loop. The short extracellular C-terminus follows after TM4.

Binding of GABA changes the conformation of the receptor, causing the ion pore to open (Sigel & Steinmann, 2012). The pore is permeable for chloride ions (Cl^-) and entrance of these ions causes hyperpolarization of the neuronal membrane. A slight permeability of the pore for bicarbonate anions is observed as well (Kaila et al., 1989). However, the precise mechanism behind pore opening has not been resolved yet, due to absence of an established crystal structure for the $GABA_A$-R. Currently, the only resolved crystal structure is for the homopentameric $GABA_A$-R consisting only in the β_3-subunit.

$GABA_A$-Rs show a complex pentameric organization. 19 subunit classes are identified from eight subunit types: six α-subunits, three β-subunits, three γ-subunits, three ρ-subunits and one δ, ε, θ and π-subunit (Kasaragod & Schindelin, 2018; Sigel & Steinmann, 2012). As for all

receptors, subunit composition regulates functional and structural properties of the receptor. It has been generally accepted that, especially in adults, the major isoform consists of two α, two β and one γ or δ-subunit (Kasaragod & Schindelin, 2018). Certain subunits show a preferential extrasynaptic localization, such as the α4-6 and the δ-subunit, whereas others, including the α1-3, β2-3 and γ2-subunit, are rather postsynaptically localized (Kasaragod & Schindelin, 2018; Sigel & Steinmann, 2012).

The majority of GABAergic transmission is mediated by the $GABA_A$-Rs, who are responsible for fast, high-amplitude inhibitory responses in the CNS (Tyagarajan & Fritschy, 2014). However, depending on their localization they give rise to different types of inhibition (Farrant & Nusser, 2005). Postsynaptic $GABA_A$-Rs respond quickly in reaction to sudden high GABA concentrations released from presynaptic vesicles (Kasaragod & Schindelin, 2018; Sigel & Steinmann, 2012). This causes a quick but transient inhibitory postsynaptic current (IPSC) and is known as phasic inhibition. On the other hand, extrasynaptic $GABA_A$-Rs are exposed to lower, ambient GABA concentrations, causing these receptors to open for longer timespans and creating the so-called tonic inhibition (Kasaragod & Schindelin, 2018; Sigel & Steinmann, 2012).

1.3.1.2 THE METABOTROPIC $GABA_B$-R

The metabotropic $GABA_B$-R is a functional heterodimer formed by the subunits $GABA_{B1}$ and $GABA_{B2}$. The $GABA_{B1}$ subunit binds orthosteric ligands, which mostly resemble the structure of GABA, whereas the $GABA_{B2}$ subunit is coupled to the inhibitory G protein (Frangaj & Fan, 2018; Mott, 2014). The $GABA_{B1}$ subunit knows two primary isoforms: $GABA_{B1a}$, which is located presynaptically, and $GABA_{B1b}$, which is located postsynaptically (Heaney & Kinney, 2016). Postsynaptic $GABA_B$-Rs cause the inhibitory effect by hyperpolarization, whereas presynaptic $GABA_B$-Rs decrease NT release (Mott, 2014). Each subunit shows the same composition as for the metabotropic mGluRs: an extracellular Venus flytrap domain, seven transmembrane helices and an intracellular C-terminal domain **(Figure 23)**.

Due to their coupling to the G-protein, the $GABA_B$-Rs show a variety of effector mechanisms. However, they are always involved in responses leading to slow, longer lasting inhibition, which can maintain up to seconds (Frangaj & Fan, 2018; Mott, 2014). Therefore, they are considered modulatory GABA-Rs. Several studies have shown their implication in LTP. A

general conclusion of all these studies is that blocking the $GABA_B$-R enables synaptic plasticity and LTP whereas activation of the $GABA_B$-R inhibits these processes (Heaney & Kinney, 2016).

1.3.2 THE GLYCINE RECEPTOR (GLYR)

The glycine receptor (GlyR) is, as the $GABA_A$-R, a member of the Cys-loop receptor family, hence sharing the same pentameric organization and individual general subunit structure as described previously **(Figure 28)**. However, the subunits composing the GlyR are different. Two subunits exist: the α-subunit and the β-subunit. Four isoforms of the α-subunit exist (α1-4) but no different isoforms of the β-subunit have been identified yet (Dresbach et al., 2008). The GlyR either forms a homopentamer consisting of only α-subunits, or a heteropentamer composed in three α and two β or two α and three β-subunits (Lynch et al., 2017).

For long time it was believed that the GlyR was only expressed in the spinal cord and brainstem, where it mediates responses related to locomotor activity and spinal reflexes, and in the retina (Legendre, 2001). However, it has become clear that the GlyR is also largely expressed in the CNS, where it mediates fast inhibitory transmission.

During development, a switch from homomeric α2 pentamers to mainly pentamers containing the α1 and α3-subunit is observed. Studies have suggested that homomeric pentamers are presynaptic, controlling glycine, GABA and glutamate release, whereas heteromeric GlyRs are rather located postsynaptically (Deleuze et al., 2005; Lynch, 2009). This is still a matter of debate. The majority of studies however has been focused on the pharmacological properties of the spinal GlyRs. Their role in inhibitory synaptic transmission at this anatomical site opens many windows for therapeutic approaches (Lynch et al., 2017).

1.3.3 GEPHYRIN

1.3.3.1 STRUCTURAL ORGANIZATION

Gephyrin was first discovered as a 93 kDa tubulin-binding protein co-immunoprecipitating with the GlyR (Kirsch et al., 1991). Later it was shown to be present as well together with $GABA_A$-Rs (Sassoè-Pognetto et al., 1995). Gephyrin binds the long intracellular loop between transmembrane 3 and 4 of the inhibitory receptors. Binding with the GlyR occurs only via its β-subunit, whereas for the $GABA_A$-R binding has been shown with postsynaptic receptors

containing the α1, α2, α3 or α5-subunit and possibly the β2 or β3-subunit (Kasaragod & Schindelin, 2018). Although gephyrin does not bind directly with the γ2-subunit, this subunit has been shown to be indispensable for $GABA_A$-R and gephyrin clustering (Essrich et al., 1998). The binding affinity of gephyrin for the GlyR is around 10 times higher than for the $GABA_A$-R, which has important structural and functional consequences (Maric et al., 2014).

Gephyrin is composed of three domains: the N-terminal G-domain, the middle C-domain and the C-terminal E-domain which binds the receptor subunit (Tyagarajan & Fritschy, 2014) **(Figure 29A)**. The G and E-domain are stable 3D structures, whereas the C-linker domain is intrinsically unstructured. This allows for high flexibility of gephyrin molecules **(Figure 29B)**. Moreover, gephyrin can multimerize with other gephyrin molecules via its G- and E-domains. The E-domains dimerize whereas the G-domains trimerize, creating dodecamers **(Figure 29B)**. The final result of all the assembled gephyrin molecules is a dense planar hexagonal lattice (Kasaragod & Schindelin, 2018) **(Figure 29A)**.

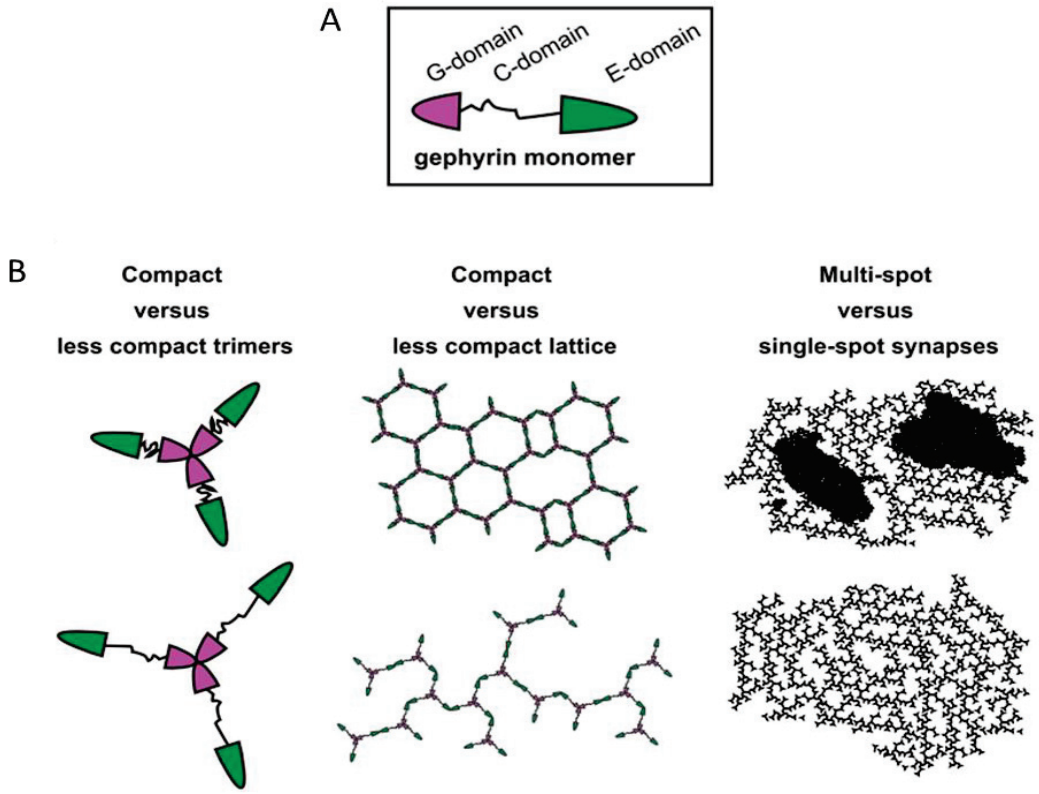

Figure 29. Structure and organization of the synaptic gephyrin lattice *(Groeneweg et al., 2018).* **A)** The gephyrin monomer consists in an N-terminal G-domain, followed by an intrinsically unstructured linking C-domain and a C-terminal E-domain. **B)** The gephyrin G-domains can trimerize with each other, whereas E-domains can dimerize. This allows for the creation of dodecamers, assembling in a planar hexagonal lattice. The flexible C-linker helps in generating a compact or less compact lattice. Nanodomains of very densely packed gephyrin can be observed at potentiated inhibitory synapses, creating multi-spot synapses.

Depending on the receptor that binds gephyrin, the resulting lattice can be very compact or less compact **(Figure 29B)**. In a study using super resolution techniques, it was found that mature glycinergic synapses can count up to 8000 gephyrin molecules per µm² whereas mature GABAergic synapses are composed of only 4000 gephyrin molecules per µm² (Specht et al., 2013). This can be partially explained by the flexible C-domain, which is more compact at glycinergic synapses (Sander et al., 2013), but can also be due to the higher binding affinity of gephyrin with GlyRs, creating compacter lattices (Groeneweg et al., 2018). Moreover, in both glycinergic and GABAergic synapses, densely packed dynamic nanodomains of gephyrin have been observed in contact with highly concentrated receptors (Specht et al., 2013) **(Figure 29B)**. LTP of inhibitory synapses increases the quantity of gephyrin nanodomains and $GABA_A$-Rs and stabilizes spontaneous IPSCs (Pennacchietti et al., 2017; Petrini et al., 2014). This demonstrates that these nanodomains and thus higher concentrations of synaptic gephyrin and inhibitory receptors, are indicative for potentiated, mature inhibitory synapses.

1.3.3.2 FUNCTION AND INTERACTIONS

Gephyrin is a highly evolutionarily conserved molecule. This lays at the basis of gephyrin to be a so-called moonlighting protein, a multifunctional protein that executes, in this case, two independent functions (Groeneweg et al., 2018; Kasaragod & Schindelin, 2018). The neuronal form, which I have been describing so far, has a receptor-anchoring and scaffolding function. The non-neuronal form is present in the cytoplasm and is related to its evolutionarily older role, namely a catalyst in molybdenum cofactor synthesis (Stallmeyer et al., 1999). Molybdenum cofactor is critical for cell viability (Schwarz et al., 2009) which could explain the presence of non-neuronal gephyrin or related polypeptides in all living organisms (Groeneweg et al., 2018).

Gephyrin knows many interaction partners, affirming its role as scaffolding and organizing protein **(Figure 30)**. The relevance of its initially evidenced interaction with tubulin (Kirsch et al., 1991) remains unclear, since gephyrin is present at the postsynaptic element, which contains mainly actin filaments and only few microtubules (Tyagarajan & Fritschy, 2014). Gephyrin does not interact directly with actin though, but via actin-associated proteins such as profilin and members of the Mena/VASP family (Giesemann et al., 2003) **(Figure 30)**. The Mena/VASP/profilin interaction is necessary for actin-dependent stabilization of dendritic spines (Ackermann & Matus, 2003) and hence may fulfil the same role in inhibitory synapses.

Two important players in gephyrin membrane localization and $GABA_A$-R surface expression are collybistin and neuroligin 2 **(Figure 30)**. Gephyrin binds via its E-domain with collybistin. The gephyrin-collybistin interaction promotes gephyrin membrane localization but does not induce $GABA_A$-R surface expression (Groeneweg et al., 2018). To allow $GABA_A$-R transport to the surface, binding of neuroligin 2 with the gephyrin E-domain is necessary as well. Upon this binding the collybistin autoinhibition domain is liberated and the tripartite complex is capable of targeting of $GABA_A$-Rs to the presynaptic membrane (Soykan et al., 2014).

The interaction between gephyrin and collybistin is specific for GABAergic synapses, since collybistin KO mice do not show abnormalities in GlyR clustering (Papadopoulos et al., 2007).

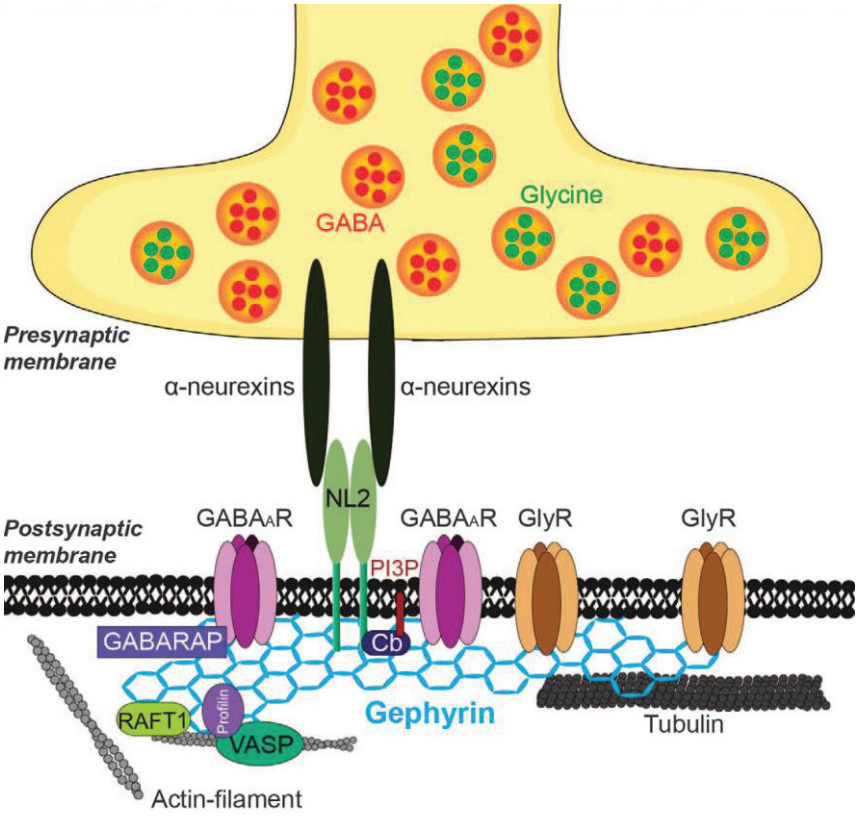

Figure 30. Molecular interactions of gephyrin at the postsynaptic inhibitory synapse *(Choii & Ko, 2015).* The main interactions of the gephyrin lattice at the inhibitory postsynaptic compartment are represented. Gephyrin interacts via proteins such as RAFT1, profilin and VASP with actin filaments and interacts directly with tubulin. The inhibitory $GABA_A$ and glycine receptors ($GABA_AR$ and GlyR respectively) are anchored in the postsynaptic plasmamembrane by intracellular attachment to gephyrin. $GABA_AR$ surface expression and gephyrin localization beneath the plasmamembrane is possible due to formation of the tripartite complex between gephyrin, collybistin (Cb) and neuroligin 2 (NL2). NL2 interacts with presynaptic α-neurexins to attach the post with the presynaptic membrane.

GABARAP: $GABA_A$ receptor-associated protein, PI3P: phosphatidylinositol 3-phosphate, RAFT1: rapamycin and FKBP12 target 1, VASP: vasodilator-stimulated phosphoprotein.

2.1 POSSIBLE SYNAPTIC LOCALIZATION FOR CASPR2

To better understand the role of CASPR2 in synaptic mechanisms, a first question to be solved is its subcellular neuronal localization. Even though neurexins are known to be located primarily at the presynaptic membrane, a synaptic localization for CASPR2 remains a matter of debate. Literature on CASPR2 synaptic localization, namely inhibitory or excitatory and pre- or postsynaptically, is scarce. The few conducted studies give some indications, although straightforward conclusions cannot be made, since the used techniques each have their advantages and disadvantages.

A first attempt to find out the localization of CASPR2 came from Bakkaloglu et al. (2008). They analyzed a preparation of crude synaptosomes obtained from P9 rat forebrain via subcellular fractionation. Crude synaptosomes are isolated neuronal synaptic terminals, consisting in both the pre- and postsynaptic compartment. Consequently, they contain a large panel of structures and molecules including mitochondria, synaptic vesicles, the plasma membrane and the PSD. Furthermore, subcellular fractionation is a rather gross technique, in which contaminating elements from the perisynaptic space are not infrequent. The authors showed presence of CASPR2 in synaptosomes, but also more precisely in synaptosomal membranes and the synaptic plasma membrane (Bakkaloglu et al., 2008). The same results were obtained using adult mice hippocampi, favoring a synaptic localization for CASPR2 (Chen et al., 2015). Other subcellular fractionation techniques allow for a more specific isolation of the PSD. The method consists in isolating the different synaptic compartments based on their solubility in different detergents (Dosemeci et al., 2005). The PSD is highly insoluble, allowing its isolation from other compartments. CASPR2 was shown to be present in the PSD fraction of adult mice whole brain, hippocampi and cortex, suggesting a postsynaptic localization (Chen et al., 2015; Fernandes et al., 2019). Interestingly, CASPR2 was also found abundantly in lipid rafts (Chen et al., 2015), specialized plasma membrane microdomains serving as organizing centers for cellular signalization.

However, given the high risk for contaminating elements from other fractions using subcellular fractionation, the results obtained with this technique need to be interpreted with caution. More accurate methods, such as microscopy, are required. An interesting result was

obtained in *in vitro* cultured rat hippocampal neurons by confocal microscopy. The authors used the serum of patients with anti-CASPR2 AILE to stain surface CASPR2, as no commercial antibody targeting the extracellular part of CASPR2 was available at that timepoint (Pinatel et al., 2015). Until DIV 7 surface CASPR2 was found to be expressed somatodendritically and along axons (see also chapter B.2.2.2). Starting from DIV 7, surface CASPR2 expression shifted towards an almost exclusively axonal localization, suggesting a presynaptic localization. These axons were mainly inhibitory axons, which was shown by staining for GAD65, an inhibitory neuronal marker **(Figure 31A)**. At DIV 21, presynaptic GAD65 clusters colocalizing with surface CASPR2 were opposed to transfected postsynaptic gephyrin clusters **(Figure 31B)**. Furthermore, at this timepoint surface CASPR2 mainly colocalized with VGAT, a presynaptic inhibitory marker **(Figure 31C)**. Moreover, staining of surface CASPR2 at DIV 21 revealed its presence in inhibitory presynaptic terminals contacting the soma of pyramidal neurons (Bonetto et al., 2019).

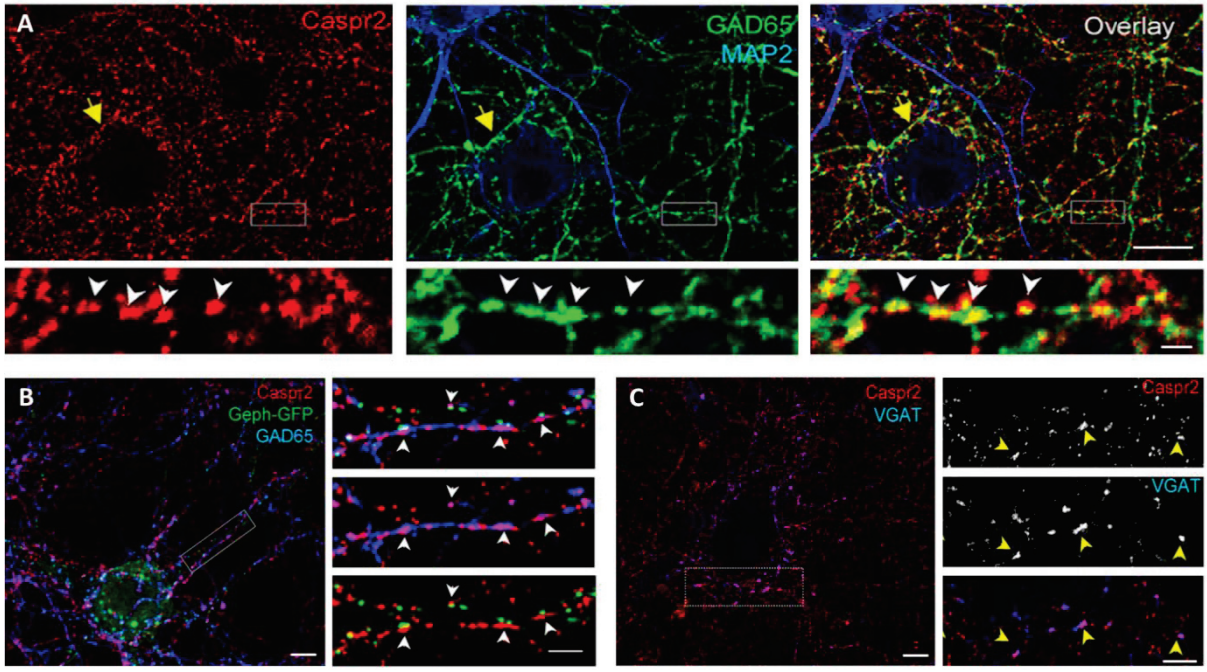

Figure 31. Surface CASPR2 is expressed in inhibitory axons and in inhibitory presynaptic sites *(Pinatel et al., 2015)*. Confocal images of rat hippocampal neurons stained for surface CASPR2 using serum of patients with anti-CASPR2 AILE. **A)** At DIV 14 CASPR2 colocalizes with GAD65, a marker for inhibitory axons (white arrowheads). Dendrites stained by MAP2 are not stained for CASPR2. GAD65-positive axons surrounding the soma of pyramidal neurons are heavily stained for CASPR2 (yellow arrows). **B)** At DIV 21 CASPR2 colocalizes with GAD65 and is opposed to postsynaptic gephyrin-GFP clusters, transfected at DIV 14 (white arrowheads). **C)** At DIV21 CASPR2 colocalizes with VGAT, a presynaptic inhibitory marker (yellow arrowheads). Scale bars represent 9 µm (A), 10 µm (B, C) and 1.5 µm (insets).

The obtained results were reinforced using CASPR2-Fc chimera, allowing to visualize binding sites of CASPR2. At DIV 7, binding sites for CASPR2 were present at postsynaptic sites, i.e. the somatodendritic compartment of both inhibitory and excitatory hippocampal neurons, whereas they were absent at presynaptic sites, i.e. the axonal surface (Pinatel et al., 2015). This suggests the presence of the CASPR2 protein itself in presynaptic compartments (Pinatel et al., 2015). Moreover, CASPR2-Fc binding was assessed at DIV 21 in neurons transfected with GFP and stained for synaptophysin as a presynaptic marker. CASPR2 binding sites were detected on dendritic shafts and spines at the contact with synaptophysin, indicating presence of receptors for CASPR2 at inhibitory and excitatory postsynaptic sites respectively (Pinatel et al., 2015). This suggests the localization of the CASPR2 protein at inhibitory and excitatory presynaptic sites (Pinatel et al., 2015). All together, these data strongly favor a presynaptic inhibitory localization for CASPR2 but do not rule out a presynaptic excitatory localization.

In support of this last possibility, surface CASPR2 colocalized at DIV 14 with VGLUT1, a presynaptic excitatory marker, albeit to a much lesser extent than with VGAT, in hippocampal neurons (Pinatel et al., 2015). An excitatory localization for CASPR2 was also demonstrated in *in vitro* rat pyramidal cortical neurons at DIV 24 (Varea et al., 2015). However, since CASPR2 was found present in dendritic spines, this pointed towards an excitatory postsynaptic localization (Varea et al., 2015). This was reaffirmed in the same study by use of high resolutive structured illumination microscopy (SIM). The authors found that CASPR2 colocalized with GluA1 in pyramidal dendritic spines and along dendritic shafts (Varea et al., 2015). Importantly, the analyzed CASPR2 spots represented total CASPR2, since staining was performed after permeabilization. This highly questions the value of the obtained results since total CASPR2 staining does not provide information concerning surface CASPR2.

Another study, using standard epifluorescent microscopy and total CASPR2 staining, showed mixed results in *in vitro* rat cortical neurons at DIV 13-18. CASPR2 was found to be present in axons and dendrites and localized in 45% of excitatory synapses and 61% of inhibitory synapses (Fernandes et al., 2019). Here as well, these results are not very informative due to staining of total CASPR2.

Taken together, currently no straightforward conclusions can be made regarding a precise synaptic localization of CASPR2 **(Table 4)**. Although valuable information coming from surface CASPR2 staining in hippocampal neurons points out a presynaptic inhibitory localization for CASPR2, this hypothesis is contradicted by hippocampal and cortical subcellular fractionation

experiments, localizing CASPR2 rather at the excitatory postsynaptic compartment. However, the observed discrepancies between studies can be attributed to differences in methodology. Furthermore, different localizations for CASPR2 depending on the brain area studied are possible.

Study	Technique	Analyzed tissue and species	Developmental stage	Synaptic localization			
				Inhibitory		Excitatory	
				Pre	Post	Pre	Post
Bakkaloglu et al., 2008	subcellular fractionation - synaptosomes	rat forebrain *ex vivo*	P9	X	X	X	X
Chen et al., 2015	subcellular fractionation - synaptosomes	mouse hippocampus *ex vivo*	adult	X	X	X	X
	subcellular fractionation - PSD fraction	mouse hippocampus *ex vivo*	adult				X
Fernandes et al., 2019	subcellular fractionation - PSD fraction	mouse whole brain *ex vivo*	adult				X
	subcellular fractionation - PSD fraction	mouse cortex *ex vivo*	adult				X
	epifluorescence microscopy - total protein staining	rat cortex *in vitro*	DIV 13-18	**X***	**X***	X*	X*
Varea et al., 2015	SIM - total protein staining	rat cortex *in vitro*	DIV 24				X
Pinatel et al., 2015	confocal microscopy - surface protein staining	rat hippocampus *in vitro*	DIV 14, DIV 21	**X**		X	
Bonetto et al., 2019	confocal microscopy - surface protein staining	rat hippocampus *in vitro*	DIV 21	X			

Table 4. Overview of evidenced synaptic localizations for CASPR2. The different studies indicating a synaptic localization for CASPR2 are listed, together with the used technique, the analyzed species and tissue, the developmental stage of the analyzed tissue and the results obtained. The obtained results, namely inhibitory or excitatory synaptic localization and pre- or postsynaptic, are indicated with an 'X'. Bold '**X**' represents the main observed localization when multiple results were obtained. * authors did not specify whether the synaptic localization was observed at the pre or postsynaptic compartment.
SIM: structured illumination microscopy, Pre: presynaptical, Post: postsynaptical.

It must be kept in mind that the synaptic cleft of excitatory synapses measures ~ 16 to 24 nm and ~ 10 to 12 nm for inhibitory synapses (High et al., 2015). Standard microscopy techniques such as confocal microscopy reach a resolution up to 180 nm laterally and 500 nm axially (Fouquet et al., 2015). SIM microscopy increases this lateral resolution twofold (Gustafsson, 2005). Thus, even though microscopy techniques are preferable in defining the precise localization of a protein, the ones used in aforementioned studies do not allow to clearly distinguish between pre and postsynaptic sites. High resolution techniques, such as stimulation emission depletion (STED) microscopy, reaching a ~ 20 nm lateral and ~ 40 nm axial resolution, or stochastical optical reconstruction microscopy (STORM), reaching a resolutive capacity of ~ 20 nm in all dimensions, allow for more reliable results.

2.2 ROLE OF CASPR2 IN DEVELOPING AND MATURE SYNAPSES

2.2.1 EVIDENCE FROM CASPR2 KO MODELS

The few existing studies aiming at unravelling the functional role of CASPR2 have been focusing on neuronal and synaptic development. One study pinpointed a role for CASPR2 in early neuronal development, before synapse formation, in *in vitro* cortical neurons established from E14.5 mice (Canali et al., 2018). Since CASPR2 was found to be present at axonal growth cones at DIV 3, the authors assessed axon length of *Cntnap2*$^{+/+}$ (WT), *Cntnap2*$^{+/-}$ (heterozygous, HET) and *Cntnap2*$^{-/-}$ (KO) neurons at DIV 2 and 3 (Canali et al., 2018). At both timepoints a decrease in axon length was observed for CASPR2 KO neurons compared with WT, and most interestingly an intermediate axon length was observed for HET neurons (Canali et al., 2018). Moreover, deficits were rescued in both KO and HET genotypes by electroporating CASPR2-HA before plating the neurons (Canali et al., 2018). This suggested that CASPR2 is capable of regulating axon elongation in a dose dependent manner. However, no difference in axon outgrowth was observed between *Cntnap2* KO and WT cortical neurons established from P0 mice (Varea et al., 2015). It is possible that the discording results find their origin in the differences in neurodevelopmental time point of the starting material, i.e. E14.5 versus P0, putting forward a role for CASPR2 in axon outgrowth in very early neurodevelopmental stages.

Regarding to dendrite outgrowth, an *in vitro* study assessed the effects of knockdown (KD) of WT CASPR2, performed by lentiviral delivery or transfection of shCASPR2 at DIV 4, on cortical dendrite morphology. A decrease in dendritic cortical arborization was observed at DIV 14-18 (Anderson et al., 2012). However, *in vitro* cortical mature CASPR2 KO neurons and *ex vivo* cortical brain slices from 4 to 6-week-old CASPR2 KO mice, did not show alterations in dendritic arborization (Gao et al., 2018; Lazaro et al., 2019; Varea et al., 2015). These opposing results could be explained by the initial presence of CASPR2 in neurons during their first stages of differentiation before knockdown, which is not the case in KO neurons. Whereas the aforementioned studies only assessed effects on cortical excitatory pyramidal neurons, one study assed effects of CASPR2 knockout on inhibitory neuronal morphology. Dendritic length and arborization were found to be decreased in *in vitro* and *in vivo* mature cortical interneurons of CASPR2 KO mice, suggesting that CASPR2 participates in the stabilization of mature interneuron dendritic trees (Gao et al., 2018) **(Figure 32)**. The different results

obtained for excitatory versus inhibitory neurons and the unclear preferential synaptic localization of CASPR2 in these neurons (see chapter C.2.1), suggest that CASPR2 may have diverging roles in excitatory and inhibitory neurons, but do not allow for clear conclusions regarding a role of CASPR2 in dendritic outgrowth or stabilization.

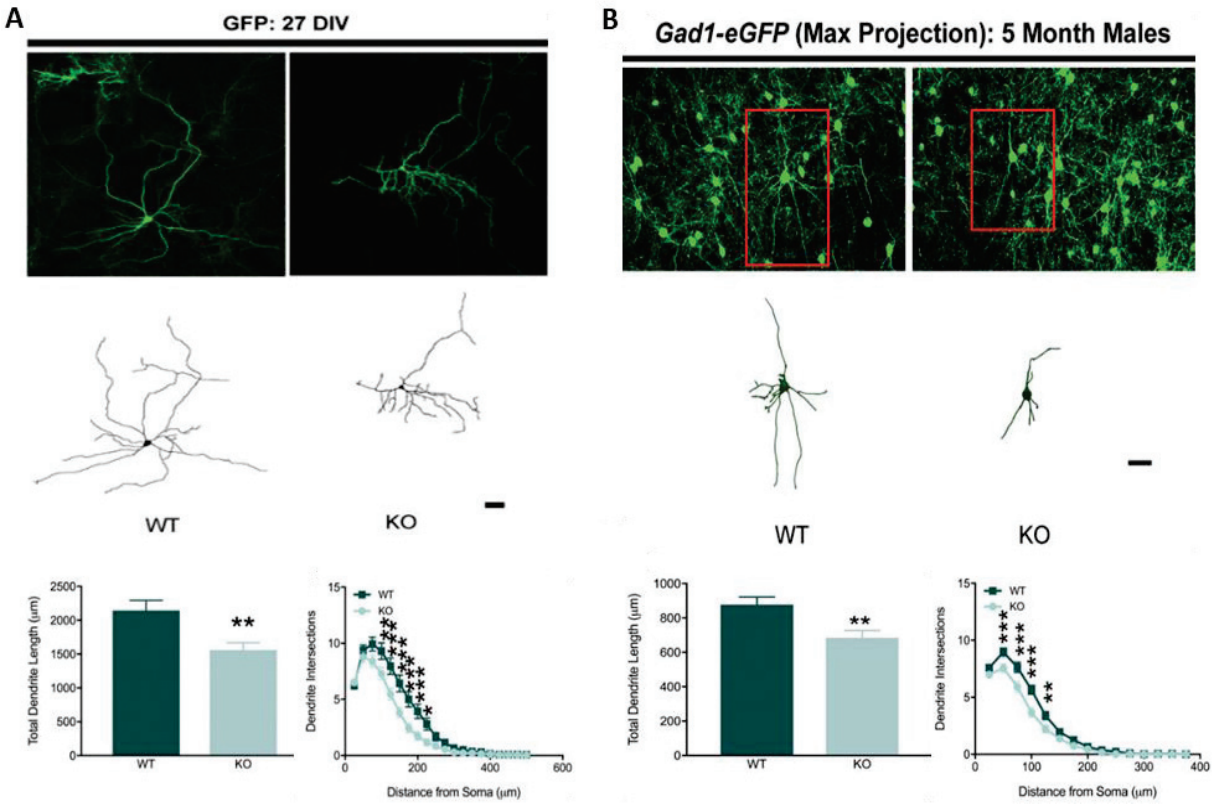

Figure 32. Dendritic length and arborization are decreased in CASPR2 KO mature cortical interneurons *(Gao et al., 2018)*. **A)** *In vitro* cortical neurons from CASPR2 WT or KO mice were transfected with GFP and stained against GABA at DIV 27 to identify interneurons. Total dendrite length and dendritic arborization are decreased in CASPR2 KO interneurons compared with WT. **B)** CASPR2 WT or KO mice were crossed with an interneuron specific reporter Gad1-eGFP transgenic line. Coronal slices from dissected brains from 5-month male mice were immunostained and interneurons from layers IV and V cingulate cortex/M2 imaged. Total dendrite length and dendritic arborization are decreased in *in vivo* CASPR2 KO interneurons compared with WT.
Scale bars represent 50 µm.

Dendritic spine density has also been investigated in several studies. After knockdown of CASPR2 at DIV 4 in *in vitro* cortical neurons, total synaptic density, analyzed by staining against synapsin, and dendritic spine density, analyzed by confocal imaging of pyramidal dendritic spines, were assessed at DIV 14-18. Both total synaptic and dendritic spine density were unchanged compared with neurons transfected with a control plasmid (Anderson et al., 2012). This was contradicted in *in vitro* cortical CASPR2 KO neurons, where a decreased spine density

was found at DIV 21 (Varea et al., 2015). This result was confirmed by an *in vivo* study, where spine density was assessed via a cranial window in the adult mouse barrel cortex using two-photon laser scanning microscopy (Gdalyahu et al., 2015). The cause of the decreased spine density in CASPR2 KO mice did not lay in altered spine formation, but in an instability of newly formed spines resulting in the observed overall spine loss (Gdalyahu et al., 2015). Thus, CASPR2 may play a role in dendritic spine stabilization in the adult mouse cortex.

Very diverging results were found regarding to dendritic spine morphology, which provides a read-out for synaptic developmental processes (see also chapter C.1.2.4). *In vitro* cortical neurons knocked down for CASPR2 by shCASPR2 at DIV 4 displayed a decreased spine head width without alteration of the spine height at DIV 14-18 (Anderson et al., 2012). In DIV 21 *in vitro* cortical CASPR2 KO neurons an increased spine width/length ratio was evidenced (Varea et al., 2015). This increased ratio could be due to an increased spine head width and no change in neck length, in accordance with results in KD neurons. On the other hand, the increased ratio could also find its origin in a decreased neck length without altering the spine head breadth. The authors sadly did not specify the parameter that altered the spine width/length ratio. Different results were observed in *ex vivo* cortical brain slices from 4 to 6-week-old CASPR2 KO mice (Lazaro et al., 2019). Using electron microscopy, the PSD length at inhibitory and excitatory synapses was assed. No alteration in PSD length was found for both types of synapses (Lazaro et al., 2019). Since for excitatory synapses the length of the PSD is an accurate reflection of the width of the spine head (see chapter C.1.2.4), the results of this study suggest an unaltered dendritic spine head width in CASPR2 KO neurons. The observed discrepancies between foregoing studies can originate from multiple factors. Inherent variations in neuronal preparations between *ex vivo* and *in vitro* studies are a first possible cause. Methodological and analytical differences between studies are a second possibility, especially for spine morphology analysis (see chapter C.1.2.4). Moreover, as mentioned before, KD and KO models are likely to produce different results, due to an initial presence of the protein before knockdown. The disparities in effects of CASPR2 KO/KD on dendritic spine morphology make it impossible to point out with certainty a precise role for CASPR2 in spine developmental processes.

Interestingly, a decrease in inhibitory and excitatory synapses in CASPR2 KO cortical brain slices from 4 to 6-week-old mice has been demonstrated (Lazaro et al., 2019) **(Figure 33)**. More specifically, using electron microscopy a decrease in multisynapse boutons was

evidenced simultaneously with an increase in perforated synapses (Lazaro et al., 2019) **(Figure 33)**. Multisynapse boutons are synapses in which multiple dendritic spines contact the same axonal terminal and are indicative for synaptogenesis (Toni et al., 1999). Perforated synapses are generally large synapses for which the pre- and postsynaptic membrane show gaps (Calverley & Jones, 1990). These gaps lay adjacent to one another and are most visible at the PSD. It is assumed that the perforations allow for increased neurotransmission and thus are indicators of well-developed synapses (Calverley & Jones, 1990). The decrease in multisynapse boutons concomitant with the increase in perforated synapses, however, is difficult to interpret. Nevertheless, all together these results indicate that CASPR2 may have important and complex functions in synaptic development and maturation.

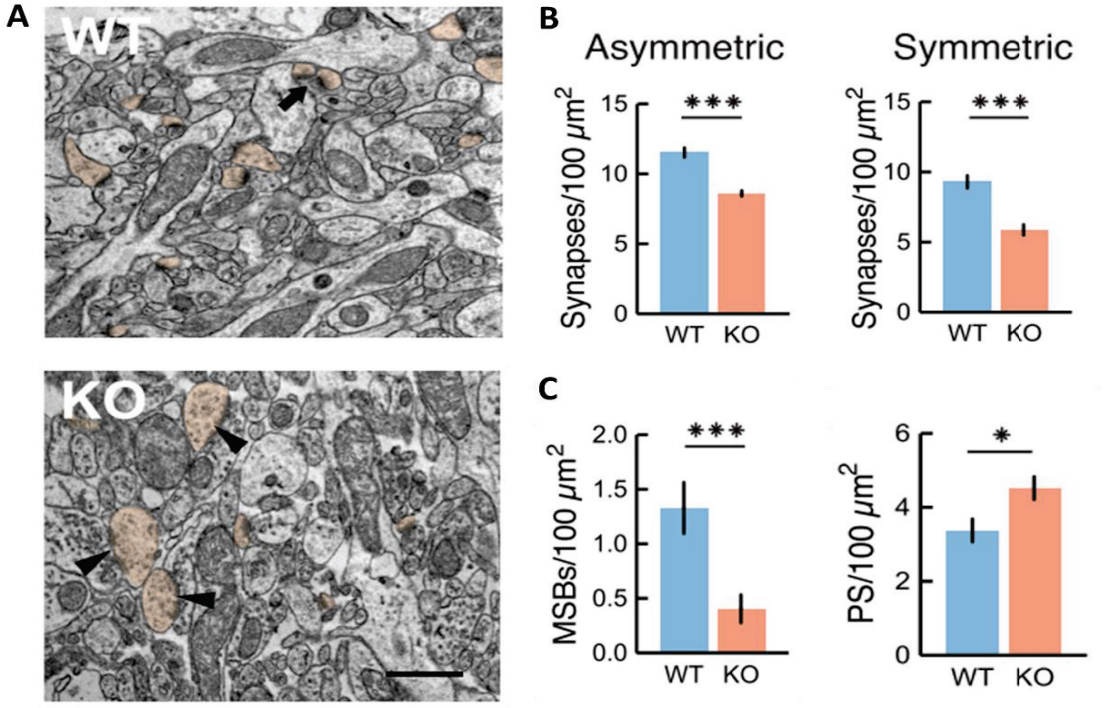

Figure 33. CASPR2 KO cortical neurons display decreased inhibitory and excitatory synapses, decreased multisynapse boutons and increased perforated synapses *(Lazaro et al., 2019)*. **A)** Electron micrograph of layer 2/3 medial prefrontal cortices of 4 to 6-week-old WT and CASPR2 KO mice. Spine profiles (orange pseudo-colored), multisynapse boutons (MSBs, black arrows) and perforated synapses (PS, black arrowheads) are depicted. **B)** CASPR2 KO mice show decreased excitatory (asymmetric) and inhibitory (symmetric) synapses. **C)** CASPR2 KO mice show a decrease in MSBs and increase in PS.
Scale bar represents 500 nm.

Recently, it has been proposed that CASPR2 plays a role in homeostatic synaptic scaling of GluA1 (Fernandes et al., 2019), a form of homeostatic synaptic plasticity which consists in adapting the synaptic AMPA-R quantity during neuronal activity perturbations to adjust

synaptic strength (Fernandes & Carvalho, 2016). In *in vitro* rat cortical neurons CASPR2 was found to be colocalized with synaptic GluA1 at DIV 13-18 (Fernandes et al., 2019). In absence of excitatory inputs, synaptic GluA1 is known to be upregulated during normal homeostatic upregulation (Ju et al., 2004; Wierenga et al., 2005). Homeostatic GluA1 upscaling, obtained by inhibiting AP firing by adding TTX or TTX+APV, was accompanied by an increase in total and excitatory synaptic CASPR2 at DIV 13-18 (Fernandes et al., 2019). *In vivo*, adult mice were deprived from light for two days to promote homeostatic GluA1 upregulation. CASPR2 levels, analyzed by western blot of whole lysates of the mouse primary visual cortex, were increased together with GluA1 (Fernandes et al., 2019). Moreover, in both experimental setups, homeostatic GluA1 upregulation was impeded by knockdown of CASPR2 (Fernandes et al., 2019). This suggests that CASPR2 is regulated by neuronal activity and is necessary for synaptic scaling of GluA1 containing AMPA-Rs in the primary visual cortex. In addition, a decreased GluA1 density in spine heads of DIV 21 *in vitro* cortical CASPR2 KO neurons has been evidenced (Varea et al., 2015). Large GluA1 aggregates which colocalized with trafficking markers were found in the soma of these neurons. Moreover, CASPR2 colocalized with GluA1 in the dendritic shafts. All together these results suggest a role for CASPR2 in AMPA-R trafficking.

From all foregoing data, it may be clear that a variety of functions for CASPR2 in neuronal and synaptic development have been proposed **(Table 5)**. However, many diverging results have been obtained and direct comparison between evidenced data is not always possible due to differences in experimental setup and more importantly in developmental stage of the material analyzed. With regard to the latter, different functions for CASPR2, depending on the neurodevelopmental stage cannot be excluded. Importantly, studies using CASPR2 KO/KD models do not allow to assess the true role of CASPR2 in mature synapses, since their proper development has been impeded. Results obtained using these models must thus be interpreted with caution.

Parameter assessed	Study	Analyzed tissue and species	Developmental stage	Method	Results
Axonal outgrowth	Canali et al., 2018	mouse cortex *in vitro*	DIV 3	KO/HET	decreased axon length
	Varea et al., 2015	mouse cortex *in vitro*	DIV 3	KO	unaltered axon length
Dendritic arborization and outgrowth	Anderson et al., 2012	mouse cortex *in vitro*	DIV 14-18	KD (DIV 4)	decreased dendritic arborization
	Varea et al., 2015	mouse cortex *in vitro*	DIV 3	KO	unaltered excitatory dendritic arborization and outgrowth
	Gao et al., 2018	mouse cortex *in vitro, in vivo*	DIV 27, adult	KO	unaltered excitatory dendritic arborization, decreased inhibitory dendritic arborization
	Lazaro et al., 2019	mouse cortex *ex vivo*	4-6-week-old	KO	unaltered excitatory dendritic arborization
Dendritic spine density	Anderson et al., 2012	mouse cortex *in vitro*	DIV 14-18	KD (DIV 4)	unaltered total and dendritic spine density
	Varea et al., 2015	mouse cortex *in vitro*	DIV 21	KO	decreased dendritic spine density
	Gdalyahu et al., 2015	mouse cortex *in vivo*	adult	KO	decreased dendritic spine density: decreased stabilization of newly formed spines
Dendritic spine morphology	Anderson et al., 2012	mouse cortex *in vitro*	DIV 14-18	KD (DIV 4)	decreased spine head width, unaltered spine height
	Varea et al., 2015	mouse cortex *in vitro*	DIV 21	KO	increased spine width/height ratio
	Lazaro et al., 2019	mouse cortex *ex vivo*	4-6-week-old	KO	unaltered inhibitory and excitatory PSD length
Synapses	Lazaro et al., 2019	mouse cortex *ex vivo*	4-6-week-old	KO	decreased inhibitory and excitatory synapses
	Fernandes et al., 2019	rat cortex *in vitro*	DIV 13-18	KD (DIV 7)	impeded homeostatic synaptic upscaling of GluA1
		mouse cortex *in vivo*	adult	KD (P21)	impeded homeostatic synaptic upscaling of GluA1
	Varea et al., 2015	mouse cortex *in vitro*	DIV 21	KO	decreased GluA1 density in dendritic spines

Table 5. Overview of possible neurodevelopmental and synaptic functions for CASPR2. The different studies indicating a neurodevelopmental and/or synaptic function for CASPR2 are listed, together with the assessed parameter, the analyzed species, brain area and type of study (*in vitro/in vivo/ex vivo*), the developmental stage of the analyzed tissue, the biological method of assessing CASPR2 function (KO or KD of CASPR2), and the obtained results.
DIV: days in vitro, KO: knockout, KD: knockdown, HET: heterozygous.

2.2.2 EVIDENCE FROM ELECTROPHYSIOLOGICAL STUDIES

Even though electrophysiological studies do not allow to draw conclusions regarding protein functions at the individual synaptic scale, they provide useful information with reference to the neuronal network and activity. Results obtained with electrophysiological measurements combined with molecular knowledge regarding neuronal/synaptic proteins allow one to better understand the assessed protein's functions on a larger scale. Neuronal activity measurements can also provide guidelines in searching a precise synaptic function for a protein. With respect to CASPR2, most electrophysiological studies have been performed

using CASPR2 KO models, not allowing to distinguish between deficits directly caused by absence of CASPR2 or indirectly by incorrectly developed neuronal networks. Taking into consideration these hindrances, some studies though may have important value in better comprehending possible CASPR2 functioning at the synapse. Therefore, I will briefly describe some of the main outcomes obtained using this technique.

Both at P14 and P60, CASPR2 KO mice display ectopic neurons in the corpus callosum and altered neuronal migration of cortical projection neurons in the somatosensory cortex (Peñagarikano et al., 2011) **(Figure 34A, B)**. In addition they also present with a decreased number of inhibitory interneurons in the somatosensory cortex and striatum at P14 (Peñagarikano et al., 2011) **(Figure 34C)**. These morphological changes are reflected *in vivo* by an asynchronous firing pattern of layer 2/3 somatosensory cortical neurons in 2-4 month old KO mice (Peñagarikano et al., 2011). The observed neuronal activity changes are found to be due to a network dysfunction in CASPR2 KO mice and not due to abnormalities in neuronal activity or conduction in se (Peñagarikano et al., 2011).

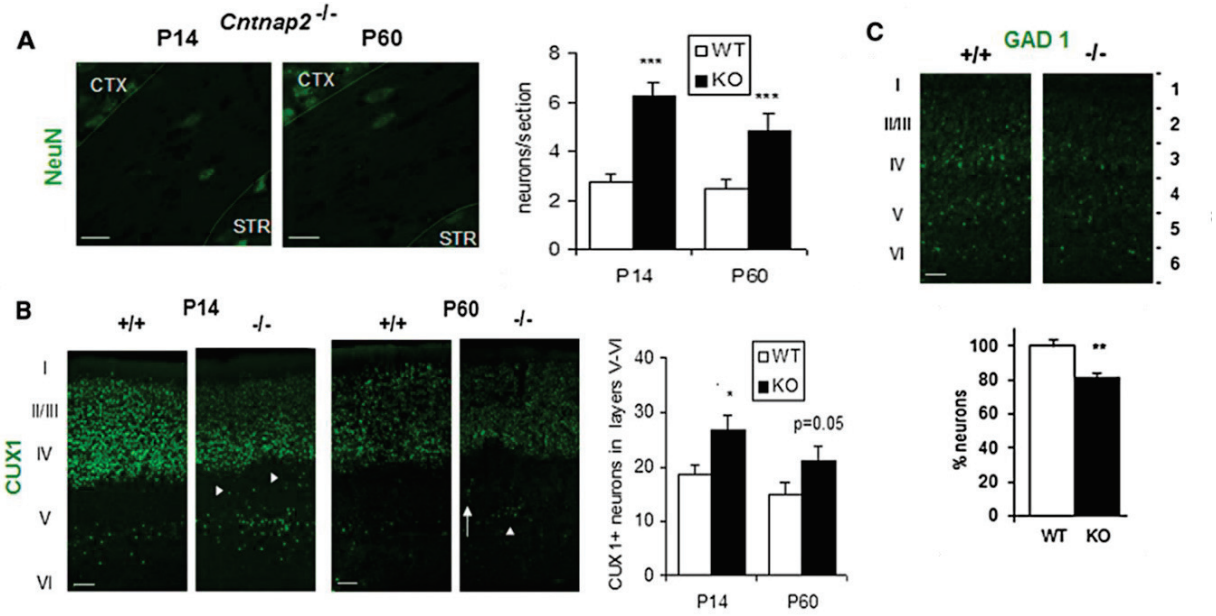

Figure 34. CASPR2 KO cortical neurons show neuronal migration abnormalities and decreased interneurons *(Peñagarikano et al., 2011)*. Immunohistochemistry was performed on cortical brain slices of CASPR2 KO and WT mice. **A)** Brain slices of P14 and P60 mice were stained against NeuN, a marker for neuronal nuclei. At both developmental stages CASPR2 KO mice display increased ectopic neurons in the corpus callosum. **B)** Brain slices of P14 and P60 mice were stained against CUX1, a marker for upper layer projection neurons. At both developmental stages CASPR2 KO mice have increased CUX1 positive cells in groups (arrowheads) and rows (arrows) in deep cortical layers of the somatosensory cortex. **C)** Brain slices of P14 mice were stained against GAD1, a marker for GABAergic interneurons. CASPR2 KO mice show decreased interneurons in the somatosensory cortex.
CTX: cortex, STR: striatum. Scale bars represent 20 µm (A) and 50 µm (B, C).

The initial observation of decreased inhibitory interneurons in CASPR2 KO mice has been confirmed by several authors using different experimental approaches (Hoffman et al., 2016; Peñagarikano et al., 2011; Vogt et al., 2018). More precisely, in P30 *ex vivo* cortical slices from CASPR2 KO mice, parvalbumin positive neurons are decreased (Vogt et al., 2018). These fast-spiking neurons also show multiple altered parameters in CASPR2 KO mice, such as slower membrane constants, more depolarized resting membrane potentials and greater adaptation ratios (Vogt et al., 2018). Repolarization after AP firing in parvalbumin-expressing neurons is mediated by voltage dependent K^+ channels. Thus, the obtained results lead to the suggestion that CASPR2 regulates properties of these Kv channels in a cell-autonomous manner (Vogt et al., 2018).

Inhibitory deficits have also been observed in hippocampal CA1 pyramidal neurons in acute slices of adult CASPR2 KO mice (Jurgensen & Castillo, 2015). Hippocampal interneurons innervate the perisomatic or dendritic compartment of pyramidal neurons, allowing for their segregation into two major classes. Here, perisomatic but not dendritic inhibitory transmission was disturbed, reflecting a selective impairment of a subpopulation of inhibitory input (Jurgensen & Castillo, 2015). The observed alterations were suggested not to be caused by a decreased neurotransmitter release, but by a decrease in parvalbumin-positive neurons, which highly innervate the perisomatic compartment of pyramidal neurons (Hu et al., 2014; Jurgensen & Castillo, 2015). Altered inhibition has also been evidenced in layer 2/3 pyramidal cells of the visual cortex of adult CASPR2 KO mice (Bridi et al., 2017). $GABA_A$-R mediated phasic and tonic inhibition was altered in adult but not in juvenile CASPR2 KO mice, suggesting different functions for CASPR2 depending on the developmental stage in formation and maintenance of inhibitory synapses (Bridi et al., 2017).

However, this was contradicted by one study, with the same experimental set-up, i.e. layer 2/3 pyramidal cortical neurons in acute slices of adult CASPR2 KO mice (Scott et al., 2017). Strangely, no defects in inhibitory neuronal distribution or transmission were observed whereas excitatory transmission was increased due to increased neurotransmitter release in presynaptic excitatory neurons with wider AP waveforms (Scott et al., 2017).

On the other hand, both inhibitory and excitatory deficits were revealed by shRNA mediated knockdown of CASPR2 at DIV 4 in *in vitro* cortical neurons (Anderson et al., 2012). At DIV 14-18 evoked EPSCs (eEPSCs) and eIPSCs showed a decrease in amplitude and miniature EPSCs (mEPSCs) and mIPSCS displayed decreased frequencies (Anderson et al., 2012). These changes

were fully rescued upon delivery of CASPR2 cDNA, evidencing that CASPR2 KD decreased neuronal transmission postsynaptically in a cell-autonomous fashion (Anderson et al., 2012).

2.2.3 EVIDENCE FROM USE OF ANTI-CASPR2 AUTOANTIBODIES

Since all foregoing studies have been performed in CASPR2 KO/KD models, the precise functions of CASPR2 in normally developed neuronal networks cannot be unambiguously concluded. Models for which CASPR2 functions are only perturbed after the neuronal network has been put into place are more useful to unravel its role at the synapse. A possible way to assess the function of CASPR2 at the mature, correctly developed synapse, is the use of patient anti-CASPR2 autoAbs. Indeed, *in vitro* neurons can be grown to a mature stage, generally DIV 18 to 21 (Biffi et al., 2013; Moutaux et al., 2018), and autoAbs added once the neuronal network and synapses have been correctly developed. For *in vivo* and *ex vivo* studies, autoAbs can be injected in the brain, mostly in the septum or ventricles, once the animal has reached a mature age. However, a disadvantage of this method is the fact that antibody specific pathological mechanisms cannot be excluded. Given the relatively recent discovery of anti-CASPR2 autoAbs, few studies exist. Moreover, the majority of studies rather assess the effect of anti-CASPR2 autoAbs on the global neuronal network and connectivity than on the synapse in se. Nevertheless, some interesting results regarding CASPR2 at the synapse have been discovered so far.

A role for CASPR2 at the mature inhibitory synapse has been assessed in *in vitro* hippocampal neurons (Pinatel et al., 2015). These neurons were transfected with gephyrin at DIV 14 and incubated with purified anti-CASPR2 autoAbs from two patients with AILE for 1h at DIV 17. The number of total and synaptic gephyrin clusters was decreased compared with neurons treated with control IgGs, purified from a healthy donor, and untreated neurons (Pinatel et al., 2015). This suggests a direct function for CASPR2 at the inhibitory synapse, or an indirect function affecting inhibitory synapses.

As mentioned, in cultured rat cortical neurons, CASPR2 was found at excitatory and inhibitory synapses, colocalizing with GluA1/PSD95 clusters and vGAT/gephyrin clusters respectively (Fernandes et al., 2019). A decrease in total and synaptic GluA1 intensity was observed after incubation for 1h or 7h with purified anti-CASPR2 autoAbs from a patient with MoS, compared with purified control IgGs or culture medium (no IgGs) (Fernandes et al., 2019). Moreover,

using antibody feeding experiments, in which the AMPA-R is forced to be internalized by short incubation with an antibody targeting an extracellular epitope of the AMPA-R thus causing its crosslinking and internalization, GluA1 internalization was assed. The GluA1 internalization ratio, defined as fluorescence signal intensities of internalized GluA1 over total GluA1, was significantly higher after treatment for 1h with patient autoAbs compared with control IgGs or no IgGs, suggesting a role for CASPR2 in AMPA-R trafficking at the cell surface (Fernandes et al., 2019). The same results were obtained after CASPR2 knock down by shRNA, meaning that the observed effects on CASPR2 are not due to autoAb specific mediated pathological mechanisms (Fernandes et al., 2019). Furthermore, functional effects of anti-CASPR2 autoAbs from the same patient were assessed by injecting the patient IgGs in layer 2/3 of the mouse primary visual cortex *in vivo* **(Figure 35A)**. 5-7h later AMPA-R mediated mEPSCs were measured *ex vivo* in layer 2/3 pyramidal neurons, where they exhibited decreased amplitudes compared with control IgGs (Fernandes et al., 2019) **(Figure 35B, C)**. In addition the cumulative distribution of mEPSC amplitudes was shifted towards smaller values for mice treated with patient autoAbs (Fernandes et al., 2019) **(Figure 35D)**. Taken together, these results imply that CASPR2 may regulate AMPA-R trafficking and that this regulation is important for AMPA-R mediated synaptic transmission in the cortex. Patient autoAbs may execute their pathogenicity by disturbing this regulatory function of CASPR2 (Fernandes et al., 2019). Interestingly, implication of CASPR2 in AMPA-R trafficking is in agreement with results of previously mentioned CASPR2 KO studies, where GluA1 cluster density in cortical dendritic spine heads was decreased (Varea et al., 2015).

A third study assessed effects of anti-CASPR2 autoAbs on peripheral myelinated dorsal root ganglia (DRG) neurons. Therefore, cultured mouse DRG neurons were incubated for 24h with complement-deactivated plasma from two different patients. One patient presented with MoS and had typical features of NMT, the second patient presented with cerebellar ataxia and neuropathic pain, without electrophysiological evidence of NMT. For both patients a reduction in membrane expression of Kv1.2 was observed together with a significant decrease in the rheobase compared with DRG neurons treated with healthy control IgGs (Dawes et al., 2018). Similar results were obtained in studies with CASPR2 KO cultured DRG neurons, suggesting that patient anti-CASPR2 autoAbs from patients with NMT/MoS increase the excitability of DRG neurons by a decrease in Kv1 channel functioning (Dawes et al., 2018).

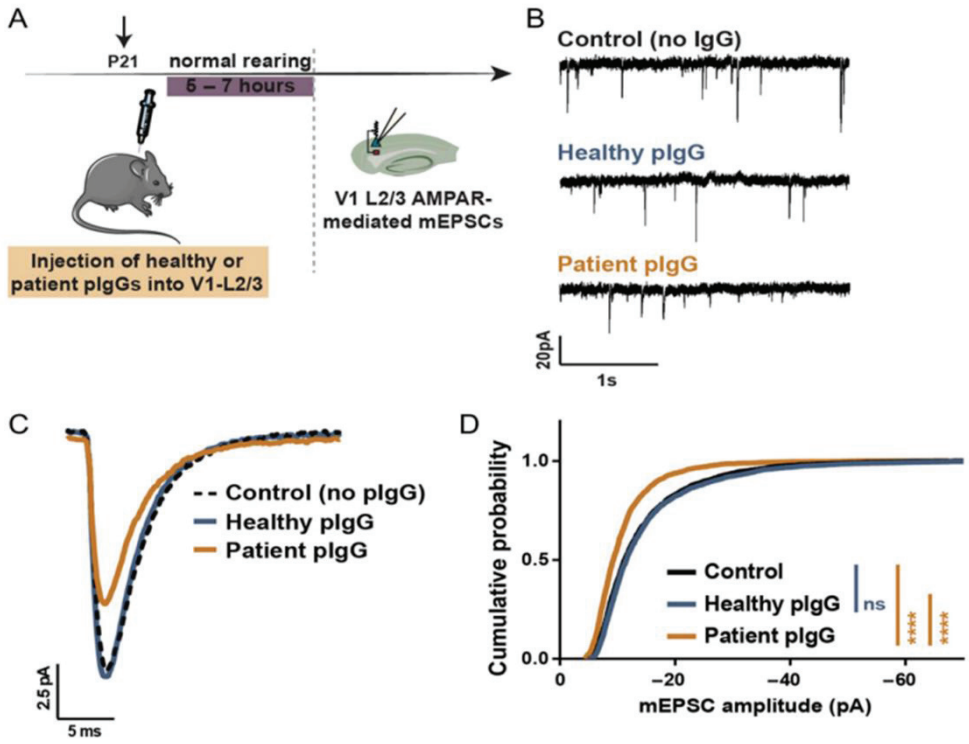

Figure 35. Anti-CASPR2 autoAbs disturb AMPA-R mediated synaptic transmission *in vivo* in the mouse primary visual cortex *(Fernandes et al., 2019)*. **A)** Purified immunoglobulins (pIgG) from a healthy donor or patient with anti-CASPR2 MoS were injected in layer 2/3 of the primary visual cortex (V1) of P21 mice. 5-7 hours later brains were dissected and V1 layer 2/3 AMPA-R mediated mEPSCs were measured in prepared cortical slices. **B)** Measured mEPSC traces from the three different conditions. **C)** Average mEPSC traces from the three different conditions show decreased amplitudes for mice injected with patient pIgG compared with healthy pIgG or control. **D)** The cumulative distribution of mEPSC amplitudes for mice injected with patient pIgG is shifted towards smaller values compared with healthy pIgG or control.

These results, even though sparse, again suggest that CASPR2 may execute different functions, depending on anatomical region and neuronal cell type. Indeed, CASPR2 may have a yet unspecified function in mature inhibitory hippocampal synapses, a regulatory role in AMPA-R trafficking in mature excitatory cortical synapses and an organizing and regulatory function in Kv1 expression in peripheral DRG neurons. However, more studies using anti-CASPR2 autoAbs are necessary to clearly elucidate the neuronal and synaptic functions of CASPR2.

RESULTS

Anti-CASPR2 autoantibodies have been found in the serum and cerebrospinal fluid of patients with autoimmune limbic encephalitis. They present with temporal lobe epilepsy as main clinical symptom, followed by memory disorders and frontal lobe dysfunction.

Initially discovered as a protein localized at the juxtaparanodal region of the node of Ranvier, CASPR2 has been shown to be present in other neuronal compartments where it appears to be an important actor in neuronal activity and connectivity. Whereas disturbing the expression or function of CASPR2 could explain the clinical presentation of patients with anti-CASPR2 autoimmune limbic encephalitis, the physiopathological properties of anti-CASPR2 autoAbs are poorly documented.

In this work, I used patients' anti-CASPR2 autoAbs as a tool not only to investigate the involvement of CASPR2 in synaptic functions, but also to unravel possible pathological mechanisms of patients' autoAbs in anti-CASPR2 autoimmune limbic encephalitis. Importantly, the use of autoAbs allows for the assessment of CASPR2 functions in a normally developed neuronal network.

During my thesis, I investigated the impact of patients' autoAbs on CASPR2 surface expression and distribution and on Kv1.2 channel expression in *in vitro* mature hippocampal neurons (DIV 21). The obtained results are part of a first article **(Article 1)**. Furthermore, I analyzed the effects of anti-CASPR2 autoAbs on inhibitory and excitatory synapses in *in vitro* hippocampal neurons at immature (DIV 14) and mature (DIV 21) developmental stages. The results obtained for this part of work are presented as an article in preparation **(Article 2)**.

Impact of anti-CASPR2 autoantibodies from patients with autoimmune encephalitis on CASPR2/TAG-1 interaction and Kv1 expression.

Saint-Martin, M.*, **Pieters, A.***, Déchelotte, B., Malleval, C., Pinatel, D., Pascual, O., Karagogeos, D., Honnorat, J., Pellier-Monnin, V., Noraz, N. **Co-first authors*

Journal of Autoimmunity, accepted May 2019.

Objectives: The presence of anti-CASPR2 autoAbs in patients with AILE suggests that these autoAbs are pathological by disturbing the functions of CASPR2. CASPR2 is mainly known for its critical role in assembling Kv1 channels at the juxtaparanodal region of the node of Ranvier, due to its direct interaction with TAG-1. Kv1 channels execute a main function in neuronal excitability, namely inhibiting repetitive AP firing, rapid membrane repolarization after AP passing and assuring stable internodal resting membrane potentials. Therefore, we wondered if upon patients' autoAbs binding with CASPR2 the interaction with its partners could be affected, leading to altered neuronal excitability. Indeed, epilepsy, a clinical feature that finds its origin in disturbing neuronal activity, is the main clinical presentation of patients with anti-CASPR2 AILE. To investigate our hypothesis, we assessed the effects of patients' anti-CASPR2 autoAbs on the interactions between CASPR2/TAG-1/Kv1 channels in HEK cells (this part of work was executed by Saint-Martin, M.). Furthermore, we explored the effects of patients' autoAbs on Kv1 channel expression and on CASPR2 surface distribution in *in vitro* mature hippocampal neurons.

Results: We showed that patients' autoAbs are capable of disturbing CASPR2/TAG-1 *cis* interaction. In addition, we studied the domains necessary for this interaction. The discoidin-like domain of CASPR2 did not interact with TAG-1, whereas the first laminin G-like domain was sufficient but not necessary for interaction between both proteins. The main interaction domains between CASPR2 and TAG-1 were the EGF2 and fourth laminin G-like domain. TAG-1 on the other hand could interact with CASPR2 via its Ig and Fn domains. Furthermore, binding of patients' autoAbs induced an increase in Kv1.2 expression in both HEK cells and *in vitro* hippocampal neurons. Interestingly, *in vitro* inhibitory hippocampal neurons expressed high levels of CASPR2 together with Kv1.2 channels. The increased Kv1.2 expression upon binding

of patients' autoAbs was accompanied *in vitro* with increased CASPR2 surface fluorescence intensity, and additionally, when neurons were transfected with CASPR2-GFP, with an increased size and number of CASPR2 clusters. Total and surface CASPR2 protein levels were not altered however, demonstrating that patients' autoAbs do not internalize CASPR2, but immobilize the protein at the surface membrane.

Conclusions: We provided evidence for two possible physiopathological mechanisms of anti-CASPR2 autoAbs. First, patients' autoAbs may execute their pathological effect by impeding the CASPR2/TAG-1 interaction. Secondly, stabilization of surface CASPR2 together with increased expression of Kv1.2 channels in inhibitory neurons upon patients' autoAbs binding might diminish inhibitory transmission, leading to increased global neuronal activity. The alteration in neuronal activity may lie at the basis of the observed epilepsy in patients with anti-CASPR2 AILE.

Journal of Autoimmunity xxx (xxxx) xxx–xxx

Contents lists available at ScienceDirect

Journal of Autoimmunity

journal homepage: www.elsevier.com/locate/jautimm

Impact of anti-CASPR2 autoantibodies from patients with autoimmune encephalitis on CASPR2/TAG-1 interaction and Kv1 expression

Margaux Saint-Martin[a,b,c,1], Alanah Pieters[a,b,c,1], Benoît Déchelotte[a,b,c], Céline Malleval[a,b,c], Delphine Pinatel[a,b,c], Olivier Pascual[a,b,c], Domna Karagogeos[e], Jérôme Honnorat[a,b,c,d], Véronique Pellier-Monnin[a,b,c], Nelly Noraz[a,b,c,*]

[a] INSERM U1217, Institut NeuroMyoGène, Lyon, F-69000, France
[b] CNRS UMR5310, Institut NeuroMyoGène, Lyon, F-69000, France
[c] University Claude Bernard Lyon 1, Lyon, F-69000, France
[d] Hospices Civils de Lyon, Lyon, F-69000, France
[e] University of Crete Medical School and IMBB-FORTH, Heraklion, Crete GR, 70013, Greece

ARTICLE INFO

Keywords:
CASPR2
TAG-1
Kv1
Autoimmune encephalitis
Autoantibody
Domains of interaction

ABSTRACT

Autoantibodies against CASPR2 (contactin-associated protein-like 2) have been linked to autoimmune limbic encephalitis that manifests with memory disorders and temporal lobe seizures. According to the growing number of data supporting a role for CASPR2 in neuronal excitability, CASPR2 forms a molecular complex with transient axonal glycoprotein-1 (TAG-1) and shaker-type voltage-gated potassium channels (Kv1.1 and Kv1.2) in compartments critical for neuronal activity and is required for Kv1 proper positioning. Whereas the perturbation of these functions could explain the symptoms observed in patients, the pathogenic role of anti-CASPR2 antibodies has been poorly studied. In the present study, we find that patient autoantibodies alter Caspr2 distribution at the cell membrane promoting cluster formation. We confirm in a HEK cellular model that the anti-CASPR2 antibodies impede CASPR2/TAG-1 interaction and we identify the domains of CASPR2 and TAG-1 taking part in this interaction. Moreover, introduction of CASPR2 into HEK cells induces a marked increase of the level of Kv1.2 surface expression and in cultures of hippocampal neurons Caspr2-positive inhibitory neurons appear to specifically express high levels of Kv1.2. Importantly, in both cellular models, anti-CASPR2 patient autoAb increase Kv1.2 expression. These results provide new insights into the pathogenic role of autoAb in the disease.

1. Introduction

Contactin-associated protein-like 2 (CASPR2) is a neuronal cell adhesion protein of the neurexin family expressed in the central and peripheral nervous system [1]. Autoantibodies (autoAb) against CASPR2 have been linked to acquired neuromyotonia (NMT) a peripheral nerve hyperexcitability syndrome [2], Morvan's syndrome (MoS), which combines NMT and encephalopathy [3] and autoimmune encephalitis (AE), a CNS-specific syndrome [4,5]. The presence of anti-CASPR2 Ab not only in serum but also in cerebrospinal fluid of AE patients was associated with rather homogeneous clinical features. They are men around 60 years of age with prevalent symptoms of limbic dysfunction, including memory disorders, temporal lobe seizures, and frontal lobe impairment [6,7]. CASPR2 autoAb were initially identified as Ab recognizing voltage-gated potassium channel (VGKC) [2]. However, it has become apparent that they principally target LGI1 or CASPR2. All these proteins belong to a complex referred as VGKC complex [8,9].

CASPR2 is a rather compact transmembrane protein with a C-terminal intracellular region that contains a 4.1B-binding motif and a type II PDZ-binding motif allowing, respectively, its interaction with cytoskeleton-associated proteins and scaffolding proteins. The extracellular part is composed of an N-terminal discoidin-like domain, four laminin G-like domains, two epidermal growth factor-like domains and a fibrinogen-like domain [10]. Anti-CASPR2 autoAb recognize multiple domains of the protein. Interestingly, all patients present autoAb directed against the discoidin and laminin G1 N-terminal domains and some, recognize only those two domains [6,7,11,12], suggesting that

* Corresponding author. INSERM U1217, CNRS UMR5310, Institut NeuroMyoGène (INMG), équipe SynatAc, Faculté de Médecine, 8 avenue Rockefeller, F-69008, Lyon, France.
E-mail address: nelly.noraz@inserm.fr (N. Noraz).
[1] Margaux Saint-Martin and Alanah Pieters have equally contributed to this work.

https://doi.org/10.1016/j.jaut.2019.05.012
Received 13 February 2019; Received in revised form 8 May 2019; Accepted 14 May 2019

Table 1
Primary and secondary antibodies. IF: Immunofluorescence; WB: Western blot; IP: Immunoprecipitation.

Antibodies	Species	Reference	Dilution
Anti-TAG-1 intra	rabbit	Millipore ABN1379	1/5000 (WB)
Anti-CASPR2 intra	rabbit	Abcam ab33994	1/5000 (WB)
Anti-CASPR2 intra	rabbit	Genscript A01426	1 µg (IP)
Anti-GFP	rabbit	ThermoFisher A-11122	1/5000 (WB), 1/1000 (IF)
Anti-HA	mouse	Sigma-Aldrich H3663	1/5000 (WB) 1/1000 (IF)
Anti-myc	mouse	Abcam ab9106	1 µg (IP)
Anti-Kv1.2 intra	mouse	NeuroMab K14/16	1/5000 (WB), 1/100 (IF)
Anti-Kv1.2 extra	rabbit	Alomone APC 162	1/100 (IF)
Anti-GAD65	mouse	Milipore MAB351	1/400 (IF)
Alexa 647 anti-rabbit	goat	Molecular Probes A21244	1/2000 (IF)
Alexa 405 anti-mouse	goat	Abcam ab175660	1/2000 (IF)
Alexa 555 anti-mouse IgG2b	goat	Molecular Probes A21147	1/1000 (IF)
Alexa 647 anti-mouse IgG2a	goat	Molecular Probes A21241	1/1000 (IF)
Alexa 488 anti-human	goat	Molecular Probes A11013	1/1000 (IF)
Alexa 488 anti-rabbit	goat	Molecular Probes A11034	1/1000 (IF)

autoAb binding to the discoidin and laminin G1 domains is involved in the development of the disease. Besides, anti-CASPR2 autoAb are mainly IgG4 [6,7], a subclass that binds weakly to Fc-γ receptors and do not activate complement. IgG4 could be considered as blocking Ab (i.e. Ab binding to its antigenic target disrupts its function).

CASPR2 forms a molecular complex with shaker-type voltage-gated potassium channels (Kv1.1 and Kv1.2) and transient axonal glycoprotein-1 (TAG-1), a glycosyl-phosphatidylinositol (GPI)-anchored adhesion molecule of the Ig superfamily also referred as Axonin-1 or Contactin-2 [13–16]. Proteins forming this complex were found co-enriched in compartments critical for neuronal activity including the axon initial segment (AIS) [17] and the juxtaparanodal region (JXP) of node of Ranvier (NOR) on myelinated axons [13,15]. Importantly, in CASPR2 KO mice, Kv1 and TAG-1 were no longer enriched at the JXP [13,18] and in the same way, in TAG-1 KO mice, Kv1 and CASPR2 were both mislocalized [15]. These data put into light the co-requirement of CASPR2 and TAG-1 for Kv1 proper positioning. In line with these findings and with the key function of Kv1 in controlling action potential propagation, CASPR2 has been involved in the regulation of intrinsic neuronal excitability [18,19]. In regards with anti-CASPR2 autoAb, some data support these findings. For instance, anti-CASPR2 autoAb impede CASPR2/TAG-1 interaction in a solid-phase binding assay [20]. Furthermore, CASPR2 autoAb enhance the excitability of DRG (dorsal root ganglion) neurons in a cell-autonomous fashion through regulation of Kv1 channel expression [19]. In the present study, experiments were conducted to bring further evidence of a pathogenic role of anti-CASPR2 autoAb in the disease.

2. Materials and methods

2.1. Patient sera and IgG purification

Sera from four patients with AE were obtained from the Centre National de Référence pour les Syndromes Neurologiques Paranéoplasiques in Lyon, France. All patients displayed temporal lobe seizures and memory disorders and were tested positive for anti-CASPR2 autoAb [6,21]. Informed consent was obtained for every patient and the present study was granted by the institutional review board of the Hospices Civils de Lyon (Comité de Protection des Personnes SUD-EST IV). We also used three control sera collected from healthy blood donors at Etablissement Français du Sang. The titer of anti-CASPR2 autoAb in the sera used in this study was previously determined using an HEK cell-based assay [6,21]. Importantly, serum antibody titers (last dilution of serum giving a positive signal) were high around 1:10.000 and equivalent among patients. To purify IgG, sera were incubated with protein-A Sepharose 4 Fast Flow™ beads (SIGMA) 2h at room temperature (RT) on rotation, transferred to columns and washed 3 times with PBS. IgG were eluted in glycine buffer pH2.8, neutralized in Tris buffer pH8.8 and dialyzed overnight at 4 °C in PBS (Slide-A-lyser G2 Dialysis Cassettes 0.5–3 ml ThermoFisher). IgG concentration was then measured using micro BCA protein assay kit (ThermoFisher). Purified IgG were sterilized on 0.22 µm filters and kept at −80 °C. Patient (Pat) and control (Ctl) IgG were either used separately or as a pool (pPat: equimolar concentration of Pat 2, Pat 3 and Pat 4 purified IgG; pCtl: equimolar concentration of Ctl 1, Ctl 2 and Ctl 3 purified IgG).

2.2. Constructs

The CASPR2-GFP plasmid, the CASPR2-HA (Hemagglutinin tag) and derived deleted constructs, CASPR2 Δ1, CASPR2 Δ2, CASPR2 Δ3, and CASPR2 Δ4, kindly provided by C. Faivre-Sarrailh, as well as CASPR2-Discoidin (D) and CASPR2-LamininG1 (L1) constructs were previously described [12]. The CASPR2-EGF2-LamininеG4 (E2L4) construct was obtained using reverse PCR on full-length CASPR2-HA plasmid and In-Fusion kit (Clontech). PCR amplified products were verified by sequencing (Eurofins). The TAG-1-GFP plasmid, TAG-1-GFP ΔFn and TAG-1-GFP ΔIg constructs, kindly provided by D. Karagogeos, were previously described [22]. The TAG-1-GFP ΔIg5 construct was obtained using reverse PCR on TAG-1-GFP full-length plasmid and In-Fusion kit (Clontech). The surface expression of proteins derived from all the plasmids used in this study has been validated in HEK cells (Fig. S1).

2.3. Antibodies

The primary and secondary antibodies used in this study are described in Table 1.

2.4. Cell lines and transfection

HEK 293 T cells were purchased from ATCC and cells referred in this paper as HEK-Kv were kindly provided by A. Morielli. HEK-Kv are HEK 293 cells stably expressing m1 mAChR, Kv1.2 and its Kvβ2 subunit [23]. Cells were grown in DMEM (ThermoFisher) SVF 10%, P/S 1% and transfected using the lipofectamine LTX kit (Invitrogen).

2.5. Immunoprecipitation and Western Blot

For immunoprecipitation (IP) and Western Blot analysis, 24 h after transfection HEK cells were lysed 10 min at 4 °C in lysis buffer pH7.5 containing NaCl 150 mM, HEPES 50 mM, Triton 1%, octyl-β-glucoside 60 mM (ThermoFisher), protease (Roche) and phosphatase (0.1 mM NaF, 0.1 mM Na3VO4, 1 mM PMSF, 1 mM benzamidine) inhibitors. Lysates were centrifuged at 4 °C, 10min 12000g, supernatant was

collected and protein concentration was evaluated using the micro BCA protein assay kit (ThermoFisher). Immunoprecipitation was performed using 150 µg of protein lysate and 1 µg of indicated Ab. Tubes were placed at 4 °C with rotation overnight and then protein G agarose fast flow beads (Millipore) were added for 2h. Supernatant was discarded and beads were washed three times in 500 µl lysis buffer. Immunoprecipitated proteins were then eluted in Laemmli DTT buffer, 5 min at 95 °C. Proteins were separated onto Criterion XT Bis-Tris precast 10% gels (Bio-Rad) and transferred onto nitrocellulose membrane (GE Healthcare). Membranes were blotted with the indicated Abs and revealed using Substrat HRP Immobilon Western (Millipore). Reactive proteins were visualized using the Chemidoc MP Imaging System (Bio-Rad). Band intensities were quantified using ImageJ and the ratio of protein co-immunoprecipitated/protein immunoprecipitated was calculated. In order to normalize for inter-experiment variations, ratios obtained for each condition were summed and results were expressed as a fraction of the summed ratios.

For surface immunoprecipitation transfected HEK cells were incubated with control or patient purified IgG (5 µg/mL) for 24 h at 37 °C. After one wash in PBS, cells were incubated with an anti-HA Ab or control anti-myc Ab (2 µg/mL) for 1h at room temperature, washed twice in PBS and lysed. Protein lysates were then processed as described above.

For the Biotinylation experiments hippocampal neurons (21 DIV) were treated for 24 h with pooled patient or control IgG and cell surface proteins were biotinylated using the Pierce Cell Surface Protein Isolation Kit (ThermoFisher) following manufacturer's instructions. The obtained total and surface fractions were denaturated for 5 min at 95 °C in Laemmli DTT and separated onto 4–15% Criterion TGX Stain-Free Precast Gels (Bio-Rad). Loaded proteins were quantified after transfer to nitrocellulose membrane using the Chemidoc MP Imaging System. Membranes were blotted with anti-CASPR2 Ab (ab33994). Reactive proteins were visualized with SuperSignal West Pico Chemiluminiscent Substrate (ThermoFisher, 34580) using the Chemidoc MP Imaging System. Band intensities were measured using Image Lab (version 5.2.1, Bio-Rad) and for each sample the ratio of Caspr2 to total loaded protein was calculated.

2.6. Flow cytometry

HEK-Kv cells were used for flow cytometry analysis. Cells were incubated with either patient or healthy control purified IgG at a concentration of 16 µg/mL for 24 h at 37 °C. HEK cells were washed with PBS one time and incubated with 154 mM sodium azide for 10 min at 37 °C, to limit endocytosis as previously described [24]. Cells were then washed with PBS and primary antibody was incubated for 1h at 4 °C in PBS 2% BSA. Cells were washed three times in PBS and secondary antibody was incubated for 30 min at 4 °C in PBS 2% BSA. After three washes in PBS, cells were then processed in the cytometer (three-laser FACS Canto II) and median of fluorescence intensity was measured for each parameter. In these experiments, Kv1.2 was labeled with anti-Kv1.2 Ab (APC 162) and Alexa647-conjugated secondary Ab; CASPR2 was labeled with anti-HA Ab and Alexa405-conjugated secondary Ab; TAG-1-GFP expression was directly measured. In order to normalize for inter-experiment variations, medians of fluorescence intensity obtained for each condition were summed and results were expressed as a fraction of the summed medians.

2.7. Primary hippocampal neuronal culture

Primary hippocampal neuron cultures were prepared from E18 Wistar rat embryos (Janvier Labs). Pregnant rats were deeply anesthetized by isoflurane (Ceva) inhalation and embryos were taken out by Caesarean section. Hippocampi were isolated in Hank's buffered salt solution (HBSS) (Gibco) and transferred for dissociation in HBSS supplemented with 10% (v/v) trypsin (Gibco) for 10 min at 37 °C. Hippocampi were then washed with 4% (w/v) bovine serum albumin (BSA) and triturated. Cells were plated onto poly-L-lysine (0.5 mg/mL) coated coverslips in Neurobasal medium (Gibco) supplemented with 2% (v/v) B27 (Gibco), 0.3% (v/v) L-glutamine (Invitrogen) and 1% (v/v) penicillin-streptomycin (invitrogen). Cells were cultured for 14 or 21 days at 37 °C in a humidified atmosphere containing 5% CO_2. Animal care and procedures were conducted according to the European Community Council Directive 2010/63/UE and the French Ethical Committee.

2.8. Immunocytofluorescence

For surface Caspr2 and total Kv1.2/GAD65 staining hippocampal neurons were treated at 20 DIV (days *in vitro*) with patient or control purified IgG at 16 µg/mL, for 24 h at 37 °C. At 21 DIV neurons were washed in Neurobasal and surface Caspr2 was stained using the pool of patient IgG (pPat) as primary Ab at 5 µg/mL, for 30 min at 37 °C. Neurons were then washed in Neurobasal, fixed in 4% (v/v) PFA for 10min, blocked with 3% (w/v) BSA in PBS for 30min and incubated for 30 min at RT with secondary Ab. After washing in PBS neurons were permeabilized for 30 min at RT with 3% (w/v) BSA in PBS 0.3% (v/v) Triton X-100 (PBS-T) and incubated for 1h at RT with anti-Kv1.2 (K14/16) and anti-GAD65 primary Ab. Neurons were then washed in PBS-T and incubated for 1h at RT with secondary Ab. After washing in PBS, nuclei were stained using 0.1 µg/mL Hoechst (ThermoFisher) for 5 min at RT.

For surface and total CASPR2-GFP staining, neurons were transfected at 18 DIV with CASPR2-GFP plasmid using the Lipofectamine LTX kit (Invitrogen) and treated at 20 DIV with pooled patient or control IgG at 16 µg/mL for 24 h at 37 °C. Neurons were washed in Neurobasal and surface CASPR2-GFP was stained with anti-GFP primary Ab for 30 min at 37 °C. Neurons were then washed in Neurobasal, fixed in 4% (v/v) PFA for 10min, blocked with 3% (w/v) BSA in PBS for 30min and incubated for 30 min at RT with alexa555 secondary Ab. After washing in PBS neurons were permeabilized for 30 min at RT with 3% (w/v) BSA in PBS-T and incubated for 1h at RT with anti-GFP primary Ab. Neurons were then washed in PBS-T and incubated for 1h with alexa488 secondary Ab. After washing in PBS, nuclei were stained using 0.1 µg/mL Hoechst (ThermoFisher) for 5 min at RT.

For all experiments coverslips were mounted in FluorPreserve Reagent (Calbiochem) and stored at 4 °C until image acquisition.

2.9. Image acquisition and analysis

Images were acquired using Zeiss Axio Imager Z.I ApoTome microscope and for the quantitative analysis a fixed exposition time was applied to the different experimental conditions. To quantify surface Caspr2 signal intensities, images were analyzed using ICY Spotdetector Plugin (version 1.9.10.0, BioImage Analysis Unit Institut Pasteur). The mean intensity of the clusters/spots detected was multiplied by cluster area to get total signal intensity per cluster. Values were summed and divided by total surface occupied by clusters. Results were expressed as mean Caspr2 signal intensity.

To analyze surface CASPR2-GFP expression, a ROI corresponding to transfected neuron was defined based on the surface occupied by green signal (total CASPR2-GFP). Red signals (surface CASPR2-GFP) included in the ROI were then quantified using ICY Spotdetector and results depicted as cluster size, cluster intensity and cluster number per μm^2 of neuron.

To analyze Kv1.2 expression, ROIs with the same surface across different experimental conditions were defined along neurites based on the red signal (surface Caspr2). Green signal intensities (total Kv1.2) included in the ROI were then quantified using ICY and results depicted as intensity arbitrary units.

2.10. Statistical analysis

GraphPad Prism software was used for all statistical tests. Depending on the experimental setting, data were compared using a Mann-Whitney, a Kruskal-Wallis or a Wilcoxon signed-rank test. Data were represented as mean ± SD and significance was set for a p value ≤ 0.05.

3. Results

3.1. Patient anti-CASPR2 autoAb impede CASPR2/TAG-1 interaction

Using an acellular solid phase binding assay, it has been shown that CASPR2 and TAG-1 directly interact through their extracellular domains and that anti-CASPR2 patient sera inhibited this interaction [20]. Here, in a first set of experiments, we asked whether anti-CASPR2 autoAb from AE patients were able to perturb CASPR2/TAG-1 interaction in a cellular model. HEK cells co-transfected with CASPR2-HA and TAG-1-GFP were incubated for 24 h with healthy donor (Ctl) or patient (Pat) IgG purified from serum to avoid any side effects due to other serum proteins. Cells were then further incubated with an anti-HA Ab before lysis to specifically immunoprecipitate the fraction of CASPR2 present at the cell surface. The ratio of TAG-1 co-immunoprecipitated (co-IP) over CASPR2 immunoprecipitated (IP) was assessed. As shown in Fig. 1A, co-IP TAG-1 was observed in surface CASPR2 immunoprecipitates obtained from cells treated with Ctl or Pat IgG, but not in the control immunoprecipitates (Ctl IP) for which co-transfected HEK cells were incubated 24 h with PBS and incubated with an irrelevant control Ab before lysis. Compared with Ctl IgG the level of co-IP TAG-1 was diminished in Pat IgG treated cells (Ctl: 0.55 ± 0.09; Pat: 0.44 ± 0.09 $p < 0.01$). Notably, a 20% and 19% decrease of TAG1-binding was observed using patient 2 and patient 3 IgG respectively whereas decreased binding was rather low on cells incubated with patient 1 IgG (7% decrease) and not observed with patient 4 IgG (Fig. 1B).

3.2. The EGF2 and laminin G4 domains of CASPR2 are critical for TAG-1 interaction

To get a better understanding of the decreased CASPR2/TAG-1 binding observed in the presence of patient autoAb, we conducted experiments to determine which domain(s) of either protein was responsible for their interaction. Notably, both CASPR2/TAG-1 cis- and trans-interactions have been reported [13,15,25] and in CASPR2 and TAG-1 co-transfected HEK cells, both types of interactions are possible. We therefore first evaluated the contribution of CASPR2/TAG-1 trans-interactions in our model. To this end, HEK cells were either, co-transfected with plasmids coding for CASPR2-HA and TAG-1-GFP proteins (C2T1) allowing cis and trans associations or, cells were separately transfected with either one plasmids and subsequently put together (C2 + T1) allowing CASPR2/TAG-1 trans-associations only (Fig. 2A left panel). Cells were lysed and CASPR2 was immunoprecipitated using a commercial antibody directed against its intracellular domain (ab33994). As shown in Fig. 2A right panel, the level of TAG-1 co-IP

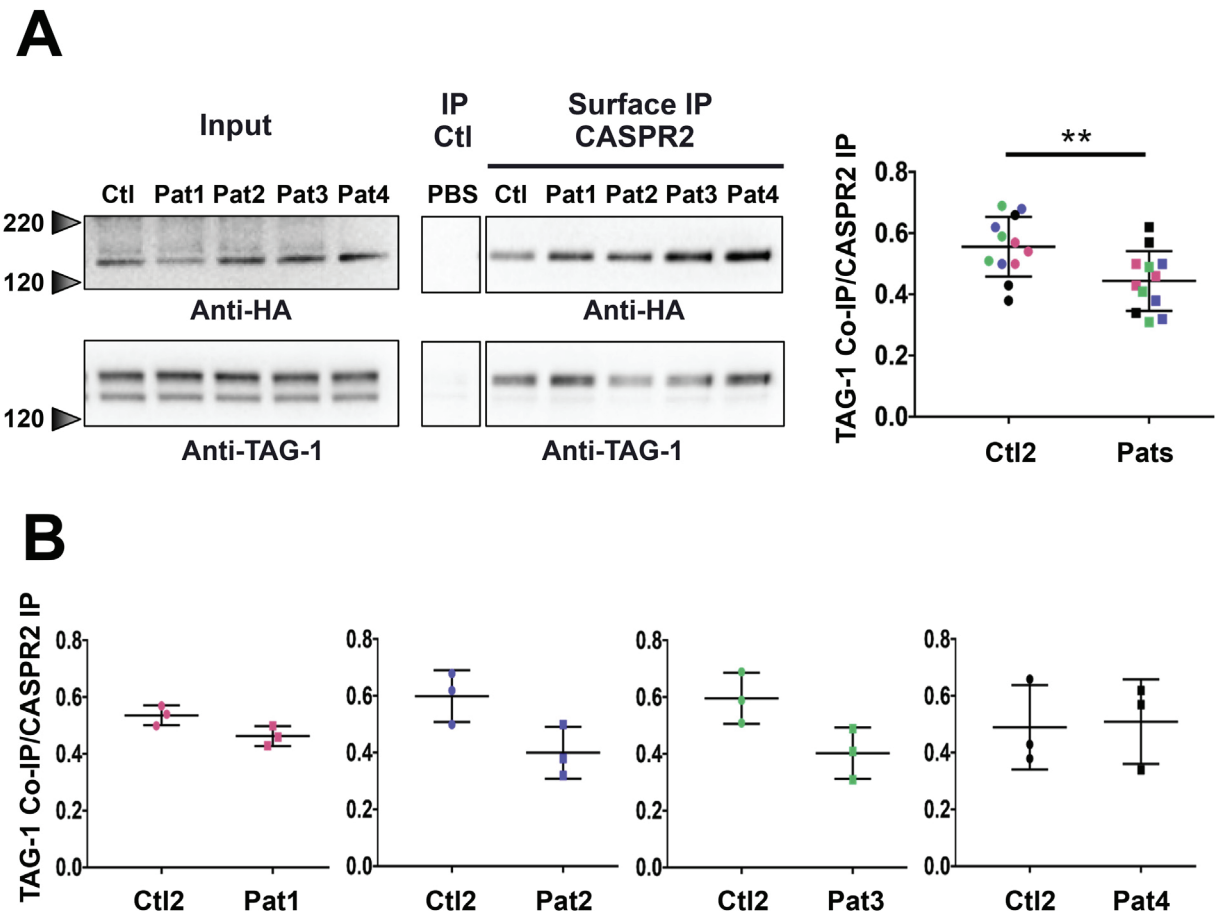

Fig. 1. Patient autoAb impede CASPR2/TAG-1 interaction A) HEK cells co-transfected with CASPR2-HA and TAG-1-GFP were incubated for 24 h with serum-purified control IgG (Ctl) or patient IgG (Pat). CASPR2 present at the cell surface was IP (surface IP) and the level of CASPR2 IP or TAG-1 co-IP, was analyzed by Western Blot. As control, co-transfected HEK cells were incubated with PBS and IP with a control Ab. The ratios of TAG-1 co-IP over CASPR2 IP signal intensities are depicted. Each color represents a different patient. n = 12 obtained from 3 independent cultures, **p < 0.01 Mann-Whitney test. **B)** Ratios of TAG-1 Co-IP over CASPR2 IP are represented separately for each patient.

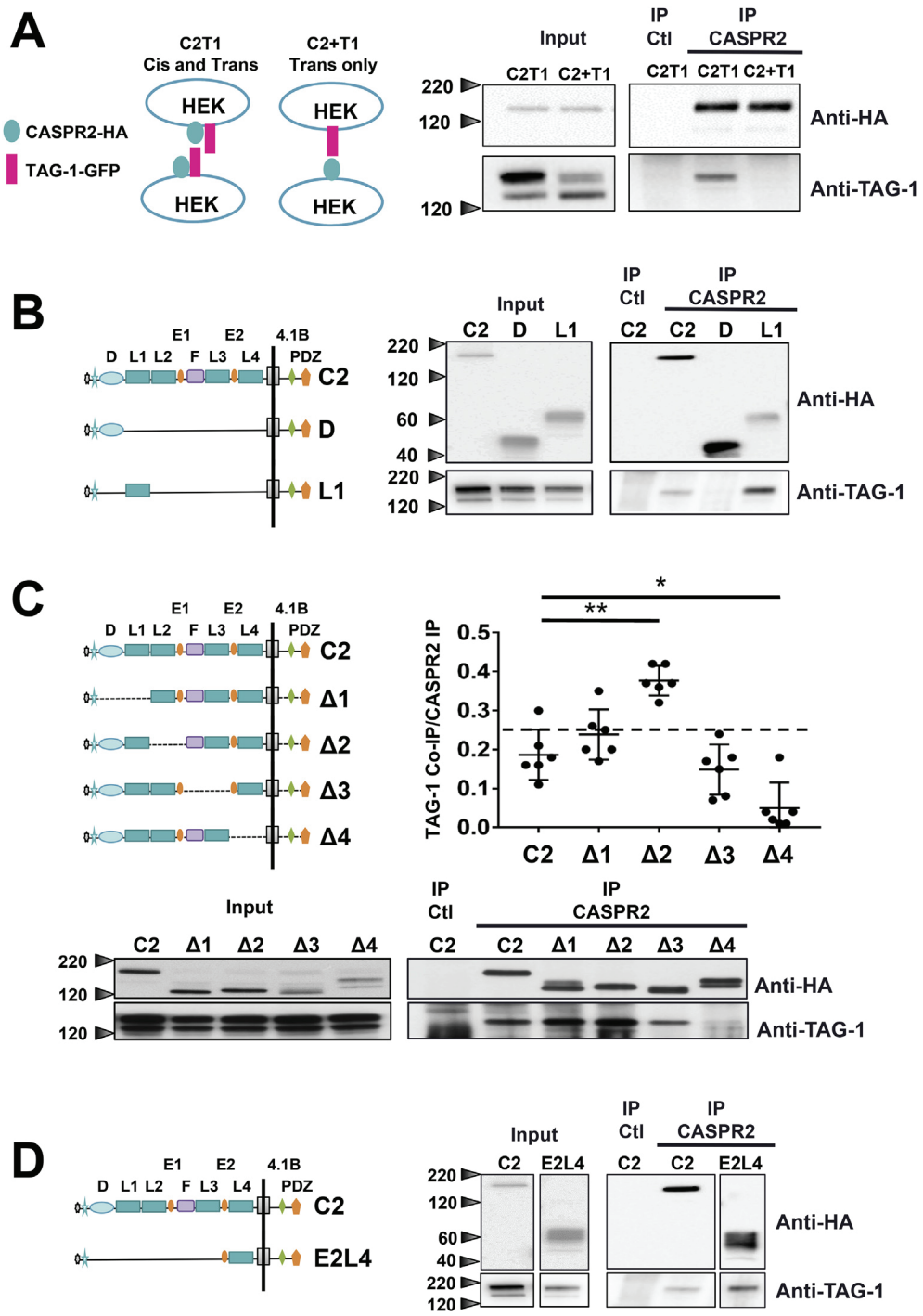

Fig. 2. The EGF2 and laminin G4 domains of CASPR2 are critical for TAG-1 interaction. A) HEK cells were co-transfected with CASPR2-HA and TAG-1-GFP (C2T1) or separately transfected with either one and subsequently put together (C2 + T1). CASPR2 was IP and the level of CASPR2 IP or TAG-1 co-IP was analyzed by Western Blot. n = 3. **B-D)** HEK cells were co-transfected with TAG-1-GFP and CASPR2-HA full-length (C2) or the indicated mutants. CASPR2 was IP and the level of CASPR2 IP and TAG-1 co-IP was analyzed by Western Blot. **(B)** CASPR2 discoidin (D) and laminin G1 (L1) mutants. n = 3. **(C)** CASPR2 Δ1 to Δ4 deletion mutants. The ratios of TAG-1 co-IP over CASPR2 IP signal intensities are depicted in a dot plot. n = 6, *p < 0.05, **p < 0.01 Mann-Whitney test. **(D)** CASPR2 EGF2-laminin G4 mutant (E2L4). n = 3. D: discoidin-like domain, L: laminin G-like domain, E: EGF-like domain, F: fibrinogen-like domain, 4.1B: 4.1B-binding motif, PDZ: PDZ-binding motifs.

was much higher in co-transfected cells (C2T1) than in cells separately transfected (C2 + T1) for which TAG-1 was barely detectable even at long exposure times. These data indicate that the majority of the TAG-1 co-IP with CASPR2 in co-transfected cells comes from cis-interaction between the two proteins.

Anti-CASPR2 autoAb from AE patients all recognize the N-terminal discoidin (D) and laminin G1 (L1) domains of CASPR2 and more importantly, 45% of patient autoAb recognize only these two domains [6], suggesting that they could be critical for CASPR2/TAG-1 interaction. To test this hypothesis, TAG-1 co-IP were repeated as described above in cells expressing the full-length (C2) or only the discoidin (D) or laminin G1 (L1) domains of CASPR2. No TAG-1 co-IP was detected in cells expressing the discoidin domain of CASPR2 (Fig. 2B). In contrast, the laminin G1 domain of CASPR2 was sufficient to co-IP TAG-1 (Fig. 2B). To further characterize the domains of CASPR2 involved in TAG-1 interaction, the same experiment was performed using deletion constructs covering the entire CASPR2 protein. CASPR2 was IP and co-IP TAG-1 was quantified (Fig. 2C). As previously shown [26], compared with CASPR2 full-length (C2), deletion of the laminin G2 and EGF1 domains of CASPR2 (Δ2) increased the quantity of TAG-1 co-IP (C2: 0.19 ± 0.06; Δ2: 0.38 ± 0.04 $p < 0.01$) (Fig. 2C). Although this result did not tell much about the TAG-1-binding propensity of the laminin G2 and EGF1 domains of CASPR2, it suggested that CASPR2/TAG-1 interaction is constrained by conformational hindrances. Equal levels of TAG-1 were co-IP in cells transfected with the CASPR2 construct lacking the discoidin and laminin G1 domains (Δ1) or the

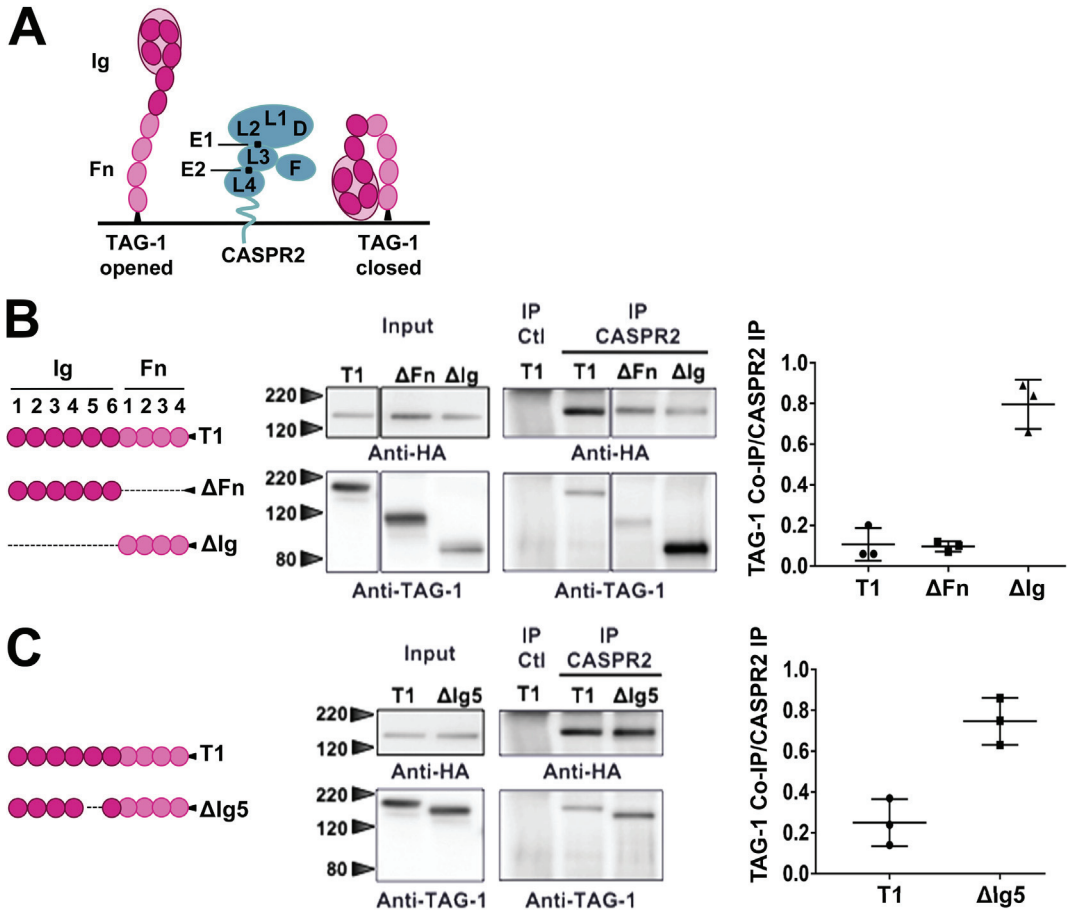

Fig. 3. Both the Ig and Fn domains of TAG-1 are involved in CASPR2/TAG-1 interaction. A) Models of CASPR2 and TAG-1 domain assignment in three dimensions. **B–C)** HEK cells were co-transfected with CASPR2-HA and TAG-1-GFP full-length (T1) or deletion mutants. (**B**) TAG-1 ΔFn and TAG-1 ΔIg. (**C**) TAG-1 ΔIg5. CASPR2 was IP and the level of CASPR2 IP and TAG-1 co-IP was analyzed by Western Blot. The ratios of TAG-1 co-IP over CASPR2 IP signal intensities are depicted in a dot plot. n = 3.

fibrinogen and laminin G3 domains (Δ3) (C2: 0.19 ± 0.06; Δ1: 0.24 ± 0.06; Δ3: 0.15 ± 0.06, $p > 0.05$) indicating that these domains are dispensable for CASPR2/TAG-1 interaction (Fig. 2C). In contrast, the Δ4 construct lacking the EGF2 and laminin G4 domains of CASPR2 led to a drastic decrease of CASPR2/TAG1 interaction (C2: 0.19 ± 0.06; Δ4: 0.05 ± 0.07 $p < 0.05$) (Fig. 2C) indicating that they are major domains of interaction. According to this, the construct expressing only the EGF2 and laminin G4 domains of CASPR2 (E2L4) was sufficient to co-IP TAG-1 (Fig. 2D).

To recapitulate, of the two discoidin and laminin G1 domains, only the laminin G1 domain is involved in CASPR2/TAG-1 interaction and the removal of these domains does not significantly hamper CASPR2/TAG-1 binding. On the contrary, the EGF2 and laminin G4 domains are critical for CASPR2/TAG-1 interaction.

3.3. Both the Ig and Fn domains of TAG-1 are involved in CASPR2/TAG-1 interaction

TAG-1 consists of 6 immunoglobulin (Ig) domains followed by 4 fibronectin domains (Fn) tethered to the cell surface by a GPI anchor (Fig. 3A). The fact that the EGF2-laminin G4 domains of CASPR2, the main interaction domains involved in CASPR2/TAG-1 interaction, are located near the membrane was difficult to conciliate with previous findings showing that CASPR2 interacts in cis with the Ig but not the Fn domains of TAG-1 [22]. Therefore, the ability of CASPR2 to interact with the Ig and Fn domains of TAG-1 was re-considered. Deletion of neither TAG-1 Fn1-4 domains (ΔFn) nor Ig1-6 domains (ΔIg) prevented CASPR2 binding to TAG-1 indicating that both are involved in CASPR2/TAG-1 interaction. Moreover, the removal of TAG-1 Ig domains increased CASPR2 binding suggesting that Ig domains placed constraints on CASPR2 accessibility to TAG-1 Fn domains (Fig. 3B). It has been proposed that TAG-1 could adopt various shapes ranging from a horseshoe-shape or closed conformation to an extended shape or opened conformation (Fig. 3A) [27]. One can therefore postulate that in the closed conformation the Fn domains could be masked by the Ig domains thus limiting their binding to CASPR2. Inversely, in the opened conformation accessibility of Fn domains to CASPR2 could be promoted. To test this hypothesis, we used the TAG-1 ΔIg5 mutant previously described to shift the conformation of the protein toward an extended shape favoring Fn domains exposure [28]. As shown in Fig. 3C, the level of TAG-1 co-IP was higher in cells transfected with TAG-1 ΔIg5 than the full-length construct.

Together, these results indicate that although both the Fn and Ig domains of TAG-1 are involved in CASPR2/TAG-1 interaction, in the TAG-1 back-folded conformation Ig domains could limit TAG-1 binding to CASPR2.

3.4. Patient autoAb do not alter CASPR2 surface expression but increase Kv1.2 surface expression

Based on findings suggesting that CASPR2 and TAG-1 affect intrinsic neuronal excitability by impacting Kv1 expression/distribution at the membrane [18,19,29], we wanted to test the hypothesis that patient anti-CASPR2 autoAb could alter Kv1.2 surface expression. As a preliminary experiment, we wished to determine whether CASPR2 or TAG-1 expression could impact Kv1.2 surface expression. To this end, we

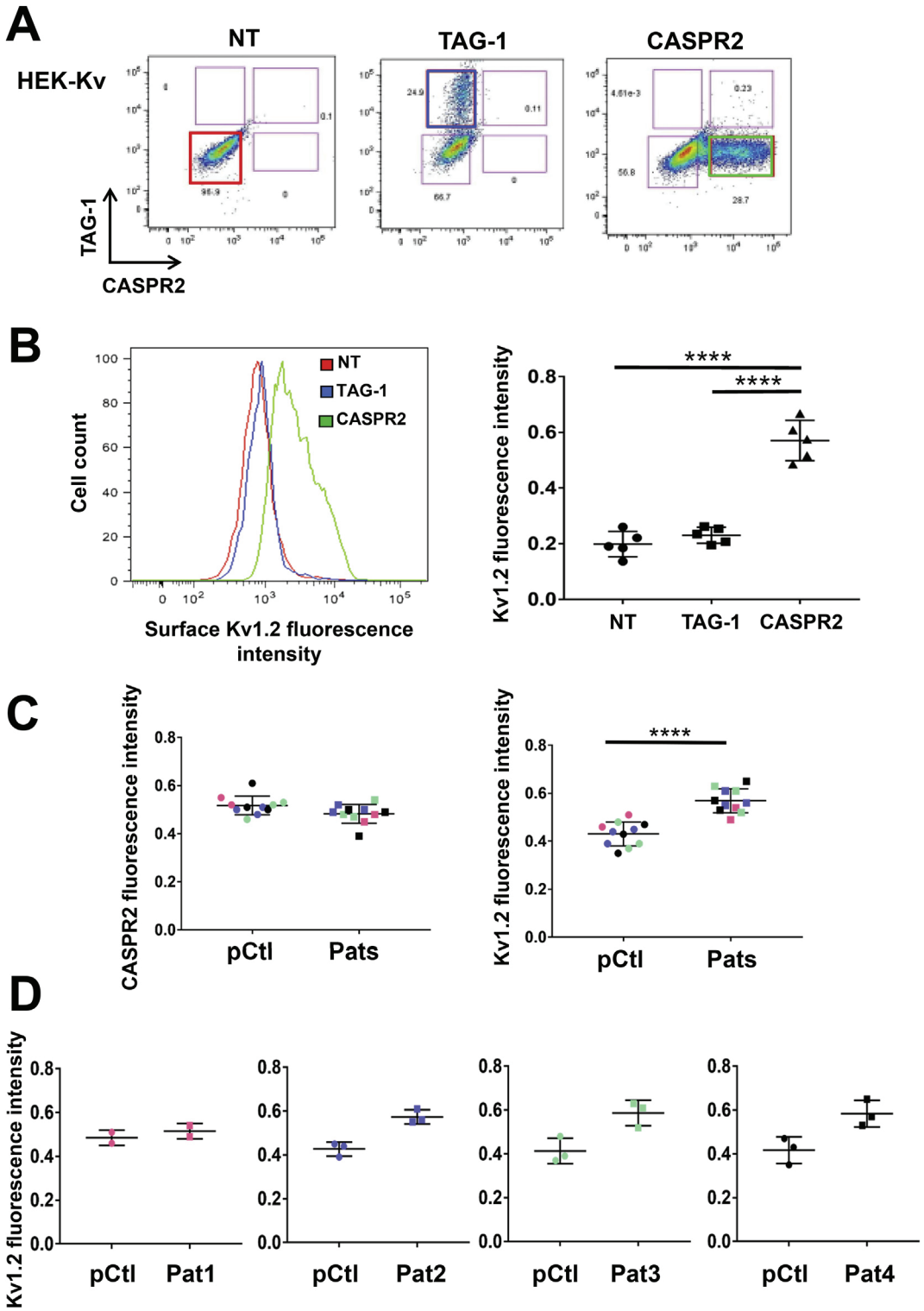

Fig. 4. Patient autoAb do not alter CASPR2 surface expression but increase Kv1.2 surface expression. HEK cells stably expressing Kv1.2 (HEK-Kv) were either non-transfected (NT) or transfected with CASPR2-HA or TAG-1-GFP. The level of Kv1.2 surface expression was quantified by flow cytometry. **A)** Dot plot representation of TAG-1 and CASPR2 fluorescence intensity in the whole population of cells. Non-transfected, TAG-1-positive and CASPR2-positive gated populations are shown in color boxes. **B)** Histogram representation of surface Kv1.2 fluorescence intensity measured in the gated populations shown in A). Results are depicted in a dot plot as mean Kv1.2 fluorescence intensity ratio. n = 5, $p < 0.0001$ Mann-Whitney test. **C)** HEK-Kv cells co-transfected with CASPR2-HA and TAG-1-GFP were incubated for 24 h with pooled control (pCtl) or Patient (Pats) IgG. CASPR2 and Kv1.2 surface fluorescence intensity was measured. Results are depicted as a fraction of the summed median fluorescence intensities. Each color represents a different patient. n = 11 obtained from 3 independent experiments, ****$p < 0.0001$ Mann-Whitney test. **D)** Surface Kv1.2 fluorescence intensity for each patient.

used HEK cells stably expressing Kv1.2 and its Kvβ2 subunit (HEK-Kv) [23]. HEK-Kv cells were transfected with CASPR2-HA or TAG-1-GFP and the level of Kv1.2 surface expression was quantified by flow cytometry (Fig. 4A). As depicted in Fig. 4B, the level of Kv1.2 in TAG-1-positive gated cells was not different from the control non-transfected cells (NT) (0.23 ± 0.03 versus 0.20 ± 0.05, $p > 0.05$). In contrast, Kv1.2 expression was markedly increased following CASPR2 transfection (CASPR2: 0.57 ± 0.07 versus NT: 0.20 ± 0.05, $p < 0.0001$).

Next, HEK-Kv co-transfected with CASPR2-HA and TAG-1-GFP were incubated for 24 h in the presence of Ctl lgG or Pat IgG and the level of CASPR2 and Kv1.2 surface expression was assessed (Fig. 4C). Whereas CASPR2 surface expression was not affected, (Ctl: 0.52 ± 0.02; Pat: 0.48 ± 0.02, $p > 0.05$), the level of Kv1.2 surface expression was significantly increased by patient IgG (Ctl: 0.44 ± 0.03; Pat: 0.56 ± 0.03, $p < 0.0001$). Patient 2, 3 and 4 increased Kv1.2 surface expression to a similar extent, 15.22%, 16.71%, and 16.52% respectively while Patient 1 only induced a 3.15% increase (Fig. 4D).

3.5. Patient autoAb alter CASPR2 surface distribution in hippocampal neurons

To study the impact of anti-CASPR2 autoAb in a more relevant cellular model, cultures of primary hippocampal neurons were treated at 20 DIV with patient IgG (Pat 2, Pat 3, Pat 4) or control IgG (Ctl 1, Ctl 2). Since no commercial Ab targeting the extracellular part of Caspr2 was available at that time, surface Caspr2 labeling was performed using a pool of patient IgG (pPat). In agreement with previous data [12], Caspr2 staining appeared as clusters of various sizes and intensities. Only a subpopulation representing approximately 20% of neurons expressed Caspr2. Moreover, Caspr2 was essentially localized along axons (Fig. 5A and data not shown).

Compared with Ctl IgG, a two-fold increase of Caspr2 surface intensity was observed upon incubation with the three patient IgG tested (Fig. 5A). To gain confidence in these results, the experiment was repeated using pooled patient (pPat) or control (pCtl) IgG and surface Caspr2 was assessed using a cell surface biotinylation assay (Fig. 5B). Notably, the level of Caspr2 in the biotinylated fraction of the proteins as well as the level of total Caspr2 was not different between the two conditions. Finally, to get a better idea of the impact of patient IgG on Caspr2 level of expression and distribution at the cell surface, hippocampal neurons were transfected with a plasmid coding for CASPR2-GFP and then treated with pooled patient IgG (pPat) or control IgG (pCtl). To analyze the fraction of CASPR2 present at the cell surface, live cells were labeled with an anti-GFP primary Ab and an anti-rabbit Alexa555-conjugated secondary Ab, therefore avoiding any interference between patient Ab used during the 24h incubation and Ab used for CASPR2 surface labeling. CASPR2 mean surface intensity per um2 of neuron was higher in cells incubated with Pat IgG than Ctl IgG (pPat: 11.62 ± 6.86; pCtl: 1.02 ± 0.81 $p < 0.0001$, data not shown). The size, intensity and number of CASPR2 clusters were then quantified for each condition and compared (Fig. 5C). Whereas patient IgG induced a two-fold increase in cluster intensity (pCtl: 16.43 ± 4.32; pPat: 32.60 ± 10.39 $p < 0.0001$), a slight increase in cluster size was observed (pCtl: 0.20 ± 0.02; pPat: 0.25 ± 0.05 $p < 0.0001$). In contrast, CASPR2 cluster number at the cell surface was markedly augmented (pCtl: 0.06 ± 0.04; pPat: 0.32 ± 0.09 $p < 0.0001$).

Taken together, these results showed that patient IgG did not induce Caspr2 internalization but altered its distribution at the cell membrane promoting Caspr2 cluster formation.

3.6. Patient autoAb increase Kv1.2 expression in hippocampal neurons

In line with the results we obtained on HEK cells, the impact of anti-CASPR2 patient autoAb on Kv1.2 expression was assessed in hippocampal neurons (21 DIV). Firstly, cells were stained for Kv1.2 surface expression but we were not able to observe any signal. Therefore, Caspr2 expression was assessed on live cells (surface) using the pool of patient IgG and Kv1.2 expression was assessed on permeabilized cells (total). As illustrated in Fig. 6A, fibers expressing high level of Kv1.2 could be clearly distinguished and strikingly an obvious co-labeling was observed with axons highly positive for Caspr2. Since in cultured hippocampal neurons Caspr2 is essentially expressed in inhibitory neurons [12], cells were stained for GAD65, a typical marker of inhibitory neurons (Fig. 6A). As expected the population of axons highly positive for Caspr2 was essentially GAD65-positive (98%) moreover, 90% of the Caspr2/GAD65-double positive axons also expressed high level of Kv1.2. Therefore, it appeared that Caspr2-positive inhibitory neurons also express high level of Kv1.2. Secondly, to determine whether anti-CASPR2 patient Ab modulate Kv1.2 expression, primary hippocampal neurons were treated at 20 DIV with the pool of patient or control IgG and stained for surface Caspr2 and total Kv1.2 (Fig. 6B). Compared with control IgG, treatment with patient IgG significantly increased Kv1.2 signal intensity (Ctl: 409.8 ± 83.2 versus Pat: 568.9 ± 193.6, $p < 0.01$).

4. Discussion

4.1. Anti-CASPR2 patient autoAb alter CASPR2 surface distribution

We show in this study that patient autoAb do not induce CASPR2 internalization using two cellular models, HEK cells and more importantly cultured primary hippocampal neurons. When tested on endogenous Caspr2, the level of Caspr2 at the cell surface remained essentially unchanged upon patient autoAb addition. However, in CASPR2 transfected neurons, patient IgG increased CASPR2 surface expression. Moreover, CASPR2 membrane distribution was altered with the formation of an elevated number of CASPR2 clusters. In view of these observations, it appears that the pathogenic effect of autoAb rely on CASPR2 redistribution at the cell membrane rather than internalization. These results are consistent with the fact that anti-CASPR2 patient autoAb are often IgG4 [6,7,12], a subclass presenting several unique biophysical properties. In particular, IgG4 can undergo half-molecule exchange rendering them bispecific and thereby functionally monovalent. This implies that IgG4 are unable to crosslink their targets which is often a prerequisite for the process of internalization [30].

4.2. Anti-CASPR2 patient autoAb impede CASPR2/TAG-1 interaction

It was suggested that patient autoAb could directly perturb CASPR2 function by preventing CASPR2/TAG-1 interaction. For instance, using an acellular solid phase binding assay, Patterson et al. [20] showed that patient Ab decrease CASPR2/TAG-1 binding by 30%–90% depending on the patient serum tested. In this paper, using purified serum IgG, we find that the decrease of CASPR2/TAG-1 binding upon anti-CASPR2 autoAb addition still occurs in a cellular environment, although to a lower extent (under 20% of decrease). Moreover, we identified regions taking part in CASPR2/TAG-1 cis-interactions, the Ig1-6 and Fn1-4 domains on TAG-1 side as well as the laminin G1 and the EGF2-laminin G4 domains on CASPR2 side. However, the removal of the laminin G1 domain of CASPR2 did not significantly hamper CASPR2/TAG-1 interaction, whereas removal of the EGF2-laminin G4 domains drastically impeded CASPR2/TAG-1 interaction, pointing the EGF2-laminin G4 domains as key domains of interaction. EGF-like domains consist of molecular hinges (small linear solenoid domain) permitting the lobes of the protein to flex with respect to each other [31,32]. In contrast, laminin G-like domains are large globular domains involved in interactions with other proteins (neuroligin, cerebellin, GABAa receptor) [33,34]. It is therefore likely that the laminin G4 domain of CASPR2, rather than the EGF2 domain, mediates CASPR2/TAG-1 interactions. Considering the molecular shape and dimension of these two molecules a model can be proposed for which the laminin G4 domain of CASPR2 interacts with the fibronectin domains of TAG-1 and the laminin G1

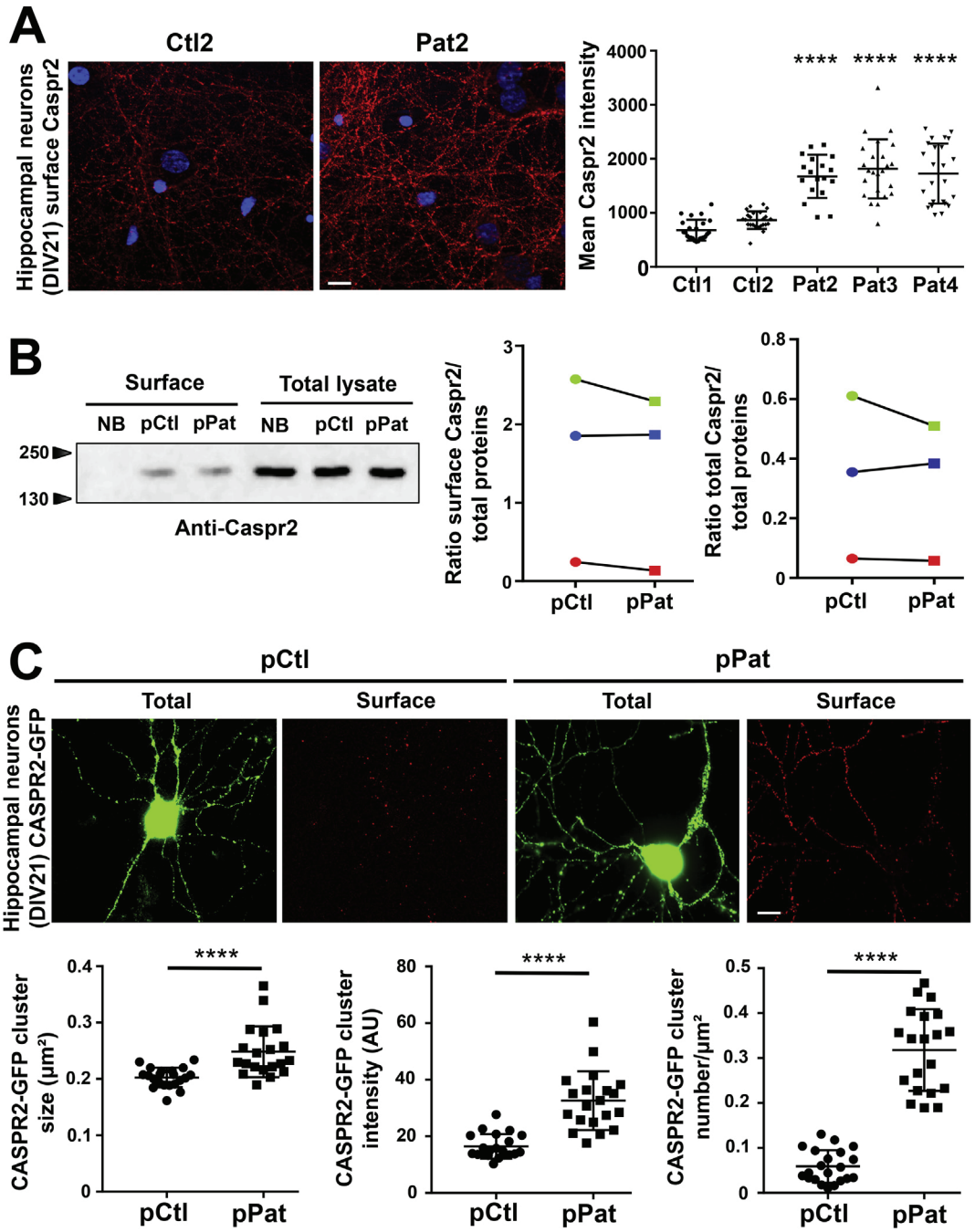

Fig. 5. Patient autoAb changed CASPR2 surface distribution in hippocampal neurons. A) hippocampal neurons (21 DIV) treated for 24h with control (Ctl) or patient (Pat) IgG were stained for surface Caspr2 and signal intensities were quantified. n = 17–24 image fields per condition, ****p < 0.0001 Kruskal-Wallis test. **B)** Hippocampal neurons (21 DIV) treated with pooled patient (pPat) or control (pCtl) IgG were subjected to cell surface biotinylation or left non-biotinylated as control (NB). Caspr2 surface and Caspr2 total proteins were quantified by Western-Blot and results expressed as ratios over total protein loaded. Each color represents a different experiment. n = 3, Wilcoxon signed-rank test. **C)** Hippocampal neurons (21 DIV) transfected with CASPR2-GFP were treated with pooled patient (pPat) or control (pCtl) IgG. The size, intensity and number of surface CASPR2-GFP clusters was analyzed on live cells using anti-GFP primary Ab/Alexa555 secondary Ab. Results are depicted as a dot plot. n = 21 neurons per condition obtained from 3 independent experiments, ****p < 0.0001 Mann-Whitney test. Scale bar 10 µm.

domain of CASPR2 interacts with the immunoglobulin domains of TAG-1 (Fig. 7A). Essentially obtained with deletion mutants, this model has nevertheless to be taken with caution since we find here that as depicted by others [32], CASPR2/TAG-1 interactions are constrained by conformational hindrances.

Regarding the impact of anti-CASPR2 autoAb on this model of interaction, we know that patient Ab are polyclonal and mostly target the N-terminal half of CASPR2 ectodomain (D-L1-L2-E1), all recognizing at least the discoidin and laminin G1 domains [6,11,12]. Moreover, patient Ab rarely target the C-terminal half of the protein (F-L3-E2-L4), where the main interaction domain of CASPR2, the laminin G4 domain, is located [11]. Thus, anti-CASPR2 autoAb would mainly perturb CASPR2/TAG-1 interaction trough the laminin G1 domain, which may explain their low propensity to impede CASPR2/TAG-1 interaction (Fig. 7B). In addition, in our cellular model, CASPR2/TAG-1 interactions are mainly occurring in cis with high constraints due to a complex environment, whereas in the solid phase binding assay, CASPR2 and TAG-1 can freely adopt several orientations. Such differences may

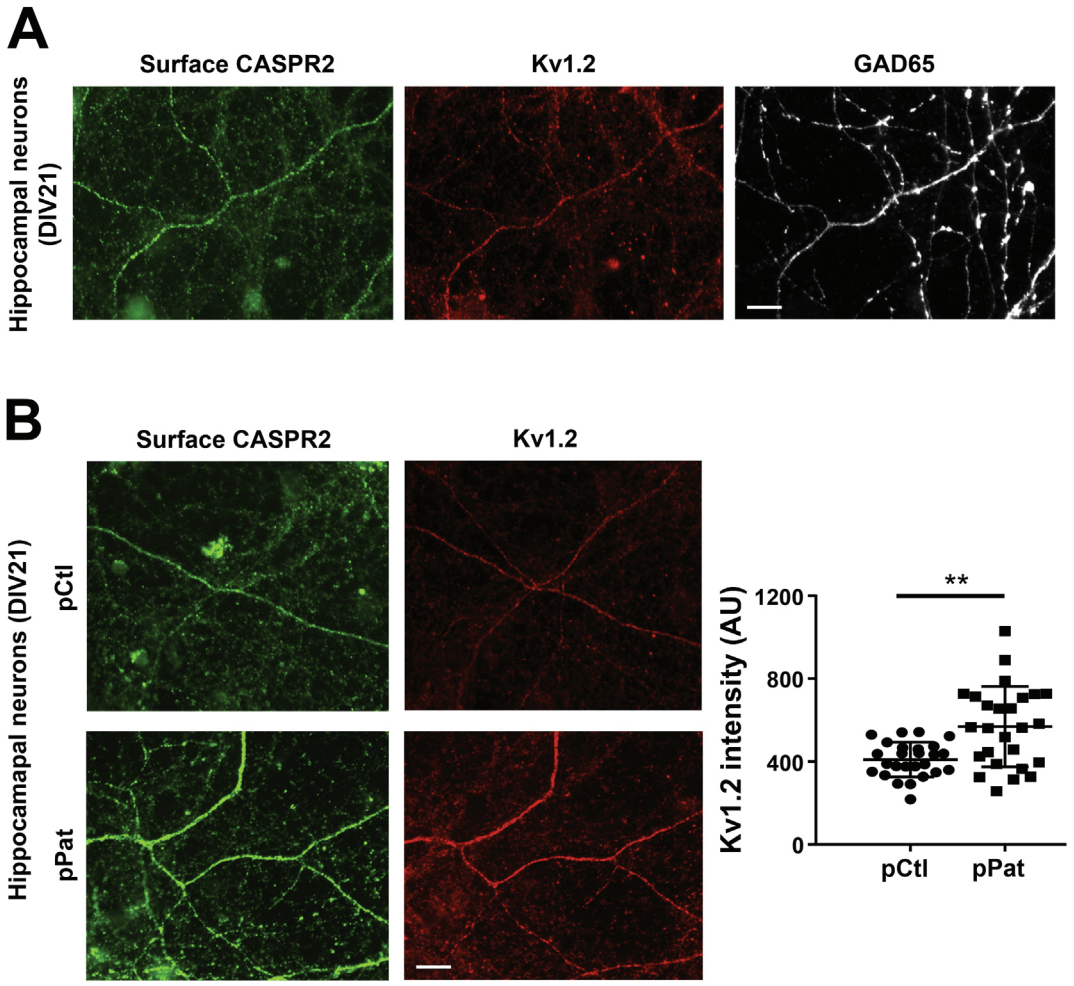

Fig. 6. Patient autoAb increase Kv1.2 expression in hippocampal neurons. A) hippocampal neurons (21 DIV) stained on live cells for surface Caspr2 and on permeabilized cells for Kv1.2 and GAD65. **B)** hippocampal neurons (21 DIV) treated for 24h with pooled patient (pPat) or control (pCtl) IgG were stained as in A) and Kv1.2 fluorescence signal intensities were quantified. n = 26 neurons per condition obtained from 3 independent experiments, **p < 0.01 Mann-Whitney test. Scale bar 10 μm.

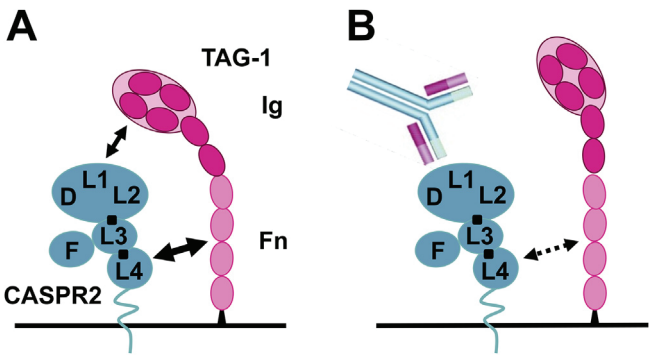

Fig. 7. Model of CASPR2/TAG-1 interaction and impact of anti-CASPR2 autoAb. A) Based on the molecular shape and dimension of these two molecules we propose a model for which laminin G4 (L4), the main interaction domain of CASPR2, interacts with the fibronectin (Fn) domains of TAG-1 and the laminin G1 (L1) domain of CASPR2 interacts with the immunoglobulin (Ig) domains of TAG-1. **B)** Since patient Ab rarely target the laminin G4 domain of the protein, anti-CASPR2 autoAb would mainly perturb CASPR2/TAG-1 interaction trough the laminin G1 domain.

explain the higher blocking propensity of patient Ab in the solid phase binding assay [20].

Besides, as for the solid phase binding assay, the extent of inhibition varied between patients although the 4 sera tested in this study presented similar anti-CASPR2 Ab titers. Differences in the localization of targeted epitopes or the Ab affinity/avidity for their targets as well as the Ab titer for each subclass of IgG (IgG1 or IgG4) may account for the variations in the degree of inhibition. Additional studies with higher number of patients are needed to determine factors responsible for the difference observed between patients.

4.3. CASPR2 and Kv1 expression are linked

We showed herein that the introduction of CASPR2 into HEK cells induces a marked increase of the level of Kv1.2 surface expression. Moreover, it appears that Caspr2-positive inhibitory neurons also express high level of Kv1.2. These results are in line with previous findings showing a decreased membrane expression of Kv1.2 in *Cntnap2* KO DRG neurons in culture. Notably, in these cells the KO of Caspr2 resulted in enhanced excitability with a large reduction in the DTX-sensitive outward current, indicating a reduction in the function of Kv1 channels [19]. Moreover, in wild-type DRG neurons cultured *in vitro* for 5 days, a spontaneous reduction in Kv1 (membrane) and Caspr2 (mRNA) expression coincided with hyperexcitabilty. Importantly, enhanced excitability was reversed by Caspr2-forced expression in a Kv1 channel-dependent manner [19]. Therefore, one can speculate that CASPR2, by interfering with surface expression of Kv1 channels is an important modulator of neuronal excitability.

4.4. Anti-CASPR2 patient autoAb increase Kv1.2 expression

In HEK cells, patient autoAb increase Kv1.2 surface expression. Importantly, such an increase is also observed in hippocampal neurons although we could not determine if this occurs at the cells surface. These results are in contrast with a previous study showing that in cultured DRG neurons treated with anti-CASPR2 patient Ab the number of cells expressing Kv1.2 at the surface was decreased [19]. Since Kv1 expression may vary with CASPR2 expression levels, it would be interesting to assess the impact of anti-CASPR2 autoAb on the level of CASPR2 surface expression in these neurons. Nevertheless, diverse mechanisms might regulate Kv1 surface expression depending on the cell type, in the same way as different mechanisms are responsible for Kv1 enrichment at the AIS and JXP. Of particular interest, a decrease of CASPR2 and Kv1.1 expression was observed at JXP following systemic injection of anti-CASPR2 patient Ab despite the fact that no patient Ab binding was detected in this region. On the other hand, a clear patient Ab binding was observed on DRG cell soma [19]. It is therefore tempting to speculate that decreased JXP expression of CASPR2 and Kv1.1 might be due to patient Ab-induced retention of these molecules at the soma, thereby impairing their axonal membrane lateral diffusion.

Since CASPR2 interacts with Kv1 channels indirectly through their intracellular cytoplasmic domains [1], the mechanism by which CASPR2 promotes Kv1.2 surface expression likely relies on intracellular motifs. Both proteins present a cytoskeleton-binding motif as well as a PDZ-binding motif, which could lead to restricted diffusion and co-clustering of CASPR2 and Kv1.2 at the membrane. For instance, the 4.1B-cytoskeleton-binding motif of CASPR2 was depicted as required for the enrichment of Kv1 channels at the NOR [35]. Kv1.2 surface expression relies on tyrosine residues present in its intracellular domain. Their phosphorylation leads to Kv1.2 reduced binding to the cytoskeleton and endocytosis [36,37]. Of particular interest, TAG-1-induced clustering of Kv1.2 along axons was shown to depend on Kv1.2 phosphorylation [29]. Whether CASPR2 could modulate Kv1 surface expression by impinging Kv1 phosphorylation directly or indirectly, by altering TAG-1 membrane distribution [15,29], remains to be established. Regarding the possible mechanism(s) by which anti-CASPR2 autoAb may lead to increased Kv1.2 expression, patient Ab binding may restrict CASPR2 diffusion thereby promoting cluster formation. This may in turn retain Kv1.2 at the membrane possibly by stabilizing CASPR2/Kv1.2 interactions, thus limiting Kv1 endocytosis.

Kv1 channels play a major role in membrane repolarization following action potential. A decrease in Kv1 expression leads to higher neuronal excitability characterized by an increase of action potential frequency and repolarization latency [38]. This results in increased neurotransmitter release at the synapse [39]. On the contrary, an increase of Kv1 expression could lead to a decrease of action potential frequency and neurotransmitter release [40]. Since CASPR2 is mainly expressed in inhibitory neurons, anti-CASPR2 autoAb, by increasing Kv1 expression, could specifically result in decreased inhibition, a defect consistent with the seizure disorders observed in patients.

In conclusion, we bring further evidences of two potential pathogenic mechanisms of anti-CASPR2 autoAb in patients with AE namely disturbing CASPR2/TAG-1 interaction and Kv1.2 expression. By impacting on neuronal excitability, these pathogenic mechanisms could contribute to the clinical features of patients with AE. Furthermore, our data provide new insights into the interaction constraints between CASPR2 and TAG-1, which might prove useful to study the relevance of this interaction in the formation and localization of the CASPR2/TAG-1/Kv1 complex.

Funding

This work was supported by INSERM, CNRS, University Lyon 1, the Agence Nationale de la Recherche (ANR-14-CE15-0001-MECANO), France, the Fondation pour la Recherche Médicale (FRM DQ20170336751), France and the fonds de dotation CSL Behring pour la recherche, France.

Acknowledgements

We are grateful to C. Faivre-Sarrailh (Institut de Neurobiologie de la Méditerranée, Aix Marseille Université, INSERM UMR1249, Marseille France) for providing the CASPR2 full-length and derived plasmids as well as scientific and technical advice. We thank Anthony Morielli (University of Vermont, Burlington USA) for providing the HEK-Kv cell line and, A. Vandermoeten, LM. Illartein, O. Martin and A. Meunier (Scar, Faculté Rockefeller, Lyon) for taking care of the animals.

Appendix A. Supplementary data

Supplementary data to this article can be found online at https://doi.org/10.1016/j.jaut.2019.05.012.

References

[1] S. Poliak, L. Gollan, R. Martinez, A. Custer, S. Einheber, J.L. Salzer, J.S. Trimmer, P. Shrager, E. Peles, Caspr2, a new member of the neurexin superfamily, is localized at the juxtaparanodes of myelinated axons and associates with K+ channels, Neuron 24 (1999) 1037–1047.

[2] P. Shillito, P.C. Molenaar, A. Vincent, K. Leys, W. Zheng, R.J. van den Berg, J.J. Plomp, G.T. van Kempen, G. Chauplannaz, A.R. Wintzen, Acquired neuromyotonia: evidence for autoantibodies directed against K+ channels of peripheral nerves, Ann. Neurol. 38 (1995) 714–722, https://doi.org/10.1002/ana.410380505.

[3] R. Liguori, A. Vincent, L. Clover, P. Avoni, G. Plazzi, P. Cortelli, A. Baruzzi, T. Carey, P. Gambetti, E. Lugaresi, P. Montagna, Morvan's syndrome: peripheral and central nervous system and cardiac involvement with antibodies to voltage-gated potassium channels, Brain J. Neurol. 124 (2001) 2417–2426.

[4] C. Buckley, J. Oger, L. Clover, E. Tüzün, K. Carpenter, M. Jackson, A. Vincent, Potassium channel antibodies in two patients with reversible limbic encephalitis, Ann. Neurol. 50 (2001) 73–78.

[5] J. Newsom-Davis, C. Buckley, L. Clover, I. Hart, P. Maddison, E. Tüzüm, A. Vincent, Autoimmune disorders of neuronal potassium channels, Ann. N. Y. Acad. Sci. 998 (2003) 202–210.

[6] B. Joubert, M. Saint-Martin, N. Noraz, G. Picard, V. Rogemond, F. Ducray, V. Desestret, D. Psimaras, J.-Y. Delattre, J.-C. Antoine, J. Honnorat, Characterization of a subtype of autoimmune encephalitis with anti-contactin-associated protein-like 2 antibodies in the cerebrospinal fluid, prominent limbic symptoms, and seizures, JAMA Neurol 73 (2016) 1115–1124, https://doi.org/10.1001/jamaneurol.2016.1585.

[7] A. van Sonderen, H. Ariño, M. Petit-Pedrol, F. Leypoldt, P. Körtvélyessy, K.-P. Wandinger, E. Lancaster, P.W. Wirtz, M.W.J. Schreurs, P.A.E. Sillevis Smitt, F. Graus, J. Dalmau, M.J. Titulaer, The clinical spectrum of Caspr2 antibody-associated disease, Neurology 87 (2016) 521–528, https://doi.org/10.1212/WNL.0000000000002917.

[8] S.R. Irani, S. Alexander, P. Waters, K.A. Kleopa, P. Pettingill, L. Zuliani, E. Peles, C. Buckley, B. Lang, A. Vincent, Antibodies to Kv1 potassium channel-complex proteins leucine-rich, glioma inactivated 1 protein and contactin-associated protein-2 in limbic encephalitis, Morvan's syndrome and acquired neuromyotonia, Brain 133 (2010) 2734–2748, https://doi.org/10.1093/brain/awq213.

[9] M. Lai, M.G.M. Huijbers, E. Lancaster, F. Graus, L. Bataller, R. Balice-Gordon, J.K. Cowell, J. Dalmau, Investigation of LGI1 as the antigen in limbic encephalitis previously attributed to potassium channels: a case series, Lancet Neurol. 9 (2010) 776–785, https://doi.org/10.1016/S1474-4422(10)70137-X.

[10] M. Saint-Martin, B. Joubert, V. Pellier-Monnin, O. Pascual, N. Noraz, J. Honnorat, Contactin-associated protein-like 2, a protein of the neurexin family involved in several human diseases, Eur. J. Neurosci. 48 (2018) 1906–1923, https://doi.org/10.1111/ejn.14081.

[11] A.L. Olsen, Y. Lai, J. Dalmau, S.S. Scherer, E. Lancaster, Caspr2 autoantibodies target multiple epitopes, Neurol. Neuroimmunol. Neuroinflammation. 2 (2015) e127, https://doi.org/10.1212/NXI.0000000000000127.

[12] D. Pinatel, B. Hivert, J. Boucraut, M. Saint-Martin, V. Rogemond, L. Zoupi, D. Karagogeos, J. Honnorat, C. Faivre-Sarrailh, Inhibitory axons are targeted in hippocampal cell culture by anti-Caspr2 autoantibodies associated with limbic encephalitis, Front. Cell. Neurosci. 9 (2015) 265, https://doi.org/10.3389/fncel.2015.00265.

[13] S. Poliak, D. Salomon, H. Elhanany, H. Sabanay, B. Kiernan, L. Pevny, C.L. Stewart, X. Xu, S.-Y. Chiu, P. Shrager, A.J.W. Furley, E. Peles, Juxtaparanodal clustering of Shaker-like K+ channels in myelinated axons depends on Caspr2 and TAG-1, J. Cell Biol. 162 (2003) 1149–1160, https://doi.org/10.1083/jcb.200305018.

[14] M.N. Rasband, E.W. Park, D. Zhen, M.I. Arbuckle, S. Poliak, E. Peles, S.G.N. Grant, J.S. Trimmer, Clustering of neuronal potassium channels is independent of their interaction with PSD-95, J. Cell Biol. 159 (2002) 663–672, https://doi.org/10.1083/jcb.200206024.

[15] M. Traka, L. Goutebroze, N. Denisenko, M. Bessa, A. Nifli, S. Havaki, Y. Iwakura, F. Fukamauchi, K. Watanabe, B. Soliven, J.-A. Girault, D. Karagogeos, Association of

TAG-1 with Caspr2 is essential for the molecular organization of juxtaparanodal regions of myelinated fibers, J. Cell Biol. 162 (2003) 1161–1172, https://doi.org/10.1083/jcb.200305078.

[16] N. Chen, F. Koopmans, A. Gordon, I. Paliukhovich, R.V. Klaassen, R.C. van der Schors, E. Peles, M. Verhage, A.B. Smit, K.W. Li, Interaction proteomics of canonical Caspr2 (CNTNAP2) reveals the presence of two Caspr2 isoforms with overlapping interactomes, Biochim. Biophys. Acta 1854 (2015) 827–833, https://doi.org/10.1016/j.bbapap.2015.02.008.

[17] M.C. Inda, J. DeFelipe, A. Muñoz, Voltage-gated ion channels in the axon initial segment of human cortical pyramidal cells and their relationship with chandelier cells, Proc. Natl. Acad. Sci. U.S.A. 103 (2006) 2920–2925, https://doi.org/10.1073/pnas.0511197103.

[18] R. Scott, A. Sánchez-Aguilera, K. van Elst, L. Lim, N. Dehorter, S.E. Bae, G. Bartolini, E. Peles, M.J.H. Kas, H. Bruining, O. Marín, Loss of Cntnap2 causes axonal excitability deficits, developmental delay in cortical myelination, and abnormal stereotyped motor behavior, Cereb. Cortex N. Y. N 29 (2019) 586–597, https://doi.org/10.1093/cercor/bhx341 1991.

[19] J.M. Dawes, G.A. Weir, S.J. Middleton, R. Patel, K.I. Chisholm, P. Pettingill, L.J. Peck, J. Sheridan, A. Shakir, L. Jacobson, M. Gutierrez-Mecinas, J. Galino, J. Walcher, J. Kühnemund, H. Kuehn, M.D. Sanna, B. Lang, A.J. Clark, A.C. Themistocleous, N. Iwagaki, S.J. West, K. Werynska, L. Carroll, T. Trendafilova, D.A. Menassa, M.P. Giannoccaro, E. Coutinho, I. Cervellini, D. Tewari, C. Buckley, M.I. Leite, H. Wildner, H.U. Zeilhofer, E. Peles, A.J. Todd, S.B. McMahon, A.H. Dickenson, G.R. Lewin, A. Vincent, D.L. Bennett, Immune or genetic-mediated disruption of CASPR2 causes pain hypersensitivity due to enhanced primary afferent excitability, Neuron 97 (2018) 806–822, https://doi.org/10.1016/j.neuron.2018.01.033 e10.

[20] K.R. Patterson, J. Dalmau, E. Lancaster, Mechanisms of Caspr2 antibodies in autoimmune encephalitis and neuromyotonia, Ann. Neurol. 83 (2018) 40–51, https://doi.org/10.1002/ana.25120.

[21] B. Joubert, F. Gobert, L. Thomas, M. Saint-Martin, V. Desestret, P. Convers, V. Rogemond, G. Picard, F. Ducray, D. Psimaras, J.-C. Antoine, J.-Y. Delattre, J. Honnorat, Autoimmune episodic ataxia in patients with anti-CASPR2 antibody-associated encephalitis, Neurol. Neuroimmunol. Neuroinflammation. 4 (2017) e371, https://doi.org/10.1212/NXI.0000000000000371.

[22] A. Tzimourakas, S. Giasemi, M. Mouratidou, D. Karagogeos, Structure-function analysis of protein complexes involved in the molecular architecture of juxtaparanodal regions of myelinated fibers, Biotechnol. J. 2 (2007) 577–583, https://doi.org/10.1002/biot.200700023.

[23] T.G. Cachero, A.D. Morielli, E.G. Peralta, The small GTP-binding protein RhoA regulates a delayed rectifier potassium channel, Cell 93 (1998) 1077–1085.

[24] E. Nesti, B. Everill, A.D. Morielli, Endocytosis as a mechanism for tyrosine kinase-dependent suppression of a voltage-gated potassium channel, Mol. Biol. Cell 15 (2004) 4073–4088, https://doi.org/10.1091/mbc.e03-11-0788.

[25] M. Savvaki, K. Theodorakis, L. Zoupi, A. Stamatakis, S. Tivodar, K. Kyriacou, F. Stylianopoulou, D. Karagogeos, The expression of TAG-1 in glial cells is sufficient for the formation of the juxtaparanodal complex and the phenotypic rescue of tag-1 homozygous mutants in the CNS, J. Neurosci. 30 (2010) 13943–13954, https://doi.org/10.1523/JNEUROSCI.2574-10.2010.

[26] D. Pinatel, B. Hivert, M. Saint-Martin, N. Noraz, M. Savvaki, D. Karagogeos, C. Faivre-Sarrailh, The Kv1-associated molecules TAG-1 and Caspr2 are selectively targeted to the axon initial segment in hippocampal neurons, J. Cell Sci. 130 (2017) 2209–2220, https://doi.org/10.1242/jcs.202267.

[27] C. Rader, B. Kunz, R. Lierheimer, R.J. Giger, P. Berger, P. Tittmann, H. Gross, P. Sonderegger, Implications for the domain arrangement of axonin-1 derived from the mapping of its NgCAM binding site, EMBO J. 15 (1996) 2056–2068.

[28] B. Kunz, R. Lierheimer, C. Rader, M. Spirig, U. Ziegler, P. Sonderegger, Axonin-1/TAG-1 mediates cell-cell adhesion by a cis-assisted trans-interaction, J. Biol. Chem. 277 (2002) 4551–4557, https://doi.org/10.1074/jbc.M109779200.

[29] C. Gu, Y. Gu, Clustering and activity tuning of Kv1 channels in myelinated hippocampal axons, J. Biol. Chem. 286 (2011) 25835–25847, https://doi.org/10.1074/jbc.M111.219113.

[30] M.G. Huijbers, L.A. Querol, E.H. Niks, J.J. Plomp, S.M. van der Maarel, F. Graus, J. Dalmau, I. Illa, J.J. Verschuuren, The expanding field of IgG4-mediated neurological autoimmune disorders, Eur. J. Neurol. 22 (2015) 1151–1161, https://doi.org/10.1111/ene.12758.

[31] E.N. Rubio-Marrero, G. Vincelli, C.M. Jeffries, T.R. Shaikh, I.S. Pakos, F.M. Ranaivoson, S. von Daake, B. Demeler, A. De Jaco, G. Perkins, M.H. Ellisman, J. Trewhella, D. Comoletti, Structural characterization of the extracellular domain of CASPR2 and insights into its association with the novel ligand Contactin1, J. Biol. Chem. 291 (2016) 5788–5802, https://doi.org/10.1074/jbc.M115.705681.

[32] Z. Lu, M.V.V.V.S. Reddy, J. Liu, A. Kalichava, J. Liu, L. Zhang, F. Chen, Y. Wang, L.M.F. Holthauzen, M.A. White, S. Seshadrinathan, X. Zhong, G. Ren, G. Rudenko, Molecular architecture of contactin-associated protein-like 2 (CNTNAP2) and its interaction with contactin 2 (CNTN2), J. Biol. Chem. (2016), https://doi.org/10.1074/jbc.M116.748236 jbc.M116.748236.

[33] F. Chen, V. Venugopal, B. Murray, G. Rudenko, The structure of neurexin 1α reveals features promoting a role as synaptic organizer, Struct. Lond. Engl. 19 (2011) 779–789, https://doi.org/10.1016/j.str.2011.03.012 1993.

[34] C. Reissner, F. Runkel, M. Missler, Neurexins, Genome Biol. 14 (2013) 213, https://doi.org/10.1186/gb-2013-14-9-213.

[35] I. Horresh, V. Bar, J.L. Kissil, E. Peles, Organization of myelinated axons by Caspr and Caspr2 requires the cytoskeletal adapter protein 4.1B, J. Neurosci. Off. J. Soc. Neurosci. 30 (2010) 2480–2489, https://doi.org/10.1523/JNEUROSCI.5225-09.2010.

[36] D. Hattan, E. Nesti, T.G. Cachero, A.D. Morielli, Tyrosine phosphorylation of Kv1.2 modulates its interaction with the actin-binding protein cortactin, J. Biol. Chem. 277 (2002) 38596–38606, https://doi.org/10.1074/jbc.M205005200.

[37] H.C. Lai, L.Y. Jan, The distribution and targeting of neuronal voltage-gated ion channels, Nat. Rev. Neurosci. 7 (2006) 548–562, https://doi.org/10.1038/nrn1938.

[38] S.L. Smart, V. Lopantsev, C.L. Zhang, C.A. Robbins, H. Wang, S.Y. Chiu, P.A. Schwartzkroin, A. Messing, B.L. Tempel, Deletion of the K(V)1.1 potassium channel causes epilepsy in mice, Neuron 20 (1998) 809–819.

[39] J.R. Geiger, P. Jonas, Dynamic control of presynaptic Ca(2+) inflow by fast-inactivating K(+) channels in hippocampal mossy fiber boutons, Neuron 28 (2000) 927–939.

[40] S. He, L.-R. Shao, W.B. Rittase, S.B. Bausch, Increased Kv1 channel expression may contribute to decreased sIPSC frequency following chronic inhibition of NR2B-containing NMDAR, Neuropsychopharmacology 37 (2012) 1338–1356, https://doi.org/10.1038/npp.2011.320.

ARTICLE 2 (IN PREPARATION)

Anti-CASPR2 autoantibodies from patients with autoimmune limbic encephalitis promote spine developmental processes and disturb mature inhibitory synapses.

Pieters, A., Malleval, C., Honnorat, J., Pascual, O., Noraz, N.

In preparation.

Objectives: CASPR2 was initially described at the node of Ranvier as a neuronal cell-adhesion protein, belonging to the neurexin family. Proteins belonging to this family are mainly present at the synapse, where they assure neuronal contacts by anchoring pre- to postsynaptic membranes. CASPR2 has also been found to be present in other neuronal compartments, including the synapse. Increasing sets of data suggest the implication of CASPR2 in synaptic functions. However, a precise role for CASPR2 in synaptic processes has not been defined yet. Interestingly, anti-CASPR2 autoAbs have been found in the serum of patients with autoimmune limbic encephalitis. We here use patients' autoAbs as a tool to assess the function of CASPR2 in correctly developed *in vitro* hippocampal WT neurons. We investigated the effects of patients' autoAbs on excitatory synapses by analyzing PSD95 clusters, dendritic spine morphology and AMPA receptor content, and on inhibitory synapses by analyzing gephyrin clusters. Our approach does not only allow to study more accurately the role of CASPR2 in synaptic functions, but also to unravel possible pathological mechanisms of anti-CASPR2 autoAbs in generation of the disease.

Results: We demonstrated that treatment of immature *in vitro* hippocampal neurons with anti-CASPR2 autoAbs from a patient with autoimmune limbic encephalitis induced an overall increase in spine density and GluA2 AMPA receptor content. The increased spine density was equally distributed over all different spine morphological subtypes. PSD95 clusters and gephyrin clusters were unaffected at this time point, whereas gephyrin cluster fluorescence intensity increased upon patients' autoAbs binding in mature *in vitro* hippocampal neurons.

Conclusions: The overall increase in spine density and in GluA2 AMPA receptor content upon anti-CASPR2 autoAbs binding, for whom we have previously shown to stabilize CASPR2 at the membrane, suggest that CASPR2 promotes spine developmental processes in a dose-

dependent fashion in immature *in vitro* hippocampal neurons. The different effects on excitatory and inhibitory synapses in immature and mature *in vitro* hippocampal neurons, suggest that CASPR2 might execute different functions depending on the neurodevelopmental stage.

Anti-CASPR2 autoantibodies from patients with autoimmune limbic encephalitis promote spine developmental processes and disturb mature inhibitory synapses.

Pieters, A.[1,2,3], Malleval, C.[1,2,3], Honnorat, J.[1,2,3,4], Pascual, O.[1,2,3], Noraz, N.[1,2,3]

[1] INSERM U1217, Institut NeuroMyoGène, Lyon, F-69000, France.

[2] CNRS UMR5310, Institut NeuroMyoGène, Lyon, F-69000, France.

[3] University Claude Bernard Lyon 1, Lyon, F-69000, France.

[4] Hospices Civils de Lyon, Lyon, F-69000, France.

Abstract

CASPR2 (contactin-associated protein-like 2) is a neuronal cell-adhesion protein that is targeted by autoantibodies (autoAbs) in autoimmune limbic encephalitis. Many studies have shown the implication of CASPR2 in synaptic functioning. However, the precise role of CASPR2 at the synapse has not been unraveled yet. To accurately assess the role of this protein in synaptic functions, correct neuronal development, implying presence of CASPR2, is required, a difficult task using currently available models. Therefore, we here assess the effects of anti-CASPR2 autoAbs from patients with autoimmune limbic encephalitis on cultures of WT hippocampal neurons, for which the neuronal network and synapses have been normally developed. This approach does not only allow to gain insight on the functions of CASPR2, but also to unravel possible molecular mechanisms that lie at the basis of the pathogenicity of anti-CASPR2 autoAbs in AILE.

In the present study, we show that in immature neurons anti-CASPR2 autoAbs increase dendritic spine density and GluA2 AMPA receptor content at the postsynaptic density, reflecting promoted spine developmental processes. Furthermore, at a mature neuronal stage inhibitory synapses are altered upon patients' autoAbs treatment. Our results suggest that CASPR2 could execute diverging roles depending on the neuronal developmental stage and provide more insight in the physiopathological role of anti-CASPR2 autoAbs.

Keywords: CASPR2, autoimmune limbic encephalitis, autoantibodies, dendritic spines, AMPA receptor

1. Introduction

Contactin-associated protein-like 2 (CASPR2) is a neuronal cell-adhesion protein belonging to the neurexin family (Poliak et al., 1999). Autoantibodies (autoAbs) directed against this protein have been found in serum and/or cerebrospinal fluid (CSF) of patients with neuromyotonia (NMT), Morvan syndrome (MoS) and autoimmune limbic encephalitis (AILE) (Buckley et al., 2001; Irani et al., 2010; Lancaster et al., 2011; Liguori et al., 2001; Shillito et al., 1995). NMT is a form of peripheral neuropathy (Isaacs, 1961; Newsom-Davis & Mills, 1993), whereas MoS is a combination of NMT with central nervous system (CNS) symptoms (Lee et al., 1998). AILE on the other hand is a pure CNS disorder. The clinical presentation of patients with AILE positive for anti-CASPR2 autoAbs is homogenous. Elderly men are mostly affected, presenting with memory disorders, partial temporal lobe epilepsy and frontal lobe dysfunction (Joubert et al., 2016; van Sonderen et al., 2016).

CASPR2 was initially found as a protein at the juxtaparanode of the node of Ranvier, an essential organization for the saltatory conduction of nervous influxes in myelinated neurons (Poliak et al., 1999). Since then, CASPR2 has been shown to be present in other neuronal compartments including the synapse. Moreover, an increasing number of data essentially obtained in the CASPR2 KO model support a role for CASPR2 in multiple aspects of synaptic processes (reviewed in Saint-Martin et al., 2018).

Mice knocked out for CASPR2 show cortical migration abnormalities, decreased inhibitory interneurons and asynchronous firing patterns (Peñagarikano et al., 2011). In addition, deficits on a synaptic scale have been observed for CASPR2 KO neurons. The number of inhibitory and excitatory synapses is diminished in *ex vivo* cortical brain slices from 4 to 6-week-old CASPR2 KO mice (Lazaro et al., 2019). Cultured cortical CASPR2 KO neurons exhibit a decreased spine density at DIV 21 accompanied with a decrease in GluA1 density in spine heads (Varea et al., 2015). The decreased spine density is also witnessed *in vivo*, due to a failure in maintaining newly developed spines in adult CASPR2 KO cortical dendrites, demonstrating a role for CASPR2 in spine stabilization (Gdalyahu et al., 2015). A more recent study depicted a role for CASPR2 in homeostatic synaptic scaling, a form of homeostatic synaptic plasticity that consists in maintaining the neuronal network in balance by adapting the synaptic AMPA receptor (AMPA-R) quantity and thereby the synaptic strength (Fernandes & Carvalho, 2016). Indeed,

CASPR2 appeared to be regulated by neuronal activity and necessary for the synaptic scaling of AMPA-Rs (Fernandes et al., 2019).

Interestingly, in accordance with the involvement of CASPR2 in the developing nervous system (neuronal connectivity and synaptic transmission), mice knocked out for CASPR2 recapitulate several features of autism spectrum disorder (ASD), a neurodevelopmental disease with early age onset (Peñagarikano et al., 2011). On the other hand, AILE occurring in patients without neurological antecedents puts forward a role for CASPR2 in the mature nervous system. Patients' autoAbs can be useful since they can be administered for a short period of time either during neuron development or once neurons have developed normally, allowing for assessment of CASPR2 functions in correctly assembled neuronal networks. With respect to this, few studies have used this principle. Therefore, in this study we assessed the impact of purified anti-CASPR2 autoAbs from patients with AILE at the synaptic scale using *in vitro* immature and mature hippocampal neurons. The obtained results shed more light on possible synaptic functions of CASPR2, but also allow to better comprehend the mechanisms of anti-CASPR2 autoAbs in generating the clinical presentation of patients with AILE.

2. Materials and methods

Patient serum and IgG purification

Serum from four patients presenting with autoimmune limbic encephalitis positive for only anti-CASPR2 autoantibodies in serum and CSF was obtained from the *Centre National de Référence pour les Syndromes Neurologiques Paranéoplasiques* in Lyon, France. A written informed consent was signed by every patient. Control serum from three healthy donors was obtained from the *Etablissement Français du Sang*. The titer of anti-CASPR2 autoantibodies in the serum was assessed using a HEK cell-based assay as previously described (Joubert et al., 2016). For IgG purification serum was incubated for 2h at RT with protein-A Sepharose 4 Fast Flow™ beads (Sigma). The serum was then transferred to columns, washed with PBS and IgGs were eluted in glycine buffer pH 2.8. Eluted IgGs were neutralized in Tris buffer pH 8.8 and dialyzed overnight at 4°C in PBS. IgG concentrations were determined by micro bicinchoninic acid (BCA) protein assay kit (Thermofisher) following manufacturer's instructions. Purified IgGs were sterilized on 0.22 µm filters and kept at -80°C until use.

Patient (Pat) and control (Ctl) IgGs were used separately or as pool (pPat and pCtl respectively). pPat consisted in equimolar concentrations of Pat2, Pat3 and Pat4 purified IgGs. pCtl consisted in equimolar concentrations of Ctl1, Ctl2 and Ctl3 purified IgGs.

Primary hippocampal neuronal cultures

Animal care and procedures were conducted according to the European Community Council Directive 2010/63/UE and the French Ethical Committee.

For PSD purification primary hippocampal neuronal cultures were prepared from E18 mouse embryos (Janvier labs). Pregnant mice were deeply anesthetized by isoflurane inhalation and embryos were taken out by Caesarean section. Hippocampi were dissected and then fragmented in Hank's buffered salt solution (HBSS) (Gibco) supplemented with 0.65% (v/v) D-glucose (Sigma-Aldrich), 1M HEPES buffer (Sigma-Aldrich) and 0.05% (v/v) penicillin/streptomycin (Invitrogen). Hippocampal tissue fragments were then transferred for dissociation in dissection medium supplemented with 10% (v/v) trypsin (Gibco) for 10 min at 37°C. 1% (v/v) DNAse (Sigma-Aldrich) was added during the last minute at room temperature. Trypsin action was stopped by adding Dulbecco's modified eagle medium (DMEM) (Gibco) supplemented with 10% (v/v) fetal calf serum (FCS) (PAA Laboratories) for 5 min. Cells were then mechanically dissociated by trituration in complete culture medium consisting of Neurobasal medium (Gibco) supplemented with 2% (v/v) B27 (Gibco), 1% (v/v) L-glutamine (Invitrogen) and 0.05% (v/v) penicillin/streptomycin. Cells were plated onto poly-L-lysine coated petri dishes in complete culture medium. Petri dishes were incubated overnight at 37°C in a humidified atmosphere with a solution containing 10 µg/ml of poly-L-lysine (Sigma-Aldrich) in HBSS and three washes in PBS were performed before plating the cells. Cells were incubated in a humidified atmosphere containing 5% CO_2 at 37°C. Culture medium was changed by half volume every three to four days.

For all other experiments primary hippocampal neuronal cultures were prepared from E18 Wistar rat embryos (Janvier Labs). Pregnant rats were deeply anesthetized by isoflurane inhalation and embryos were taken out by Caesarean section. Hippocampi were isolated in Hank's buffered salt solution (HBSS) (Gibco) and transferred for dissociation in HBSS supplemented with 10% (v/v) trypsin (Gibco) for 10 min at 37°C. Trypsin action was stopped by washing with HBSS supplemented with 4% (w/v) bovine serum albumin (BSA). Cells were then mechanically dissociated by trituration in complete culture medium consisting of

Neurobasal medium (Gibco) supplemented with 2% (v/v) B27 (Gibco), 0.3% (v/v) L-glutamine (Invitrogen) and 1% (v/v) penicillin/streptomycin. Cells were plated onto poly-L-lysine coated coverslips in complete culture medium. Glass coverslips were incubated overnight at 37°C in a humidified atmosphere with a solution containing 0.5 mg/ml of poly-L-lysine (Sigma-Aldrich) in borate buffer pH 8.5 and 3 washes in water were performed before plating the cells. Cells were incubated in a humidified atmosphere containing 5% CO_2 at 37°C.

Transfection and treatment with IgGs

For spine analysis neurons were transfected at 11 *days in vitro* (DIV) with a plasmid coding for eGFP (Clontech) using the Lipofectamine LTX kit (Invitrogen) following manufacturer's instructions.

In all experiments neurons were treated at DIV 13 or DIV 20 with 16 µg/ml purified Pat IgGs or Ctl IgGs for 24h at 37°C.

Immunocytochemistry

At DIV 14 or DIV 21 neurons were washed three times with Neurobasal and fixed in 4% PFA for 10 min at RT. Cells were then washed with PBS, followed by blocking and permeabilization in 3% (w/v) BSA, 0.3% (v/v) Triton X-100 in PBS (PBS-T) for 30 min at RT. Neurons were incubated for 1h at room temperature (RT) with primary antibodies, washed three times with PBS-T and incubated with secondary antibodies for 1h at RT. After three washes in PBS nuclei were stained by 0.1 µg/ml Hoescht (Thermofisher) followed by three washes with PBS. Coverslips were mounted in FluorPreserve Reagent (Calbiochem) and stored at 4°C until image acquisition.

Image acquisition and analysis

For PSD95 and gephyrin analysis images were acquired using Zeiss Axio Imager Z.I ApoTome microscope at x63 magnification with use of apotome. The same fixed exposition time was applied for the different experimental conditions. Quantitative analysis was performed using ICY software (version 1.9.10.0, BioImage Analysis Unit Institut Pasteur) and the ICY Spotdetector plugin. Spots were detected using a scale 2 and size filtering of minimum 2 pixels. For spine morphology analysis hippocampal pyramidal cells expressing eGFP were selected based on their typical morphology. For each pyramidal neuron three regions of interest (ROI)

of 20 to 40 µm were selected on secondary or tertiary apical dendrites. Images were acquired using a laser scanning confocal microscope (Leica TCS SP5X CLSM, Leica Microsystems, Heidelberg, Germany) equipped with an x63 oil-immersion objective (numerical aperture (NA) = 1.40). Z-series of the entire thickness of the ROI were performed with a stepsize of 0.25 µm to obtain a field of 1024 x 1024 pixels, with a voxel size of 80.2 x 80.2 x 251.8 nm. A 3X zoom factor was used and typically 40 to 60 z-slices were necessary. To improve spatial resolution z-stack images were deconvoluted using Huygens Professional software (version 15.10, Scientific Volume Imaging). Dendritic shafts and spines were semi-automatically reconstructed in 3D using Imaris 3D software (version x64 7.6.5, Bitplane AG) with Filament Tracer module and a Gaussian filter. Dendritic spines were manually selected and following equations were used to categorize spines into four types (filopodia, stubby, thin and mushroom) depending on their morphology: *Stubby: length(spine)<1 and 2*min_width(neck)>max_width(head)*; *Mushroom: max_width(head)>min_width(neck)*2 and length(neck)<max_width(head)*2*; *Long thin: max_width(head)>min_width(neck)*2 and length(neck)>max_width(head)*2; Filopodia: mean_width(neck)>=mean_width(head) and length(spine)>2.* This equation has been validated and routinely used in our laboratory. Unclassifiable spines were referred to as 'others'.

Total spine densities and spine subtype densities were calculated as the number of total spines or spine subtype respectively per µm of the analyzed ROI. Spine percentages were calculated by expressing spine subtypes as a percentage of total spines per ROI analyzed.

PSD content analysis

All steps were executed on ice, at 4°C. Cells were rinsed twice with PBS and incubated for 10 min in HEPES buffer (10 mM HEPES buffer, 0.32 M sucrose, pH 7.4) at 4°C. All buffers were supplemented before use with phosphatase and protease inhibitors (cOmplete tablets, Roche) following manufacturer's instructions. Cells were then harvested and mechanically dissociated by 15 rounds of aspiration/expulsion in a 1 ml syringe (Terumo) equipped with a 23 mm, ∅ 0.45 mm needle (Terumo). A small amount of the resulting homogenate corresponding to the total lysate was lysed in lysis buffer (50 mM Tris-HCl, 150 mM NaCl, 1 mM EDTA, 1% NP-40, 0.5% deoxycholic acid, 0.1% SDS, pH 7.5) for 10 min. Homogenates were then centrifuged at 1 000 g for 10 min in order to remove nuclei and large debris. Supernatants were centrifuged at 12 000 g for 20 min and the pellet containing the crude membrane

fraction was resuspended in EDTA buffer, 4 mM HEPES, 1 mM EDTA (Sigma-Aldrich) pH 7.4. This step was repeated twice. The resulting pellet corresponding to the synaptosomal preparation was resuspended in a low-triton buffer (20 mM HEPES, 100 mM NaCl, 0.5% (v/v) Triton X-100, pH 7.2), incubated for 1h at 4°C and then centrifuged at 12 000 g for 20 min. The supernatant containing the non-PSD or Triton X-100-soluble fraction was collected. The remaining pellet containing the PSD or Triton X-100-insoluble fraction was resuspended in a high stringent buffer (20 mM HEPES, 0.15 mM NaCl, 1% (v/v) Triton X-100, 1% (v/v) deoxycholic acid (Sigma-Aldrich), 1% (v/v) sodium dodecyl sulfate (SDS) (Sigma-Aldrich), pH 7.5) for 1h at 4°C. After centrifugation at 10 000 g for 15 min, the supernatant corresponding to the PSD fraction was collected. Protein concentrations in PSD and non-PSD fractions were determined using a BCA assay kit (Thermo Scientific) following instructions provided by the manufacturer. All samples were kept at -20°C until use.

Western Blotting

Samples were diluted in Laemmli-DTT solution (275 mM tromethamine pH 6.8, 5% (v/v) SDS, 0.025% (m/v) bromophenol blue (Sigma-Aldrich), 40% (v/v) glycerol, 200 mM dithiothreitol (DTT) (Sigma-Aldrich)) and denaturated for 5 min at 95°C. Equal protein amounts were loaded on 10% bis-tris electrophoresis gels (Criterion™ XT, Biorad), separated by molecular weight and then transferred to a nitrocellulose membrane (GE Healthcare). Non-specific interactions were blocked by incubating the membrane in blocking solution consisting of dry milk 2% (w/v) in TBS-T (150 mM NaCl, 20 mM Tris, 0.1% (v/v) Tween). Membranes were then incubated with primary antibodies in blocking solution overnight at 4°C. Afterwards the membrane was washed three times for 10 min with TBS-T and incubated with corresponding secondary peroxidase conjugated goat antibodies (Jackson ImmunoResearch) (1:5000) for 1h at room temperature. After 3 washes in TBS-T for 10 min and 2 washes in TBS for 5 min, proteins were revealed by chemiluminescence detection using an ECL kit (Millipore). Signal intensities were quantified using ImageJ (NIH).

Statistical analysis

All data were obtained from at least three independent experiments. Data were analysed using GraphPad Prism software (version 7.00, GraphPad Software, Inc.). P-values equal or inferior to 0.05 were considered statistically significant. Depending on the experimental

setting, data were compared using a Mann-Whitney U test or a Wilcoxon signed-rank test. Data were represented as mean ± SD and significance was set for a p value ≤ 0.05.

List of antibodies

Antibody	Host species	Reference	Dilution
Anti-actin	mouse	Sigma A1978	1/60000 (WB)
Anti-eGFP	rabbit	ThermoFisher A-11122	1/1000 (IF)
Anti-gephyrin	mouse	Synaptic Systems 147021	1/300 (IF)
Anti-GluA2	rabbit	Abcam ab133477	1/500 (WB)
Anti-MAP2	mouse	Sigma M4403	1/500 (IF)
Anti-PSD95	mouse	Thermofisher MA1-045	1/2000 (IF), 1/500 (WB)
Anti-synaptophysin	mouse	Millipore MAB368	1/60000 (WB)
Anti-mouse Alexa 488	goat	Molecular Probes A11029	1/1000 (IF)
Anti-mouse Alexa 647	goat	Molecular Probes A21236	1/2000 (IF)
Anti-mouse Alexa 555	goat	Molecular Probes A21422	1/1000 (IF)
Anti-rabbit Alexa 488	goat	Molecular Probes A11034	1/2000 (IF)

3. Results

3.1 Patient autoAbs do not alter immature excitatory or inhibitory synapses

In a first attempt to determine if anti-CASPR2 autoAbs are capable of perturbing synaptic functions we treated cultured hippocampal neurons with purified IgGs from one patient (Pat1) or purified IgGs from a healthy donor (Ctl1). Neurons were treated for 24h starting at DIV 13 and fixed at DIV 14. We chose this time point, since CASPR2 has been shown to play a role in dendritic spine stabilization, a process in which newly formed spines are converted into stable mature spines (Gdalyahu et al., 2015; Yoshihara et al., 2009). This process requires neuronal activity, since spines' activity allow for enhanced neurotransmission and strengthened synapses (Harris, 1999; Yoshihara et al., 2009). Neuronal activity peaks *in vitro* at DIV 16-18 (Biffi et al., 2013) and formation of synaptic contacts reaches a plateau between DIV 14-21 (Moutaux et al., 2018). Therefore, we considered DIV 13, a time point corresponding to immature spines, the appropriate developmental stage to assess the impact of patient autoAbs on spine stabilization. To assess effects of autoAbs on excitatory synapses, we stained neurons against PSD95, a typical postsynaptic excitatory marker. Inhibitory synapses were

investigated by staining against gephyrin, the major inhibitory postsynaptic scaffolding protein. Size, number and intensity of detected clusters in the total neuronal population were assessed on whole field images. No difference in PSD95 or gephyrin cluster size, number or intensity was observed for neurons treated with patient IgGs compared with neurons treated with control IgGs **(Fig. 1A and 1B)**. Thus, excitatory and inhibitory synapses in immature neurons do not show alterations upon patient autoAbs treatment when using this analytical technique.

3.2 Patient autoAbs affect different spine subtypes

We next wanted to analyze the effects of patient autoAbs on a more refined scale. Excitatory dendritic spines are highly dynamic protrusions which undergo morphological changes depending on neuronal activity (Harris & Stevens, 1989; Parnass et al., 2000). In response to increased neuronal activity, the spine and its spine head enlarge to form a stable spine, assuring adequate neuronal transmission and increased synaptic strength. Based on their morphology, spines can be artificially classified into different subtypes, namely filopodia, long fine spines without a spine head; stubby spines, small protrusions where distinction between spine head and neck is not possible; thin spines, which have a long and narrow neck followed by a small head, and mushroom spines, which have a short neck and a large head (Jones & Powell, 1969; Peters & Kaiserman-Abramof, 1970) **(Fig. 2A)**. To study the impact of autoAbs on dendritic spine morphology neurons were transfected at DIV 11 with a plasmid coding for eGFP, allowing for visualization of dendritic spines. After treatment for 24h with Pat1 or Ctl1 IgGs, neurons were fixed and stained against eGFP to enhance the signal and against MAP2 to assess correct neuronal network formation. Spines were semi-automatically categorized into the different spine classes and unclassifiable spines were categorized as 'others' **(Fig 2A)**. Spine density, defined as the number of spines per µm of analyzed dendrite, was increased for neurons treated with patient IgGs compared with neurons treated with control IgGs (Pat1: 1.03 ± 0.40 vs Ctl1: 0.84 ± 0.29, $p<0.05$) **(Fig. 2B)**. A significant increase in 'other spine' density (Pat1: 0.20 ± 0.15 vs Ctl1: 0.13 ± 0.10, $p<0.01$) and mushroom spine density (Pat1: 0.19 ± 0.12 vs Ctl1: 0.14 ± 0.07, $p<0.05$) was observed **(Fig. 2C)**. This trend in increased density after treatment with patient IgGs was also observed for other spine subtypes but did not reach significance level **(Fig. 2C)**. We also assessed spine subtype distribution, defined as the number

of each spine subtype per dendrite analyzed divided by the total amount of spines on that dendrite. An increase in 'other' spines percentage was observed for neurons treated with patient IgGs compared with control IgGs (Pat1: 18.55 ± 9.53 vs Ctl1: 15.14 ± 9.68, $p<0.05$) **(Fig. 2C)**. The spine subtype percentage was not significantly altered for other spine subtypes **(Fig. 2C)**.

All together, these results demonstrate that patient autoAbs increase spine density in immature neurons, with a more pronounced increase in mushroom an 'other' spines density.

3.3 Patient autoAbs increase GluA2 amount at the PSD

The increase in spine head is accompanied with an enlargement of the postsynaptic density (PSD) (Harris & Stevens, 1989; Harris et al., 1992). The PSD is enriched in several proteins important in neuronal signaling, adhesion and trafficking. The AMPA-R is a typical component of the PSD for which surface expression augments with synaptic activity (Harris et al., 1992; Nusser et al., 1998). Since we observed an overall increase in spine density, and more precisely in mushroom spines, when neurons were treated with patient autoAbs, we wanted to verify if this was accompanied with an increased AMPA-R content at the PSD. Neurons were incubated with Pat1 or Ctl1 IgGs at DIV 13 and lysed at DIV 14 to perform a PSD purification protocol. Synaptic PSD fractions were isolated from non-PSD fractions by subcellular fractionation, a method that consists in separating both fractions depending on their different solubility in detergents. Equal amounts of both fractions were then western blotted against different proteins **(Fig. 3)**. To validate correct PSD enrichment, signal ratios of synaptophysin, an exclusively presynaptic protein, present in the PSD fraction over synaptophysin present in the non-PSD fraction were calculated. A value higher or equal at ten was considered to be representative for contamination of the PSD fraction with non-PSD proteins and these experiments were excluded for analysis. Membranes were also blotted against PSD95, representative for the PSD fraction, and GluA2, the main AMPA-R subunit. For the PSD fractions, the signal intensity ratios of GluA2 over PSD95 were calculated and compared between Ctl1 and Pat1. A significant increase in GluA2 content was observed when neurons were incubated with patient IgGs (Pat1: 1.87 ± 0.98 vs Ctl1: 1.31 ± 0.60, $p<0.05$) **(Fig. 3)**. This evidences that treatment with patient autoAbs increases the GluA2 amount at the PSD in immature neurons.

3.4 Patient autoantibodies disturb mature inhibitory synapses.

We then wanted to determine if anti-CASPR2 autoAbs are capable of perturbing mature synapses. Therefore, we created a pool of patients' autoAbs (pPat), which consisted in purified serum IgGs from three patients (Pat2, Pat3, Pat4) presenting with typical features of anti-CASPR2 AILE. Similarly, we created a pool of three healthy donors (pCtl: Ctl1, Ctl2, Ctl3). Neurons were treated for 24h at DIV 20 with pPat or pCtl and fixed at DIV 21, a neuronal stage characterized by the presence of mature synapses (Bourke et al., 2013; Moutaux et al., 2018). Excitatory synapses were assessed by staining neurons against PSD95 **(Fig 4A)** and inhibitory synapses were investigated by staining against gephyrin **(Fig 4B)**. Size, number and intensity of observed clusters were quantified. Treatment with patients' autoAbs did not disturb PSD95 clusters compared with treatment with controls' autoAbs. In contrast, an increase in gephyrin cluster intensity was observed (pPat: 953.19 ± 343.17 vs pCtl: 698.32 ± 217.08, $p<0.0001$) **(Fig. 4)**. This suggests that patients' autoAbs specifically disturb mature inhibitory synapses.

4. Discussion

In this study we show that autoAbs from a patient with anti-CASPR2 AILE increase GluA2 content at the PSD and increase total spine density in *in vitro* immature hippocampal neurons at DIV 14. No alterations in PSD95 clusters or gephyrin clusters were observed after treatment with patient autoAbs at this time point. In DIV 21 mature hippocampal neurons, PSD95 clusters remained unchanged whereas gephyrin cluster intensity increased after treatment with a pool of patients compared with a pool of controls.

The increased total spine density upon treatment with anti-CASPR2 autoAbs from a patient with AILE can be significantly attributed to an augmentation in mushroom spines and unclassifiable spines. However, a trend in increased density was present for all other spine subtypes. The relative percentages of spines subtypes remained unaltered for all subtypes except for unclassifiable spines, where only a slight significant increase was observed, meaning that spine distribution overall remained unaltered upon treatment with patient autoAbs. Together, these results suggest that patient autoAbs cause a global increase in spine density, with a more noticeable increase for mushroom and unclassifiable spines. Interestingly, the most significant increase in spine density and percentage was present for unclassifiable spines. This result remains difficult to interpret since, to our knowledge, this is

the first study taking into account spines that cannot be morphologically categorized for calculations of total spine percentages and densities. Indeed, other studies reject unclassifiable spines for analysis, which is very likely to alter outcomes since percentages up to 30% for uncategorizable spines have already been described (Harris et al., 1992). Furthermore, currently no clearly defined 'rules' exist for spine measurements. Most studies assess spine morphology visually, whereas others use calculations, which are decided by the experimenter, based on spine measurements. Hence, comparisons between different studies is complicated. Regarding to the effect of CASPR2 on dendritic spines, to our knowledge no studies assessing spine morphology have been performed yet. Therefore, comparing our data with other studies is a difficult if not impossible task. In our interpretation, the total increase of spine density for each spine subtype after treatment with patient autoAbs demonstrates the capacity of CASPR2 to globally promote spine development. Indeed, in previous results, we have shown that patients' autoAbs do not internalize CASPR2, but immobilize the protein at the membrane (Saint-Martin et al., 2019).

Since increased spine heads also increase their PSD-content, including the AMPA-R, the observed increase of the GluA2 subunit of the AMPA-R after treatment with patient autoAbs is in agreement with the increase in mushroom spine density. However, since there was a tendency for other subtypes to augment in density as well in addition with unaltered relative subtypes percentages, the higher GluA2 amount could originate from a global increase in spines and thus spine heads, and is not necessarily attributed to mushroom spines. Indeed, we analyzed total PSD GluA2 amounts, thus the spine subtype to whom the increased GluA2 stems is unknown.

Strangely, no alterations in PSD95, the major component of the PSD, were observed after treatment with patient autoAbs using classical microscopy analysis. Given the positive correlation between PSD content and spine head, we would expect an augmentation for this protein as well. However, it must be kept in mind that spine head widths measure ~ 0.1 to 1.6 µm (Bourne & Harris, 2011). The classic microscopy technique used in this study does not reach such high resolution. Therefore, PSD95 spots present in small spines could have passed undetected. Moreover, we analyzed PSD95 present in whole fields of the total neuronal population, and not specifically in spine heads of pyramidal neurons, the neuronal subtype we analyzed for spine morphology calculations. Given the slight but significant increase in spine

density, the concomitant expected subtle increase in PSD95 is most likely to have been submerged with this rather gross analytical immunohistochemical method.

We also assessed excitatory and inhibitory synapses after patient autoAbs incubation at DIV 21, a mature neuronal stage. No differences in size, number or intensity were observed for PSD95 when neurons were treated with pooled patient compared with pooled control IgGs. However, a significant increase in gephyrin intensity was observed compared with pooled Ctl IgGs. In previous results, we have shown that treatment with patients' autoAbs caused increased Kv1.2 expression in inhibitory neurons compared with control treated neurons (Saint-Martin et al., 2019). The increase in Kv1.2 channel expression is supposed to increase refractory periods and decrease action potential frequency, causing diminished inhibitory NT release, which would lead to a global increase of neuronal network activity. Since we treat neurons for 24h with anti-CASPR2 autoAbs, a period sufficient for homeostatic mechanisms to take place, it is plausible that the increase in gephyrin expression is an adaptive response to increased neuronal network activity upon patients' autoAbs binding (Lushnikova et al., 2011; Turrigiano, 2017; Zenke et al., 2017).

Our results are in agreement with other studies where a decrease in spine density and GluA1 amount was found in CASPR2 KO neurons (Gdalyahu et al., 2015; Varea et al., 2015). Indeed, since we have shown previously that patients' autoAbs do not internalize CASPR2, an opposite outcome in comparison with neurons absent from CASPR2 is expected, as is reflected here by an increase in spine density and GluA2 content. Our proposal that CASPR2 surface expression is positively linked with the extent to which the protein performs its functions is in line with results obtained by others. Canali et al. (2018) showed that cortical axon length at DIV 3 was decreased in CASPR2 KO neurons compared with WT, while an intermediate axon length was observed for heterozygous neurons, supporting the idea that CASPR2 executes its functions in a dose-dependent manner.

The diverging effects on excitatory and inhibitory synapses depending on neuronal developmental stage could reflect different time dependent functions of CASPR2. Whereas alteration of immature synapses is indicative for an implication of CASPR2 in neurodevelopmental disorders such as ASD (for review Takumi et al., 2019), altered mature synapses might lie at the basis of the observed epilepsy in AILE, occurring in elderly patients.

References

Biffi, E., Regalia, G., Menegon, A., Ferrigno, G., & Pedrocchi, A. (2013). The influence of neuronal density and maturation on network activity of hippocampal cell cultures: A methodological study. *PLoS ONE*, *8*(12). https://doi.org/10.1371/journal.pone.0083899

Bourke, J. L., Coleman, H. A., Pham, V., Forsythe, J. S., & Parkington, H. C. (2013). Neuronal Electrophysiological Function and Control of Neurite Outgrowth on Electrospun Polymer Nanofibers Are Cell Type Dependent. *Tissue Engineering Part A*. https://doi.org/10.1089/ten.tea.2013.0295

Bourne, J. N., & Harris, K. M. (2011). Coordination of size and number of excitatory and inhibitory synapses results in a balanced structural plasticity along mature hippocampal CA1 dendrites during LTP. *Hippocampus*, *21*(4), 354–373. https://doi.org/10.1002/hipo.20768

Buckley, C., Oger, J., Clover, L., Tüzün, E., Carpenter, K., Jackson, M., & Vincent, A. (2001). Potassium channel antibodies in two patients with reversible limbic encephalitis. *Annals of Neurology*, *50*(1), 73–78. https://doi.org/10.1002/ana.1097

Fernandes, D., & Carvalho, A. L. (2016). Mechanisms of homeostatic plasticity in the excitatory synapse. *Journal of Neurochemistry*, *139*(6), 973–996. https://doi.org/10.1111/jnc.13687

Fernandes, D., Santos, S. D., Coutinho, E., Whitt, J. L., Beltrão, N., Rondão, T., … Carvalho, A. L. (2019). Disrupted AMPA Receptor Function upon Genetic- or Antibody-Mediated Loss of Autism-Associated CASPR2. *Cerebral Cortex*. https://doi.org/10.1093/cercor/bhz032

Gdalyahu, A., Lazaro, M., Penagarikano, O., Golshani, P., Trachtenberg, J. T., & Gescwind, D. H. (2015). The autism related protein contactin-associated protein-like 2 (CNTNAP2) stabilizes new spines: An in vivo mouse study. *PLoS ONE*, *10*(5), 1–7. https://doi.org/10.1371/journal.pone.0125633

Harris, K M, & Stevens, J. K. (1989). Dendritic spines of CA 1 pyramidal cells in the rat hippocampus: serial electron microscopy with reference to their biophysical characteristics. *The Journal of Neuroscience : The Official Journal of the Society for Neuroscience*, *9*(8), 2982–2997.

Harris, Kristen M. (1999). Structure, development, and plasticity of dendritic spines. *Current Opinion in Neurobiology*, *9*(3), 343–348. https://doi.org/10.1016/S0959-4388(99)80050-6

Harris, Kristen M, Jensen, F. E., & Tsao, B. (1992). Three-dimensional structure of dendritic spines and synapses in rat hippocampus (CA1) at postnatal day 15 and adult ages: implications for the maturation of synaptic physiology and long-term potentiation [published erratum appears in J Neurosci 1992 Aug;1. *The Journal of Neuroscience*, *12*(7), 2685–2705. https://doi.org/10.1016/j.tcb.2009.06.001

Irani, S. R., Alexander, S., Waters, P., Kleopa, K. A., Pettingill, P., Zuliani, L., … Vincent, A. (2010). Antibodies to Kv1 potassium channel-complex proteins leucine-rich, glioma inactivated 1 protein and contactin-associated protein-2 in limbic encephalitis, Morvan's syndrome and acquired neuromyotonia. *Brain*, *133*(9), 2734–2748. https://doi.org/10.1093/brain/awq213

Isaacs, H. (1961). A syndrome of continuous muscle-fibre activity. *Journal of Neurology, Neurosurgery & Psychiatry*, *24*(4), 319–325. https://doi.org/10.1136/jnnp.24.4.319

Jones, E. G., & Powell, T. P. S. (1969). Morphological variations in the dendritic spines of the neorcortex. *J. Cell Sci. S*, *5*(2), 509–529.

Joubert, B., Saint-Martin, M., Noraz, N., Picard, G., Rogemond, V., Ducray, F., … Honnorat, J. (2016). Characterization of a subtype of autoimmune encephalitis with anti-Contactin-Associated

protein-like 2 antibodies in the cerebrospinal fluid, prominent limbic symptoms, and seizures. *JAMA Neurology*, *73*(9), 1115–1124. https://doi.org/10.1001/jamaneurol.2016.1585

Lancaster, E., Huijbers, M. G. M., Bar, V., Boronat, A., Wong, A., Martinez-Hernandez, E., … Dalmau, J. (2011). Investigations of caspr2, an autoantigen of encephalitis and neuromyotonia. *Annals of Neurology*, *69*(2), 303–311. https://doi.org/10.1002/ana.22297

Lazaro, M. T., Taxidis, J., Shuman, T., Bachmutsky, I., Ikrar, T., Santos, R., … Golshani, P. (2019). Reduced Prefrontal Synaptic Connectivity and Disturbed Oscillatory Population Dynamics in the CNTNAP2 Model of Autism. *Cell Reports*, 2567–2578. https://doi.org/10.1016/j.celrep.2019.05.006

Lee, E. K., Maselli, R. A., Ellis, W. G., & Agius, M. A. (1998). Morvan's fibrillary chorea: A paraneoplastic manifestation of thymoma. *Journal of Neurology Neurosurgery and Psychiatry*, *65*(6), 857–862. https://doi.org/10.1136/jnnp.65.6.857

Liguori, R., Vincent, A., Clover, L., Avoni, P., Plazzi, G., Cortelli, P., … Montagna, P. (2001). Morvan's syndrome: peripheral and central nervous system and cardiac involvement with antibodies to voltage-gated potassium channels. *Brain*, *124*(12), 2417–2426. https://doi.org/10.1093/brain/124.12.2417

Lushnikova, I., Skibo, G., Muller, D., & Nikonenko, I. (2011). Excitatory synaptic activity is associated with a rapid structural plasticity of inhibitory synapses on hippocampal CA1 pyramidal cells. *Neuropharmacology*, *60*(5), 757–764. https://doi.org/10.1016/j.neuropharm.2010.12.014

Moutaux, E., Christaller, W., Scaramuzzino, C., Genoux, A., Charlot, B., Cazorla, M., & Saudou, F. (2018). Neuronal network maturation differently affects secretory vesicles and mitochondria transport in axons. *Scientific Reports*. https://doi.org/10.1038/s41598-018-31759-x

Newsom-Davis, J., & Mills, K. R. (1993). Immunological associations of acquired neuromyotonia (Isaacs' syndrome). *Brain*, *116*(2), 453–469. https://doi.org/10.1093/brain/116.2.453

Nusser, Z., Lujan, R., Laube, G., Roberts, J. D., Molnar, E., & Somogyi, P. (1998). Cell type and pathway dependence of synaptic AMPA receptor number and variability in the hippocampus. *Neuron*, *21*(3), 545–559. https://doi.org/10.1016/S0896-6273(00)80565-6

Parnass, Z., Tashiro, A., & Yuste, R. (2000). Analysis of spine morphological plasticity in developing hippocampal pyramidal neurons. *Hippocampus*, *10*(5), 561–568. https://doi.org/10.1002/1098-1063(2000)10:5<561::AID-HIPO6>3.0.CO;2-X

Peñagarikano, O., Abrahams, B. S., Herman, E. I., Winden, K. D., Gdalyahu, A., Dong, H., … Geschwind, D. H. (2011). Absence of CNTNAP2 leads to epilepsy, neuronal migration abnormalities, and core autism-related deficits. *Cell*, *147*(1), 235–246. https://doi.org/10.1016/j.cell.2011.08.040

Peters, A., & Kaiserman-Abramof, I. R. (1970). The small pyramidal neuron of the rat cerebral cortex. The perikaryon, dendrites and spines. *American Journal of Anatomy*, *127*(4), 321–355. https://doi.org/10.1002/aja.1001270402

Poliak, S., Gollan, L., Martinez, R., Custer, A., Einheber, S., Salzer, J. L., … Peles, E. (1999). Caspr2, a new member of the Neurexin superfamily, is localized at the juxtaparanodes of myelinated axons and associates with K+channels. *Neuron*, *24*(4), 1037–1047. https://doi.org/10.1016/S0896-6273(00)81049-1

Saint-Martin, M., Joubert, B., Pellier-Monnin, V., Pascual, O., Noraz, N., & Honnorat, J. (2018). Contactin-associated protein-like 2, a protein of the neurexin family involved in several human diseases. *European Journal of Neuroscience*, *48*(3), 1906–1923. https://doi.org/10.1111/ejn.14081

Saint-Martin, M., Pieters, A., Déchelotte, B., Malleval, C., Pinatel, D., Pascual, O., … Noraz, N. (2019). Impact of anti-CASPR2 autoantibodies from patients with autoimmune encephalitis on CASPR2/TAG-1 interaction and Kv1 expression. *Journal of Autoimmunity*. https://doi.org/10.1016/j.jaut.2019.05.012

Shillito, P., Molenaar, P. C., Vincent, A., Leys, K., Zheng, W., van den Berg, R. J., … Newsom-Davis, J. (1995). Acquired neuromyotonia: Evidence for autoantibodies directed against K + channels of peripheral nerves. *Annals of Neurology*, *38*(5), 714–722. https://doi.org/10.1002/ana.410380505

Takumi, T., Tamada, K., Hatanaka, F., Nakai, N., & Bolton, P. F. (2019, May). Behavioral neuroscience of autism. *Neuroscience and Biobehavioral Reviews*. https://doi.org/10.1016/j.neubiorev.2019.04.012

Turrigiano, G. G. (2017). The dialectic of hebb and homeostasis. *Philosophical Transactions of the Royal Society B: Biological Sciences*, *372*(1715). https://doi.org/10.1098/rstb.2016.0258

van Sonderen, A., Ariño, H., Petit-Pedrol, M., Leypoldt, F., Körtvélyessy, P., Wandinger, K.-P., … Titulaer, M. J. (2016). The clinical spectrum of Caspr2 antibody-associated disease. *Neurology*, *87*(5), 521–528. https://doi.org/10.1212/WNL.0000000000002917

Varea, O., Martin-de-Saavedra, M. D., Kopeikina, K. J., Schürmann, B., Fleming, H. J., Fawcett-Patel, J. M., … Penzes, P. (2015). Synaptic abnormalities and cytoplasmic glutamate receptor aggregates in contactin associated protein-like 2 */Caspr2* knockout neurons. *Proceedings of the National Academy of Sciences*, *112*(19), 6176–6181. https://doi.org/10.1073/pnas.1423205112

Yoshihara, Y., De Roo, M., & Muller, D. (2009). Dendritic spine formation and stabilization. *Current Opinion in Neurobiology*, Vol. 19, pp. 146–153. https://doi.org/10.1016/j.conb.2009.05.013

Zenke, F., Gerstner, W., & Ganguli, S. (2017). The temporal paradox of Hebbian learning and homeostatic plasticity. *Current Opinion in Neurobiology*, Vol. 43, pp. 166–176. https://doi.org/10.1016/j.conb.2017.03.015

Fig 1

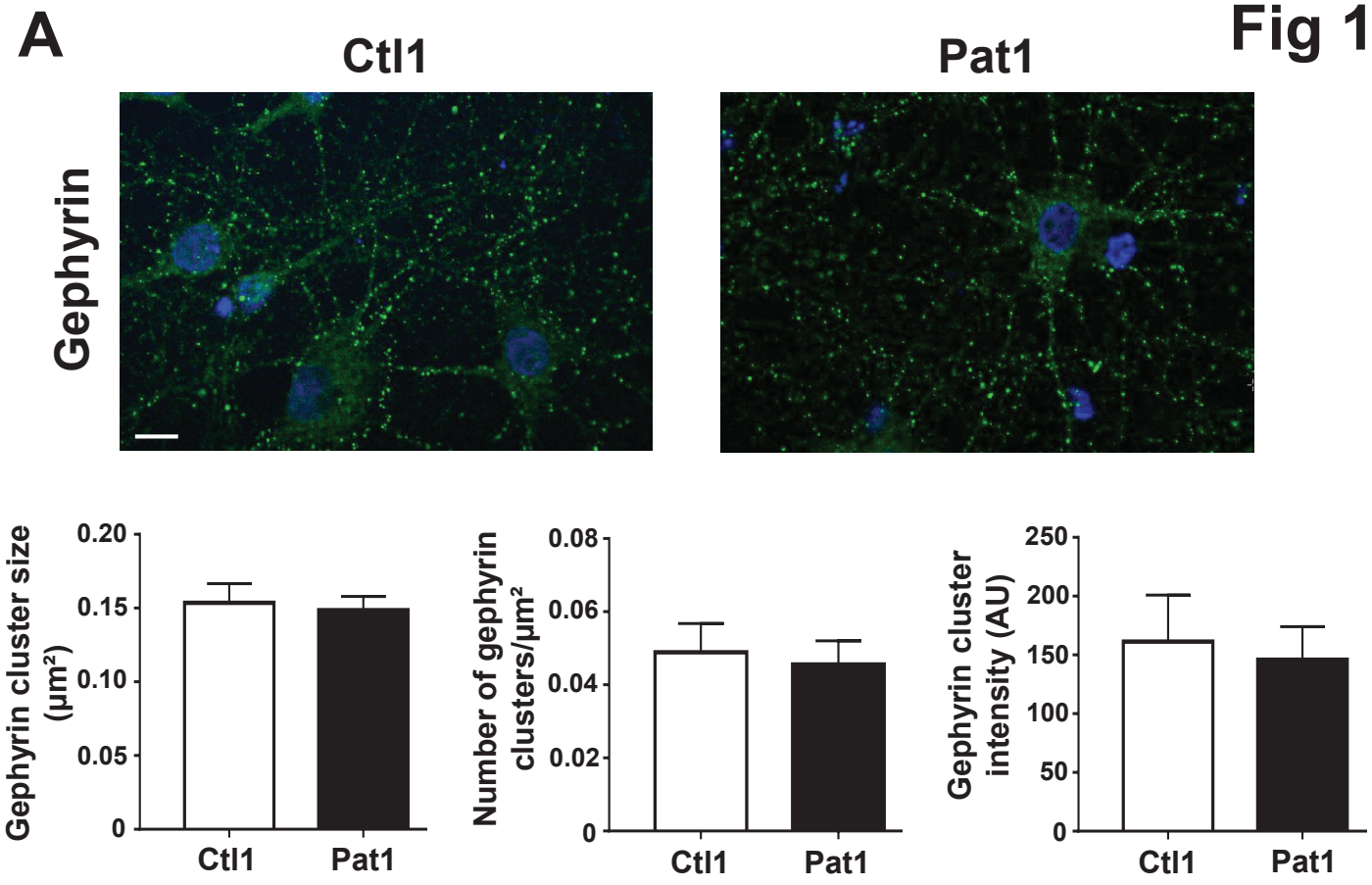
A
Ctl1
Pat1
Gephyrin
Gephyrin cluster size (µm²)
0.20
0.15
0.10
0.05
0
Ctl1
Pat1
Number of gephyrin clusters/µm²
0.08
0.06
0.04
0.02
0
Ctl1
Pat1
Gephyrin cluster intensity (AU)
250
200
150
100
50
0
Ctl1
Pat1

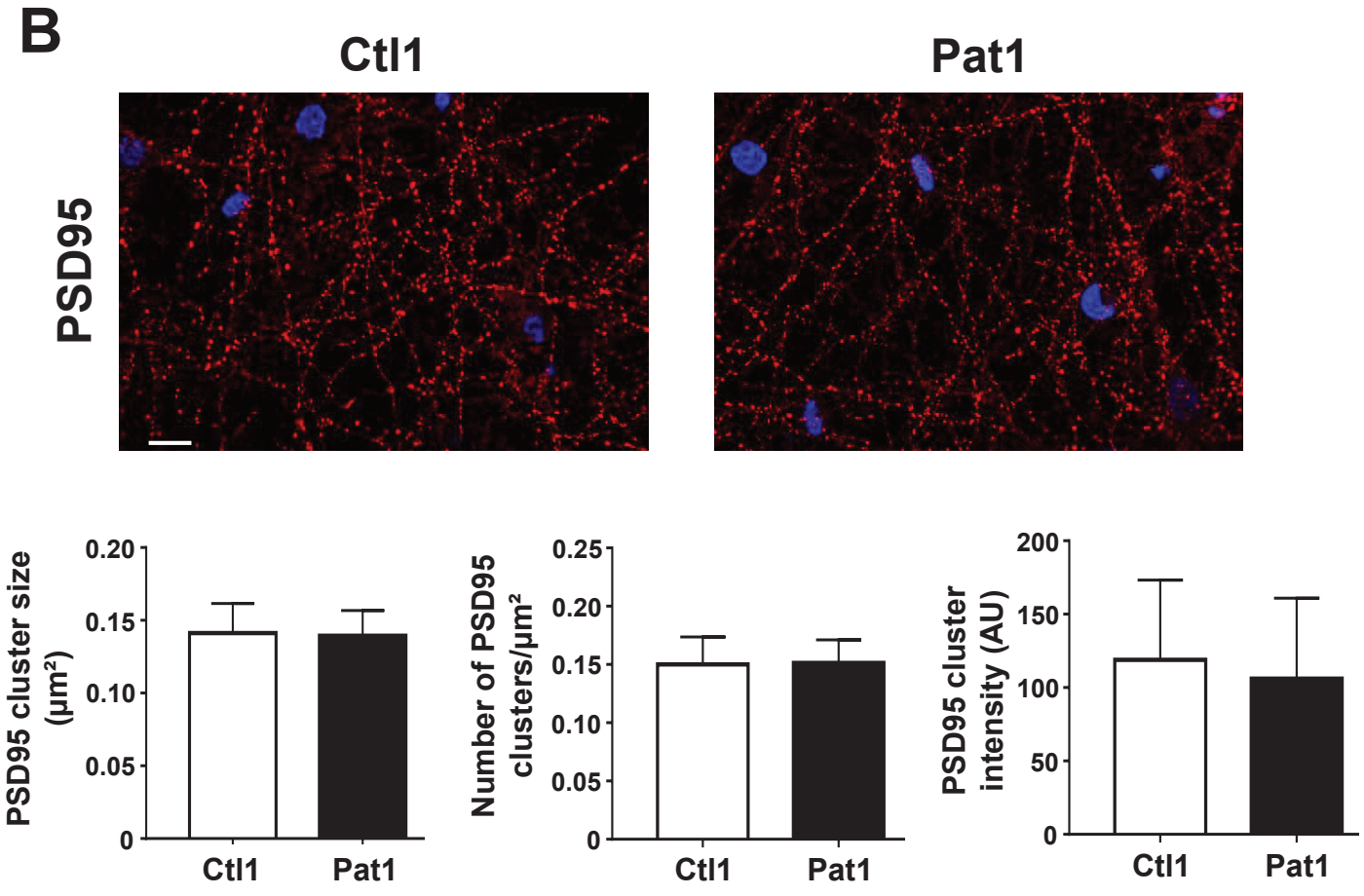
B
Ctl1
Pat1
PSD95
PSD95 cluster size (µm²)
0.20
0.15
0.10
0.05
0
Ctl1
Pat1
Number of PSD95 clusters/µm²
0.25
0.20
0.15
0.10
0.05
0
Ctl1
Pat1
PSD95 cluster intensity (AU)
200
150
100
50
0
Ctl1
Pat1

Fig 2

A

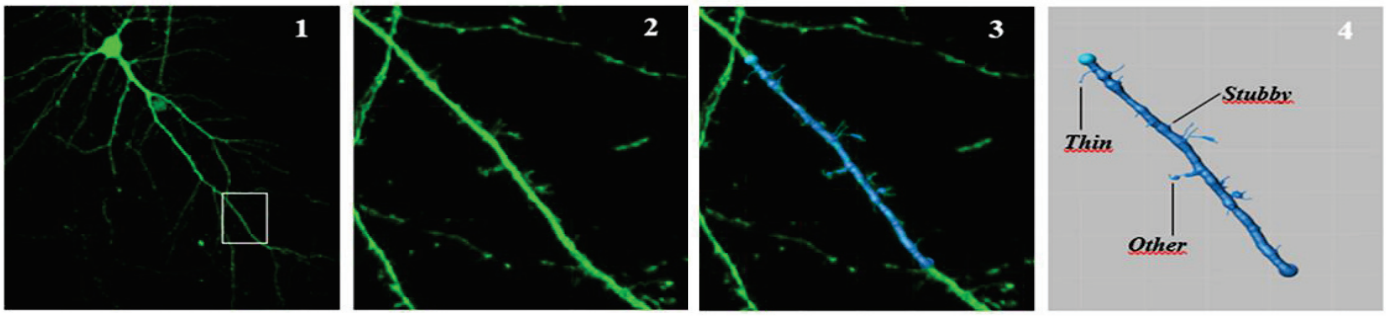
1
2
3
4
Stubby
Thin
Other

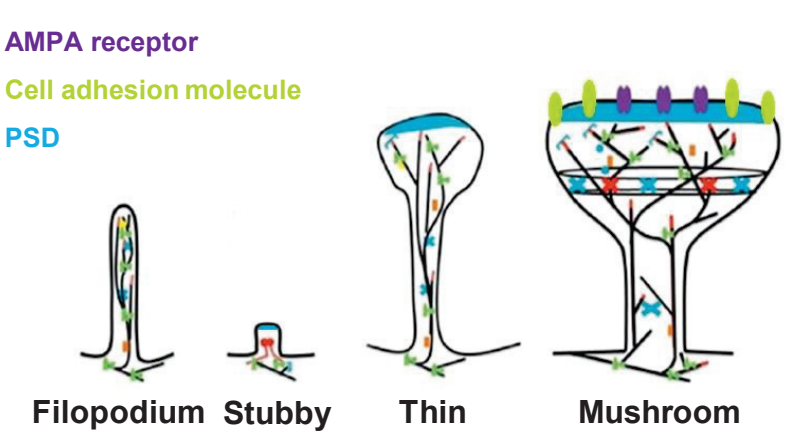
AMPA receptor
Cell adhesion molecule
PSD
Filopodium
Stubby
Thin
Mushroom

B

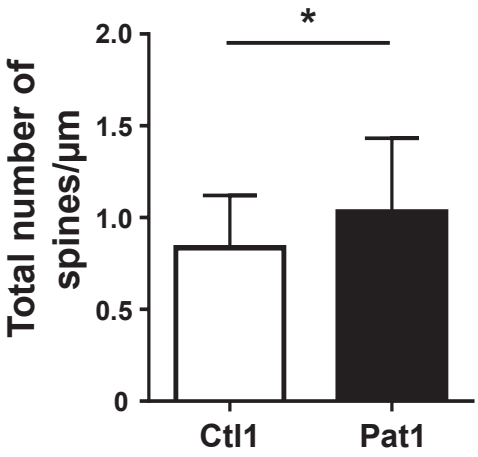
Total number of spines/μm
2.0
1.5
1.0
0.5
0
*
Ctl1
Pat1

C

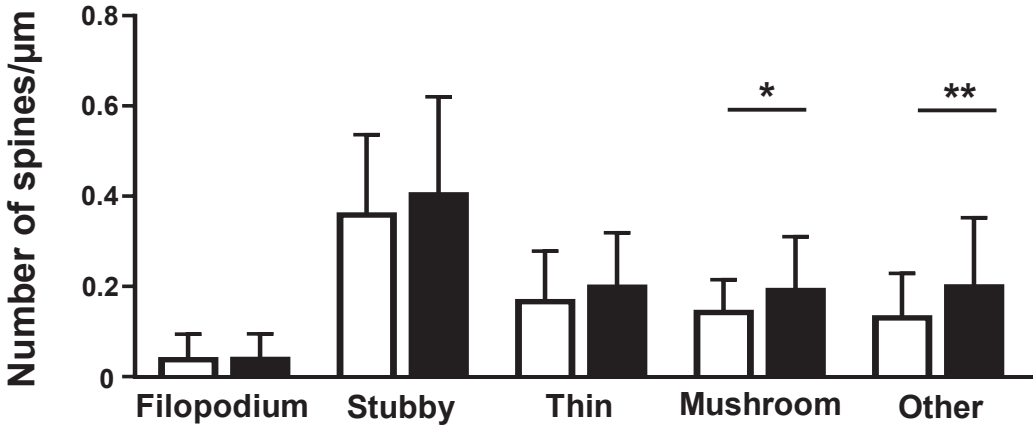
Number of spines/μm
0.8
0.6
0.4
0.2
0
*
**
Filopodium
Stubby
Thin
Mushroom
Other

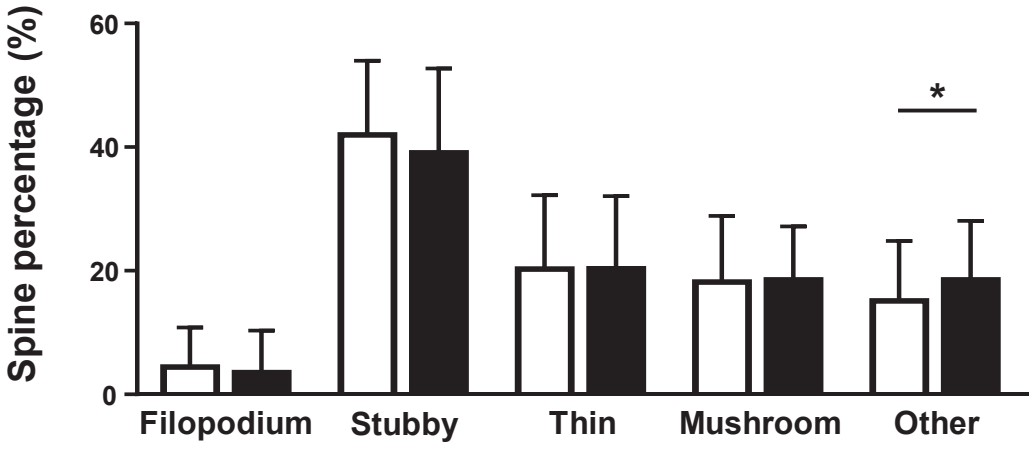
Spine percentage (%)
60
40
20
0
*
Filopodium
Stubby
Thin
Mushroom
Other

Fig 3

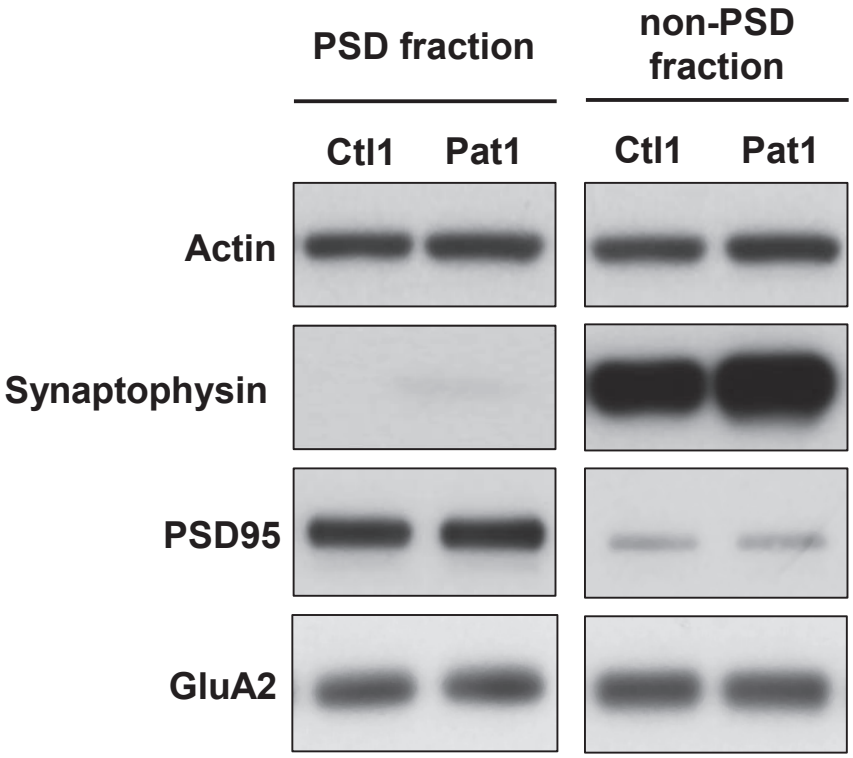
PSD fraction
non-PSD fraction
Ctl1
Pat1
Ctl1
Pat1
Actin
Synaptophysin
PSD95
GluA2

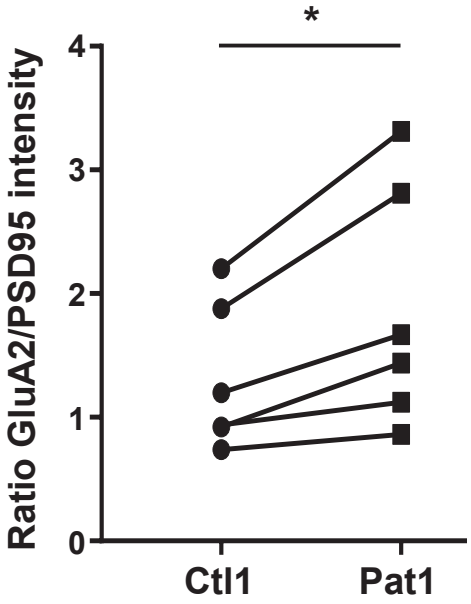
*
Ratio GluA2/PSD95 intensity
4
3
2
1
0
Ctl1
Pat1

Fig 4

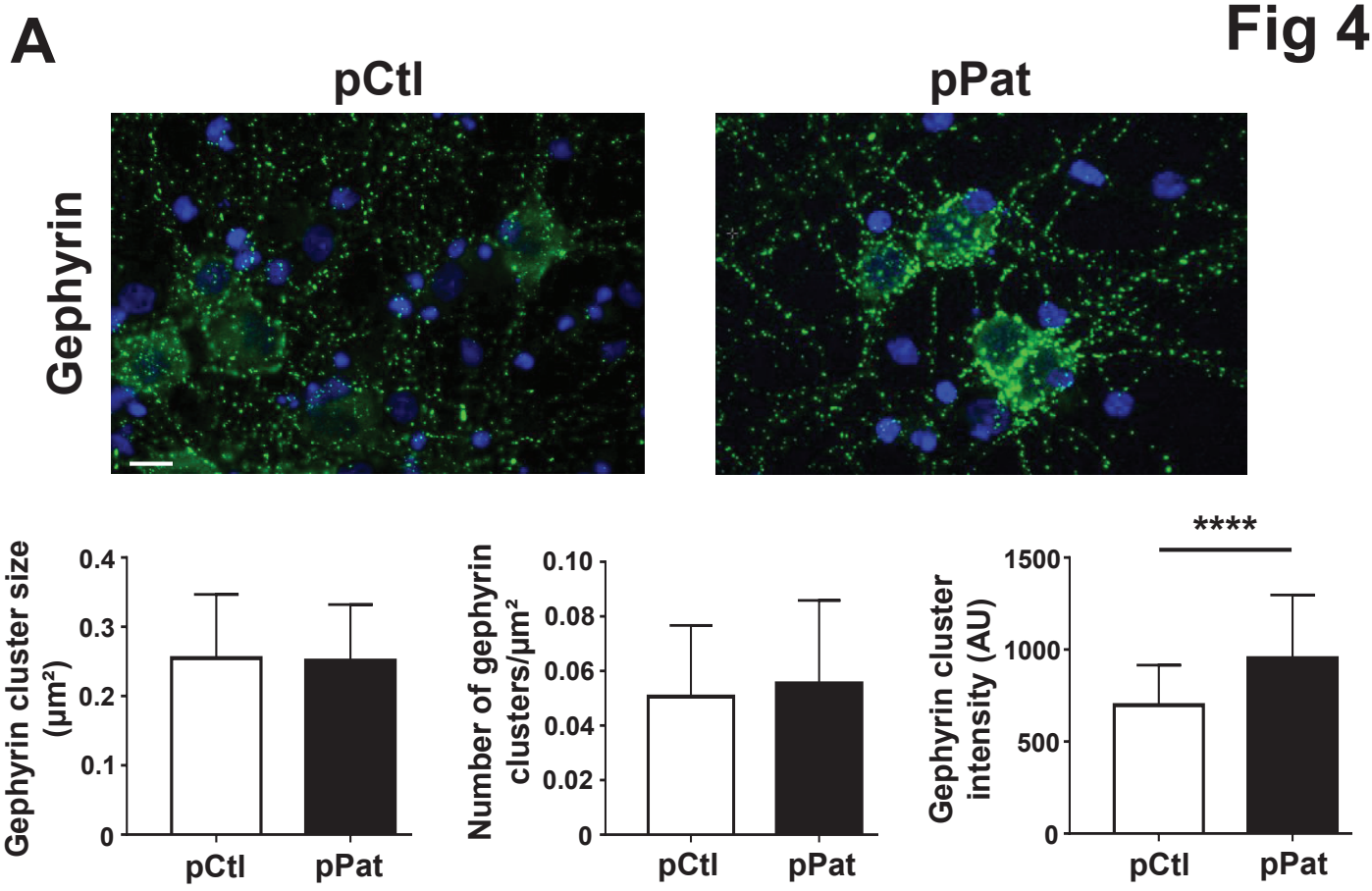
A
pCtl
pPat
Gephyrin
Gephyrin cluster size (µm²)
0.4
0.3
0.2
0.1
0
pCtl
pPat
Number of gephyrin clusters/µm²
0.10
0.08
0.06
0.04
0.02
0
pCtl
pPat
****
Gephyrin cluster intensity (AU)
1500
1000
500
0
pCtl
pPat

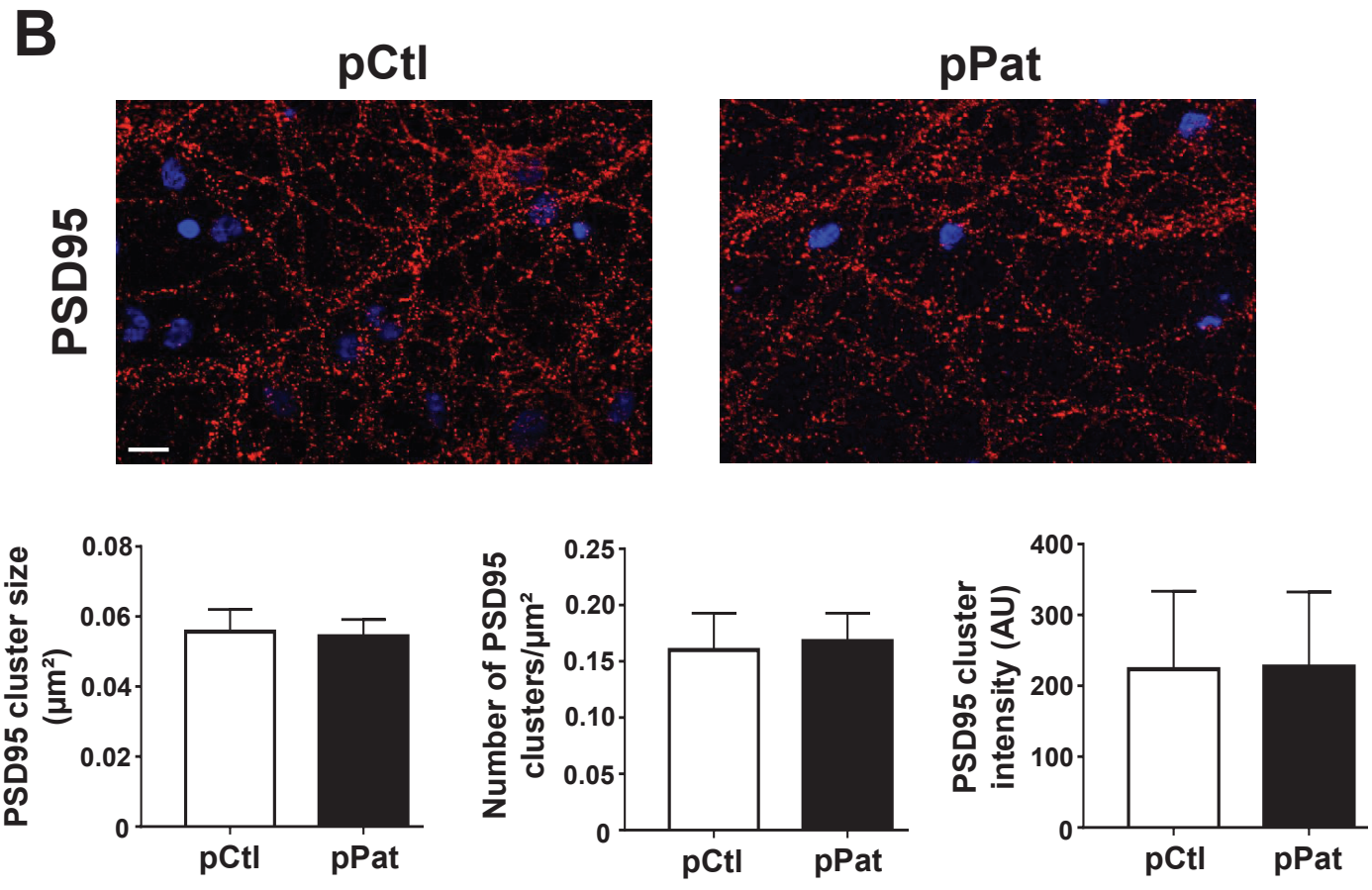
B
pCtl
pPat
PSD95
PSD95 cluster size (µm²)
0.08
0.06
0.04
0.02
0
pCtl
pPat
Number of PSD95 clusters/µm²
0.25
0.20
0.15
0.10
0.05
0
pCtl
pPat
PSD95 cluster intensity (AU)
400
300
200
100
0
pCtl
pPat

Figure legends

Figure 1. Patient autoAbs do not alter inhibitory or excitatory synapses at DIV 14. A) Hippocampal neurons (DIV 14) were treated for 24h with control (Ctl1) or patient (Pat1) IgGs. Neurons were stained against gephyrin and cluster size, number and intensity quantified. **B)** Hippocampal neurons (DIV 14) were treated for 24h with control (Ctl1) or patient (Pat1) IgGs. Neurons were stained against PSD95 and cluster size, number and intensity quantified.
n = minimum 19 fields per condition, Mann-Withney U test, $p<0.05$. Scale bars represent 10 µm.

Figure 2. Patient autoAbs increase dendritic spine density at DIV 14. A) Illustration of 3D spine reconstruction using Imaris. (1) Secondary and tertiary apical dendrites from eGFP transfected pyramidal neurons were selected for analysis (white quadrant). (2) Z-stacked images of the selected dendrite were taken by confocal microscopy and deconvoluted. (3) Dendrites and spines were semi-automatically reconstructed in 3D using Imaris software. (4) Reconstructed spines were categorized into four different spine subtypes, depending on their morphology: filopodium, stubby, thin or mushroom spines. Unclassifiable spines were categorized as 'other'. The different spine subtypes are schematically represented with their typical morphological features. The AMPA receptor is represented in purple, cell adhesion molecules in green and the PSD in blue. **B)** Hippocampal neurons (DIV 14) were treated for 24h with control (Ctl1) or patient (Pat1) IgGs and analyzed as described in A). Spine density, defined as the total number of spines per µm dendrite, was calculated. **C)** Spine subtype densities and spine subtype percentages were calculated. White bars depict results for neurons treated with Ctl1, black bars depict results for neurons treated with Pat1.
n = minimum 18 neurons and 1200 spines per condition, Mann-Withney U test, $*p<0.05$, $**p<0.01$.

Figure 3. Patient autoAbs increase GluA2 content at the PSD at DIV 14. Hippocampal neurons (DIV 14) were treated for 24h with control (Ctl1) or patient (Pat1) IgGs. Neurons were lysed and non-PSD fraction separated from PSD fraction. Both fractions were analyzed by western blot and stained against actin, synaptophysin, PSD95 and GluA2. Signal intensity ratios from

the PSD fraction of GluA2 over PSD95 were calculated. n = 6 independent experiments, Wilcoxon signed-rank test, *p<0.05.

Figure 4. Patients' autoAbs alter inhibitory synapses at DIV 21. A) Hippocampal neurons (DIV 21) were treated for 24h with pooled control (pCtl) or pooled patient (pPat) IgGs. Neurons were stained against gephyrin and cluster size, number and intensity quantified. **B)** Hippocampal neurons (DIV 21) were treated for 24h with pooled control (pCtl) or pooled patient (pPat) IgGs. Neurons were stained against PSD95 and cluster size, number and intensity quantified.

n = minimum 24 fields per condition, Mann-Withney U test, ****p<0.0001. Scale bars represent 10 µm.

DISCUSSION AND PERSPECTIVES

In this part I would like to consider some points that have not been entirely covered in the foregoing articles, but that seem important to me to discuss considering the ensemble of my obtained results, unpublished data from our laboratory and current literature.

1. CASPR2 surface expression and distribution: impact of autoantibodies

My results demonstrate that patient anti-CASPR2 autoAbs do not induce Caspr2 internalization but alter its distribution at the cell membrane promoting CASPR2 cluster formation in DIV 21 hippocampal neurons transfected with CASPR2-GFP **(article 1)**. Furthermore, CASPR2 surface and total expression is unaltered upon treatment with patient autoAbs. Intriguingly, treatment with patients' autoAbs of untransfected neurons only caused an increase in endogenous surface CASPR2 fluorescence intensity, but not in size or number of clusters. Since transfection experiments allow high levels of protein expression, effects on size and number of clusters are more likely to be visible using this approach compared to the endogenous situation, where small alterations in size and number are difficult to evidence, in particular when assessed by classical microscopy techniques. However, another hypothesis different from cluster formation upon patients' autoAb binding is possible. We and others have shown that patients' autoAbs are capable of impeding CASPR2/TAG-1 interaction (Patterson et al., 2018) **(article 1)**. The altered interaction between both proteins is presumed to take place due to conformational changes of CASPR2 upon autoAb binding. This might cause previously inaccessible epitopes to be exposed, allowing additional binding of autoAbs. Indeed, since we use polyclonal patients' autoAbs as primary staining autoAb when assessing endogenous CASPR2, the increase in fluorescence intensity might reflect increased staining autoAb binding to CASPR2, after initial conformational changes due to treatment with patients' autoAbs. This could explain why in the endogenous situation no alterations in size or number of clusters are observed.

Interestingly, in preliminary live trafficking experiments performed using STED microscopy, we observed that CASPR2 is a highly dynamic protein, moving along axons with a straight and directed trajectory (Malleval, C., unpublished preliminary results), which is in agreement with

its linkage to the actin cytoskeleton via its C-terminal 4.1B binding domain. Upon treatment with patients' autoAbs, CASPR2 movements along neurons were less dynamic (Malleval, C., unpublished preliminary results), which supports the idea that patients' autoAbs cause immobilization of CASPR2 at the membrane. A possible pathogenic mechanism of anti-CASPR2 autoAbs could thus rely on the immobilization of CASPR2 at the neuronal surface giving rise to multiple functional consequences. As for axon outgrowth (Canali et al., 2018) CASPR2 functioning could be promoted in a manner proportional to its quantity at the surface. Immobilization could affect CASPR2 subcellular localization, thus hindering to execute its function at the required neuronal compartments. In addition, downstream events, such as recruitment of intracellular signaling actors regulating for example phosphorylation events could also be altered upon CASPR2 immobilization

To gain more insight on the effect of patients' autoAbs on endogenous CASPR2 surface expression and distribution, we are currently analyzing size and number of CASPR2 spots after treatment with patients' autoAbs on a more refined scale by STORM and STED microscopy.

2. CASPR2 synaptic localization and impact of autoantibodies

In *in vitro* cultures of hippocampal neurons, staining on permeabilized cells (total CASPR2) reveals that CASPR2 is present in almost all cells, localized in dendrites, axons and somas. Live staining of cells (surface CASPR2) on the other hand demonstrates that surface CASPR2 is mainly present at the surface of inhibitory axons **(article 1)**. The same results were previously observed by Pinatel et al. (2015). In addition, in that study, the authors showed by confocal microscopy that CASPR2 is mainly localized in the presynaptic compartment of inhibitory synapses. Since we wanted to assess the impact of autoAbs on the synaptic localization of CASPR2, we started by verifying if in our hands as well CASPR2 was localized synaptically. Therefore, cultures of hippocampal neurons (DIV 21) were stained for surface CASPR2 together with gephyrin and homer, a postsynaptic excitatory marker. Unexpectedly, we did not observe obvious synaptic localization for CASPR2. When fixing the colocalization radius between CASPR2 and the synaptic markers at 200 nm (indicative of a strict synaptic localization at the synaptic cleft or at close proximity) we found that 95% of CASPR2 spots were localized extrasynaptically for both inhibitory and excitatory synapse labeling (Malleval, C., unpublished results). The synaptic localization of the 5% colocalizing spots remains

uncertain since this percentage lies in a range of potential non-relevant random colabeling. When we increased the colocalization radius to 500 nm, thus including the perisynaptic region, 15% of CASPR2 spots were found in this radius, with a higher colocalization frequency with inhibitory synapses (60% for inhibitory synapses versus 40% for excitatory synapses) (Malleval, C., unpublished results).

Altogether, it appears that in our hands, CASPR2 is essentially localized extrasynaptically or in proximity of the synapse, with a preference near the inhibitory synapse, but does not show a synaptic localization. These results argue that at least in this cellular model of DIV 21 hippocampal neurons the synaptic processes in which CASPR2 has been associated do not rely on its localization at the synapse.

3. Effect of anti-CASPR2 autoantibodies on synaptic related processes

3.1 In mature neurons (DIV 21)

I provided evidence that patients' autoAbs increase Kv1.2 expression along axons of inhibitory neurons in cultured hippocampal neurons at DIV 21 **(article 1)**. According to the role of Kv1 channels in repolarizing the neuronal membrane following APs, neurons absent from Kv1 channels displayed higher neuronal excitability characterized by latency in repolarization and increased action potential frequency (Smart et al., 1998). On the contrary, increased axonal Kv1 channel expression could consequently lead to decreased AP frequency and thus diminished synaptic activity (He et al., 2012). In the case of inhibitory neurons, this would imply decreased GABA release and decreased inhibitory transmission, leading to an overall hyperexcitability of the neuronal network. This hypothesis is under investigation in our laboratory by assessing the global neuronal network activity using calcium imaging. In this technique, a calcium indicator dye which emits a fluorescent signal upon calcium binding is loaded into neurons. Since intracellular calcium concentrations are directly related to NT release, the emitted fluorescence intensity is a reflection of the neuronal network activity. In preliminary results we observed an increase in neuronal activity upon treatment of *in vitro* mature hippocampal neurons for 24h with patients' autoAbs, suggesting that indeed inhibitory transmission could be decreased in presence of anti-CASPR2 autoAbs (Guery, D. and Pascual, O., unpublished results). In addition, we plan on performing electrophysiological

experiments, assessing IPSCs and EPSCs of *in vitro* hippocampal neurons after treatment with patients' autoAbs.

At first sight, a decrease in inhibitory transmission seems inconsistent with the increase in gephyrin cluster fluorescence intensity observed after treatment with patients' autoAbs **(article 2)**. Indeed, the level of gephyrin at the postsynaptic compartment is upregulated after long-term potentiation of inhibition (iLTP) (Pennacchietti et al., 2017; Petrini et al., 2014). However, in our experiments we treat neurons for 24h with patient autoAbs. During this time period, homeostatic mechanisms aimed to equilibrate the excitatory/inhibitory (E/I) balance and typically occurring in a temporal space ranging from hours to days, can take place (Lushnikova et al., 2011; Turrigiano, 2008, 2017; Zenke et al., 2017). Thus, the increased gephyrin cluster fluorescence intensity might reflect the adaptive response of the neuronal network to the autoAb-mediated increased excitatory neuronal activity.

Regarding to the effect of patients' autoAbs on gephyrin, an augmentation in this postsynaptic protein is representative of functional synapses if the GABA-R is upregulated as well. The expression of the GABA-R upon treatment with anti-CASPR2 autoAbs is at present being examined using high resolutive STORM and STED microscopy where we analyze size, number and fluorescence intensity of the GABA-R (Malleval, C.). Furthermore, since we presume that the increased gephyrin intensity is caused by homeostatic mechanisms, it would be interesting to assess the effects of patients' autoAbs on Kv1.2 channels and gephyrin clusters after different incubation times. This would allow to define if both events (namely increased Kv1.2 fluorescence intensity and increased gephyrin fluorescence intensity) occur concomitantly, or, if indeed the effects witnessed for gephyrin clusters install after increased Kv1.2 expression, indicative for homeostatic mechanisms.

Interestingly, increased Kv1.2 expression occurred concomitantly with changes in surface CASPR2 distribution after treatment with patients' autoAbs. Since the cytoplasmic parts of both proteins interact indirectly via a yet unknown mechanism (Poliak et al., 1999), this raises the question if CASPR2 might regulate Kv1.2 expression. The immobilization of CASPR2 at the surface upon patients' autoAbs binding might strengthen the interaction between CASPR2 and Kv1 channels and thus limit Kv1 endocytosis. Since Kv1 channel endocytosis is induced by phosphorylation of intracellular tyrosine residues of the channel (Hattan et al., 2002; Nesti et al., 2004), we are currently investigating if binding of patients' autoAbs could impact these processes either at basal level or upon NMDA activation, which leads to Kv channel

phosphorylation (Lei et al.,2008; Tao et al., 2005). We therefore perform immunoprecipitation experiments using an anti-phosphotyrosin antibody. Immunoprecipitated fractions are then western blotted and revealed with an anti-Kv1.2 antibody to verify if upon treatment with patients' autoAbs the quantity of phosphorylated Kv channels is altered. In addition, since in our experiments we were not able to distinguish between surface and intracellular Kv1.2 channels, an interesting way to verify surface Kv1.2 channel expression upon patients' autoAbs treatment would be the use of transfected Kv1.2 channels. Indeed, we could couple Kv channels' intracellular part to a fluorescent protein such as mCherry and the extracellular loop to superecliptic pHluorin (SEP), a protein emitting fluorescence depending on the environmental pH, hence allowing concomitant visualization of Kv1.2 intracellular and surface expression.

3.2 In immature neurons (DIV 14)

I showed that in immature DIV 14 cultured hippocampal neurons patient autoAbs induced increased excitatory dendritic spine density together with increased GluA2 AMPA-R content at the PSD **(article 2)**. All spine subtypes were increased in number suggesting a rather global speed-up/promoting effect of spine development upon autoAb binding. In regard to our findings that patients' autoAbs do not induce CASPR2 internalization and rather immobilize CASPR2 at the surface of inhibitory neurons, these results are in a way in agreement with other data obtained in CASPR2 KO models. Indeed, as recapitulated in **Table 5** (see chapter C.2.2.1), decreased spine densities and decreased GluA1 AMPA-R expression in dendritic spines have been documented using CASPR2 KO models (Gdalyahu et al., 2015; Varea et al., 2015). However, since dendritic spines are present on excitatory neurons, the mechanisms behind our result are difficult to conceive. Interestingly CASPR2 appears to affect neurons in a cell-type specific manner. For instance, CASPR2 stabilizes dendritic arborization in interneurons but not in excitatory neurons (Gao et al., 2018). Furthermore, it has recently been shown that CASPR2, by interaction with the scaffolding protein CASK, regulates AMPA-R trafficking and expression level, with opposite effects in excitatory and inhibitory neurons (Gao et al., 2018, 2019; Varea et al., 2015). Whereas CASPR2 promotes GluA1 surface expression in excitatory neurons (Fernandes et al., 2019; Varea et al., 2015) in inhibitory neurons CASPR2 rather restricts it (Gao et al., 2019). All these data were collected in mature

cortical neurons and whether they apply for immature hippocampal neurons remains to be established. Hence, to gain more insight in our results many questions remain to be solved. First, CASPR2 cellular distribution, namely presence in inhibitory or excitatory neurons, must be assessed at DIV 14 in our model (*in vitro* hippocampal neurons). The subcellular distribution of the protein also has to be verified, i.e. the surface expression of CASPR2 in dendrites, soma and axons and a possible synaptic localization. Secondly, the impact of anti-CASPR2 autoAbs on CASPR2 surface expression and distribution and on Kv1.2 channel expression must be analyzed. In addition, to assess functional consequences of increased spine densities and GluA2 content upon autoAbs treatment, it would be informative to measure neuronal network activity using electrophysiological techniques.

CONCLUSION

In this work, I used anti-CASPR2 autoAbs from patients with AILE as a tool to investigate the function of CASPR2 in normally developed WT hippocampal neurons and to reveal possible pathological mechanisms of patients' autoAbs in generating the disease. I demonstrated that patients' autoAbs do not induce internalization of CASPR2 but immobilize the protein at the surface, and concomitantly increase Kv1.2 channel expression. This could result in altered neuronal activity, leading to the observed epilepsy as the predominant symptom in patients with anti-CASPR2 AILE. I also evidenced that anti-CASPR2 autoAbs affect excitatory dendritic spines and inhibitory synapses in immature and mature *in vitro* hippocampal neurons respectively. The diverging effects on different neurodevelopmental time points suggest variable functions for CASPR2 in synaptic processes, depending on the neurodevelopmental stage, and highlight the importance of CASPR2 in immature developing neurons and in mature normally developed neurons. This adds evidence to the association of CASPR2 with neurodevelopmental disorders upon early perturbations of the *CNTNAP2* gene and to the pathological effects of anti-CASPR2 autoAbs in elderly patients without previous neurological antecedents.

My obtained results provide more insight on the function of CASPR2 in synaptic processes and reveal possible physiopathological mechanisms of anti-CASPR2 autoAbs in autoimmune limbic encephalitis.

REFERENCES

Aalberse, R. C., Stapel, S. O., Schuurman, J., & Rispens, T. (2009). Immunoglobulin G4: an odd antibody. *Clinical & Experimental Allergy*, *39*(4), 469–477. https://doi.org/10.1111/j.1365-2222.2009.03207.x

Aalberse, Rob C, & Schuurman, J. (2002, January). IgG4 breaking the rules. *Immunology*, Vol. 105, pp. 9–19. https://doi.org/10.1046/j.0019-2805.2001.01341.x

Abrahams, B. S., Tentler, D., Perederiy, J. V, Oldham, M. C., Coppola, G., & Geschwind, D. H. (2007). Genome-wide analyses of human perisylvian cerebral cortical patterning. *Proceedings of the National Academy of Sciences of the United States of America*, *104*(45), 17849–17854. https://doi.org/10.1073/pnas.0706128104

Ackermann, M., & Matus, A. (2003). Activity-induced targeting of profilin and stabilization of dendritic spine morphology. *Nature Neuroscience*, *6*(11), 1194–1200. https://doi.org/10.1038/nn1135

Al-din, A. N., Anderson, M., Bickerstaff, E. R., & Harvey, I. (1982). Brainstem encephalitis and the syndrome of miller fisher a clinical study. *Brain*. https://doi.org/10.1093/brain/105.3.481

American Psychiatric Association (2013). *Diagnostic and Statistical Manual of Mental Disorders (DSM-5)*, 5th edn. Washington, DC: American Psychiatric Association Publishing.

Ances, B. M., Vitaliani, R., Taylor, R. A., Liebeskind, D. S., Voloschin, A., Houghton, D. J., … Dalmau, J. (2005). Treatment-responsive limbic encephalitis identified by neuropil antibodies: MRI and PET correlates. *Brain*, *128*(8), 1764–1777. https://doi.org/10.1093/brain/awh526

Anderson, G. R., Galfin, T., Xu, W., Aoto, J., Malenka, R. C., & Sudhof, T. C. (2012). Candidate autism gene screen identifies critical role for cell-adhesion molecule CASPR2 in dendritic arborization and spine development. *Proceedings of the National Academy of Sciences*, *109*(44), 18120–18125. https://doi.org/10.1073/pnas.1216398109

Anderson, Garret R., Galfin, T., Xu, W., Aoto, J., Malenka, R. C., & Südhof, T. C. (2012). Candidate autism gene screen identifies critical role for cell-adhesion molecule CASPR2 in dendritic arborization and spine development. *Proceedings of the National Academy of Sciences of the United States of America*, *109*(44), 18120–18125. https://doi.org/10.1073/pnas.1216398109

Ang, C. W., Laman, J. D., Willison, H. J., Wagner, E. R., Endtz, H. P., De Klerk, M. A., … Van Doorn, P. A. (2002). Structure of Campylobacter jejuni lipopolysaccharides determines antiganglioside specificity and clinical features of Guillain-Barré and Miller Fisher patients. *Infection and Immunity*, *70*(3), 1202–1208. https://doi.org/10.1128/iai.70.3.1202-1208.2002

Arikkath, J. (2012). Molecular mechanisms of dendrite morphogenesis. *Frontiers in Cellular Neuroscience*, *6*(December), 1–14. https://doi.org/10.3389/fncel.2012.00061

Armangue, T., Leypoldt, F., Málaga, I., Raspall-Chaure, M., Marti, I., Nichter, C., … Dalmau, J. (2014). Herpes simplex virus encephalitis is a trigger of brain autoimmunity. *Annals of Neurology*, *75*(2), 317–323. https://doi.org/10.1002/ana.24083

Aronica, E., Gorter, J. A., Ijlst-Keizers, H., Rozemuller, A. J., Yankaya, B., Leenstra, S., & Troost, D. (2003). Expression and functional role of mGluR3 and mGluR5 in human astrocytes and glioma cells: opposite regulation of glutamate transporter proteins. *European Journal of Neuroscience*, *17*(10), 2106–2118. https://doi.org/10.1046/j.1460-9568.2003.02657.x

Bahn, S., Volk, B., & Wisden, W. (1994). Kainate receptor gene expression in the developing rat brain.

The Journal of Neuroscience. https://doi.org/10.1523/jneurosci.14-09-05525.1994

Bakkaloglu, B., O'Roak, B. J., Louvi, A., Gupta, A. R., Abelson, J. F., Morgan, T. M., … State, M. W. (2008). Molecular Cytogenetic Analysis and Resequencing of Contactin Associated Protein-Like 2 in Autism Spectrum Disorders. *American Journal of Human Genetics*, *82*(1), 165–173. https://doi.org/10.1016/j.ajhg.2007.09.017

Banks, W. A. (2005). Blood-brain barrier transport of cytokines: a mechanism for neuropathology. *Current Pharmaceutical Design*, *11*(8), 973–984. Retrieved from http://www.ncbi.nlm.nih.gov/pubmed/15777248

Bataller, L., Wade, D. F., Graus, F., Stacey, H. D., Rosenfeld, M. R., & Dalmau, J. (2004). Antibodies to Zic4 in paraneoplastic neurologic disorders and small-cell lung cancer. *Neurology*, *62*(5), 778–782. https://doi.org/10.1212/01.wnl.0000113749.77217.01

Bats, C., Groc, L., & Choquet, D. (2007). The Interaction between Stargazin and PSD-95 Regulates AMPA Receptor Surface Trafficking. *Neuron*, *53*(5), 719–734. https://doi.org/10.1016/j.neuron.2007.01.030

Battefeld, A., Tran, B. T., Gavrilis, J., Cooper, E. C., & Kole, M. H. P. (2014). Heteromeric Kv7.2/7.3 channels differentially regulate action potential initiation and conduction in neocortical myelinated axons. *The Journal of Neuroscience : The Official Journal of the Society for Neuroscience*, *34*(10), 3719–3732. https://doi.org/10.1523/JNEUROSCI.4206-13.2014

Baumgartner, S., Littleton, J. T., Broadie, K., Bhat, M. A., Harbecke, R., Lengyel, J. A., … Bellen, H. J. (1996). A Drosophila neurexin is required for septate junction and blood-nerve barrier formation and function. *Cell*, *87*(6), 1059–1068. Retrieved from http://www.ncbi.nlm.nih.gov/pubmed/8978610

Bel, C., Oguievetskaia, K., Pitaval, C., Goutebroze, L., & Faivre-Sarrailh, C. (2009). Axonal targeting of Caspr2 in hippocampal neurons via selective somatodendritic endocytosis. *Journal of Cell Science*, *122*(18), 3403–3413. https://doi.org/10.1242/jcs.050526

Bellen, H. J., Lu, Y., Beckstead, R., & Bhat, M. A. (1998). Neurexin IV, caspr and paranodin--novel members of the neurexin family: encounters of axons and glia. *Trends in Neurosciences*, *21*(10), 444–449. Retrieved from http://www.ncbi.nlm.nih.gov/pubmed/9786343

Berghs, S., Aggujaro, D., Dirkx, R., Maksimova, E., Stabach, P., Hermel, J. M., … Solimena, M. (2000). βIV spectrin, a new spectrin localized at axon initial segments and nodes of ranvier in the central and peripheral nervous system. *Journal of Cell Biology*, *151*(5), 985–1001. https://doi.org/10.1083/jcb.151.5.985

Bhat, M. A., Rios, J. C., Lu, Y., Garcia-Fresco, G. P., Ching, W., St Martin, M., … Bellen, H. J. (2001). Axon-glia interactions and the domain organization of myelinated axons requires neurexin IV/Caspr/Paranodin. *Neuron*, *30*(2), 369–383. https://doi.org/10.1016/S0896-6273(01)00294-X

Bien, C. G., Mirzadjanova, Z., Baumgartner, C., Onugoren, M. D., Grunwald, T., Holtkamp, M., … May, T. W. (2017). Anti-contactin-associated protein-2 encephalitis: relevance of antibody titres, presentation and outcome. *European Journal of Neurology*, *24*(1), 175–186. https://doi.org/10.1111/ene.13180

Bien, Christian G., Vincent, A., Barnett, M. H., Becker, A. J., Blümcke, I., Graus, F., … Bauer, J. (2012). Immunopathology of autoantibody-associated encephalitides: Clues for pathogenesis. *Brain*, *135*(5), 1622–1638. https://doi.org/10.1093/brain/aws082

Biffi, E., Regalia, G., Menegon, A., Ferrigno, G., & Pedrocchi, A. (2013). The influence of neuronal density and maturation on network activity of hippocampal cell cultures: A methodological study.

PLoS ONE, *8*(12). https://doi.org/10.1371/journal.pone.0083899

Black, J. A., & Waxman, S. G. (1988). The perinodal astrocyte. *Glia*, Vol. 1, pp. 169–183. https://doi.org/10.1002/glia.440010302

Boeckers, T. M. (2006). The postsynaptic density. In *Cell and tissue research* (pp. 409–422). https://doi.org/10.1007/978-1-4939-3474-4_17

Bonetto, G., Hivert, B., Goutebroze, L., Karagogeos, D., Crépel, V., & Faivre-Sarrailh, C. (2019). Selective axonal expression of the Kv1 channel complex in pre-myelinated GABAergic hippocampal neurons. *Frontiers in Cellular Neuroscience*, *13*(May), 1–17. https://doi.org/10.3389/fncel.2019.00222

Bourke, J. L., Coleman, H. A., Pham, V., Forsythe, J. S., & Parkington, H. C. (2013). Neuronal Electrophysiological Function and Control of Neurite Outgrowth on Electrospun Polymer Nanofibers Are Cell Type Dependent. *Tissue Engineering Part A*. https://doi.org/10.1089/ten.tea.2013.0295

Bourne, J. N., & Harris, K. M. (2011). Coordination of size and number of excitatory and inhibitory synapses results in a balanced structural plasticity along mature hippocampal CA1 dendrites during LTP. *Hippocampus*, *21*(4), 354–373. https://doi.org/10.1002/hipo.20768

Boyle, M. E. T., Berglund, E. O., Murai, K. K., Weber, L., Peles, E., & Ranscht, B. (2001). Contactin orchestrates assembly of the septate-like junctions at the paranode in myelinated peripheral nerve. *Neuron*, *30*(2), 385–397. https://doi.org/10.1016/S0896-6273(01)00296-3

Brew, H. M., Gittelman, J. X., Silverstein, R. S., Hanks, T. D., Demas, V. P., Robinson, L. C., … Tempel, B. L. (2007). Seizures and Reduced Life Span in Mice Lacking the Potassium Channel Subunit Kv1.2, but Hypoexcitability and Enlarged Kv1 Currents in Auditory Neurons. *Journal of Neurophysiology*, *98*(3), 1501–1525. https://doi.org/10.1152/jn.00640.2006

Bridi, M. S., Park, S. M., & Huang, S. (2017). Developmental Disruption of GABA A R-Meditated Inhibition in Cntnap2 KO Mice. *Eneuro*, *4*(5), ENEURO.0162-17.2017. https://doi.org/10.1523/eneuro.0162-17.2017

Brimberg, L., Mader, S., Jeganathan, V., Berlin, R., Coleman, T. R., Gregersen, P. K., … Diamond, B. (2016). Caspr2-reactive antibody cloned from a mother of an ASD child mediates an ASD-like phenotype in mice. *Molecular Psychiatry*, *21*(12), 1663–1671. https://doi.org/10.1038/mp.2016.165

Brimberg, L., Sadiq, A., Gregersen, P. K., & Diamond, B. (2013). *Brain-reactive IgG correlates with autoimmunity in mothers of a child with an autism spectrum disorder*. *18*. https://doi.org/10.1038/mp.2013.101

Brivio, V., Faivre-Sarrailh, C., Peles, E., Sherman, D. L., & Brophy, P. J. (2017). Assembly of CNS Nodes of Ranvier in Myelinated Nerves Is Promoted by the Axon Cytoskeleton. *Current Biology*, *27*(7), 1068–1073. https://doi.org/10.1016/j.cub.2017.01.025

Browne, D. L., Gancher, S. T., Nutt, J. G., Brunt, E. R. P., Smith, E. A., Kramer, P., & Litt, M. (1994). Episodic ataxia/myokymia syndrome is associated with point mutations in the human potassium channel gene, KCNA1. *Nature Genetics*, *8*(2), 136–140. https://doi.org/10.1038/ng1094-136

Buckley, C., Oger, J., Clover, L., Tüzün, E., Carpenter, K., Jackson, M., & Vincent, A. (2001). Potassium channel antibodies in two patients with reversible limbic encephalitis. *Annals of Neurology*, *50*(1), 73–78. https://doi.org/10.1002/ana.1097

Buttiglione, M., Revest, J.-M., Pavlou, O., Karagogeos, D., Furley, A., Rougon, G., & Faivre-Sarrailh, C.

(1998). A Functional Interaction between the Neuronal Adhesion Molecules TAG-1 and F3 Modulates Neurite Outgrowth and Fasciculation of Cerebellar Granule Cells. *The Journal of Neuroscience*, *18*(17), 6853–6870. https://doi.org/10.1523/jneurosci.18-17-06853.1998

Calverley, R. K. S., & Jones, D. G. (1990, September 1). Contributions of dendritic spines and perforated synapses to synaptic plasticity. *Brain Research Reviews*, Vol. 15, pp. 215–249. https://doi.org/10.1016/0165-0173(90)90002-6

Campomanes, C. R., Carroll, K. I., Manganas, L. N., Hershberger, M. E., Gong, B., Antonucci, D. E., … Trimmer, J. S. (2002). Kvβ subunit oxidoreductase activity and Kv1 potassium channel trafficking. *Journal of Biological Chemistry*. https://doi.org/10.1074/jbc.M110276200

Canali, G., Garcia, M., Hivert, B., Pinatel, D., Goullancourt, A., Oguievetskaia, K., … Goutebroze, L. (2018). Genetic variants in autism-related CNTNAP2 impair axonal growth of cortical neurons. *Human Molecular Genetics*, *27*(11), 1941–1954. https://doi.org/10.1093/hmg/ddy102

Chan, K. H., Vernino, S., & Lennon, V. A. (2001). ANNA-3 anti-neuronal nuclear antibody: marker of lung cancer-related autoimmunity. *Annals of Neurology*, *50*(3), 301–311. Retrieved from http://www.ncbi.nlm.nih.gov/pubmed/11558786

Chang, K. J., Zollinger, D. R., Susuki, K., Sherman, D. L., Makara, M. A., Brophy, P. J., … Rasband, M. N. (2014). Glial ankyrins facilitate paranodal axoglial junction assembly. *Nature Neuroscience*, *17*(12), 1673–1681. https://doi.org/10.1038/nn.3858

Charles, P., Tait, S., Faivre-Sarrailh, C., Barbin, G., Gunn-Moore, F., Denisenko-Nehrbass, N., … Lubetzki, C. (2002). Neurofascin is a glial receptor for the paranodin/Caspr-contactin axonal complex at the axoglial junction. *Current Biology : CB*, *12*(3), 217–220. https://doi.org/10.1016/S0960-9822(01)00680-7

Chen, N., Koopmans, F., Gordon, A., Paliukhovich, I., Klaassen, R. V., Van Der Schors, R. C., … Li, K. W. (2015). Interaction proteomics of canonical Caspr2 (CNTNAP2) reveals the presence of two Caspr2 isoforms with overlapping interactomes. *Biochimica et Biophysica Acta - Proteins and Proteomics*, *1854*(7), 827–833. https://doi.org/10.1016/j.bbapap.2015.02.008

Chicurel, M. E., & Harris, K. M. (1992). Three-dimensional analysis of the structure and composition of CA3 branched dendritic spines and their synaptic relationships with mossy fiber boutons in the rat hippocampus. *The Journal of Comparative Neurology*, *325*(2), 169–182. https://doi.org/10.1002/cne.903250204

Chiu, S. Y., Zhou, L., Zhang, C. L., & Messing, A. (1999). Analysis of potassium channel functions in mammalian axons by gene knockouts. *Journal of Neurocytology*, *28*(4–5), 349–364. Retrieved from http://www.ncbi.nlm.nih.gov/pubmed/10739576

Choii, G., & Ko, J. (2015). Gephyrin: a central GABAergic synapse organizer. *Experimental & Molecular Medicine*, Vol. 47, p. e158. https://doi.org/10.1038/emm.2015.5

Christensen, D. L., Braun, K. V. N., Baio, J., Bilder, D., Charles, J., Constantino, J. N., … Yeargin-Allsopp, M. (2018). Prevalence and Characteristics of Autism Spectrum Disorder Among Children Aged 8 Years — Autism and Developmental Disabilities Monitoring Network, 11 Sites, United States, 2012. *MMWR. Surveillance Summaries*. https://doi.org/10.15585/mmwr.ss6513a1

Cifuentes-Diaz, C., Chareyre, F., Garcia, M., Devaux, J., Carnaud, M., Levasseur, G., … Goutebroze, L. (2011). Protein 4.1B contributes to the organization of peripheral myelinated axons. *PLoS ONE*, *6*(9). https://doi.org/10.1371/journal.pone.0025043

Clarke, P., Leser, J. S., Bowen, R. A., & Tyler, K. L. (2014). Virus-induced transcriptional changes in the brain include the differential expression of genes associated with interferon, apoptosis,

interleukin 17 receptor A, and glutamate signaling as well as flavivirus-specific upregulation of tRNA synthetases. *MBio*, *5*(2), e00902-14. https://doi.org/10.1128/mBio.00902-14

Colman, H., Nabekura, J., & Lichtman, J. W. (1997). Alterations in synaptic strength preceding axon withdrawal. *Science (New York, N.Y.)*, *275*(5298), 356–361. Retrieved from http://www.ncbi.nlm.nih.gov/pubmed/8994026

Conn, P. J., & Pin, J.-P. (1997). Pharmacology and functions of metabotropuc glutamate receptors. *Annual Review of Pharmacology and Toxicology*, *37*(1), 205–237. https://doi.org/10.1146/annurev.pharmtox.37.1.205

Contractor, A., Mulle, C., & Swanson, G. T. (2011, March). Kainate receptors coming of age: Milestones of two decades of research. *Trends in Neurosciences*, Vol. 34, pp. 154–163. https://doi.org/10.1016/j.tins.2010.12.002

Corsellis, J. A. N., Goldberg, G. J., & Norton, A. R. (1968). "limbic encephalitis" and its association with carcinoma. *Brain*, *91*(3), 481–496. https://doi.org/10.1093/brain/91.3.481

Coutinho, E., Menassa, D. A., Jacobson, L., West, S. J., Domingos, J., Moloney, T. C., … Vincent, A. (2017). Persistent microglial activation and synaptic loss with behavioral abnormalities in mouse offspring exposed to CASPR2-antibodies in utero. *Acta Neuropathologica*, *134*(4), 567–583. https://doi.org/10.1007/s00401-017-1751-5

Dale, R. C., Merheb, V., Pillai, S., Wang, D., Cantrill, L., Murphy, T. K., … Brilot, F. (2012). Antibodies to surface dopamine-2 receptor in autoimmune movement and psychiatric disorders. *Brain : A Journal of Neurology*, *135*(Pt 11), 3453–3468. https://doi.org/10.1093/brain/aws256

Dalmau, J., Geis, C., & Graus, F. (2017). Autoantibodies to Synaptic Receptors and Neuronal Cell Surface Proteins in Autoimmune Diseases of the Central Nervous System. *Physiological Reviews*, *97*(2), 839–887. https://doi.org/10.1152/physrev.00010.2016

Dalmau, J., Gultekin, S. H., Voltz, R., Hoard, R., DesChamps, T., Balmaceda, C., … Rosenfeld, M. R. (1999). Ma1, a novel neuron- and testis-specific protein, is recognized by the serum of patients with paraneoplastic neurological disorders. *Brain*, *122*(1), 27–39. https://doi.org/10.1093/brain/122.1.27

Dalmau, J., & Rosenfeld, M. R. (2008, April). Paraneoplastic syndromes of the CNS. *The Lancet Neurology*, Vol. 7, pp. 327–340. https://doi.org/10.1016/S1474-4422(08)70060-7

Dalmau, J., Tüzün, E., Wu, H.-Y., Masjuan, J., Rossi, J. E., Voloschin, A., … Lynch, D. R. (2007). Paraneoplastic Anti-N-methyl-D-aspartate Receptor Encephalitis Associated with Ovarian Teratoma. *Ann Neurol*, *61*, 25–36. https://doi.org/10.1002/ana.21050

Davies, A. M., & Sutton, B. J. (2015, November). Human IgG4: A structural perspective. *Immunological Reviews*, Vol. 268, pp. 139–159. https://doi.org/10.1111/imr.12349

Davis, J. Q., Lambert, S., & Bennett, V. (1996). Molecular composition of the node of Ranvier: identification of ankyrin-binding cell adhesion molecules neurofascin (mucin+/third FNIII domain-) and NrCAM at nodal axon segments. *The Journal of Cell Biology*, *135*(5), 1355–1367. https://doi.org/10.1083/jcb.135.5.1355

Dawes, J. M., Weir, G. A., Middleton, S. J., Patel, R., Chisholm, K. I., Pettingill, P., … Bennett, D. L. (2018). Immune or Genetic-Mediated Disruption of CASPR2 Causes Pain Hypersensitivity Due to Enhanced Primary Afferent Excitability. *Neuron*, *97*(4), 806-822.e10. https://doi.org/10.1016/j.neuron.2018.01.033

De Camilli, P., Thomas, A., Cofiell, R., Folli, F., Lichte, B., Piccolo, G., … Kilimann, M. W. (1993). The

synaptic vesicle-associated protein amphiphysin is the 128-kD autoantigen of Stiff-Man syndrome with breast cancer. *The Journal of Experimental Medicine*, *178*(6), 2219–2223. https://doi.org/10.1084/jem.178.6.2219

de Graaff, E., Maat, P., Hulsenboom, E., van den Berg, R., van den Bent, M., Demmers, J., … Sillevis Smitt, P. (2012). Identification of delta/notch-like epidermal growth factor-related receptor as the Tr antigen in paraneoplastic cerebellar degeneration. *Annals of Neurology*, *71*(6), 815–824. https://doi.org/10.1002/ana.23550

de Waegh, S. M., Lee, V. M., & Brady, S. T. (1992). Local modulation of neurofilament phosphorylation, axonal caliber, and slow axonal transport by myelinating Schwann cells. *Cell*, *68*(3), 451–463. Retrieved from http://www.ncbi.nlm.nih.gov/pubmed/1371237

Dean, C., & Dresbach, T. (2006). Neuroligins and neurexins: Linking cell adhesion, synapse formation and cognitive function. *Trends in Neurosciences*, Vol. 29, pp. 21–29. https://doi.org/10.1016/j.tins.2005.11.003

Deleuze, C., Alonso, G., Lefevre, I. A., Duvoid-Guillou, A., & Hussy, N. (2005). Extrasynaptic localization of glycine receptors in the rat supraoptic nucleus: Further evidence for their involvement in glia-to-neuron communication. *Neuroscience*, *133*(1), 175–183. https://doi.org/10.1016/j.neuroscience.2005.01.060

Denaxa, M., Chan, C. H., Schachner, M., Parnavelas, J. G., & Karagogeos, D. (2001). The adhesion molecule TAG-1 mediates the migration of cortical interneurons from the ganglionic eminence along the corticofugal fiber system. *Development (Cambridge, England)*, *128*(22), 4635–4644. Retrieved from http://www.ncbi.nlm.nih.gov/pubmed/11714688

Denisenko-Nehrbass, N., Oguievetskaia, K., Goutebroze, L., Galvez, T., Yamakawa, H., Ohara, O., … Girault, J. A. (2003). Protein 4.1B associates with both Caspr/paranodin and Caspr2 at paranodes and juxtaparanodes of myelinated fibres. *European Journal of Neuroscience*, *17*(2), 411–416. https://doi.org/10.1046/j.1460-9568.2003.02441.x

Devaux, J. J., Kleopa, K. A., Cooper, E. C., & Scherer, S. S. (2004). KCNQ2 Is a Nodal K+ Channel. *Journal of Neuroscience*, *24*(5), 1236–1244. https://doi.org/10.1523/jneurosci.4512-03.2004

Devaux, Jérôme, Alcaraz, G., Grinspan, J., Bennett, V., Joho, R., Crest, M., & Scherer, S. S. (2003). Kv3.1b is a novel component of CNS nodes. *The Journal of Neuroscience : The Official Journal of the Society for Neuroscience*, *23*(11), 4509–4518. https://doi.org/10.1523/JNEUROSCI.23-11-04509.2003

Devaux, Jerome, Gola, M., Jacquet, G., & Crest, M. (2002). Effects of K + Channel Blockers on Developing Rat Myelinated CNS Axons: Identification of Four Types of K + Channels. *Journal of Neurophysiology*, *87*(3), 1376–1385. https://doi.org/10.1152/jn.00646.2001

Devaux, Jerome, Gola, M., Jacquet, G., & Crest, M. (2017). Effects of K + Channel Blockers on Developing Rat Myelinated CNS Axons: Identification of Four Types of K + Channels. *Journal of Neurophysiology*, *87*(3), 1376–1385. https://doi.org/10.1152/jn.00646.2001

Devaux, Jerome, & Gow, A. (2008). Tight junctions potentiate the insulative properties of small CNS myelinated axons. *Journal of Cell Biology*. https://doi.org/10.1083/jcb.200808034

Diamond, B, Honig, G., Mader, S., Brimberg, L., & Volpe, B. T. (2013). Brain-Reactive Antibodies and Disease. *Annual Review of Immunology*, *31*(1), 345–385. https://doi.org/10.1146/annurev-immunol-020711-075041

Diamond, Betty, Huerta, P. T., Mina-Osorio, P., Kowal, C., & Volpe, B. T. (2009). Losing your nerves? Maybe it's the antibodies. *Nature Reviews Immunology*, *9*(6), 449–456.

https://doi.org/10.1016/j.bmcl.2009.08.098

Didelot, A., & Honnorat, J. (2009). Update on paraneoplastic neurological syndromes. *Current Opinion in Oncology*, *21*(6), 566–572. https://doi.org/10.1097/CCO.0b013e3283306647

Dingledine, R. (1991). New wave of non-NMDA excitatory amino acid receptors. *Trends in Pharmacological Sciences*, *12*(10), 360–362. Retrieved from http://www.ncbi.nlm.nih.gov/pubmed/1662419

Dosemeci, A., Tao-Cheng, J.-H., Vinade, L., & Jaffe, H. (2005). *Preparation of postsynaptic density fraction from hippocampal slices and proteomic analysis*. https://doi.org/10.1016/j.bbrc.2005.11.069

Doumazane, E., Scholler, P., Zwier, J. M., Trinquet, E., Rondard, P., & Pin, J.-P. (2011). A new approach to analyze cell surface protein complexes reveals specific heterodimeric metabotropic glutamate receptors. *The FASEB Journal*, *25*(1), 66–77. https://doi.org/10.1096/fj.10-163147

Dresbach, T., Nawrotzki, R., Kremer, T., Schumacher, S., Quinones, D., Kluska, M., … Kirsch, J. (2008). Molecular architecture of glycinergic synapses. *Histochemistry and Cell Biology*, Vol. 130, pp. 617–633. https://doi.org/10.1007/s00418-008-0491-y

Duflocq, A., Chareyre, F., Giovannini, M., Couraud, F., & Davenne, M. (2011). Characterization of the axon initial segment (AIS) of motor neurons and identification of a para-AIS and a juxtapara-AIS, organized by protein 4.1B. *BMC Biology*, *9*(September). https://doi.org/10.1186/1741-7007-9-66

Dumas, T. C. (2005). Developmental regulation of cognitive abilities: Modified composition of a molecular switch turns on associative learning. *Progress in Neurobiology*, Vol. 76, pp. 189–211. https://doi.org/10.1016/j.pneurobio.2005.08.002

Einheber, S., Meng, X., Rubin, M., Lam, I., Mohandas, N., An, X., … Salzer, J. L. (2013). The 4.1B cytoskeletal protein regulates the domain organization and sheath thickness of myelinated axons. *GLIA*, *61*(2), 240–253. https://doi.org/10.1002/glia.22430

Engelhardt, B., & Wolburg, H. (2004). Mini-review: Transendothelial migration of leukocytes: through the front door or around the side of the house? *European Journal of Immunology*, *34*(11), 2955–2963. https://doi.org/10.1002/eji.200425327

Essrich, C., Lorez, M., Benson, J. A., Fritschy, J.-M., & Lüscher, B. (1998). Postsynaptic clustering of major GABAA receptor subtypes requires the γ2 subunit and gephyrin. *Nature Neuroscience*, *1*(7), 563–571. https://doi.org/10.1038/2798

Evans, A. J., Gurung, S., Henley, J. M., Nakamura, Y., & Wilkinson, K. A. (2019). Exciting Times: New Advances Towards Understanding the Regulation and Roles of Kainate Receptors. *Neurochemical Research*, *44*(3), 572–584. https://doi.org/10.1007/s11064-017-2450-2

Faivre-sarrailh, C., Gauthier, F., Denisenko-nehrbass, N., Bivic, A. Le, Rougon, G., & Girault, J. (2000). The Glycosylphosphatidyl Inositol-anchored Adhesion Molecule F3 / Contactin Is Required for Surface Transport of Paranodin / Contactin-associated Protein (caspr). *Cell*, *149*(2), 491–501.

Falivelli, G., De jaco, A., Favaloro, F. L., Kim, H., Wilson, J., Dubi, N., … Comoletti, D. (2012). Inherited genetic variants in autism-related CNTNAP2 show perturbed trafficking and ATF6 activation. *Human Molecular Genetics*, *21*(21), 4761–4773. https://doi.org/10.1093/hmg/dds320

Fang, B., McKeon, A., Hinson, S. R., Kryzer, T. J., Pittock, S. J., Aksamit, A. J., & Lennon, V. A. (2016). Autoimmune Glial Fibrillary Acidic Protein Astrocytopathy. *JAMA Neurology*, *73*(11), 1297. https://doi.org/10.1001/jamaneurol.2016.2549

Farrant, M., & Nusser, Z. (2005). Variations on an inhibitory theme: Phasic and tonic activation of GABA

A receptors. *Nature Reviews Neuroscience*, *6*(3), 215–229. https://doi.org/10.1038/nrn1625

Feldt-Rasmussen, U. (1996). Analytical and clinical performance goals for testing autoantibodies to thyroperoxidase, thyroglobulin, and thyrotropin receptor. In *Clinical (hernistiy* (Vol. 42). Retrieved from http://clinchem.aaccjnls.org/content/clinchem/42/1/160.full.pdf

Fernandes, D., & Carvalho, A. L. (2016). Mechanisms of homeostatic plasticity in the excitatory synapse. *Journal of Neurochemistry*, *139*(6), 973–996. https://doi.org/10.1111/jnc.13687

Fernandes, D., Santos, S. D., Coutinho, E., Whitt, J. L., Beltrão, N., Rondão, T., … Carvalho, A. L. (2019). Disrupted AMPA Receptor Function upon Genetic- or Antibody-Mediated Loss of Autism-Associated CASPR2. *Cerebral Cortex*. https://doi.org/10.1093/cercor/bhz032

Fiala, J. C., Feinberg, M., Popov, V., & Harris, K. M. (1998). Synaptogenesis via dendritic filopodia in developing hippocampal area CA1. *J Neurosci*, *18*(21), 8900–8911. https://doi.org/1998/10/24 00:01

Fouquet, C., Gilles, J.-F., Heck, N., Dos Santos, M., Schwartzmann, R., Cannaya, V., … Bolte, S. (2015). Improving axial resolution in confocal microscopy with new high refractive index mounting media. *PloS One*, *10*(3), e0121096. https://doi.org/10.1371/journal.pone.0121096

Frangaj, A., & Fan, Q. R. (2018). Structural biology of GABA B receptor. *Neuropharmacology*, *136*, 68–79. https://doi.org/10.1016/j.neuropharm.2017.10.011

Freigang, J., Proba, K., Leder, L., Diederichs, K., Sonderegger, P., & Welte, W. (2000). The Crystal Structure of the Ligand Binding Module of Axonin-1/TAG-1 Suggests a Zipper Mechanism for Neural Cell Adhesion. *Cell*, *101*(4), 425–433. https://doi.org/10.1016/S0092-8674(00)80852-1

Fukamauchi, F., Aihara, O., Wang, Y. J., Akasaka, K., Takeda, Y., Horie, M., … Iwakura, Y. (2001). Tag-1-deficient mice have marked elevation of adenosine A1 receptors in the hippocampus. *Biochemical and Biophysical Research Communications*, *281*(1), 220–226. https://doi.org/10.1006/bbrc.2001.4334

Fukata, Y., Lovero, K. L., Iwanaga, T., Watanabe, A., Yokoi, N., Tabuchi, K., … Fukata, M. (2010). Disruption of LGI1-linked synaptic complex causes abnormal synaptic transmission and epilepsy. *Proceedings of the National Academy of Sciences*, *107*(8), 3799–3804. https://doi.org/10.1073/pnas.0914537107

Fukata, Yuko, Adesnik, H., Iwanaga, T., Bredt, D. S., Nicoll, R. A., & Fukata, M. (2006). Epilepsy-related ligand/receptor complex LGI1 and ADAM22 regulate synaptic transmission. *Science*, *313*(5794), 1792–1795. https://doi.org/10.1126/science.1129947

Furley, A. J., Morton, S. B., Dodd, J., & Jessell, T. M. (1990). The Axond Glycoprotein TAG1 Is an ImmunogiobuMn SuperfamHy Member with Neurite Outgrowth-Promoting Activity. *Cell*, *61*, 157–170.

Furneaux, H. M., Rosenblum, M. K., Dalmau, J., Wong, E., Woodruff, P., Graus, F., & Posner, J. B. (1990). Selective Expression of Purkinje-Cell Antigens in Tumor Tissue from Patients with Paraneoplastic Cerebellar Degeneration. *New England Journal of Medicine*, *322*(26), 1844–1851. https://doi.org/10.1056/NEJM199006283222604

Gao, R., Piguel, N. H., Melendez-Zaidi, A. E., Martin-de-Saavedra, M. D., Yoon, S., Forrest, M. P., … Penzes, P. (2018). CNTNAP2 stabilizes interneuron dendritic arbors through CASK. *Molecular Psychiatry*, *23*(9), 1832–1850. https://doi.org/10.1038/s41380-018-0027-3

Gao, R., Zaccard, C. R., Shapiro, L. P., Dionisio, L. E., Martin-de-Saavedra, M. D., Piguel, N. H., … Penzes, P. (2019). The CNTNAP2-CASK complex modulates GluA1 subcellular distribution in interneurons.

Neuroscience Letters, *701*, 92–99. https://doi.org/10.1016/j.neulet.2019.02.025

Garner, C. C., Zhai, R. G., Gundelfinger, E. D., & Ziv, N. E. (2002). Molecular mechanisms of CNS synaptogenesis. *Trends in Neurosciences*, Vol. 25, pp. 243–250. https://doi.org/10.1016/S0166-2236(02)02152-5

Gdalyahu, A., Lazaro, M., Penagarikano, O., Golshani, P., Trachtenberg, J. T., & Gescwind, D. H. (2015). The autism related protein contactin-associated protein-like 2 (CNTNAP2) stabilizes new spines: An in vivo mouse study. *PLoS ONE*, *10*(5), 1–7. https://doi.org/10.1371/journal.pone.0125633

Gelpi, E., Höftberger, R., Graus, F., Ling, H., Holton, J. L., Dawson, T., … Kovacs, G. G. (2016). Neuropathological criteria of anti-IgLON5-related tauopathy. *Acta Neuropathologica*, *132*(4), 531–543. https://doi.org/10.1007/s00401-016-1591-8

Gibb, A. J., & Colquhoun, D. (1992). Activation of N-methyl-D-aspartate receptors by L-glutamate in cells dissociated from adult rat hippocampus. *The Journal of Physiology*, *456*(1), 143–179. https://doi.org/10.1113/jphysiol.1992.sp019331

Giesemann, T., Schwarz, G., Nawrotzki, R., Berhörster, K., Rothkegel, M., Schlüter, K., … Jockusch, B. M. (2003). Complex formation between the postsynaptic scaffolding protein gephyrin, profilin, and Mena: a possible link to the microfilament system. *The Journal of Neuroscience : The Official Journal of the Society for Neuroscience*, *23*(23), 8330–8339. Retrieved from http://www.ncbi.nlm.nih.gov/pubmed/12967995

Gollan, L., Sabanay, H., Poliak, S., Berglund, E. O., Ranscht, B., & Peles, E. (2002). Retention of a cell adhesion complex at the paranodal junction requires the cytoplasmic region of Caspr. *The Journal of Cell Biology*, *157*(7), 1247–1256. https://doi.org/10.1083/jcb.200203050

Gordon, A., Salomon, D., Barak, N., Pen, Y., Tsoory, M., Kimchi, T., & Peles, E. (2016). Expression of Cntnap2 (Caspr2) in multiple levels of sensory systems. *Molecular and Cellular Neuroscience*, *70*, 42–53. https://doi.org/10.1016/j.mcn.2015.11.012

Granerod, J., Ambrose, H. E., Davies, N. W., Clewley, J. P., Walsh, A. L., Morgan, D., … Crowcroft, N. S. (2010). Causes of encephalitis and differences in their clinical presentations in England: A multicentre, population-based prospective study. *The Lancet Infectious Diseases*, *10*(12), 835–844. https://doi.org/10.1016/S1473-3099(10)70222-X

Graus, F., Elkon, K. B., Lloberes, P., Ribalta, T., Torres, A., Ussetti, P., … Agusti-Vidal, A. (1987). Neuronal antinuclear antibody (anti-Hu) in paraneoplastic encephalomyelitis simulating acute polyneuritis. *Acta Neurologica Scandinavica*, *75*(4), 249–252. Retrieved from http://www.ncbi.nlm.nih.gov/pubmed/3035860

Gray, E. G. (1959). Axo-somatic and axo-dendritic synapses of the cerebral cortex. *Journal of Anatomy*, *93*(Pt 4), 420–433. Retrieved from https://www.ncbi.nlm.nih.gov/pmc/articles/PMC1244535/pdf/janat00446-0039.pdf

Gresa-Arribas, N., Planagumà, J., Petit-Pedrol, M., Kawachi, I., Katada, S., Glaser, C. A., … Dalmau, J. (2016). Human neurexin-3α antibodies associate with encephalitis and alter synapse development. *Neurology*, *86*(24), 2235–2242. https://doi.org/10.1212/WNL.0000000000002775

Gresa-Arribas, N., Titulaer, M. J., Torrents, A., Aguilar, E., McCracken, L., Leypoldt, F., … Dalmau, J. (2014). Diagnosis and significance of antibody titers in anti-NMDA receptor encephalitis, a retrospective study. *Lancet Neurology*, *13*(2), 167. https://doi.org/10.1016/S1474-4422(13)70282-5

Griffiths, I., Klugmann, M., Anderson, T., Yool, D., Thomson, C., Schwab, M. H., … Nave, K. A. (1998). Axonal swellings and degeneration in mice lacking the major proteolipid of myelin. *Science (New*

York, N.Y.), *280*(5369), 1610–1613. https://doi.org/10.1126/SCIENCE.280.5369.1610

Groc, L., Gustafsson, B., & Hanse, E. (2006). AMPA signalling in nascent glutamatergic synapses: There and not there! *Trends in Neurosciences*, Vol. 29, pp. 132–139. https://doi.org/10.1016/j.tins.2006.01.005

Groc, L., Heine, M., Cognet, L., Brickley, K., Stephenson, F. A., Lounis, B., & Choquet, D. (2004). Differential activity-dependent regulation of the lateral mobilities of AMPA and NMDA receptors. *Nature Neuroscience*, *7*(7), 695–696. https://doi.org/10.1038/nn1270

Groeneweg, F. L., Trattnig, C., Kuhse, J., Nawrotzki, R. A., & Kirsch, J. (2018). Gephyrin: a key regulatory protein of inhibitory synapses and beyond. *Histochemistry and Cell Biology*, Vol. 150, pp. 489–508. https://doi.org/10.1007/s00418-018-1725-2

Gu, C., & Gu, Y. (2011). Clustering and activity tuning of Kv1 channels in myelinated hippocampal axons. *Journal of Biological Chemistry*, *286*(29), 25835–25847. https://doi.org/10.1074/jbc.M111.219113

Gulbis, J. M., Zhou, M., Mann, S., & MacKinnon, R. (2000). Structure of the cytoplasmic β subunit - T1 assembly of voltage- dependent K+ channels. *Science*, *289*(5476), 123–127. https://doi.org/10.1126/science.289.5476.123

Gustafsson, M. G. L. (2005). Nonlinear structured-illumination microscopy: wide-field fluorescence imaging with theoretically unlimited resolution. *Proceedings of the National Academy of Sciences of the United States of America*, *102*(37), 13081–13086. https://doi.org/10.1073/pnas.0406877102

Hadden, R. D. M., Karch, H., Hartung, H. P., Zielasek, J., Weissbrich, B., Schubert, J., … Toyka, K. V. (2001). Preceding infections, immune factors, and outcome in Guillain-Barré syndrome. *Neurology*. https://doi.org/10.1212/WNL.56.6.758

Halbach, M., Hömberg, V., & Freund, H. J. (1987). Neuromuscular, autonomic and central cholinergic hyperactivity associated with thymoma and acetylcholine receptor-binding antibody. *Journal of Neurology*, *234*(6), 433–436. https://doi.org/10.1007/BF00314093

Hansen, K. B., Yi, F., Perszyk, R. E., Furukawa, H., Wollmuth, L. P., Gibb, A. J., & Traynelis, S. F. (2018). Structure, function, and allosteric modulation of NMDA receptors. *J. Gen. Physiol*, *150*(8), 1081–1105. https://doi.org/10.1085/jgp.201812032

Harris, K M, & Stevens, J. K. (1989). Dendritic spines of CA 1 pyramidal cells in the rat hippocampus: serial electron microscopy with reference to their biophysical characteristics. *The Journal of Neuroscience : The Official Journal of the Society for Neuroscience*, *9*(8), 2982–2997.

Harris, Kristen M. (1999). Structure, development, and plasticity of dendritic spines. *Current Opinion in Neurobiology*, *9*(3), 343–348. https://doi.org/10.1016/S0959-4388(99)80050-6

Harris, Kristen M, Jensen, F. E., & Tsao, B. (1992). Three-dimensional structure of dendritic spines and synapses in rat hippocampus (CA1) at postnatal day 15 and adult ages: implications for the maturation of synaptic physiology and long-term potentiation [published erratum appears in J Neurosci 1992 Aug;1. *The Journal of Neuroscience*, *12*(7), 2685–2705. https://doi.org/10.1016/j.tcb.2009.06.001

Harris, Kristen M, & Weinberg, R. J. (2012, May 1). Ultrastructure of synapses in the mammalian brain. *Cold Spring Harbor Perspectives in Biology*, Vol. 4, p. 7. https://doi.org/10.1101/cshperspect.a005587

Harris, M., & Jensen, E. (1992). Hospital and Harvard Medical School, Boston,. *Journal of Neuroscience*,

12(July), 2665–2705. https://doi.org/10.1523/JNEUROSCI.12-07-02685.1992

Hart, I. K., Waters, C., Vincent, A., Newland, C., Beeson, D., Pongs, O., … Newsom-Davis, J. (1997). Autoantibodies detected to expressed K + channels are implicated in neuromyotonia. *Annals of Neurology*, *41*(2), 238–246. https://doi.org/10.1002/ana.410410215

Hattan, D., Nesti, E., Cachero, T. G., & Morielli, A. D. (2002). Tyrosine phosphorylation of Kv1.2 Modulates its interaction with the actin-binding protein cortactin. *Journal of Biological Chemistry*, *277*(41), 38596–38606. https://doi.org/10.1074/jbc.M205005200

He, S., Shao, L.-R., Rittase, W. B., & Bausch, S. B. (2012). Increased Kv1 channel expression may contribute to decreased sIPSC frequency following chronic inhibition of NR2B-containing NMDAR. *Neuropsychopharmacology : Official Publication of the American College of Neuropsychopharmacology*, *37*(6), 1338–1356. https://doi.org/10.1038/npp.2011.320

Heaney, C. F., & Kinney, J. W. (2016). Role of GABA B receptors in learning and memory and neurological disorders. *Neuroscience and Biobehavioral Reviews*, *63*, 1–28. https://doi.org/10.1016/j.neubiorev.2016.01.007

High, B., Cole, A. A., Chen, X., & Reese, T. S. (2015). Electron microscopic tomography reveals discrete transcleft elements at excitatory and inhibitory synapses. *Frontiers in Synaptic Neuroscience*, *7*, 9. https://doi.org/10.3389/fnsyn.2015.00009

Hivert, B., Marien, L., Agbam, K. N., & Faivre-Sarrailh, C. (2019). ADAM22 and ADAM23 modulate the targeting of the Kv1 channel-associated protein LGI1 to the axon initial segment. *Journal of Cell Science*, *132*(2), jcs219774. https://doi.org/10.1242/jcs.219774

Hoffman, E. J., Turner, K. J., Fernandez, J. M., Cifuentes, D., Ghosh, M., Ijaz, S., … Giraldez, A. J. (2016). Estrogens Suppress a Behavioral Phenotype in Zebrafish Mutants of the Autism Risk Gene, CNTNAP2. *Neuron*. https://doi.org/10.1016/j.neuron.2015.12.039

Holtmaat, A. J. G. D., Trachtenberg, J. T., Wilbrecht, L., Shepherd, G. M., Zhang, X., Knott, G. W., & Svoboda, K. (2005). Transient and persistent dendritic spines in the neocortex in vivo. *Neuron*, *45*(2), 279–291. https://doi.org/10.1016/j.neuron.2005.01.003

Honnorat, J., Antoine, J. C., Derrington, E., Aguera, M., & Belin, M. F. (1996). Antibodies to a subpopulation of glial cells and a 66 kDa developmental protein in patients with paraneoplastic neurological syndromes. *Journal of Neurology, Neurosurgery, and Psychiatry*, *61*(3), 270–278. https://doi.org/10.1136/jnnp.61.3.270

Horresh, I., Bar, V., Kissil, J. L., & Peles, E. (2010). Organization of Myelinated Axons by Caspr and Caspr2 Requires the Cytoskeletal Adapter Protein 4.1B. *Journal of Neuroscience*, *30*(7), 2480–2489. https://doi.org/10.1523/JNEUROSCI.5225-09.2010

Horresh, I., Poliak, S., Grant, S., Bredt, D., Rasband, M. N., & Peles, E. (2008). Multiple Molecular Interactions Determine the Clustering of Caspr2 and Kv1 Channels in Myelinated Axons. *Journal of Neuroscience*, *28*(52), 14213–14222. https://doi.org/10.1523/JNEUROSCI.3398-08.2008

Hotulainen, P., & Hoogenraad, C. C. (2010). Actin in dendritic spines: Connecting dynamics to function. *Journal of Cell Biology*, *189*(4), 619–629. https://doi.org/10.1083/jcb.201003008

Hou, R., Wu, J., He, D., Yan, Y., & Li, L. (2019). Anti-N-methyl-D-aspartate receptor encephalitis associated with reactivated Epstein-Barr virus infection in pediatric patients: Three case reports. *Medicine*, *98*(20), e15726. https://doi.org/10.1097/MD.0000000000015726

Høyer, H., Braathen, G. J., Eek, A. K., Nordang, G. B. N., Skjelbred, C. F., & Russell, M. B. (2015). Copy Number Variations in a Population-Based Study of Charcot-Marie-Tooth Disease. *BioMed*

Research International. https://doi.org/10.1155/2015/960404

Hu, H., Gan, J., & Jonas, P. (2014). Fast-spiking, parvalbumin+ GABAergic interneurons: From cellular design to microcircuit function. *Science*. https://doi.org/10.1126/science.1255263

Huettner, J. E. (2003). Kainate receptors and synaptic transmission. *Progress in Neurobiology*. https://doi.org/10.1016/S0301-0082(03)00122-9

Hunt, D. L., & Castillo, P. E. (2012). Synaptic plasticity of NMDA receptors: mechanisms and functional implications. *Current Opinion in Neurobiology*, *22*(3), 496–508. https://doi.org/10.1016/j.conb.2012.01.007

Hutchinson, M., Waters, P., McHugh, J., Gorman, G., O'Riordan, S., Connolly, S., … Vincent, A. (2008). Progressive encephalomyelitis, rigidity, and myoclonus: A novel glycine receptor antibody. *Neurology*, *71*(16), 1291–1292. https://doi.org/10.1212/01.wnl.0000327606.50322.f0

Ichimura, T., & Ellisman, M. H. (1991). Three-dimensional fine structure of cytoskeletal-membrane interactions at nodes of Ranvier. *Journal of Neurocytology*, *20*(8), 667–681. Retrieved from http://www.ncbi.nlm.nih.gov/pubmed/1719139

Inda, M. C., DeFelipe, J., & Muñoz, A. (2006). Voltage-gated ion channels in the axon initial segment of human cortical pyramidal cells and their relationship with chandelier cells. *Proceedings of the National Academy of Sciences of the United States of America*, *103*(8), 2920–2925. https://doi.org/10.1073/pnas.0511197103

Irani, S. R., Buckley, C., Vincent, A., Cockerell, O. C., Rudge, P., Johnson, M. R., & Smith, S. (2008). Immunotherapy-responsive seizure-like episodes with potassium channel antibodies. *Neurology*, *71*(20), 1647–1648. https://doi.org/10.1212/01.wnl.0000326572.93762.51

Irani, Sarosh R, Alexander, S., Waters, P., Kleopa, K. A., Pettingill, P., Zuliani, L., … Vincent, A. (2010). Antibodies to Kv1 potassium channel-complex proteins leucine-rich, glioma inactivated 1 protein and contactin-associated protein-2 in limbic encephalitis, Morvan's syndrome and acquired neuromyotonia. *Brain*, *133*(9), 2734–2748. https://doi.org/10.1093/brain/awq213

Isaacs, H. (1961). A syndrome of continuous muscle-fibre activity. *Journal of Neurology, Neurosurgery & Psychiatry*, *24*(4), 319–325. https://doi.org/10.1136/jnnp.24.4.319

Jacob, T. C., Moss, S. J., & Jurd, R. (2008, May). GABAA receptor trafficking and its role in the dynamic modulation of neuronal inhibition. *Nature Reviews Neuroscience*, Vol. 9, pp. 331–343. https://doi.org/10.1038/nrn2370

Jacobi, E., & von Engelhardt, J. (2018). AMPA receptor complex constituents: Control of receptor assembly, membrane trafficking and subcellular localization. *Molecular and Cellular Neuroscience*, Vol. 91, pp. 67–75. https://doi.org/10.1016/j.mcn.2018.05.008

Jammalamadaka, A., Banerjee, S., Manjunath, B. S., & Kosik, K. S. (2013). Statistical analysis of dendritic spine distributions in rat hippocampal cultures. *BMC Bioinformatics*, *14*(1), 287. https://doi.org/10.1186/1471-2105-14-287

Jane, D. E., Lodge, D., & Collingridge, G. L. (2009). Kainate receptors: Pharmacology, function and therapeutic potential. *Neuropharmacology*, Vol. 56, pp. 90–113. https://doi.org/10.1016/j.neuropharm.2008.08.023

Johnson, J. W., & Ascher, P. (1987). Glycine potentiates the NMDA response in cultured mouse brain neurons. *Nature*, *325*(6104), 529–531. https://doi.org/10.1038/325529a0

Jones, E. G., & Powell, T. P. S. (1969). Morphological variations in the dendritic spines of the neorcortex. *J. Cell Sci. S*, *5*(2), 509–529.

Joubert, B., Gobert, F., Thomas, L., Saint-Martin, M., Desestret, V., Convers, P., … Honnorat, J. (2017). Autoimmune episodic ataxia in patients with anti-CASPR2 antibody-associated encephalitis. *Neurology: Neuroimmunology and NeuroInflammation*, *4*(4). https://doi.org/10.1212/NXI.0000000000000371

Joubert, B., Saint-Martin, M., Noraz, N., Picard, G., Rogemond, V., Ducray, F., … Honnorat, J. (2016). Characterization of a subtype of autoimmune encephalitis with anti-Contactin-Associated protein-like 2 antibodies in the cerebrospinal fluid, prominent limbic symptoms, and seizures. *JAMA Neurology*, *73*(9), 1115–1124. https://doi.org/10.1001/jamaneurol.2016.1585

Ju, W., Morishita, W., Tsui, J., Gaietta, G., Deerinck, T. J., Adams, S. R., … Malenka, R. C. (2004). Activity-dependent regulation of dendritic synthesis and trafficking of AMPA receptors. *Nature Neuroscience*, *7*(3), 244–253. https://doi.org/10.1038/nn1189

Jurgensen, S., & Castillo, P. E. (2015). Selective Dysregulation of Hippocampal Inhibition in the Mouse Lacking Autism Candidate Gene CNTNAP2. *Journal of Neuroscience*, *35*(43), 14681–14687. https://doi.org/10.1523/JNEUROSCI.1666-15.2015

Kaila, K., Pasternack, M., Saarikoski, J., & Voipio, J. (1989). Influence of GABA-gated bicarbonate conductance on potential, current and intracellular chloride in crayfish muscle fibres. *The Journal of Physiology*, *416*, 161–181. https://doi.org/10.1113/jphysiol.1989.sp017755

Karagogeos, D., Morton, S. B., Casano, F., Dodd, J., & Jessell, T. M. (1991). Developmental expression of the axonal glycoprotein TAG-1: differential regulation by central and peripheral neurons in vitro. *Development (Cambridge, England)*, *112*(1), 51–67. Retrieved from http://dev.biologists.org/content/develop/112/1/51.full.pdf

Kasai, H., Fukuda, M., Watanabe, S., Hayashi-Takagi, A., & Noguchi, J. (2010). Structural dynamics of dendritic spines in memory and cognition. *Trends in Neurosciences*, *33*(3), 121–129. https://doi.org/10.1016/j.tins.2010.01.001

Kasaragod, V. B., & Schindelin, H. (2018). Structure–Function Relationships of Glycine and GABAA Receptors and Their Interplay With the Scaffolding Protein Gephyrin. *Frontiers in Molecular Neuroscience*, *11*. https://doi.org/10.3389/fnmol.2018.00317

Kazarinova-Noyes, K., Malhotra, J. D., McEwen, D. P., Mattei, L. N., Berglund, E. O., Ranscht, B., … Xiao, Z.-C. (2001). Contactin Associates with Na+ Channels and Increases Their Functional Expression. *Journal of Neuroscience*, *21*(19), 7517–7525. https://doi.org/10.1523/JNEUROSCI.21-19-07517.2001

Kegel, L., Jaegle, M., Driegen, S., Aunin, E., Leslie, K., Fukata, Y., … Meijer, D. (2014). Functional phylogenetic analysis of LGI proteins identifies an interaction motif crucial for myelination. *Development (Cambridge, England)*, *141*(8), 1749–1756. https://doi.org/10.1242/dev.107995

Keith, D., & El-Husseini, A. (2008). Excitation control: balancing PSD-95 function at the synapse. *Frontiers in Molecular Neuroscience*, *1*. https://doi.org/10.3389/neuro.02.004.2008

Kenny, P. J., & Markou, A. (2004, May). The ups and downs of addiction: Role of metabotropic glutamate receptors. *Trends in Pharmacological Sciences*, Vol. 25, pp. 265–272. https://doi.org/10.1016/j.tips.2004.03.009

Kim, E., Niethammer, M., Rothschild, A., Nung Jan, Y., & Sheng, M. (1995). Clustering of Shaker-type K+ channels by interaction with a family of membrane-associated guanylate kinases. *Nature*, *378*(6552), 85–88. https://doi.org/10.1038/378085a0

King, C. H., Lancaster, E., Salomon, D., Peles, E., & Scherer, S. S. (2014). Kv7.2 regulates the function of peripheral sensory neurons. *Journal of Comparative Neurology*, *522*(14), 3262–3280.

https://doi.org/10.1002/cne.23595

Kirsch, J., Langosch, D., Prior, P., Littauer, U. Z., Schmitt, B., & Betz, H. (1991). The 93-kDa glycine receptor-associated protein binds to tubulin. *Journal of Biological Chemistry*, *266*(33), 22242–22245. Retrieved from http://www.jbc.org/content/266/33/22242.full.pdf

Kirvan, C. A., Swedo, S. E., Heuser, J. S., & Cunningham, M. W. (2003). Mimicry and autoantibody-mediated neuronal cell signaling in Sydenham chorea. *Nature Medicine*, *9*(7), 914–920. https://doi.org/10.1038/nm892

Kleckner, N. W., & Dingledine, R. (1988). Requirement for glycine in activation of NMDA receptors expressed in xenopus oocytes. *Science*, *241*(4867), 835–837. https://doi.org/10.1126/science.2841759

Kleopa, K. A., Elman, L. B., Lang, B., Vincent, A., & Scherer, S. S. (2006). Neuromyotonia and limbic encephalitis sera target mature Shaker-type K + channels: Subunit specificity correlates with clinical manifestations. *Brain*, *129*(6), 1570–1584. https://doi.org/10.1093/brain/awl084

Koga, M., Gilbert, M., Li, J., Koike, S., Takahashi, M., Furukawa, K., … Yuki, N. (2005). Antecedent infections in Fisher syndrome. *Neurology*, *64*(9), 1605. https://doi.org/10.1212/01.WNL.0000160399.08456.7C

Kordeli, E., Lambert, S., & Bennett, V. (1995). AnkyrinG. A new ankyrin gene with neural-specific isoforms localized at the axonal initial segment and node of Ranvier. *The Journal of Biological Chemistry*, *270*(5), 2352–2359. https://doi.org/10.1074/jbc.270.5.2352

Körtvelyessy, P., Bauer, J., Stoppel, C. M., Brück, W., Gerth, I., Vielhaber, S., … Bien, C. G. (2015). Complement-associated neuronal loss in a patient with CASPR2 antibody-associated encephalitis. *Neurology(R) Neuroimmunology & Neuroinflammation*, *2*(2), e75. https://doi.org/10.1212/NXI.0000000000000075

Krisher, K., & Cunningham, M. W. (1985). Myosin: A link between streptococci and heart. *Science*, *227*(4685), 413–415. https://doi.org/10.1126/science.2578225

Kuang, F., Wang, B.-R., Zhang, P., Fei, L.-L., Jia, Y., Duan, X.-L., … Ju, G. (2004). Extravasation of blood-borne immunoglobulin G through blood-brain barrier during adrenaline-induced transient hypertension in the rat. *The International Journal of Neuroscience*, *114*(6), 575–591. https://doi.org/10.1080/00207450490422731

Kuhlmann, C. R. W., Zehendner, C. M., Gerigk, M., Closhen, D., Bender, B., Friedl, P., & Luhmann, H. J. (2009). MK801 blocks hypoxic blood–brain-barrier disruption and leukocyte adhesion. *Neuroscience Letters*, *449*(3), 168–172. https://doi.org/10.1016/J.NEULET.2008.10.096

Kuhn, T. B., Stoeckli, E. T., Condrau, M. A., Rathjen, F. G., & Sonderegger, P. (1991). Neurite Outgrowth on Immobilized Axonin-1 Is Mediated by a Heterophilic Interaction with LI(G4). In *The Journal of Cell Biology* (Vol. 115).

Kunz, B., Lierheimer, R., Rader, C., Spirig, M., Ziegler, U., & Sonderegger, P. (2002). Axonin-1/TAG-1 mediates cell-cell adhesion by a cis-assisted trans-interaction. *Journal of Biological Chemistry*, *277*(6), 4551–4557. https://doi.org/10.1074/jbc.M109779200

Lai, H. C., & Jan, L. Y. (2006). The distribution and targeting of neuronal voltage-gated ion channels. *Nature Reviews Neuroscience*, Vol. 7, pp. 548–562. https://doi.org/10.1038/nrn1938

Lai, M., Hughes, E. G., Peng, X., Zhou, L., Gleichman, A. J., Shu, H., … Dalmau, J. (2009). AMPA receptor antibodies in limbic encephalitis alter synaptic receptor location. *Annals of Neurology*, *65*(4), 424–434. https://doi.org/10.1002/ana.21589

Lai, M., Huijbers, M. G. M., Lancaster, E., Graus, F., Bataller, L., Balice-Gordon, R., … Dalmau, J. (2010). Investigation of LGI1 as the antigen in limbic encephalitis previously attributed to potassium channels: a case series. *The Lancet. Neurology*, *9*(8), 776–785. https://doi.org/10.1016/S1474-4422(10)70137-X

Lancaster, E, Martinez-Hernandez, E., Titulaer, M. J., Boulos, M., Weaver, S., Antoine, J. C., … Dalmau, J. (2011). Antibodies to metabotropic glutamate receptor 5 in the Ophelia syndrome. *Neurology*, *77*(18), 1698–1701. https://doi.org/10.1212/WNL.0b013e3182364a44

Lancaster, Eric. (2016). The diagnosis and treatment of autoimmune encephalitis. *Journal of Clinical Neurology (Korea)*, Vol. 12, pp. 1–13. https://doi.org/10.3988/jcn.2016.12.1.1

Lancaster, Eric, Huijbers, M. G. M., Bar, V., Boronat, A., Wong, A., Martinez-Hernandez, E., … Dalmau, J. (2011). Investigations of caspr2, an autoantigen of encephalitis and neuromyotonia. *Annals of Neurology*, *69*(2), 303–311. https://doi.org/10.1002/ana.22297

Lancaster, Eric, Lai, M., Peng, X., Hughes, E., Constantinescu, R., Raizer, J., … Dalmau, J. (2010). Antibodies to the GABAB receptor in limbic encephalitis with seizures: case series and characterisation of the antigen. *The Lancet Neurology*, *9*(1), 67–76. https://doi.org/10.1016/S1474-4422(09)70324-2

Lazaro, M. T., Taxidis, J., Shuman, T., Bachmutsky, I., Ikrar, T., Santos, R., … Golshani, P. (2019). Reduced Prefrontal Synaptic Connectivity and Disturbed Oscillatory Population Dynamics in the CNTNAP2 Model of Autism. *Cell Reports*, 2567–2578. https://doi.org/10.1016/j.celrep.2019.05.006

Lee, E. K., Maselli, R. A., Ellis, W. G., & Agius, M. A. (1998). Morvan's fibrillary chorea: A paraneoplastic manifestation of thymoma. *Journal of Neurology Neurosurgery and Psychiatry*, *65*(6), 857–862. https://doi.org/10.1136/jnnp.65.6.857

Legendre, P. (2001). The glycinergic inhibitory synapse. *Cellular and Molecular Life Sciences*, Vol. 58, pp. 760–793. https://doi.org/10.1007/PL00000899

Lei, Z., Deng, P., & Xu, Z. C. (2008). Regulation of Kv4.2 channels by glutamate in cultured hippocampal neurons. *Journal of Neurochemistry*, *106*(1), 182–192. https://doi.org/10.1111/j.1471-4159.2008.05356.x

Leterrier, C. (2018). The axon initial segment: An updated viewpoint. *Journal of Neuroscience*, *38*(9), 2135–2145. https://doi.org/10.1523/JNEUROSCI.1922-17.2018

Leypoldt, F., Wandinger, K.-P., Bien, C. G., & Dalmau, J. (2012). Autoimmune Encephalitis. *European Neurological Review*, *8*(1), 31. https://doi.org/10.17925/ENR.2013.08.01.31

Liguori, R., Vincent, A., Clover, L., Avoni, P., Plazzi, G., Cortelli, P., … Montagna, P. (2001). Morvan's syndrome: peripheral and central nervous system and cardiac involvement with antibodies to voltage-gated potassium channels. *Brain*, *124*(12), 2417–2426. https://doi.org/10.1093/brain/124.12.2417

Linnoila, J. J., Binnicker, M. J., Majed, M., Klein, C. J., & McKeon, A. (2016). CSF herpes virus and autoantibody profiles in the evaluation of encephalitis. *Neurology - Neuroimmunology Neuroinflammation*, *3*(4), e245. https://doi.org/10.1212/nxi.0000000000000245

Lu, Z., Reddy, M. V. V. V. S., Liu, J., Kalichava, A., Liu, J., Zhang, L., … Rudenko, G. (2016). Molecular architecture of contactin-Associated protein-like 2 (CNTNAP2) and its interaction with contactin 2 (CNTN2). *Journal of Biological Chemistry*, *291*(46), 24133–24147. https://doi.org/10.1074/jbc.M116.748236

Luque, F. A., Furneaux, H. M., Ferziger, R., Rosenblum, M. K., Wray, S. H., Schold, S. C., … Posner, J. B.

(1991). Anti-Ri: An antibody associated with paraneoplastic opsoclonus and breast cancer. *Annals of Neurology*, *29*(3), 241–251. https://doi.org/10.1002/ana.410290303

Lüscher, C., Xia, H., Beattie, E. C., Carroll, R. C., von Zastrow, M., Malenka, R. C., & Nicoll, R. A. (1999). Role of AMPA Receptor Cycling in Synaptic. *Neuron*, *24*(3), 649–658. Retrieved from https://pdf.sciencedirectassets.com/272195/1-s2.0-S0896627300X00529/1-s2.0-S0896627300811198/main.pdf?x-amz-security-token=AgoJb3JpZ2luX2VjEHcaCXVzLWVhc3QtMSJHMEUCIQDIheEYeSHue6fzYx8ABeDo0PdVNgs5XhX%252FCTxXbzfB%252BQIgSICLcgjrm8nm%252F530l5meuAfpcahpIaIPoqGKy%25

Lushnikova, I., Skibo, G., Muller, D., & Nikonenko, I. (2011). Excitatory synaptic activity is associated with a rapid structural plasticity of inhibitory synapses on hippocampal CA1 pyramidal cells. *Neuropharmacology*, *60*(5), 757–764. https://doi.org/10.1016/j.neuropharm.2010.12.014

Lynch, J. W. (2009). Native glycine receptor subtypes and their physiological roles. *Neuropharmacology*, *56*(1), 303–309. https://doi.org/10.1016/j.neuropharm.2008.07.034

Lynch, J. W., Zhang, Y., Talwar, S., & Estrada-Mondragon, A. (2017). Glycine Receptor Drug Discovery. In *Advances in pharmacology (San Diego, Calif.)* (Vol. 79, pp. 225–253). https://doi.org/10.1016/bs.apha.2017.01.003

Malinow, R., Zhu, J. J., Esteban, J. A., & Hayashi, Y. (2000). Postnatal synaptic potentiation: Delivery of GluR4-containing AMPA receptors by spontaneous activity. *Nature Neuroscience*, *3*(11), 1098–1106. https://doi.org/10.1038/80614

Mangler, M., Trebesch De Perez, I., Teegen, B., Stöcker, W., Prüss, H., Meisel, A., … Speiser, D. (2013). Seroprevalence of anti-N-methyl-d-aspartate receptor antibodies in women with ovarian teratoma. *Journal of Neurology*, *260*(11), 2831–2835. https://doi.org/10.1007/s00415-013-7074-0

Mansour, M., Nagarajan, N., Nehring, R. B., Clements, J. D., & Rosenmund, C. (2001). Heteromeric AMPA receptors assemble with a preferred subunit stoichiometry and spatial arrangement. *Neuron*, *32*(5), 841–853. https://doi.org/10.1016/S0896-6273(01)00520-7

Marco, E. J., Hinkley, L. B. N., Hill, S. S., & Nagarajan, S. S. (2011). Sensory processing in autism: A review of neurophysiologic findings. *Pediatric Research*, *69*(5 PART 2). https://doi.org/10.1203/PDR.0b013e3182130c54

Maric, H. M., Kasaragod, V. B., Hausrat, T. J., Kneussel, M., Tretter, V., Strømgaard, K., & Schindelin, H. (2014). Molecular basis of the alternative recruitment of GABAA versus glycine receptors through gephyrin. *Nature Communications*, *5*(1), 5767. https://doi.org/10.1038/ncomms6767

Martinez-Hernandez, E., Horvath, J., Shiloh-Malawsky, Y., Sangha, N., Martinez-Lage, M., & Dalmau, J. (2011). Analysis of complement and plasma cells in the brain of patients with anti-NMDAR encephalitis. *Neurology*, *77*(6), 589–593. https://doi.org/10.1212/WNL.0b013e318228c136

Mason, W. (1997). Small-cell lung cancer, paraneoplastic cerebellar degeneration and the Lambert-Eaton myasthenic syndrome. *Brain*, *120*(8), 1279–1300. https://doi.org/10.1093/brain/120.8.1279

Mayer, M. L., & Westbrook, G. L. (1987). Permeation and block of N-methyl-D-aspartic acid receptor channels by divalent cations in mouse cultured central neurones. *The Journal of Physiology*. https://doi.org/10.1113/jphysiol.1987.sp016883

Meir, A., Ginsburg, S., Butkevich, A., Kachalsky, S. G., Kaiserman, I., Ahdut, R., … Rahamimoff, R. (1999). Ion channels in presynaptic nerve terminals and control of transmitter release. *Physiological Reviews*, *79*(3), 1019–1088. https://doi.org/10.1152/physrev.1999.79.3.1019

Meyer Sauteur, P. M., Hackenberg, A., Tio-Gillen, A. P., Van Rossum, A. M. C., Berger, C., & Jacobs, B. C. (2015). Intrathecal Anti-GalC Antibodies in Bickerstaff Brain Stem Encephalitis. *Neuropediatrics*, Vol. 46, pp. 428–430. https://doi.org/10.1055/s-0035-1566730

Milev, P., Maurel, P., Häring, M., Margolis, R. K., & Margolis, R. U. (1996). TAG-1/axonin-1 is a high-affinity ligand of neurocan, phosphacan/protein-tyrosine phosphatase-ζ/β, and N-CAM. *Journal of Biological Chemistry*. https://doi.org/10.1074/jbc.271.26.15716

Mohammad-Rezazadeh, I., Frohlich, J., Loo, S. K., & Jeste, S. S. (2016, April 1). Brain connectivity in autism spectrum disorder. *Current Opinion in Neurology*, Vol. 29, pp. 137–147. https://doi.org/10.1097/WCO.0000000000000301

Mörtl, M., Sonderegger, P., Diederichs, K., & Welte, W. (2007). The crystal structure of the ligand-binding module of human TAG-1 suggests a new mode of homophilic interaction. *Protein Science*, *16*(10), 2174–2183. https://doi.org/10.1110/ps.072802707

Morvan, A. (1890). De la chorée fibrillaire. *Gazette Hebdomadaire de Médicine et de Chirurgie,* Vol. 27, pp 173–200.

Mott, D. (2014). The metabotropic GABAB receptors. *Cellular and Molecular Neurophysiology*, 245–267. https://doi.org/10.1016/B978-0-12-397032-9/00011-X

Moutaux, E., Christaller, W., Scaramuzzino, C., Genoux, A., Charlot, B., Cazorla, M., & Saudou, F. (2018). Neuronal network maturation differently affects secretory vesicles and mitochondria transport in axons. *Scientific Reports*. https://doi.org/10.1038/s41598-018-31759-x

Mueller, S. H., Färber, A., Prüss, H., Melzer, N., Golombeck, K. S., Kümpfel, T., … Leypoldt, F. (2018). Genetic predisposition in anti-LGI1 and anti-NMDA receptor encephalitis. *Annals of Neurology*, *83*(4), 863–869. https://doi.org/10.1002/ana.25216

Nair, D., Hosy, E., Petersen, J. D., Constals, A., Giannone, G., Choquet, D., & Sibarita, J.-B. (2013). Super-Resolution Imaging Reveals That AMPA Receptors Inside Synapses Are Dynamically Organized in Nanodomains Regulated by PSD95. *Journal of Neuroscience*, *33*(32), 13204–13224. https://doi.org/10.1523/JNEUROSCI.2381-12.2013

Nakabayashi, K., & Scherer, S. W. (2001). The human contactin-associated protein-like 2 gene (CNTNAP2) spans over 2 Mb of DNA at chromosome 7q35. *Genomics*, *73*(1), 108–112. https://doi.org/10.1006/geno.2001.6517

Nelson, A. D., & Jenkins, P. M. (2017, May 9). Axonal membranes and their domains: Assembly and function of the axon initial segment and node of Ranvier. *Frontiers in Cellular Neuroscience*, Vol. 11. https://doi.org/10.3389/fncel.2017.00136

Nesti, E. (2004). Endocytosis as a Mechanism for Tyrosine Kinase-dependent Suppression of a Voltage-gated Potassium Channel. *Molecular Biology of the Cell*, *15*(9), 4073–4088. https://doi.org/10.1091/mbc.E03-11-0788

Newsom-Davis, J., & Mills, K. R. (1993). Immunological associations of acquired neuromyotonia (Isaacs' syndrome). *Brain*, *116*(2), 453–469. https://doi.org/10.1093/brain/116.2.453

Nowak, L., Bregestovski, P., Ascher, P., Herbet, A., & Prochiantz, A. (1984). Magnesium gates glutamate-activated channels in mouse central neurones. *Nature*. https://doi.org/10.1038/307462a0

Nusser, Z., Lujan, R., Laube, G., Roberts, J. D., Molnar, E., & Somogyi, P. (1998). Cell type and pathway dependence of synaptic AMPA receptor number and variability in the hippocampus. *Neuron*, *21*(3), 545–559. https://doi.org/10.1016/S0896-6273(00)80565-6

Ogawa, Y., Oses-Prieto, J., Kim, M. Y., Horresh, I., Peles, E., Burlingame, A. L., … Rasband, M. N. (2010). ADAM22, A Kv1 Channel-Interacting Protein, Recruits Membrane-Associated Guanylate Kinases to Juxtaparanodes of Myelinated Axons. *Journal of Neuroscience*, *30*(3), 1038–1048. https://doi.org/10.1523/JNEUROSCI.4661-09.2010

Ogawa, Yasuhiro, Horresh, I., Trimmer, J. S., Bredt, D. S., Peles, E., & Rasband, M. N. (2008). *PSD-93 clusters Kv1 channels at axon initial segments independent of CASPR2*. *28*(22), 5731–5739. https://doi.org/10.1523/JNEUROSCI.4431-07.2008.PSD-93

Ogawa, Yasuhiro, Schafer, D. P., Horresh, I., Bar, V., Hales, K., Yang, Y., … Rasband, M. N. (2006). Spectrins and ankyrinB constitute a specialized paranodal cytoskeleton. *The Journal of Neuroscience : The Official Journal of the Society for Neuroscience*, *26*(19), 5230–5239. https://doi.org/10.1523/JNEUROSCI.0425-06.2006

Okabe, S. (2007). Molecular anatomy of the postsynaptic density. *Molecular and Cellular Neuroscience*, *34*(4), 503–518. https://doi.org/10.1016/j.mcn.2007.01.006

Olsen, A. L., Lai, Y., Dalmau, J., Scherer, S. S., & Lancaster, E. (2015). Caspr2 autoantibodies target multiple epitopes. *Neurology: Neuroimmunology and NeuroInflammation*, *2*(4), 1–9. https://doi.org/10.1212/NXI.0000000000000127

Onugoren, M. D., Golombeck, K. S., Bien, C., Abu-Tair, M., Brand, M., Bulla-Hellwig, M., … Bien, C. G. (2016). Immunoadsorption therapy in autoimmune encephalitides. *Neurology: Neuroimmunology and NeuroInflammation*, *3*(2). https://doi.org/10.1212/NXI.0000000000000207

Ozkaynak, E., Abello, G., Jaegle, M., van Berge, L., Hamer, D., Kegel, L., … Meijer, D. (2010). Adam22 is a major neuronal receptor for Lgi4-mediated Schwann cell signaling. *The Journal of Neuroscience : The Official Journal of the Society for Neuroscience*, *30*(10), 3857–3864. https://doi.org/10.1523/JNEUROSCI.6287-09.2010

Paoletti, P., Bellone, C., & Zhou, Q. (2013). NMDA receptor subunit diversity: Impact on receptor properties, synaptic plasticity and disease. *Nature Reviews Neuroscience*, Vol. 14, pp. 383–400. https://doi.org/10.1038/nrn3504

Papadopoulos, T., Korte, M., Eulenburg, V., Kubota, H., Retiounskaia, M., Harvey, R. J., … Betz, H. (2007). Impaired GABAergic transmission and altered hippocampal synaptic plasticity in collybistin-deficient mice. *The EMBO Journal*, *26*(17), 3888–3899. https://doi.org/10.1038/sj.emboj.7601819

Parham, P. (1988). Function and polymorphism of human leukocyte antigen-A,B,C molecules. *The American Journal of Medicine*, *85*(6A), 2–5. Retrieved from http://www.ncbi.nlm.nih.gov/pubmed/2462346

Parnass, Z., Tashiro, A., & Yuste, R. (2000). Analysis of spine morphological plasticity in developing hippocampal pyramidal neurons. *Hippocampus*, *10*(5), 561–568. https://doi.org/10.1002/1098-1063(2000)10:5<561::AID-HIPO6>3.0.CO;2-X

Paroder-Belenitsky, M., & Pham, H. P. (2019). Immunoadsorption. In *Transfusion Medicine and Hemostasis* (pp. 497–500). https://doi.org/10.1016/B978-0-12-813726-0.00081-7

Paterson, R. W., Zandi, M. S., Armstrong, R., Vincent, A., & Schott, J. M. (2014). Clinical relevance of positive voltage-gated potassium channel (VGKC)-complex antibodies: experience from a tertiary referral centre. *Journal of Neurology, Neurosurgery, and Psychiatry*, *85*(6), 625–630. https://doi.org/10.1136/jnnp-2013-305218

Patterson, K. R., Dalmau, J., & Lancaster, E. (2018). Mechanisms of Caspr2 antibodies in autoimmune

encephalitis and neuromyotonia. *Annals of Neurology*, *83*(1), 40–51. https://doi.org/10.1002/ana.25120

Peñagarikano, O., Abrahams, B. S., Herman, E. I., Winden, K. D., Gdalyahu, A., Dong, H., … Geschwind, D. H. (2011). Absence of CNTNAP2 leads to epilepsy, neuronal migration abnormalities, and core autism-related deficits. *Cell*, *147*(1), 235–246. https://doi.org/10.1016/j.cell.2011.08.040

Peñagarikano, O., & Geschwind, D. H. (2012, March). What does CNTNAP2 reveal about autism spectrum disorder? *Trends in Molecular Medicine*, Vol. 18, pp. 156–163. https://doi.org/10.1016/j.molmed.2012.01.003

Pennacchietti, F., Vascon, S., Nieus, T., Rosillo, C., Das, S., Tyagarajan, S. K., … Cella Zanacchi, F. (2017). Nanoscale Molecular Reorganization of the Inhibitory Postsynaptic Density Is a Determinant of GABAergic Synaptic Potentiation. *The Journal of Neuroscience*, *37*(7), 1747–1756. https://doi.org/10.1523/jneurosci.0514-16.2016

Peters, A., & Kaiserman-Abramof, I. R. (1970). The small pyramidal neuron of the rat cerebral cortex. The perikaryon, dendrites and spines. *American Journal of Anatomy*, *127*(4), 321–355. https://doi.org/10.1002/aja.1001270402

Petit-Pedrol, M., Armangue, T., Peng, X., Bataller, L., Cellucci, T., Davis, R., … Dalmau, J. (2014). Encephalitis with refractory seizures, status epilepticus, and antibodies to the GABAAreceptor: A case series, characterisation of the antigen, and analysis of the effects of antibodies. *The Lancet Neurology*, *13*(3), 276–286. https://doi.org/10.1016/S1474-4422(13)70299-0

Petralia, R. S., Sans, N., Wang, Y. X., & Wenthold, R. J. (2005). Ontogeny of postsynaptic density proteins at glutamatergic synapses. *Molecular and Cellular Neuroscience*, *29*(3), 436–452. https://doi.org/10.1016/j.mcn.2005.03.013

Petrini, E. M., Ravasenga, T., Hausrat, T. J., Iurilli, G., Olcese, U., Racine, V., … Barberis, A. (2014). Synaptic recruitment of gephyrin regulates surface GABAA receptor dynamics for the expression of inhibitory LTP. *Nature Communications*, *5*, 3921. https://doi.org/10.1038/ncomms4921

Piepgras, J., Höltje, M., Michel, K., Li, Q., Otto, C., Drenckhahn, C., … Ruprecht, K. (2015). Anti-DPPX encephalitis: pathogenic effects of antibodies on gut and brain neurons. *Neurology*, *85*(10), 890–897. https://doi.org/10.1212/WNL.0000000000001907

Pinatel, D., Hivert, B., Boucraut, J., Saint-Martin, M., Rogemond, V., Zoupi, L., … Faivre-Sarrailh, C. (2015). Inhibitory axons are targeted in hippocampal cell culture by anti-Caspr2 autoantibodies associated with limbic encephalitis. *Frontiers in Cellular Neuroscience*, *9*(July), 1–16. https://doi.org/10.3389/fncel.2015.00265

Pinatel, D., Hivert, B., Saint-Martin, M., Noraz, N., Savvaki, M., Karagogeos, D., & Faivre-Sarrailh, C. (2017). The Kv1-associated molecules TAG-1 and Caspr2 are selectively targeted to the axon initial segment in hippocampal neurons. *Journal of Cell Science*, *130*(13), 2209–2220. https://doi.org/10.1242/jcs.202267

Pinheiro, P. S., & Mulle, C. (2008). Presynaptic glutamate receptors: physiological functions and mechanisms of action. *Nature Reviews. Neuroscience*, Vol. 9, pp. 423–436. https://doi.org/10.1038/nrn2379

Platt, M. P., Agalliu, D., & Cutforth, T. (2017, April 21). Hello from the other side: How autoantibodies circumvent the blood-brain barrier in autoimmune encephalitis. *Frontiers in Immunology*, Vol. 8, p. 442. https://doi.org/10.3389/fimmu.2017.00442

Poliak, S., Gollan, L., Martinez, R., Custer, A., Einheber, S., Salzer, J. L., … Peles, E. (1999). Caspr2, a new member of the Neurexin superfamily, is localized at the juxtaparanodes of myelinated axons and

associates with K+channels. *Neuron*, *24*(4), 1037–1047. https://doi.org/10.1016/S0896-6273(00)81049-1

Poliak, S., & Peles, E. (2003). The local differentiation of myelinated axons at nodes of ranvier. *Nature Reviews Neuroscience*, Vol. 4, pp. 968–980. https://doi.org/10.1038/nrn1253

Poliak, S., Salomon, D., Elhanany, H., Sabanay, H., Kiernan, B., Pevny, L., … Peles, E. (2003). Juxtaparanodal clustering of Shaker-like K+channels in myelinated axons depends on Caspr2 and TAG-1. *Journal of Cell Biology*, *162*(6), 1149–1160. https://doi.org/10.1083/jcb.200305018

Poot, M. (2015). Connecting the CNTNAP2 networks with neurodevelopmental disorders. *Molecular Syndromology*, *6*(1), 7–22. https://doi.org/10.1159/000371594

Poot, M. (2017). Intragenic CNTNAP2 Deletions: A Bridge Too Far? *Molecular Syndromology*, *8*(3), 118–130. https://doi.org/10.1159/000456021

Prüss, H., Finke, C., Höltje, M., Hofmann, J., Klingbeil, C., Probst, C., … Wandinger, K. P. (2012). N-methyl-D-aspartate receptor antibodies in herpes simplex encephalitis. *Annals of Neurology*, *72*(6), 902–911. https://doi.org/10.1002/ana.23689

Purves, D., Aigustine G.J., Fitzpatrick, D., Hall, W.C., LaMantia, A.-S., McNamara, J.O., White, L.E. (2013). *Neurosciences*, 4th edn. Brussel: De Boeck.

Rader, C., Kunz, B., Lierheimer, R., Giger, R. J., Berger, P., Tittmann, P., … Sonderegger, P. (1996). Implications for the domain arrangement of axonin-1 derived from the mapping of its NgCAM binding site. *The EMBO Journal*, *15*(9), 2056–2068. https://doi.org/10.1002/j.1460-2075.1996.tb00559.x

Rader, C., Stoeckli, E. T., Ziegler, U., Osterwalder, T., K, B., & Sonderegger, P. (1993). Cell-cell adhesion by homophilic interaction of the neuronal recognition molecule axonin-1. *European Journal of Biochemistry*, *215*(1), 133–141. https://doi.org/10.1111/j.1432-1033.1993.tb18015.x

Rajmohan, V., & Mohandas, E. (2007). The limbic system. *Indian Journal of Psychiatry*, *49*(2), 132–139. https://doi.org/10.4103/0019-5545.33264

Rakic, P., Bourgeois, J. P., Eckenhoff, M. F., Zecevic, N., & Goldman-Rakic, P. S. (1986). Concurrent overproduction of synapses in diverse regions of the primate cerebral cortex. *Science (New York, N.Y.)*, *232*(4747), 232–235. Retrieved from http://www.ncbi.nlm.nih.gov/pubmed/3952506

Rasband, M. N. (2010). The axon initial segment and the maintenance of neuronal polarity. *Nature Reviews Neuroscience*, *11*(8), 552–562. https://doi.org/10.1038/nrn2852

Rasband, M. N., Park, E. W., Zhen, D., Arbuckle, M. I., Poliak, S., Peles, E., … Trimmer, J. S. (2002). Clustering of neuronal potassium channels is independent of their interaction with PSD-95. *Journal of Cell Biology*, *159*(4), 663–672. https://doi.org/10.1083/jcb.200206024

Rasband, M. N., & Peles, E. (2016). The nodes of Ranvier: Molecular assembly and maintenance. *Cold Spring Harbor Perspectives in Biology*, *8*(3). https://doi.org/10.1101/cshperspect.a020495

Rasband, M. N., & Trimmer, J. S. (2001). Subunit composition and novel localization of K+ channels in spinal cord. *Journal of Comparative Neurology*, *429*(1), 166–176. https://doi.org/10.1002/1096-9861(20000101)429:1<166::AID-CNE13>3.0.CO;2-Y

Rasband, M. N., Trimmer, J. S., Schwarz, T. L., Levinson, S. R., Ellisman, M. H., Schachner, M., & Shrager, P. (1998). Potassium Channel Distribution, Clustering, and Function in Remyelinating Rat Axons. *Journal of Neuroscience*, *18*(1), 36–47. https://doi.org/10.1523/JNEUROSCI.18-01-00036.1998

Reeves, H. M., & Winters, J. L. (2014, February). The mechanisms of action of plasma exchange. *British*

Journal of Haematology, Vol. 164, pp. 342–351. https://doi.org/10.1111/bjh.12629

Rhodes, K. J., Strassle, B. W., Monaghan, M. M., Bekele-Arcuri, Z., Matos, M. F., & Trimmer, J. S. (1997). Association and colocalization of the Kvbeta1 and Kvbeta2 beta-subunits with Kv1 alpha-subunits in mammalian brain K+ channel complexes. *The Journal of Neuroscience : The Official Journal of the Society for Neuroscience*, *17*(21), 8246–8258. https://doi.org/10.1523/JNEUROSCI.17-21-08246.1997

Rios, J. C., Melendez-Vasquez, C. V, Einheber, S., Lustig, M., Grumet, M., Hemperly, J., … Salzer, J. L. (2000). Contactin-associated protein (Caspr) and contactin form a complex that is targeted to the paranodal junctions during myelination. *The Journal of Neuroscience : The Official Journal of the Society for Neuroscience*, *20*(22), 8354–8364. https://doi.org/10.1523/JNEUROSCI.20-22-08354.2000

Robbins, C. A., & Tempel, B. L. (2012). Kv1.1 and Kv1.2: Similar channels, different seizure models. *Epilepsia*, *53*, 134–141. https://doi.org/10.1111/j.1528-1167.2012.03484.x

Rodenas-Cuadrado, P., Ho, J., & Vernes, S. C. (2014). Shining a light on CNTNAP2: Complex functions to complex disorders. *European Journal of Human Genetics*, *22*(2), 171–178. https://doi.org/10.1038/ejhg.2013.100

Rodenas-Cuadrado, P., Pietrafusa, N., Francavilla, T., La Neve, A., Striano, P., & Vernes, S. C. (2016). Characterisation of CASPR2 deficiency disorder--a syndrome involving autism, epilepsy and language impairment. *BMC Medical Genetics*, *17*, 8. https://doi.org/10.1186/s12881-016-0272-8

Rodríguez-Moreno, A., & Lerma, J. (1998). Kainate receptor modulation of GABA release involves a metabotropic function. *Neuron*. https://doi.org/10.1016/S0896-6273(00)80501-2

Rosenbluth, J., Mierzwa, A., & Shroff, S. (2013). Molecular architecture of myelinated nerve fibers: Leaky paranodal junctions and paranodal dysmyelination. *Neuroscientist*, *19*(6), 629–641. https://doi.org/10.1177/1073858413504627

Roth, J., Harré, E.-M., Rummel, C., Gerstberger, R., & Hübschle, T. (2004). Signaling the brain in systemic inflammation: role of sensory circumventricular organs. *Frontiers in Bioscience : A Journal and Virtual Library*, *9*, 290–300. Retrieved from http://www.ncbi.nlm.nih.gov/pubmed/14766367

Rubenstein, J. L. R., & Merzenich, M. M. (2003). Model of autism: increased ratio of excitation/inhibition in key neural systems. *Genes, Brain, and Behavior*, *2*(5), 255–267. Retrieved from http://www.ncbi.nlm.nih.gov/pubmed/14606691

Rubio-Marrero, E. N., Vincelli, G., Jeffries, C. M., Shaikh, T. R., Pakos, I. S., Ranaivoson, F. M., … Comoletti, D. (2016). Structural characterization of the extracellular domain of caSPR2 and insights into its association with the novel ligand contactin1. *Journal of Biological Chemistry*, *291*(11), 5788–5802. https://doi.org/10.1074/jbc.M115.705681

Sabater, L., Titulaer, M., Saiz, A., Verschuuren, J., Güre, A. O., & Graus, F. (2008). SOX1 antibodies are markers of paraneoplastic Lambert-Eaton myasthenic syndrome. *Neurology*, *70*(12), 924–928. https://doi.org/10.1212/01.wnl.0000281663.81079.24

Sabater, Lidia, Gaig, C., Gelpi, E., Bataller, L., Lewerenz, J., Torres-Vega, E., … Graus, F. (2014). A novel non-rapid-eye movement and rapid-eye-movement parasomnia with sleep breathing disorder associated with antibodies to IgLON5: a case series, characterisation of the antigen, and post-mortem study. *The Lancet Neurology*, *13*(6), 575–586. https://doi.org/10.1016/S1474-4422(14)70051-1

Sagane, K., Ishihama, Y., & Sugimoto, H. (2008). LGI1 and LGI4 bind to ADAM22, ADAM23 and ADAM11. *International Journal of Biological Sciences*, *4*(6), 387–396. Retrieved from

http://www.ncbi.nlm.nih.gov/pubmed/18974846

Saint-Martin, M., Joubert, B., Pellier-Monnin, V., Pascual, O., Noraz, N., & Honnorat, J. (2018). Contactin-associated protein-like 2, a protein of the neurexin family involved in several human diseases. *European Journal of Neuroscience*, *48*(3), 1906–1923. https://doi.org/10.1111/ejn.14081

Saint-Martin, M., Pieters, A., Déchelotte, B., Malleval, C., Pinatel, D., Pascual, O., … Noraz, N. (2019). Impact of anti-CASPR2 autoantibodies from patients with autoimmune encephalitis on CASPR2/TAG-1 interaction and Kv1 expression. *Journal of Autoimmunity*. https://doi.org/10.1016/j.jaut.2019.05.012

Saito, Y., Murakami, F., Song, W. J., Okawa, K., Shimono, K., & Katsumaru, H. (1992). Developing corticorubral axons of the cat form synapses on filopodial dendritic protrusions. *Neuroscience Letters*, *147*(1), 81–84. https://doi.org/10.1016/0304-3940(92)90779-7

Sander, B., Tria, G., Shkumatov, A. V., Kim, E.-Y., Grossmann, J. G., Tessmer, I., … Schindelin, H. (2013). Structural characterization of gephyrin by AFM and SAXS reveals a mixture of compact and extended states. *Acta Crystallographica Section D Biological Crystallography*, *69*(10), 2050–2060. https://doi.org/10.1107/S0907444913018714

Santos, S. D., Carvalho, A. L., Caldeira, M. V, & Duarte, C. B. (2009). Regulation of AMPA receptors and synaptic plasticity. *Neuroscience*, Vol. 158, pp. 105–125. https://doi.org/10.1016/j.neuroscience.2008.02.037

Sassoè-Pognetto, M., Kirsch, J., Grünert, U., Greferath, U., Fritschy, J. M., Möhler, H., … Wässle, H. (1995). Colocalization of gephyrin and GABA $_A$ -receptor subunits in the rat retina. *Journal of Comparative Neurology*, *357*(1), 1–14. https://doi.org/10.1002/cne.903570102

Savvaki, M., Panagiotaropoulos, T., Stamatakis, A., Sargiannidou, I., Karatzioula, P., Watanabe, K., … Kleopa, K. A. (2008). Impairment of learning and memory in TAG-1 deficient mice associated with shorter CNS internodes and disrupted juxtaparanodes. *Molecular and Cellular Neuroscience*, *39*(3), 478–490. https://doi.org/10.1016/j.mcn.2008.07.025

Savvaki, M., Theodorakis, K., Zoupi, L., Stamatakis, A., Tivodar, S., Kyriacou, K., … Karagogeos, D. (2010). The Expression of TAG-1 in Glial Cells Is Sufficient for the Formation of the Juxtaparanodal Complex and the Phenotypic Rescue of Tag-1 Homozygous Mutants in the CNS. *Journal of Neuroscience*, *30*(42), 13943–13954. https://doi.org/10.1523/JNEUROSCI.2574-10.2010

Schools, G. P., & Kimelberg, H. K. (1999). mGluR3 and mGluR5 are the predominant metabotropic glutamate receptor mRNAs expressed in hippocampal astrocytes acutely isolated from young rats. *Journal of Neuroscience Research*, *58*(4), 533–543. https://doi.org/10.1002/(SICI)1097-4547(19991115)58:4<533::AID-JNR6>3.0.CO;2-G

Schulte, U., Thumfart, J. O., Klöcker, N., Sailer, C. A., Bildl, W., Biniossek, M., … Fakler, B. (2006). The epilepsy-linked Lgi1 protein assembles into presynaptic Kv1 channels and inhibits inactivation by Kvβ1. *Neuron*, *49*(5), 697–706. https://doi.org/10.1016/j.neuron.2006.01.033

Schwarz, G., Mendel, R. R., & Ribbe, M. W. (2009). Molybdenum cofactors, enzymes and pathways. *Nature*, *460*(7257), 839–847. https://doi.org/10.1038/nature08302

Schwenk, J., Harmel, N., Brechet, A., Zolles, G., Berkefeld, H., Müller, C. S., … Fakler, B. (2012). High-Resolution Proteomics Unravel Architecture and Molecular Diversity of Native AMPA Receptor Complexes. *Neuron*, *74*(4), 621–633. https://doi.org/10.1016/j.neuron.2012.03.034

Scott, R., Sánchez-Aguilera, A., van Elst, K., Lim, L., Dehorter, N., Bae, S. E., … Marín, O. (2017). Loss of Cntnap2 Causes Axonal Excitability Deficits, Developmental Delay in Cortical Myelination, and

Abnormal Stereotyped Motor Behavior. *Cerebral Cortex*, 1–12. https://doi.org/10.1093/cercor/bhx341

Shi, G., Nakahira, K., Hammond, S., Rhodes, K. J., Schechter, L. E., & Trimmer, J. S. (1996). β Subunits promote K+ channel surface expression through effects early in biosynthesis. *Neuron*. https://doi.org/10.1016/S0896-6273(00)80104-X

Shillito, P., Molenaar, P. C., Vincent, A., Leys, K., Zheng, W., van den Berg, R. J., … Newsom-Davis, J. (1995). Acquired neuromyotonia: Evidence for autoantibodies directed against K + channels of peripheral nerves. *Annals of Neurology*, *38*(5), 714–722. https://doi.org/10.1002/ana.410380505

Shin, Y. W., Lee, S. T., Park, K. Il, Jung, K. H., Jung, K. Y., Lee, S. K., & Chu, K. (2018). Treatment strategies for autoimmune encephalitis. *Therapeutic Advances in Neurological Disorders*, Vol. 11. https://doi.org/10.1177/1756285617722347

Shu, Y., Qiu, W., Zheng, J., Sun, X., Yin, J., Yang, X., … Yu, X. (2019). HLA class II allele DRB1∗16:02 is associated with anti-NMDAR encephalitis. *Journal of Neurology, Neurosurgery and Psychiatry*, (May 2018), 1–7. https://doi.org/10.1136/jnnp-2018-319714

Siegelman, J., Fleit, H. B., & Peress, N. S. (1987). Characterization of immunoglobulin G-Fe receptor activity in the outflow system of the cerebrospinal fluid. *Cell and Tissue Research*, *248*(3), 599–605. https://doi.org/10.1007/BF00216489

Sigel, E., & Steinmann, M. E. (2012). Structure, function, and modulation of GABAA receptors. *Journal of Biological Chemistry*, Vol. 287, pp. 40224–40231. https://doi.org/10.1074/jbc.R112.386664

Sihra, T. S., Flores, G., & Rodríguez-Moreno, A. (2014). Kainate receptors: Multiple roles in neuronal plasticity. *Neuroscientist*, *20*(1), 29–43. https://doi.org/10.1177/1073858413478196

Sillevis Smitt, P., Kinoshita, A., De Leeuw, B., Moll, W., Coesmans, M., Jaarsma, D., … Shigemoto, R. (2002). Paraneoplastic Cerebellar Ataxia Due to Autoantibodies against a Glutamate Receptor. *New England Journal of Medicine*, *342*(1), 21–27. https://doi.org/10.1056/nejm200001063420104

Singer, H. S., Morris, C. M., Gause, C. D., Gillin, P. K., Crawford, S., & Zimmerman, A. W. (2008). Antibodies against fetal brain in sera of mothers with autistic children. *Journal of Neuroimmunology*, *194*(1–2), 165–172. https://doi.org/10.1016/j.jneuroim.2007.11.004

Sinha, S., Newsom-Davis, J., Byrne, N., Lang, B., Vincent, A., & Mills, K. R. (1991). Autoimmune aetiology for acquired neuromyotonia (Isaacs' syndrome). *The Lancet*, *338*(8759), 75–77. https://doi.org/10.1016/0140-6736(91)90073-X

Smart, S. L., Lopantsev, V., Zhang, C. L., Robbins, C. A., Wang, H., Chiu, S. Y., … Tempel, B. L. (1998). Deletion of the K(v)1.1 Potassium channel causes epilepsy in mice. *Neuron*, *20*(4), 809–819. https://doi.org/10.1016/S0896-6273(00)81018-1

Solimena, M., Folli, F., Denis-Donini, S., Comi, G. C., Pozza, G., De Camilli, P., & Vicari, A. M. (1988). Autoantibodies to glutamic acid decarboxylase in a patient with stiff-man syndrome, epilepsy, and type I diabetes mellitus. *The New England Journal of Medicine*, *318*(16), 1012–1020. https://doi.org/10.1056/NEJM198804213181602

Solís, N., Salazar, L., & Hasbun, R. (2016). Anti-NMDA Receptor antibody encephalitis with concomitant detection of Varicella zoster virus. *Journal of Clinical Virology*, *83*, 26–28. https://doi.org/10.1016/j.jcv.2016.08.292

Sorra, & Harris. (1999). Overview on the structure, composition, function, development, and plasticity of hippocampal dendritic spines. *Hippocampus*, *10*(5), 501–511. https://doi.org/10.1002/1098-

1063(2000)10:5<501::AID-HIPO1>3.0.CO;2-T

Soykan, T., Schneeberger, D., Tria, G., Buechner, C., Bader, N., Svergun, D., … Brose, N. (2014). A conformational switch in collybistin determines the differentiation of inhibitory postsynapses. *The EMBO Journal*, *33*(18), 2113–2133. https://doi.org/10.15252/embj.201488143

Specht, C., Izeddin, I., Rodriguez, P., ElBeheiry, M., Rostaing, P., Darzacq, X., … Triller, A. (2013). Quantitative nanoscopy of inhibitory synapses: Counting gephyrin molecules and receptor binding sites. *Neuron*, *79*(2), 308–321. https://doi.org/10.1016/j.neuron.2013.05.013

Stallmeyer, B., Schwarz, G., Schulze, J., Nerlich, A., Reiss, J., Kirsch, J., & Mendel, R. R. (1999). The neurotransmitter receptor-anchoring protein gephyrin reconstitutes molybdenum cofactor biosynthesis in bacteria, plants, and mammalian cells. *Proceedings of the National Academy of Sciences of the United States of America*, *96*(4), 1333–1338. https://doi.org/10.1073/pnas.96.4.1333

Stephen F. Traynelis, Lonnie P. Wollmuth, Chris J. McBain, Frank S. Menniti, Katie M. Vance, Kevin K. Ogden, K. B. H., & Hongjie Yuan, Scott J. Myers, R. D. (2010). Glutamate Receptor Ion Channels: Structure, Regulation, and Function. *Pharmacological Reviews*, *62*(3), 405–439. https://doi.org/10.1124/pr.109.002451.405

Stoeckli, E. T., Kuhn, T. B., Duc, C. O., Ruegg, M. A., & Sonderegger, P. (1991). The axonally secreted protein axonin-1 is a potent substratum for neurite growth. *Journal of Cell Biology*, *112*(3), 449–455. https://doi.org/10.1083/jcb.112.3.449

Strauss, K. A., Puffenberger, E. G., Huentelman, M. J., Gottlieb, S., Dobrin, S. E., Parod, J. M., … Morton, D. H. (2006). Recessive Symptomatic Focal Epilepsy and Mutant Contactin-Associated Protein-like 2. *New England Journal of Medicine*, *354*(13), 1370–1377. https://doi.org/10.1056/NEJMoa052773

Suh, Y. H., Chang, K., & Roche, K. W. (2018). Metabotropic glutamate receptor trafficking. *Molecular and Cellular Neuroscience*, Vol. 91, pp. 10–24. https://doi.org/10.1016/j.mcn.2018.03.014

Tabata, E., Masuda, M., Eriguchi, M., Yokoyama, M., Takahashi, Y., Tanaka, K., … Hara, H. (2014). Immunopathological significance of ovarian teratoma in patients with anti-N-Methyl-D-Aspartate receptor encephalitis. *European Neurology*, *71*(1–2), 42–48. https://doi.org/10.1159/000353982

Tabone, C. J., & Ramaswami, M. (2012). Is NMDA Receptor-Coincidence Detection Required for Learning and Memory? *Neuron*. https://doi.org/10.1016/j.neuron.2012.05.008

Takumi, T., Tamada, K., Hatanaka, F., Nakai, N., & Bolton, P. F. (2019, May). Behavioral neuroscience of autism. *Neuroscience and Biobehavioral Reviews*. https://doi.org/10.1016/j.neubiorev.2019.04.012

Takumi, Y., Ramirez-Leon, V., Laake, P., Rinvik, E., & Ottersen, O. P. (1999). Different modes of expression of AMPA and NMDA receptors in hippocampal synapses. *Nat Neurosci*, *2*(7), 618-24. https://doi.org/10.1038/10172

Tanabe, Y., Fujita-Jimbo, E., Momoi, M. Y., & Momoi, T. (2015). CASPR2 forms a complex with GPR37 via MUPP1 but not with GPR37(R558Q), an autism spectrum disorder-related mutation. *Journal of Neurochemistry*, *134*(4), 783–793. https://doi.org/10.1111/jnc.13168

Tao, C.-L., Liu, Y.-T., Sun, R., Zhang, B., Qi, L., Shivakoti, S., … Bi, G.-Q. (2018). Differentiation and Characterization of Excitatory and Inhibitory Synapses by Cryo-electron Tomography and Correlative Microscopy. *The Journal of Neuroscience*, *38*(6), 1493–1510. https://doi.org/10.1523/jneurosci.1548-17.2017

Tao, Y., Zeng, R., Shen, B., Jia, J., & Wang, Y. (2005). Neuronal transmission stimulates the phosphorylation of Kv1.4 channel at Ser229 through protein kinase A1. *Journal of Neurochemistry*, *94*(6), 1512–1522. https://doi.org/10.1111/j.1471-4159.2005.03297.x

Titulaer, M. J., McCracken, L., Gabilondo, I., Armangué, T., Glaser, C., Iizuka, T., … Dalmau, J. (2013). Treatment and prognostic factors for long-term outcome in patients with anti-NMDA receptor encephalitis: an observational cohort study. *The Lancet. Neurology*, *12*(2), 157–165. https://doi.org/10.1016/S1474-4422(12)70310-1

Toni, N., Buchs, P. A., Nikonenko, I., Bron, C. R., & Muller, D. (1999). LTP promotes formation of multiple spine synapses between a single axon terminal and a dendrite. *Nature*, *402*(6760), 421–425. https://doi.org/10.1038/46574

Traka, M., Dupree, J. L., Popko, B., & Karagogeos, D. (2002). The neuronal adhesion protein TAG-1 is expressed by Schwann cells and oligodendrocytes and is localized to the juxtaparanodal region of myelinated fibers. *The Journal of Neuroscience : The Official Journal of the Society for Neuroscience*, *22*(8), 3016–3024. https://doi.org/20026306

Traka, M., Goutebroze, L., Denisenko, N., Bessa, M., Nifli, A., Havaki, S., … Karagogeos, D. (2003). Association of TAG-1 with Caspr2 is essential for the molecular organization of juxtaparanodal regions of myelinated fibers. *Journal of Cell Biology*, *162*(6), 1161–1172. https://doi.org/10.1083/jcb.200305078

Tretter, V., Mukherjee, J., Maric, H.-M., Schindelin, H., Sieghart, W., & Moss, S. J. (2012). Gephyrin, the enigmatic organizer at GABAergic synapses. *Frontiers in Cellular Neuroscience*, *6*. https://doi.org/10.3389/fncel.2012.00023

Tunkel, A. R., Glaser, C. A., Bloch, K. C., Sejvar, J. J., Marra, C. M., Roos, K. L., … Whitley, R. J. (2008). The Management of Encephalitis: Clinical Practice Guidelines by the Infectious Diseases Society of America. *Clinical Infectious Diseases*, *47*(3), 303–327. https://doi.org/10.1086/589747

Turrigiano, G. G. (2008). The Self-Tuning Neuron: Synaptic Scaling of Excitatory Synapses. *Cell*. https://doi.org/10.1016/j.cell.2008.10.008

Turrigiano, G. G. (2017). The dialectic of hebb and homeostasis. *Philosophical Transactions of the Royal Society B: Biological Sciences*, *372*(1715). https://doi.org/10.1098/rstb.2016.0258

Tüzün, E., Rossi, J. E., Karner, S. F., Centurion, A. F., & Dalmau, J. (2007). Adenylate kinase 5 autoimmunity in treatment refractory limbic encephalitis. *Journal of Neuroimmunology*, *186*(1–2), 177–180. https://doi.org/10.1016/j.jneuroim.2007.03.015

Tyagarajan, S. K., & Fritschy, J. M. (2014). Gephyrin: A master regulator of neuronal function? *Nature Reviews Neuroscience*, Vol. 15, pp. 141–156. https://doi.org/10.1038/nrn3670

Ushkaryov, Y. A., Petrenko, A. G., Geppert, M., & Südhof, T. C. (1992). Neurexins: synaptic cell surface proteins related to the alpha-latrotoxin receptor and laminin. *Science (New York, N.Y.)*, *257*(5066), 50–56. Retrieved from http://www.ncbi.nlm.nih.gov/pubmed/1621094

Vabnick, I., Trimmer, J. S., Schwarz, T. L., Levinson, S. R., Risal, D., & Shrager, P. (1999). Dynamic Potassium Channel Distributions during Axonal Development Prevent Aberrant Firing Patterns. *Journal of Neuroscience*, *19*(2), 747–758. https://doi.org/10.1523/JNEUROSCI.19-02-00747.1999

van der Neut Kolfschoten, M., Schuurman, J., Losen, M., Bleeker, W. K., Martinez-Martinez, P., Vermeulen, E., … Parren, P. W. H. I. (2007). Anti-Inflammatory Activity of Human IgG4 Antibodies by Dynamic Fab Arm Exchange. *Science*, *317*(5844), 1554–1557. https://doi.org/10.1126/science.1144603

van Sonderen, A., Ariño, H., Petit-Pedrol, M., Leypoldt, F., Körtvélyessy, P., Wandinger, K.-P., … Titulaer, M. J. (2016a). The clinical spectrum of Caspr2 antibody-associated disease. *Neurology*, *87*(5), 521–528. https://doi.org/10.1212/WNL.0000000000002917

van Sonderen, A., Ariño, H., Petit-Pedrol, M., Leypoldt, F., Körtvélyessy, P., Wandinger, K.-P., … Titulaer, M. J. (2016b). The clinical spectrum of Caspr2 antibody–associated disease. *Neurology*, *87*(5), 521–528. https://doi.org/10.1212/wnl.0000000000002917

van Sonderen, A., Roelen, D. L., Stoop, J. A., Verdijk, R. M., Haasnoot, G. W., Thijs, R. D., … Titulaer, M. J. (2017). Anti-LGI1 encephalitis is strongly associated with HLA-DR7 and HLA-DRB4. *Annals of Neurology*, *81*(2), 193–198. https://doi.org/10.1002/ana.24858

Varea, O., Martin-de-Saavedra, M. D., Kopeikina, K. J., Schürmann, B., Fleming, H. J., Fawcett-Patel, J. M., … Penzes, P. (2015). Synaptic abnormalities and cytoplasmic glutamate receptor aggregates in contactin associated protein-like 2 */Caspr2* knockout neurons. *Proceedings of the National Academy of Sciences*, *112*(19), 6176–6181. https://doi.org/10.1073/pnas.1423205112

Venkatesan, A, Tunkel, A. R., Bloch, K. C., Lauring, A. S., Sejvar, J., Bitnun, A., … Cherry, J. (2013). Case definitions, diagnostic algorithms, and priorities in encephalitis: Consensus statement of the international encephalitis consortium. *Clinical Infectious Diseases*, *57*(8), 1114–1128. https://doi.org/10.1093/cid/cit458

Venkatesan, Arun, & Benavides, D. R. (2015, March 1). Autoimmune Encephalitis and Its Relation to Infection. *Current Neurology and Neuroscience Reports*, Vol. 15, p. 3. https://doi.org/10.1007/s11910-015-0529-1

Verkerk, A. J. M. H., Mathews, C. A., Joosse, M., Eussen, B. H. J., Heutink, P., & Oostra, B. A. (2003). *CNTNAP2 is disrupted in a family with Gilles de la Tourette syndrome and obsessive compulsive disorder*. https://doi.org/10.1016/S0888-7543(03)00097-1

Vernino, S., & Lennon, V. A. (2000). New Purkinje cell antibody (PCA-2): marker of lung cancer-related neurological autoimmunity. *Annals of Neurology*, *47*(3), 297–305. Retrieved from http://www.ncbi.nlm.nih.gov/pubmed/10716248

Vidarsson, G., Dekkers, G., & Rispens, T. (2014). IgG subclasses and allotypes: From structure to effector functions. *Frontiers in Immunology*, *5*(OCT), 1–17. https://doi.org/10.3389/fimmu.2014.00520

Vogt, D., Cho, K. K. A., Shelton, S. M., Paul, A., Huang, Z. J., Sohal, V. S., & Rubenstein, J. L. R. (2018). Mouse Cntnap2 and Human CNTNAP2 ASD Alleles Cell Autonomously Regulate PV+ Cortical Interneurons. *Cerebral Cortex (New York, N.Y. : 1991)*, *28*(11), 3868–3879. https://doi.org/10.1093/cercor/bhx248

Voltz, R., Gultekin, S. H., Rosenfeld, M. R., Gerstner, E., Eichen, J., Posner, J. B., & Dalmau, J. (2002). A Serologic Marker of Paraneoplastic Limbic and Brain-Stem Encephalitis in Patients with Testicular Cancer. *New England Journal of Medicine*, *340*(23), 1788–1795. https://doi.org/10.1056/nejm199906103402303

Wang, H., Kunkel, D. D., Martin, T. M., Schwartzkroin, P. A., & Tempel, B. L. (1993). Heteromultimeric K+ channels in terminal and juxtaparanodal regions of neurons. *Nature*, *365*(6441), 75–79. https://doi.org/10.1038/365075a0

Watson, C. M., Crinnion, L. A., Tzika, A., Mills, A., Coates, A., Pendlebury, M., … Bonthron, D. T. (2014). Diagnostic whole genome sequencing and split-read mapping for nucleotide resolution breakpoint identification in CNTNAP2 deficiency syndrome. *American Journal of Medical Genetics, Part A*, *164*(10), 2649–2655. https://doi.org/10.1002/ajmg.a.36679

Waxman, S. G., & Ritchie, J. M. (1993). Molecular dissection of the myelinated axon. *Annals of Neurology*, *33*(2), 121–136. https://doi.org/10.1002/ana.410330202

Wenthold, R. J., Petralia, R. S., & Niedzielski, A. S. (1996). Evidence for Multiple AMPA Receptor Complexes in Hippocampal CAllCA2 Neurons. In *The Journal of Neuroscience* (Vol. 76). Retrieved from http://www.jneurosci.org/content/jneuro/16/6/1982.full.pdf

Wierenga, C. J. (2005). Postsynaptic Expression of Homeostatic Plasticity at Neocortical Synapses. *Journal of Neuroscience*, *25*(11), 2895–2905. https://doi.org/10.1523/jneurosci.5217-04.2005

Willard, S. S., & Koochekpour, S. (2013). Glutamate, Glutamate Receptors, and Downstream Signaling Pathways. *International Journal of Biological Sciences*, *9*(9), 948–959. https://doi.org/10.7150/ijbs.6426

Yoshihara, Y., De Roo, M., & Muller, D. (2009). Dendritic spine formation and stabilization. *Current Opinion in Neurobiology*, Vol. 19, pp. 146–153. https://doi.org/10.1016/j.conb.2009.05.013

Yuan, L. L., & Ganetzky, B. (1999). A glial-neuronal signaling pathway revealed by mutations in a neurexin-related protein. *Science (New York, N.Y.)*, *283*(5406), 1343–1345. Retrieved from http://www.ncbi.nlm.nih.gov/pubmed/10037607

Yuste, R., & Bonhoeffer, T. (2004). Genesis of dendritic spines: Insights from ultrastructural and imaging studies. *Nature Reviews Neuroscience*, *5*(1), 24–34. https://doi.org/10.1038/nrn1300

Zenke, F., Gerstner, W., & Ganguli, S. (2017). The temporal paradox of Hebbian learning and homeostatic plasticity. *Current Opinion in Neurobiology*, Vol. 43, pp. 166–176. https://doi.org/10.1016/j.conb.2017.03.015

Zhang, J., & Diamond, J. S. (2006). Distinct perisynaptic and synaptic localization of NMDA and AMPA receptors on ganglion cells in rat retina. *The Journal of Comparative Neurology*, *498*(6), 810. https://doi.org/10.1002/CNE.21089

Zhang, Y., & Pardridge, W. M. (2001). Mediated efflux of IgG molecules from brain to blood across the blood-brain barrier. *Journal of Neuroimmunology*, *114*(1–2), 168–172. Retrieved from http://www.ncbi.nlm.nih.gov/pubmed/11240028

Zhou, L., Messing, A., & Chiu, S. Y. (2018). Determinants of Excitability at Transition Zones in Kv1.1-Deficient Myelinated Nerves. *The Journal of Neuroscience*, *19*(14), 5768–5781. https://doi.org/10.1523/jneurosci.19-14-05768.1999

Zweier, C., de Jong, E. K., Zweier, M., Orrico, A., Ousager, L. B., Collins, A. L., … Rauch, A. (2009). CNTNAP2 and NRXN1 Are Mutated in Autosomal-Recessive Pitt-Hopkins-like Mental Retardation and Determine the Level of a Common Synaptic Protein in Drosophila. *American Journal of Human Genetics*. https://doi.org/10.1016/j.ajhg.2009.10.004